

The Simplest B Decay, Precisely

CLAUDIA CORNELLA^a, MAX FERRÉ^b, MATTHIAS KÖNIG^b AND MATTHIAS NEUBERT^{b,c}

^a*CERN, Theory Department, 1211 Geneva 23, Switzerland*

^b*PRISMA⁺⁺ Cluster of Excellence & Mainz Institute for Theoretical Physics
Johannes Gutenberg University, Staudingerweg 9, D-55128 Mainz, Germany*

^c*Department of Physics & LEPP, Cornell University, Ithaca, NY 14853, U.S.A.*

Abstract

We derive the QCD×QED factorization theorem governing the leptonic decay $B^- \rightarrow \mu^- \bar{\nu}_\mu(\gamma)$ at all orders in α_s and α . Electromagnetic corrections to this decay probe multiple scales, which we disentangle through a sequence of effective field theories (EFTs). The resulting state-of-the-art prediction for the photon-vetoed rate includes the complete structure-dependent component and is accurate at the percent level, establishing the theoretical framework required for future high-precision measurements of this channel, which will allow for a clean determination of $|V_{ub}|$ and powerful tests of new physics. Our work presents the first complete study of QED effects to an exclusive B -meson decay at next-to-leading power (NLP) in the heavy-quark expansion. Important milestones are (i) the construction of the complete NLP operator basis in soft-collinear effective theory (SCET); (ii) the proposal of a “SCET-friendly” reduction scheme for the Dirac structures of four-fermion operators in dimensional regularization, which avoids power-enhanced evanescent operators; (iii) the consistent refactorization of endpoint-divergent convolution integrals and the first complete resummation of “rapidity logarithms” arising at the boundary between the contributions involving soft and hard-collinear quarks; (iv) the systematic discussion of the EFT below the scale of QCD confinement and the non-perturbative matching of SCET onto this low-energy theory; (v) the decoupling of pseudoscalar mesons in the context of heavy-hadron chiral perturbation theory, so that they can be integrated out for processes in which they do not appear as external particles. We perform a phenomenological analysis of direct and indirect contributions to the decay rate and radiation-energy spectrum, highlighting the importance of the chiral anomaly.

Contents

1	Introduction and strategy	2
2	Effective weak interactions below the weak scale	9
3	Matching to Soft-Collinear Effective Theory	11
3.1	Ingredients of SCET-1	12
3.2	Construction of the SCET-1 operator basis	15
3.3	Evanescient operators in SCET	21
3.4	Results for the bare hard matching coefficients	23
3.5	Simplifications arising at $\mathcal{O}(\alpha)$ in perturbation theory	28
3.6	Renormalization of the hard functions	28
3.7	RG evolution equations	33
4	Matching to SCET-2	38
4.1	Systematics of the SCET-1 \rightarrow SCET-2 matching	39
4.2	Construction of the SCET-2 operator basis	45
4.3	Results for the bare jet functions	47
4.4	Endpoint divergent convolution integrals	52
4.5	Renormalized jet functions	56
4.6	Two-scale RG evolution of the hard function H_1^C	57
4.7	RG evolution in SCET-2	59
4.8	SCET-2 matrix elements	61
4.9	The virtual $B^- \rightarrow \ell^- \bar{\nu}_\ell$ amplitude	67
4.10	Power-enhanced QED corrections from new physics	72
5	Low-energy description and real corrections	74
5.1	Heavy-particle effective theory	74
5.2	Heavy-hadron chiral effective theory	82
5.3	Integrating out the pseudoscalar mesons	88
5.4	Matching SCET-2 to $\text{HH}\chi\text{PT}$	91
5.5	Direct contribution to the decay rate	93
5.6	Indirect contributions to the decay rate	99
5.7	Electromagnetic radiation spectrum	104
6	Phenomenology	105
6.1	Non-perturbative input parameters	105
6.2	Numerical estimates	107
7	Conclusions	113

A	SCET Lagrangians	115
B	Reduction of Dirac structures	116
B.1	Scheme dependence and conversion	116
B.2	Reduction identities in light-cone components	117
B.3	Cancellation of power-enhanced contributions	118
C	Soft anomalous dimension of $F_{\mp}(\Lambda, \mu)$	118
D	RG resummation with a running QED coupling	120

1 Introduction and strategy

Weak decays of B mesons are fundamental probes of the flavor structure of the Standard Model (SM) and its extensions. As the Belle II and LHCb experiments accumulate data, the precision in the measurements of several such decays is expected to reach the percent level. Achieving a comparable precision in theoretical predictions is essential for meaningful comparisons, in particular to accurately determine Cabibbo–Kobayashi–Maskawa (CKM) matrix elements and extract possible new-physics signals. To reach this level of accuracy, electroweak (EW) and QED effects must be incorporated into theoretical predictions. Electroweak corrections, being short-distance effects, are straightforward to calculate. In contrast, the inclusion of QED corrections introduces additional challenges.

In Monte-Carlo generators like PHOTOS [1], the standard way of treating electromagnetic corrections is to dress the charged final states with eikonal emissions. A proper assessment of electromagnetic effects, however, requires including also radiation from the initial state as well as virtual corrections. This is commonly achieved by modeling the decaying meson as a point-like particle, as was done for $B \rightarrow \ell\nu$ in [2]. Explicit studies of other B -meson decays in this approximation include, e.g., the decays $\bar{B} \rightarrow \bar{K}\ell^+\ell^-$ [3–5] and $B \rightarrow M_1M_2$ [6]. This treatment allows one to describe and exponentiate all large logarithms of the type $\ln(m_B/E_{\text{cut}})$, where E_{cut} denotes the cut on the total energy of final-state real radiation. These structure-independent QED corrections are typically dominant, because they appear as double logarithms of the form $\frac{\alpha}{\pi} \ln(m_B/E_{\text{cut}}) \ln(m_B/m_f)$, where m_f denotes the mass of a charged final-state particle.

Once experimental uncertainties reach the percent level, structure-dependent QED effects associated with the finite size of the B meson can no longer be neglected. For the inclusive decay $\bar{B} \rightarrow X_c \ell \nu_\ell$, a complete calculation of $\mathcal{O}(\alpha)$ corrections to the total decay width and the moments of the electron energy spectrum has been performed in [7] in the context of the heavy-quark expansion. Exclusive processes are, however, notoriously more difficult to describe theoretically. For the $B^- \rightarrow \ell^- \bar{\nu}_\ell$ process, as we will show, the structure-dependent contributions contain single logarithms of the mass ratio m_B/m_ℓ , as well as single and double logarithms of the ratio Λ_{QCD}/m_B . These corrections can naturally be at the few percent level, since $\frac{\alpha}{\pi} \ln(m_B/m_\ell) \approx 1.9\%$ (for $\ell = \mu$) and $\frac{\alpha}{\pi} \ln^2(m_B/\Lambda_{\text{QCD}}) \sim (1.5\text{--}5.4)\%$ for $\Lambda_{\text{QCD}} \sim (0.5\text{--}1.5)$ GeV. Unlike for lighter mesons, where dedicated lattice studies of structure-dependent

QED effects exist [8–17], lattice calculations of QED corrections for B -meson decays are not yet available. On the continuum side, a systematic way to separate structure-dependent from point-like QED effects is to use effective field theory (EFT) techniques to factorize the contribution of photons associated to different energy scales. The investigation of such effects along these lines and the derivation of the corresponding factorization theorems is a fairly recent endeavor, so far limited to hadronic two-body decays of B mesons [18–21] and the leptonic decays $B_q \rightarrow \mu^+ \mu^-$ [22, 23] and $B^- \rightarrow \mu^- \bar{\nu}_\mu$ [24], with the latter forming the focus of the present work. As an alternative to this EFT approach, a model based on gauge-invariant interpolating operators for charged hadrons has been developed in [25], and applied in a sum-rule calculation of QED corrections to $B^- \rightarrow \ell^- \bar{\nu}_\ell$ decays in [26]. This method is less rigorous than our framework and does not capture the fine details of the structure-dependent virtual corrections. While it may still lead to reasonable numerical results, it does not allow for a systematic estimate of theoretical uncertainties. For completeness, we also note earlier studies focusing on structure-dependent effects arising from real photons only [27, 28].

The leptonic decay $B^- \rightarrow \ell^- \bar{\nu}_\ell$ (with $\ell = e, \mu, \tau$) is arguably the simplest B -meson decay. Phenomenologically, it is relevant for several reasons. First, once measured precisely, it can provide an independent determination of $|V_{ub}|$ with minimal hadronic uncertainties compared to semileptonic channels such as $B \rightarrow X_u \ell^- \bar{\nu}_\ell$ or $B \rightarrow \pi \ell^- \bar{\nu}_\ell$. Second, it is a sensitive probe of new scalar and pseudoscalar interactions, whose contributions would not feature the chiral suppression of the decay amplitude in the SM. Third, the comparison of different lepton channels could provide a valuable probe of lepton-flavor universality. To date, only the branching ratio for the τ channel has been measured, with a rather large uncertainty, by the Babar and Belle collaborations [29–32] and, more recently, by Belle II [33]. For the e and μ channels only upper bounds are available. The Particle Data Group (PDG) quotes the averaged values [34]¹

$$\begin{aligned} \text{Br}(B^- \rightarrow \tau^- \bar{\nu}_\tau) &= (1.09 \pm 0.24) \cdot 10^{-4}, \\ \text{Br}(B^- \rightarrow \mu^- \bar{\nu}_\mu) &< 8.6 \cdot 10^{-7} \quad (90\% \text{CL}), \\ \text{Br}(B^- \rightarrow e^- \bar{\nu}_e) &< 9.8 \cdot 10^{-7} \quad (90\% \text{CL}). \end{aligned} \tag{1.1}$$

This picture will change in the next decades, as Belle II aims at measuring the $B^- \rightarrow \mu^- \bar{\nu}_\mu$ and $B^- \rightarrow \tau^- \bar{\nu}_\tau$ branching fractions with $\mathcal{O}(5 - 6\%)$ accuracy, assuming 50 ab^{-1} of integrated luminosity [35, 36]. On a longer timescale, a future high-energy lepton collider such as FCC-ee and/or CEPC would further improve these measurements (for dedicated feasibility studies on $B_{(c)}^- \rightarrow \tau^- \bar{\nu}_\tau$ at FCC-ee, see [37, 38]). These prospects motivate a systematic assessment of QED corrections to these channels, including structure-dependent effects.

At first glance, the decay $B^- \rightarrow \ell^- \bar{\nu}_\ell$ appears to be a very simple process. Neglecting QED effects, the non-perturbative contributions to the rate are completely accounted for by the decay constant of the B meson, defined by the (QCD-only) matrix element

$$\langle 0 | \bar{u} \gamma^\mu \gamma_5 b | B^-(p) \rangle = i f_B p^\mu, \tag{1.2}$$

which is currently known to sub-percent precision from lattice simulations of QCD. Including

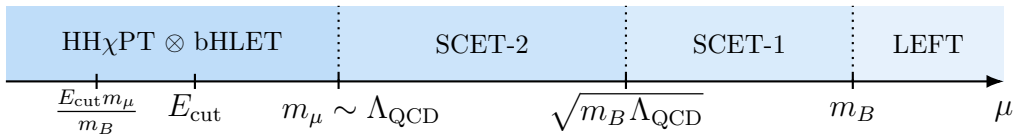
¹The averages quoted here do not include the Belle II result for $\text{Br}(B^- \rightarrow \tau^- \bar{\nu}_\tau)$ [33]. Including it shifts the central value upward by about 10%, with negligible impact on the quoted uncertainty.

QED effects significantly complicates the picture. First, as anticipated above, there is a loss of universality in the non-perturbative quantities entering a given process. The reason is simple: whenever external states carry electric charges, photons – unlike gluons – can mediate interactions among them, and in particular spoil the naive factorization of the amplitude in a hadronic and a leptonic contribution. As a result, quantities which are universal in QCD, such as meson decay constants, light-cone distribution amplitudes (LCDAs) and form factors, must be generalized to quantities that depend on the directions and charges of all initial- and final-state particles. As discussed in [18, 19, 21, 23] for the case of the B -meson decay constant and LCDAs, this generalization is non-trivial. For example, it requires a rearrangement of infrared divergences between soft and collinear functions and leads to LCDAs with support for both positive and negative light-cone momenta. A further complication arises from the fact that the chirally-suppressed decay $B^- \rightarrow \ell^- \bar{\nu}_\ell$ is genuinely a “next-to-leading power (NLP) observable”; its amplitude is suppressed by a factor m_ℓ/m_B relative to that for the decay $B^{*-} \rightarrow \ell^- \bar{\nu}_\ell$. This fact notoriously complicates the derivation of a factorization theorem. The analysis of QCD corrections to exclusive non-leptonic and radiative weak decays of B mesons [39–42] has shown that, while decay amplitudes can be factorized at leading order in Λ_{QCD}/m_b , some power-suppressed corrections contain divergent convolution integrals of hard-scattering kernels with meson LCDAs, which spoil a naive separation of scales. Endpoint-divergent convolutions were also encountered in the analysis of non-local power corrections to the inclusive radiative decay $B \rightarrow X_s \gamma$ [43, 44]. These endpoint divergences are now understood to be a generic feature of subleading-power factorization theorems, see e.g. [45–54] for some early references. In order to establish scale factorization, they must be regularized and removed in a systematic way. A consistent framework to do so is provided by the refactorization-based subtraction (RBS) scheme, in which operators with energetic fields are related, in their low-energy limit, to corresponding operators involving soft fields [51, 52, 54, 55]. In recent years, this scheme has been applied to derive factorization theorems for numerous NLP observables [56–59]. In the present study, we apply the RBS method in a non-perturbative context, which requires a redefinition of hadronic parameters related to the B -meson decay constant [24].

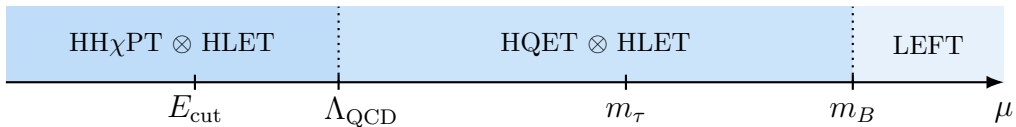
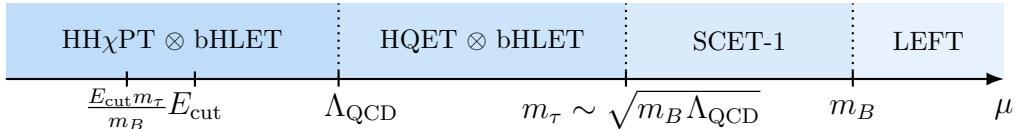
Electromagnetic corrections to $B^- \rightarrow \ell^- \bar{\nu}_\ell$ arise from several energy scales. The largest one is the electroweak scale, $\mu_{\text{EW}} \sim m_Z$, which sets the characteristic scale of the weak interactions underlying the process in the SM. The internal dynamics of the B meson is governed by the scale m_b set by the mass of the heavy b quark, and the confinement scale $\Lambda_{\text{QCD}} \sim 500 \text{ MeV}$, which determines the momentum fluctuations of light partons inside hadronic bound states. Below this scale, the appropriate degrees of freedom of QCD are hadrons rather than quarks and gluons. The kinematics of the decay is controlled by the mass of the decaying B meson and the mass of the charged lepton, as well as by experimental cuts. In what follows we assume that events are selected by imposing an upper cut on the total energy of additional real-photon radiation in the B -meson rest frame, $E_{\text{rad}}^{\text{tot}} < E_{\text{cut}}$, with the cut chosen such that $E_{\text{cut}} \ll \Lambda_{\text{QCD}}$.

The effects associated with these scales can be disentangled by an appropriate sequence of effective field theories, schematically illustrated in Figure 1, whose construction is based on expansions in several small scale ratios. In the effective theory below the weak scale, the

Muon channel



Tau channel



Electron channel

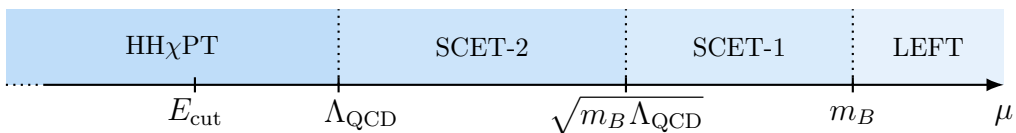


Figure 1: Illustration of the appropriate effective theories below the electroweak scale to treat the $B^- \rightarrow \ell^- \bar{\nu}_\ell$ process for the cases $\ell = \mu, \tau, e$. In the case of the τ lepton, two options are shown, in which the lepton is either treated as a hard-collinear or a hard particle. The dots in the electron case indicate the scales m_e and $E_{\text{cut}}(m_e/m_B)$, which are both much smaller than E_{cut} .

relevant expansion parameters are

$$\lambda \sim \frac{\Lambda_{\text{QCD}}}{m_B}, \quad \lambda_\ell \sim \frac{m_\ell}{m_B}, \quad \zeta \sim \frac{E_{\text{cut}}}{\Lambda_{\text{QCD}}}, \quad (1.3)$$

where we use the fact that m_b and m_B are of the same order. The first two ratios provide the basis for systematic expansions at scales above Λ_{QCD} , while the third controls the structure of the low-energy theory below Λ_{QCD} .

Below the electroweak scale, for all lepton flavors the appropriate description of $B^- \rightarrow \ell^- \bar{\nu}_\ell$ is provided by the effective weak Hamiltonian [60], referred to as Low-Energy Effective Theory (LEFT) in more recent literature [61, 62]. The starting point of our investigation is the LEFT Lagrangian at the scale $\mu_h \sim m_B$, which we refer to as the “hard” scale. In the SM only a single $(V-A) \times (V-A)$ four-fermion operator contributes, and we denote its Wilson coefficient by K_{EW} . At scales below μ_h , the B meson and the heavy b quark therein are described in heavy-quark effective theory (HQET) [63–66]. The rest of the construction depends on the mass of the charged lepton. For $\ell = \mu, e$, QED interactions of the light spectator quark with the final-state charged lepton probe an intermediate “hard-collinear” scale $\mu_{hc} \sim \sqrt{m_B \Lambda_{\text{QCD}}}$, which can resolve the inner structure of the meson [24]. The appropriate effective field theory describing these effects is the soft-collinear effective theory (SCET) [67–70], in the variant

called SCET-1. The Wilson coefficients arising in the matching of the LEFT onto SCET-1 are referred to as *hard functions* and denoted by H_i . These functions depend on the hard scales m_B and m_b as well as on the large light-cone energies of hard-collinear particles. In the next step, the hard-collinear modes are integrated out by matching SCET-1 onto a second variant of SCET, commonly called SCET-2. The matching coefficients arising in this step are referred to as *jet functions* and denoted J_i . These functions depend on the large light-cone energies of the hard-collinear fluctuations integrated out, but also on soft light-cone momenta of the light constituents (light quarks and gluons) of the B meson. The hierarchy $m_\ell \ll \mu_{hc}$ implies that the charged-lepton mass is a power-suppressed parameter in SCET-1. In SCET-2, the soft hadronic dynamics and the collinear leptonic dynamics are factorized, because interactions between soft and collinear particles are forbidden by momentum conservation. The B -meson matrix elements of the (non-local) SCET-2 operators define the *soft functions* S_i . These can be parameterized in terms of two HQET decay constants F_\mp as well as the two-particle and three-particle LCDAs of the B meson defined in HQET. The matrix elements of the leptonic current operators in SCET-2, on the other hand, can be calculated in perturbation theory and expressed in terms of functions K_i of the lepton mass m_ℓ .

The situation is different for the τ channel, for which the parameter $\lambda_\ell \approx 0.34$ is not particularly small. Here two approaches seem reasonable. Either one treats m_τ as a hard-collinear scale, $m_\tau \sim \sqrt{m_B \Lambda_{\text{QCD}}}$, in which case it enters as an additional parameter in the jet functions J_i . Below the scale μ_{hc} , the tau lepton is then treated in heavy-lepton effective theory (HLET). Or one treats m_τ as a hard scale, $m_\tau \sim m_B$, in analogy with the standard treatment of charm mesons in $B \rightarrow D^{(*)}$ transitions in HQET [71–73], in which case m_τ enters in the hard functions H_i instead. In this case, the effective theory below μ_h consists of HQET \times HLET, and it does not involve any hard-collinear or collinear modes.

Below the hadronic scale Λ_{QCD} , the strong and electromagnetic dynamics of B mesons and their excitations can be described in a systematic way using heavy-hadron chiral perturbation theory (HH χ PT) [74–76]. Hadrons containing a b quark can be classified as multiplets under the heavy-quark spin symmetry, with the ground state consisting of the doublet (B, B^*) of the lowest-lying pseudoscalar and vector mesons, whose masses are degenerate in the heavy-quark limit [71, 77]. Photons with energies $E_\gamma \ll \Lambda_{\text{QCD}}$ cannot resolve the internal structure of the mesons, and their interactions can therefore be described by treating the mesons as point-like objects. The corresponding eikonal emissions are then encoded in Wilson lines associated with the mesons. This forbids transitions of the form $B \rightarrow X_b \gamma$, since $m_{X_b} - m_B \gtrsim \mathcal{O}(\Lambda_{\text{QCD}})$ for excited states containing a b quark.² Importantly, the only exception is the case $X_b = B^*$, which is special since the mass splitting $m_{B^*} - m_B \sim \Lambda_{\text{QCD}}^2/m_B$ vanishes in the heavy-quark limit. The transition $B \rightarrow B^* \gamma$ is unsuppressed for $E_\gamma \sim \Lambda_{\text{QCD}}^2/m_B$. A second possibility is the transition $B \rightarrow B^* \pi^0$ with an on-shell pion, which then decays to two photons. In both cases, the B^* meson can subsequently decay leptonically, $B^{*-} \rightarrow \ell^- \bar{\nu}_\ell$, without suffering the chiral suppression of the pseudo-scalar channel. The relevance of these contributions relative to the direct $B^- \rightarrow \ell^- \bar{\nu}_\ell$ decay scales with $(m_B/m_\ell)^2 \times (E_{\text{cut}}/\Lambda_{\text{QCD}})^2$ times a phase-space

²Virtual hard-collinear photons in SCET-1 can excite such transitions. This effect is calculated in our framework using quark and gluon degrees of freedom. Specifically, the hard-collinear \bar{u} -quark propagator in diagrams such as the second graph in Figure 5, combined with the heavy-quark, is dual to the sum over the entire tower of excited states X_b .

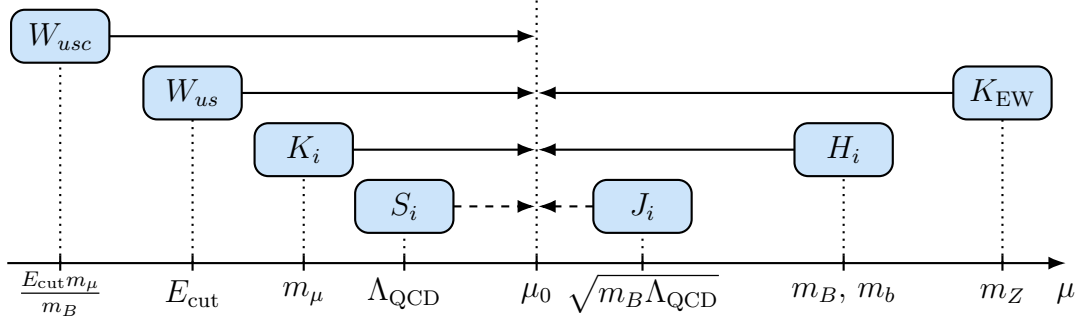


Figure 2: Ingredients of the $B^- \rightarrow \mu^- \bar{\nu}_\mu$ factorization formula and their respective natural scales. Solid arrows denote RG evolution to a common renormalization scale μ_0 . Dashed arrows indicate that the corresponding component functions are evaluated at $\mu = \mu_0$ without resummation.

function, which also depends on E_{cut} . As a consequence, they turn out to be relevant for the cases where $\ell = \mu, e$. Real photons emitted in the low-energy effective theory come with two different momentum scalings, which we refer to as “ultrasoft” and “ultrasoft-collinear”. Ultrasoft photons have homogeneously small momentum components of order E_{cut} in the rest frame of the B meson, while ultrasoft-collinear photons have homogeneously small momentum components of order $E_{\text{cut}}(m_\ell/m_B)$ in the rest frame of the charged lepton. When boosted to the B -meson rest frame, they become collinear, with their largest light-cone momentum component of order E_{cut} . The charged leptons in the low-energy effective theory are described by a boosted version of HLET, since they appear heavy on the energy scale $E_{\text{cut}}(m_\ell/m_B)$ of the ultrasoft-collinear radiation. In the factorization theorem, the real-photon emissions give rise to the ultrasoft and ultrasoft-collinear functions W_{us} and W_{usc} , living at the scales E_{cut} and $E_{\text{cut}}(m_\ell/m_B)$, respectively. The matching of SCET-2 onto $\text{HH}\chi\text{PT}$ is non-perturbative. The soft functions S_i mentioned above appear as the matching coefficients in this transition.

In the present work we focus on the decay $B^- \rightarrow \mu^- \bar{\nu}_\mu$, postponing a detailed treatment of the τ channel to future work. Our analysis of the muon channel is general enough to carry over to the electron case. However, due to the very strong chiral suppression in this case, the “direct” contribution to the decay rate is completely negligible, and only “indirect” decay modes such as $B^- \rightarrow B^{*-} \gamma \rightarrow e^- \bar{\nu}_e \gamma$ would be observable. We derive the general multi-scale QCD \times QED factorization theorem for these decays, valid to all orders in QCD and QED interactions. The functions entering this factorization formula, together with their natural scales, are summarized in Figure 2. We provide explicit expressions for the component functions needed for the evaluation of the decay amplitude at one-loop order. We also derive the renormalization-group (RG) evolution equations of the hard functions, which allows us to resum the leading logarithmic corrections of order $(\alpha_s L^2)^n$, $(\alpha_s L)^n$, and $(\alpha L^2)^n$ (with L a logarithm of a large scale ratio) to all orders of perturbation theory. We also include the most relevant mixed corrections of $\mathcal{O}(\alpha\alpha_s)$. All component functions, including the non-perturbative hadronic decay constants and LCDAs, are evaluated at a common perturbative scale $\mu_0 = 1.5 \text{ GeV}$, chosen sufficiently large to be in the perturbative domain, but sufficiently

low to ensure that all large logarithms are resummed. With the hard-collinear scale being of order 1.6 GeV (for $\Lambda_{\text{QCD}} \sim 0.5 \text{ GeV}$), the RG evolution of the jet functions from the hard-collinear scale to the scale μ_0 can be safely neglected. For all other functions we perform RG evolution from their natural scale to μ_0 .

This paper is organized as follows. We begin in Section 2 by describing the relevant operators in the LEFT, which contribute to leptonic B decays in the effective theory below the electroweak scale. In Section 3 we then construct the effective theory SCET-1. Since we need to work beyond leading order in SCET power counting, the general operator basis required for our analysis is rather large, containing 26 physical, plus six evanescent operators needed at one-loop order. We calculate the bare Wilson coefficients of these operators – the hard functions – to the perturbative order needed for our analysis and show how the $1/\epsilon$ pole terms in the bare coefficients are removed by renormalization. The latter step is non-trivial, since different hard functions mix under renormalization, and some of the mixing terms contain endpoint-divergent convolution integrals. In Section 3.7, we solve the RG evolution equations for the renormalized hard functions and present our final results for these objects. In Section 4, we present the analogous construction of the effective theory SCET-2. After explaining the systematics of the SCET-1 \rightarrow SCET-2 matching procedure, which exploits the symmetries of the effective theories, we construct the SCET-2 operator basis relevant to our problem, which consists of 12 operators. We then present the bare expressions for the Wilson coefficients of these operators – the jet functions – to one-loop order. The convolution integrals of the hard and jet functions exhibit endpoint divergences in the regions where some of the hard-collinear particles carry soft momenta. We explain in Section 4.4 how these divergences are treated in the RBS scheme, and how this leads to a redefinition of four of the basis operators and requires a novel, two-scale RG evolution of the related hard functions. We then discuss the renormalization of the jet functions and the derivation of their RG evolution equations. Finally, the matrix elements of the SCET-2 operators, which factorize into independent matrix elements of hadronic and leptonic currents, are either expressed in terms of well-defined hadronic quantities in HQET – form factors and LCDAs – (hadronic currents), or calculated at one-loop order in perturbation theory (leptonic currents). In Section 4.9, we then present our final, RG-improved result for the virtual $B^- \rightarrow \ell^- \bar{\nu}_\ell$ decay amplitude. In Section 5, we discuss in detail the low-energy effective theory below the hadronic scale, in which the B meson is described as a point-like object interacting with low-energetic photons and light pseudoscalar mesons. We perform the non-perturbative matching of SCET-2 onto this theory. We also show that the pseudoscalar mesons can be integrated out (for processes in which they do not appear as final-state particles), but this generates non-local effective $B^{(*)}B^{(*)}\gamma\gamma$ vertices from the chiral anomaly, which has an important impact on phenomenology. We present a detailed phenomenological study of our findings in Section 6. Finally, we summarize our main findings and give our conclusions in Section 7. Additional technical details of the calculations are relegated to four appendices.

Our discussion in Sections 3 and 4 is necessarily technical, since we are dealing with a NLP SCET factorization theorem affected by endpoint divergences. The reader not interested in the details can skip these sections and consult directly the final result for the virtual $B^- \rightarrow \ell^- \bar{\nu}_\ell$ decay amplitude given in (4.99), (4.113) and (4.116), and then proceed with Section 5.

2 Effective weak interactions below the weak scale

Since B -meson decays occur at energies well below the electroweak scale, they can be described in terms of operators involving only light SM fields. Using the LEFT operator basis [61], the most general effective Lagrangian describing $B^- \rightarrow \ell^- \bar{\nu}_\ell$ decays can be written as

$$\begin{aligned} \mathcal{L}_{\text{LEFT}} \ni & L_\ell^{V,LL} (\bar{\ell} \gamma^\mu P_L \nu_\ell) (\bar{u} \gamma_\mu P_L b) + L_\ell^{V,LR} (\bar{\ell} \gamma^\mu P_L \nu_\ell) (\bar{u} \gamma_\mu P_R b) \\ & + L_\ell^{S,RL} (\bar{\ell} P_L \nu_\ell) (\bar{u} P_R b) + L_\ell^{S,RR} (\bar{\ell} P_L \nu_\ell) (\bar{u} P_L b) + L_\ell^{T,RR} (\bar{\ell} \sigma^{\mu\nu} P_L \nu_\ell) (\bar{u} \sigma_{\mu\nu} P_L b) \\ & + [L_{\nu e}^{V,LL}]_{2112} (\bar{\nu}_\mu \gamma_\mu P_L \nu_e) (\bar{e} \gamma^\mu P_L \mu), \end{aligned} \quad (2.1)$$

where we have defined $L_\ell^X \equiv [L_{\nu e d u}^X]_{\ell\ell 31}^*$ for compactness, and for convenience we included also the operator mediating the decay of the muon, from which the Fermi constant is extracted. In scenarios with new exotic states heavier than the EW scale, all coefficients in (2.1) can be non-zero. At tree level, the $B^- \rightarrow \ell^- \bar{\nu}_\ell$ decay rate obtained from this Lagrangian reads

$$\Gamma_{\text{LEFT}} = \frac{m_\ell^2 m_B (f_B)^2}{64\pi} \left(1 - \frac{m_\ell^2}{m_B^2} \right) \left| L_\ell^{V,LL} - L_\ell^{V,LR} + \frac{m_B^2}{m_\ell (m_b + m_u)} (L_\ell^{S,RL} - L_\ell^{S,RR}) \right|^2, \quad (2.2)$$

where the Wilson coefficients and running quark masses are evaluated at a scale $\mu_b \sim m_B$. Note that the scalar operators give chirally unsuppressed contributions to the rate.

In this work, we are primarily interested in QED corrections to the prediction in the SM, where only the two vector-current operators in (2.1) have non-vanishing Wilson coefficients. These read [78]

$$\begin{aligned} [L_{\nu e}^{V,LL}]_{1212} &= -\frac{4G_F}{\sqrt{2}} K_\ell \equiv -\frac{4G_F^{(\mu)}}{\sqrt{2}}, \\ L_\ell^{V,LL} &= -\frac{4G_F}{\sqrt{2}} V_{ub} K_q \equiv -\frac{4G_F^{(\mu)}}{\sqrt{2}} V_{ub} K_{\text{EW}}(\mu), \end{aligned} \quad (2.3)$$

where G_F denotes the Fermi constant obtained from integrating out the W boson at tree level, and the parameters K_ℓ and K_q contain the one-loop matching corrections. In practice, one extracts the Fermi constant from the lifetime of the muon and identifies it with the Wilson coefficient of the purely leptonic operator in the last line of (2.1), yielding $G_F^{(\mu)} = G_F K_\ell$. This implies the relation

$$K_{\text{EW}}(\mu) = \frac{K_q(\mu)}{K_\ell} = 1 + \frac{Q_\ell \alpha}{4\pi} \left[3Q_u \left(\ln \frac{\mu^2}{m_Z^2} + \frac{11}{2} \right) + (Q_b + Q_u) \left(1 + \frac{\kappa}{4} \right) \right] + \mathcal{O}(\alpha^2), \quad (2.4)$$

which reproduces the well-known result of [79] up to scheme-dependent constant terms.

Throughout this paper we work in the naive dimensional regularization scheme with anti-commuting γ_5 , in which the vector and axial-vector currents obey analogous matching relations and hence the chirality of the states is preserved. The parameter κ is introduced to encode the scheme choice when extending four-dimensional Dirac reductions to $d = 4 - 2\epsilon$ dimensions, using the identity

$$\gamma_\mu \gamma_\nu \gamma_\rho P_L \otimes \gamma^\mu \gamma^\nu \gamma^\rho P_L = (16 + \kappa \epsilon) \gamma_\mu P_L \otimes \gamma^\mu P_L. \quad (2.5)$$

As we will show in Section 3.3, this parameter cancels out in the matching of the LEFT onto SCET-1.

The scale dependence of $K_{\text{EW}}(\mu)$ is governed by the RG equation

$$\frac{dK_{\text{EW}}(\mu)}{d \ln \mu} = \gamma_{\text{EW}} K_{\text{EW}}(\mu) \quad \text{with} \quad \gamma_{\text{EW}} = 3Q_\ell Q_u \frac{\alpha}{2\pi} + \mathcal{O}(\alpha^2), \quad (2.6)$$

whose solution can be written as

$$K_{\text{EW}}(\mu) = U_{\text{EW}}(\mu, m_Z) K_{\text{EW}}(m_Z). \quad (2.7)$$

For $m_b < \mu < m_Z$, the evolution function takes the simple form

$$U_{\text{EW}}(\mu, m_Z) = \left(\frac{\alpha(m_Z)}{\alpha(\mu)} \right)^{\gamma_0^{\text{EW}}/2\beta_0^{\text{QED}}} = \left(\frac{\alpha(m_Z)}{\alpha(\mu)} \right)^{\frac{9}{40}}, \quad (2.8)$$

where $\gamma_0^{\text{EW}} = 6Q_\ell Q_u$ and $\beta_0^{\text{QED}} = -\frac{4}{3} \sum_f N_c^f Q_f^2$ are the one-loop coefficients of the anomalous dimension of K_{EW} and the QED β -function, respectively, where the sum includes all electrically charged fermions except the top quark. Here and in the following, we use the conventions

$$\gamma(\alpha) = \sum_{n=0}^{\infty} \gamma_n \left(\frac{\alpha}{4\pi} \right)^{n+1}, \quad \beta(\alpha) = -2\alpha \sum_{n=0}^{\infty} \beta_n \left(\frac{\alpha}{4\pi} \right)^{n+1}. \quad (2.9)$$

Given the values of the QED running coupling at the scales of relevance to our analysis, namely $\alpha^{-1}(m_Z) \simeq 127.9$, $\alpha^{-1}(m_B) \simeq 132.0$ and $\alpha^{-1}(\mu_0) \simeq 133.6$, it is sufficient for our purposes to include the running of α between the weak scale m_Z and the hard scale m_B , while treating the coupling as fixed in the low-energy theory. For $\mu < m_B$ we therefore approximate the evolution factor as

$$U_{\text{EW}}(\mu, m_Z) = \left(\frac{\alpha(m_Z)}{\alpha(m_B)} \right)^{\frac{9}{40}} \left[1 + 3Q_\ell Q_u \frac{\alpha(\mu_0)}{4\pi} \ln \frac{\mu^2}{m_B^2} \right]. \quad (2.10)$$

3 Matching to Soft-Collinear Effective Theory

At the scale $\mu_h \sim m_B$ we match the LEFT onto SCET, which is the appropriate effective theory describing B -meson decays into light particles [67–70]. These light particles can either be soft, with energies of order the QCD scale, or carry large energies scaling with the B -meson mass. In the following discussion we focus on the SM, in which the decay $B^- \rightarrow \ell^- \bar{\nu}_\ell$ is mediated solely by the operator proportional to $L_\ell^{V,LL}$ in (2.1),

$$\mathcal{O}_\ell^{V,LL} = (\bar{u} \gamma_\mu P_L b) (\bar{\ell} \gamma^\mu P_L \nu_\ell), \quad (3.1)$$

and both the u -quark and the neutrino are described by left-handed fields. As mentioned in the introduction, the matching onto SCET is performed in two steps [80–82]:

1. At the hard scale $\mu_h \sim m_B$, modes with momenta of order m_B are integrated out and the theory is matched onto SCET-1, an effective theory containing soft and hard-collinear particles. The latter have virtualities of order $p_{hc}^2 \sim m_B \Lambda_{\text{QCD}}$, which is parametrically higher than the QCD scale and the charged-lepton mass (for $\ell = \mu, e$). The Wilson coefficients arising in this first matching step are the hard functions H_i , and they can depend on all scales of order m_B .
2. After the effective theory SCET-1 has been evolved down to the hard-collinear scale $\mu_{hc} \sim \sqrt{m_B \Lambda_{\text{QCD}}}$ (sometimes referred to as the “jet” scale), the hard-collinear modes are integrated out and one matches to the final effective theory SCET-2 containing soft and collinear particles. The Wilson coefficients arising in this second matching step are the jet functions J_i . The low-energy matrix elements remaining in SCET-2 capture all long-distance hadronic dynamics in the decay process as well as the dependence on the charged-lepton mass.

In our discussion, we will closely follow the detailed treatments of the two-step matching procedure presented in [81, 82]. The power counting in the two versions of SCET is controlled by the small parameters λ and λ_ℓ defined in (1.3), where $\ell = \mu$ or e , so that λ_ℓ is at most of order λ . Without loss of generality we work in the B -meson rest frame, where the 4-velocity v^μ of the B meson (with $v^2 = 1$) is chosen as $v^\mu = (1, \mathbf{0})$. In SCET it is convenient to define two light-like reference vectors n^μ and \bar{n}^μ , with $n^2 = \bar{n}^2 = 0$ and $n \cdot \bar{n} = 2$, which, up to power corrections, are aligned with the momenta of the charged lepton (p_ℓ) and anti-neutrino ($p_{\bar{\nu}_\ell}$), respectively. Any 4-vector can be decomposed in the light-cone basis spanned by n and \bar{n} , such that

$$p^\mu = (n \cdot p) \frac{\bar{n}^\mu}{2} + (\bar{n} \cdot p) \frac{n^\mu}{2} + p_\perp^\mu \equiv p_+^\mu + p_-^\mu + p_\perp^\mu. \quad (3.2)$$

In our reference frame, it follows that $v_\perp = p_{\ell\perp} = p_{\bar{\nu}_\ell\perp} = 0$ and $(n \cdot v)(\bar{n} \cdot v) = 1$. One often chooses the reference vectors such that $n \cdot v = \bar{n} \cdot v = 1$, but we will refrain from making this choice. All operators and Wilson coefficients in SCET must be invariant under the reparameterization transformation [83, 84]

$$n^\mu \rightarrow \zeta n^\mu, \quad \bar{n}^\mu \rightarrow \zeta^{-1} \bar{n}^\mu, \quad (3.3)$$

with $\zeta = \mathcal{O}(1)$, which is a consequence of the fact that the effective theory must be independent of the choice of the reference vectors n and \bar{n} , as long as $n^2 = \bar{n}^2 = 0$ and $n \cdot \bar{n} = 2$. This invariance enforces important constraints on the form of the operators.

Below the weak scale the neutrino is effectively a sterile particle, which does not interact and does not propagate in any loop diagram. Therefore, it is possible to choose an operator basis where the neutrino momentum does not appear as a hard scale. The relevant hard scales are then given by

$$m_b, \quad \frac{\bar{n} \cdot p_\ell}{\bar{n} \cdot v} = m_B, \quad 2v \cdot p_\ell = \frac{m_B^2 + m_\ell^2}{m_B} = \frac{\bar{n} \cdot p_\ell}{\bar{n} \cdot v} + \mathcal{O}(\lambda_\ell^2), \quad (3.4)$$

which are all of similar magnitude.

For a detailed discussion of the effective Lagrangian of SCET-1, including the leading power corrections, we refer the reader to the founding papers [67–70] (see [85] for a review). A brief summary can be found in Appendix A.

3.1 Ingredients of SCET-1

The effective field theory SCET-1 describes physics at or below the hard scale μ_h . It contains interacting hard-collinear (hc) and soft (s) particles, which differ in the scalings of their momenta. Using the decomposition (3.2), and collecting the components in a tuple $(p_+^\mu, p_-^\mu, p_\perp^\mu)$ with well-defined scaling properties, hard-collinear and soft momenta scale as

$$p_{hc}^\mu \sim m_B (\lambda, 1, \lambda^{\frac{1}{2}}), \quad p_s^\mu \sim m_B (\lambda, \lambda, \lambda). \quad (3.5)$$

From here on we will drop the hard scale m_B in such relations.

We will express the relevant SCET-1 operators in terms of so-called hard-collinear building blocks, which are invariant under hard-collinear gauge transformations and transform covariantly under soft gauge transformations [69, 86]. The corresponding effective fermion and gauge-boson fields have scalings

$$\begin{aligned} \mathcal{X}_{hc} &\sim \lambda^{\frac{1}{2}}, & \mathcal{A}_{hc}^\mu &\sim (\lambda, 1, \lambda^{\frac{1}{2}}), \\ u_s, b_v &\sim \lambda^{\frac{3}{2}}, & A_s^\mu &\sim (\lambda, \lambda, \lambda). \end{aligned} \quad (3.6)$$

Here u_s is the ordinary QCD spinor field for a massless up-quark, and b_v is the effective b -quark field in HQET [64, 66], defined as

$$b_v(x) = e^{im_b v \cdot x} \frac{1 + \not{v}}{2} b(x), \quad (3.7)$$

where $b(x)$ denotes the b -quark field in full QCD. In our kinematics, the Fourier components of the soft fields b_v and u_s are restricted to carry soft momenta. The hard-collinear building block for the charged lepton is defined as

$$\mathcal{X}_{hc}^{(\ell)}(x) = \frac{\not{v} \not{\bar{v}}}{4} W_{hc}^{(\ell)\dagger}(x) \psi_{hc}^{(\ell)}(x), \quad (3.8)$$

where the hard-collinear Wilson line

$$W_{hc}^{(\ell)}(x) = \exp \left[i Q_\ell e \int_{-\infty}^0 ds \bar{n} \cdot A_{hc}(x + s\bar{n}) \right] \quad (3.9)$$

contains the photon field with charge $Q_\ell = -1$, and $\psi_{hc}^{(\ell)}(x)$ denotes the field for the charged lepton with its Fourier components restricted to the region of hard-collinear momenta. In the construction of the SCET-1 operator basis we also need a hard-collinear field for the light spectator quark in the B meson (an up-quark in the present case), which is defined in an analogous way. In this case, the hard-collinear Wilson line contains both gluon and photon fields, i.e.

$$W_{hc}^{(u)}(x) = \exp \left[i Q_u e \int_{-\infty}^0 ds \bar{n} \cdot A_{hc}(x + s\bar{n}) \right] \mathbf{P} \exp \left[i g_s t^a \int_{-\infty}^0 ds \bar{n} \cdot G_{hc}^a(x + s\bar{n}) \right]. \quad (3.10)$$

The hard-collinear gauge fields can also appear in isolated form. The corresponding building blocks for the hard-collinear gluon and photon fields are defined as [69, 86]

$$\begin{aligned} \mathcal{G}_{hc}^\mu(x) &= W_{hc}^\dagger(x) [i D^\mu W_{hc}(x)] = g_s \int_{-\infty}^0 ds \bar{n}_\alpha [W_{hc}^\dagger G_{hc}^{\alpha\mu} W_{hc}](x + s\bar{n}) \equiv t^a \mathcal{G}_{hc}^{\mu,a}(x), \\ \mathcal{A}_{hc}^{(\ell)\mu}(x) &= W_{hc}^{(\ell)\dagger}(x) [i D^\mu W_{hc}^{(\ell)}(x)] = Q_\ell e \int_{-\infty}^0 ds \bar{n}_\alpha F_{hc}^{\alpha\mu}(x + s\bar{n}) \equiv Q_\ell \mathcal{A}_{hc}^\mu(x), \end{aligned} \quad (3.11)$$

where W_{hc} without a superscript denotes the hard-collinear Wilson line including the gluon field only. It follows from these definitions that the hard-collinear fields are subject to the constraints

$$\not{n} \mathcal{X}_{hc}^{(\ell)} = \not{n} \mathcal{X}_{hc}^{(u)} = 0, \quad \bar{n} \cdot \mathcal{G}_{hc} = \bar{n} \cdot \mathcal{A}_{hc} = 0, \quad (3.12)$$

while the effective heavy-quark field satisfies $\not{v} b_v = b_v$. The scalings of the fields indicated in (3.6) can be derived from the scaling of the corresponding propagators. The spinor field $\nu_{\bar{c}}$ for the neutrino is non-interacting and satisfies $\not{n} \nu_{\bar{c}} = 0$ with our choice of reference frame. It is not necessary to assign a power counting to this field.

The effective Lagrangian of SCET-1 has the generic form

$$\mathcal{L}_{\text{eff}}^{\text{SCET-1}} = \mathcal{L}_{hc} + \mathcal{L}_s + \mathcal{L}_{\text{HQET}} + \mathcal{L}_{hc+s}. \quad (3.13)$$

The first term on the right-hand side is known in exact form, while the soft Lagrangian is given by the ordinary QCD Lagrangian for the soft quark and the HQET Lagrangian for the heavy quark, where the latter contains an infinite series of operators in a $1/m_b$ expansion. The interaction terms connecting the hard-collinear sector to the soft sector can be systematically expanded in powers of λ .

When a LEFT operator is matched onto SCET-1, the hard-collinear fields in the effective theory can be smeared out along the light-like direction \bar{n} , because the corresponding momentum components $\bar{n} \cdot p_{hc}$ are $\mathcal{O}(1)$ in power counting. A generic term in the SCET-1 effective Lagrangian for our problem is thus of the form

$$\mathcal{L}_{\text{eff}}^{\text{SCET-1}} \ni \int dt_1 \dots \int dt_n \tilde{H}(m_b, t_1, \dots, t_n, \mu) \phi_{hc}^{(1)}(x + t_1 \bar{n}) \dots \phi_{hc}^{(n)}(x + t_n \bar{n}) \prod_j \Phi_j(x), \quad (3.14)$$

where Φ_j represent the soft fields, and \tilde{H} is the hard matching coefficient. Using translational invariance, we have

$$\phi_{hc}^{(i)}(x + t_i \bar{n}) = e^{t_i \bar{n} \cdot \partial_x} \phi_{hc}^{(i)}(x) \equiv e^{i t_i \bar{n} \cdot \mathcal{P}_{hc}^{(i)}} \phi_{hc}^{(i)}(x), \quad (3.15)$$

where the label operator $\bar{n} \cdot \mathcal{P}_{hc}^{(i)}$ projects out the large momentum component $\bar{n} \cdot p_i$ of the i^{th} hard-collinear particle. We then obtain

$$\mathcal{L}_{\text{eff}}^{\text{SCET-1}} \ni H(m_b, \bar{n} \cdot \mathcal{P}_{hc}^{(1)}, \dots, \bar{n} \cdot \mathcal{P}_{hc}^{(n)}, \mu) \phi_{hc}^{(1)}(x) \dots \phi_{hc}^{(n)}(x) \prod_j \Phi_j(x), \quad (3.16)$$

where we have introduced the Fourier-transformed hard matching coefficient

$$H(m_b, \bar{n} \cdot \mathcal{P}_{hc}^{(1)}, \dots, \bar{n} \cdot \mathcal{P}_{hc}^{(n)}, \mu) = \int dt_1 e^{i t_1 \bar{n} \cdot \mathcal{P}_{hc}^{(1)}} \dots \int dt_n e^{i t_n \bar{n} \cdot \mathcal{P}_{hc}^{(n)}} \tilde{H}(m_b, t_1, \dots, t_n, \mu). \quad (3.17)$$

If a SCET-1 operator contains $n > 1$ hard-collinear fields, these fields share the large component of the total hard-collinear momentum, given by $\bar{n} \cdot p_\ell$ in our case. Since the large components of hard-collinear momenta are always positive, we can assign variables $y_i \in [0, 1]$ with $i = 1, \dots, n$ to the fields, which specify the fraction of the total large moment carried by the individual fields. Specifically, we define [87]

$$\phi_{hc[y_i]}^{(i)}(x) = \delta\left(y_i - \frac{\bar{n} \cdot \mathcal{P}_{hc}^{(i)}}{\bar{n} \cdot \mathcal{P}_{hc}}\right) \phi_{hc}^{(i)}(x), \quad (3.18)$$

where the label operator $\bar{n} \cdot \mathcal{P}_{hc}$ projects out the large component of the total hard-collinear momentum carried by an operator. We write the Wilson coefficients as functions of $\bar{n} \cdot \mathcal{P}_{hc}$ and the variables $\{y_i\}$, and in the effective Lagrangian one must integrate over these variables. The condition $\sum_{i=1}^n \bar{n} \cdot \mathcal{P}_{hc}^{(i)} = \bar{n} \cdot \mathcal{P}_{hc}$ implies that one of these integrations is trivial, since the last δ -distribution can be rewritten as

$$\delta\left(y_n - \frac{\bar{n} \cdot \mathcal{P}_{hc}^{(n)}}{\bar{n} \cdot \mathcal{P}_{hc}}\right) = \delta\left(\sum_{i=1}^n y_i - 1\right). \quad (3.19)$$

This leaves us with the final form (for $n > 1$)

$$\begin{aligned} \mathcal{L}_{\text{eff}}^{\text{SCET-1}} \ni & \int_0^1 dy_1 \dots \int_0^1 dy_{n-1} \theta\left(1 - \sum_{i=1}^{n-1} y_i\right) H(m_b, \bar{n} \cdot \mathcal{P}_{hc}, y_1, \dots, y_{n-1}, \mu) \\ & \times \phi_{hc[y_1]}^{(1)}(x) \dots \phi_{hc[y_{n-1}]}^{(n-1)}(x) \phi_{hc}^{(n)}(x) \prod_j \Phi_j(x). \end{aligned} \quad (3.20)$$

Reparameterization invariance requires that, besides the scaling variables y_i , the hard functions can depend on the hard scales m_b and $\bar{n} \cdot \mathcal{P}_{hc}/\bar{n} \cdot v$.

The Dirac basis can be spanned by the 16 matrices

$$1, \gamma_5, \gamma_\perp^\mu, \gamma_\perp^\mu \gamma_5, \not{v}, \not{v} \gamma_5, \not{v} \gamma_\perp^\mu, \not{v}, \not{v} \gamma_5, \not{v} \gamma_\perp^\mu, \not{v} \not{v}, [\gamma_\perp^\mu, \gamma_\perp^\nu], \quad (3.21)$$

where the transverse Lorentz indices can take two distinct values. We will express all SCET operators in terms of fermion fields with definite chirality, and hence there is no need to write out factors of γ_5 . Lorentz invariance requires that all open transverse Lorentz indices in the SCET operators must be contracted using the symbols (we use the convention $\epsilon^{0123} = -1$)

$$g_{\perp}^{\mu\nu} = g^{\mu\nu} - \frac{n^{\mu}\bar{n}^{\nu} + \bar{n}^{\mu}n^{\nu}}{2}, \quad \epsilon_{\perp}^{\mu\nu} = \frac{1}{2}\epsilon^{\mu\nu\alpha\beta}\bar{n}_{\alpha}n_{\beta}. \quad (3.22)$$

For $n^{\mu} = (1, 0, 0, 1)$ and $\bar{n}^{\mu} = (1, 0, 0, -1)$ these definitions imply $g_{\perp}^{11} = g_{\perp}^{22} = -1$ and $\epsilon_{\perp}^{12} = -\epsilon_{\perp}^{21} = 1$, and all other entries vanish. When $\epsilon_{\perp}^{\mu\nu}$ is contracted with a Dirac matrix next to a hard-collinear or anti-hard-collinear spinor, it can be traded for $g_{\perp}^{\mu\nu}$ using the relations [88]

$$\begin{aligned} \not{n} i\epsilon_{\perp}^{\mu\nu}\gamma_{\perp\nu} &= -\not{n} g_{\perp}^{\mu\nu}\gamma_{\perp\nu}\gamma_5 = -\not{n}\gamma_{\perp}^{\mu}\gamma_5, \\ i\epsilon_{\perp}^{\mu\nu}\gamma_{\perp\nu}\not{\bar{n}} &= -g_{\perp}^{\mu\nu}\gamma_{\perp\nu}\gamma_5\not{\bar{n}} = -\gamma_{\perp}^{\mu}\gamma_5\not{\bar{n}}, \end{aligned} \quad (3.23)$$

which hold in four spacetime dimensions. As an important corollary of these relations, we note the remarkable identities

$$\begin{aligned} \not{n}\gamma_{\perp}^{\mu}P_{L,R} \otimes \not{n}\gamma_{\perp\mu}P_{L,R} &= 0, \\ \not{\bar{n}}\gamma_{\perp}^{\mu}P_{L,R} \otimes \not{\bar{n}}\gamma_{\perp\mu}P_{L,R} &= 0, \\ \not{n}\gamma_{\perp}^{\mu}P_{L,R} \otimes \not{\bar{n}}\gamma_{\perp\mu}P_{R,L} &= 0, \end{aligned} \quad (3.24)$$

which can be used to eliminate several operators from the basis. In our analysis, we will employ a projection scheme in which these relations are maintained even in $d = 4 - 2\epsilon$ spacetime dimensions (see Section 3.3). Note also that there is no need to allow for the commutator $[\gamma_{\perp}^{\mu}, \gamma_{\perp}^{\nu}]$ next to a hard-collinear or anti-collinear spinor, because the identities [88]

$$\not{n}[\gamma_{\perp}^{\mu}, \gamma_{\perp}^{\nu}] = \not{n}2i\epsilon_{\perp}^{\mu\nu}\gamma_5, \quad [\gamma_{\perp}^{\mu}, \gamma_{\perp}^{\nu}]\not{\bar{n}} = 2i\epsilon_{\perp}^{\mu\nu}\gamma_5\not{\bar{n}} \quad (3.25)$$

can be used to eliminate these structures.

We now lay out the construction of the SCET-1 operator basis needed to describe the decay $B^- \rightarrow \ell^- \bar{\nu}_{\ell}$, working at leading non-trivial order in the expansion parameters $\lambda \sim \Lambda_{\text{QCD}}/m_B$ and $\lambda_{\ell} \sim m_{\ell}/m_B$. (For most of the discussion we have in mind the process $B^- \rightarrow \mu^- \bar{\nu}_{\mu}$, for which it seems reasonable to adopt a power counting where $m_{\ell} = m_{\mu} \sim \Lambda_{\text{QCD}}$, but our analysis does not rely on this counting.) We will show that the problem at hand is intrinsically a SCET factorization problem at next-to-leading power, and therefore the discussion will be rather technical.

3.2 Construction of the SCET-1 operator basis

The lepton current in SCET-1 must be of the form (modulo additional gauge fields or derivatives, see below)

$$\bar{\chi}_{hc}^{(\ell)} \Gamma \nu_{\bar{\ell}}, \quad (3.26)$$

where the Dirac basis is spanned by $\Gamma \in \{1, \gamma_{\perp}^{\alpha}\}$. For the case where $\Gamma = 1$ the charged lepton is right-handed, and the chirality flip introduces a factor $m_{\ell} \sim \lambda_{\ell}$, which we include

in the definition of the operators. This factor must be compensated by a hard scale in the denominator. In SCET-1, the spectator quark in the B meson is described either by a soft field or a hard-collinear field. In the latter case, the large momentum carried by the field needs to be transferred to the charged lepton via the exchange of a hard-collinear photon (in the matching onto SCET-2) or a collinear photon (in the evaluation of the SCET-2 matrix elements), and a soft spectator quark remains.

The simplest operator one can write down in SCET-1 is

$$O_0^A = (\bar{u}_s \gamma_\perp^\alpha P_L b_v) (\bar{\chi}_{hc}^{(\ell)} \gamma_\alpha^\perp P_L \nu_{\bar{c}}) \sim \lambda^{\frac{7}{2}}, \quad (3.27)$$

where for simplicity we count the sterile neutrino field as $\mathcal{O}(\lambda^0)$. The analogous operator in which the soft quark field is replaced by a hard-collinear field vanishes due to the first identity in (3.24). Converting the hard-collinear lepton field into a collinear one in SCET-2 costs a factor $\lambda_\ell/\lambda^{\frac{1}{2}}$, and hence O_0^A matches onto a SCET-2 operator scaling as $\sim \lambda_\ell \lambda^3$. This operator can mediate the decay $B^{*-} \rightarrow \ell^- \bar{\nu}_\ell$ with an amplitude of $\mathcal{O}(\lambda^{\frac{3}{2}})$, corresponding to the scaling of the decay constant of the B^* meson.³ However, it has a vanishing projection onto the B -meson state and thus does not contribute to the $B^- \rightarrow \ell^- \bar{\nu}_\ell$ decay amplitude, the leading contributions to which arise from SCET-2 operators with scaling $\sim \lambda_\ell^2 \lambda^3$. This observation shows that our process of interest requires the construction of a SCET-1 operator basis beyond the leading power, which as we will see is a rather challenging task.

Concretely, our task is to find all relevant SCET-1 operators which can match onto $\mathcal{O}(\lambda_\ell^2 \lambda^3)$ operators in SCET-2. If these operators do not include the lepton mass explicitly, they must contain additional hard-collinear fields or derivatives, so that a factor of m_ℓ can be produced either in the matching onto SCET-2, when hard-collinear loop graphs are evaluated, or in the calculation of collinear matrix elements in SCET-2. In deriving the structure of the relevant operators, one needs to understand the systematics of the matching onto SCET-2, which will be discussed in detail in Section 4. These considerations lead to the following four simple rules:

1. For $\ell = \mu, e$ the lepton mass is a power-suppressed parameter in SCET-1, and a mass insertion costs a factor $\lambda_\ell/\lambda^{\frac{1}{2}}$.
2. The conversion of a hard-collinear into a soft quark field costs a factor $\lambda^{\frac{1}{2}}$.
3. The conversion of a hard-collinear into a collinear lepton field costs a factor $\lambda_\ell/\lambda^{\frac{1}{2}}$. The same is true for the conversion of a hard-collinear gauge field into a collinear gauge field.
4. The conversion of a soft into a collinear lepton field costs a factor λ_ℓ . Obtaining a mass term from a soft lepton propagator costs another factor λ_ℓ/λ .

The first rule implies that operators not containing the lepton mass can have one additional “transverse object” (either a transversely polarized gauge field or a transverse derivative) compared with the corresponding operators containing a factor of m_ℓ . Since a soft quark field has power counting $\lambda^{\frac{3}{2}}$ and a hard-collinear quark field has power counting $\lambda^{\frac{1}{2}}$, the second rule

³The external B -meson and lepton states in SCET-2 “eat up” factors of $\lambda^{-\frac{3}{2}}$ and λ_ℓ^{-1} , respectively.

further implies that operators with a hard-collinear quark field may contain one additional transverse object compared to operators with a soft quark field. Operators with a hard-collinear quark field and no factor of m_ℓ can therefore contain up to two additional transverse objects. The second and the fourth rule imply that operators containing a soft lepton field along with a hard-collinear quark field must at most be of $\mathcal{O}(\lambda^{\frac{7}{2}})$ in power counting and hence cannot contain any additional fields or derivatives. It follows from these observations that we can distinguish six different classes of operators:

Type-A operators containing a hc lepton field:

$$\begin{aligned}
O_1^A &= \frac{m_\ell}{\bar{n} \cdot \mathcal{P}_{hc}} (\bar{u}_s \not{\bar{n}} P_L b_v) (\bar{\mathcal{X}}_{hc}^{(\ell)} P_L \nu_{\bar{c}}) && \sim \lambda_\ell \lambda^{\frac{7}{2}} \\
O_2^A &= \frac{m_\ell (\bar{n} \cdot v)^2}{\bar{n} \cdot \mathcal{P}_{hc}} (\bar{u}_s \not{\bar{n}} P_L b_v) (\bar{\mathcal{X}}_{hc}^{(\ell)} P_L \nu_{\bar{c}}) && \sim \lambda_\ell \lambda^{\frac{7}{2}} \\
O_3^A &= \frac{1}{\bar{n} \cdot \mathcal{P}_{hc}} (\bar{u}_s \not{\bar{n}} P_L b_v) [\bar{\mathcal{X}}_{hc}^{(\ell)} (-i \overleftarrow{\not{\partial}}_\perp) P_L \nu_{\bar{c}}] && \sim \lambda^4 \\
O_4^A &= \frac{(\bar{n} \cdot v)^2}{\bar{n} \cdot \mathcal{P}_{hc}} (\bar{u}_s \not{\bar{n}} P_L b_v) [\bar{\mathcal{X}}_{hc}^{(\ell)} (-i \overleftarrow{\not{\partial}}_\perp) P_L \nu_{\bar{c}}] && \sim \lambda^4
\end{aligned} \tag{3.28}$$

Type-B operators containing a hc lepton field and a hc gauge field:

$$\begin{aligned}
O_1^B &= \frac{1}{\bar{n} \cdot \mathcal{P}_{hc}} (\bar{u}_s \not{\bar{n}} P_L b_v) (\bar{\mathcal{X}}_{hc}^{(\ell)} \mathcal{A}_{hc[y]}^\perp P_L \nu_{\bar{c}}) && \sim \lambda^4 \\
O_2^B &= \frac{(\bar{n} \cdot v)^2}{\bar{n} \cdot \mathcal{P}_{hc}} (\bar{u}_s \not{\bar{n}} P_L b_v) (\bar{\mathcal{X}}_{hc}^{(\ell)} \mathcal{A}_{hc[y]}^\perp P_L \nu_{\bar{c}}) && \sim \lambda^4 \\
O_3^B &= \frac{1}{\bar{n} \cdot \mathcal{P}_{hc}} (\bar{u}_s \not{\bar{n}} P_L \mathcal{G}_{hc[y]}^{\perp\alpha} b_v) (\bar{\mathcal{X}}_{hc}^{(\ell)} \gamma_\alpha^\perp P_L \nu_{\bar{c}}) && \sim \lambda^4 \\
O_4^B &= \frac{(\bar{n} \cdot v)^2}{\bar{n} \cdot \mathcal{P}_{hc}} (\bar{u}_s \not{\bar{n}} P_L \mathcal{G}_{hc[y]}^{\perp\alpha} b_v) (\bar{\mathcal{X}}_{hc}^{(\ell)} \gamma_\alpha^\perp P_L \nu_{\bar{c}}) && \sim \lambda^4
\end{aligned} \tag{3.29}$$

Type-C operators containing a hc lepton field and a hc quark field:

$$\begin{aligned}
O_1^C &= \frac{m_\ell}{\bar{n} \cdot \mathcal{P}_{hc}} (\bar{\mathcal{X}}_{hc[y]}^{(u)} \not{\bar{n}} P_L b_v) (\bar{\mathcal{X}}_{hc}^{(\ell)} P_L \nu_{\bar{c}}) && \sim \lambda_\ell \lambda^{\frac{5}{2}} \\
O_2^C &= \frac{m_\ell \bar{n} \cdot v}{(\bar{n} \cdot \mathcal{P}_{hc})^2} [\bar{\mathcal{X}}_{hc[y]}^{(u)} (-i \overleftarrow{\not{\partial}}_\perp) \not{\bar{n}} P_R b_v] (\bar{\mathcal{X}}_{hc}^{(\ell)} P_L \nu_{\bar{c}}) && \sim \lambda_\ell \lambda^3 \\
O_3^C &= \frac{1}{\bar{n} \cdot \mathcal{P}_{hc}} [\bar{\mathcal{X}}_{hc[y]}^{(u)} (-i \overleftarrow{D}_{s\perp}^\alpha) \not{\bar{n}} P_L b_v] (\bar{\mathcal{X}}_{hc}^{(\ell)} \gamma_\alpha^\perp P_L \nu_{\bar{c}}) && \sim \lambda^3, \lambda^{\frac{7}{2}} \\
O_4^C &= \frac{1}{\bar{n} \cdot \mathcal{P}_{hc}} (\bar{\mathcal{X}}_{hc[y]}^{(u)} \not{\bar{n}} P_L b_v) [\bar{\mathcal{X}}_{hc}^{(\ell)} (-i \overleftarrow{\not{D}}_{s\perp}) P_L \nu_{\bar{c}}] && \sim \lambda^3, \lambda^{\frac{7}{2}} \\
O_5^C &= \frac{\bar{n} \cdot v}{(\bar{n} \cdot \mathcal{P}_{hc})^2} [\bar{\mathcal{X}}_{hc[y]}^{(u)} (-i \overleftarrow{\not{\partial}}_\perp) \not{\bar{n}} P_R b_v] [\bar{\mathcal{X}}_{hc}^{(\ell)} (-i \overleftarrow{\not{\partial}}_\perp) P_L \nu_{\bar{c}}] && \sim \lambda^{\frac{7}{2}}
\end{aligned} \tag{3.30}$$

Type- D operators containing three hc fields:

$$\begin{aligned}
O_1^D &= \frac{m_\ell \bar{n} \cdot v}{(\bar{n} \cdot \mathcal{P}_{hc})^2} (\bar{\mathcal{X}}_{hc[y_1]}^{(u)} \mathcal{A}_{hc[y_2]}^\perp \not{n} P_R b_v) (\bar{\mathcal{X}}_{hc}^{(\ell)} P_L \nu_{\bar{c}}) && \sim \lambda_\ell \lambda^3 \\
O_2^D &= \frac{m_\ell \bar{n} \cdot v}{(\bar{n} \cdot \mathcal{P}_{hc})^2} (\bar{\mathcal{X}}_{hc[y_1]}^{(u)} \mathcal{G}_{hc[y_2]}^\perp \not{n} P_R b_v) (\bar{\mathcal{X}}_{hc}^{(\ell)} P_L \nu_{\bar{c}}) && \sim \lambda_\ell \lambda^3 \\
O_3^D &= \frac{1}{\bar{n} \cdot \mathcal{P}_{hc}} (\bar{\mathcal{X}}_{hc[y_1]}^{(u)} \not{n} P_L b_v) (\bar{\mathcal{X}}_{hc}^{(\ell)} \mathcal{A}_{hc[y_2]}^\perp P_L \nu_{\bar{c}}) && \sim \lambda^3 \\
O_4^D &= \frac{1}{\bar{n} \cdot \mathcal{P}_{hc}} (\bar{\mathcal{X}}_{hc[y_1]}^{(u)} \mathcal{G}_{hc[y_2]}^{\perp\alpha} \not{n} P_L b_v) (\bar{\mathcal{X}}_{hc}^{(\ell)} \gamma_\alpha^\perp P_L \nu_{\bar{c}}) && \sim \lambda^3 \\
O_5^D &= \frac{\bar{n} \cdot v}{(\bar{n} \cdot \mathcal{P}_{hc})^2} [\bar{\mathcal{X}}_{hc[y_1]}^{(u)} (-i \overleftarrow{\not{\partial}}_\perp) \not{n} P_R b_v] (\bar{\mathcal{X}}_{hc}^{(\ell)} \mathcal{A}_{hc[y_2]}^\perp P_L \nu_{\bar{c}}) && \sim \lambda^{\frac{7}{2}} \\
O_6^D &= \frac{\bar{n} \cdot v}{(\bar{n} \cdot \mathcal{P}_{hc})^2} [\bar{\mathcal{X}}_{hc[y_1]}^{(u)} (-i \overleftarrow{\not{\partial}}_\perp) \mathcal{G}_{hc[y_2]}^{\perp\alpha} \not{n} P_R b_v] (\bar{\mathcal{X}}_{hc}^{(\ell)} \gamma_\alpha^\perp P_L \nu_{\bar{c}}) && \sim \lambda^{\frac{7}{2}} \\
O_7^D &= \frac{\bar{n} \cdot v}{(\bar{n} \cdot \mathcal{P}_{hc})^2} (\bar{\mathcal{X}}_{hc[y_1]}^{(u)} \mathcal{A}_{hc[y_2]}^\perp \not{n} P_R b_v) [\bar{\mathcal{X}}_{hc}^{(\ell)} (-i \overleftarrow{\not{\partial}}_\perp) P_L \nu_{\bar{c}}] && \sim \lambda^{\frac{7}{2}} \\
O_8^D &= \frac{\bar{n} \cdot v}{(\bar{n} \cdot \mathcal{P}_{hc})^2} (\bar{\mathcal{X}}_{hc[y_1]}^{(u)} \mathcal{G}_{hc[y_2]}^\perp \not{n} P_R b_v) [\bar{\mathcal{X}}_{hc}^{(\ell)} (-i \overleftarrow{\not{\partial}}_\perp) P_L \nu_{\bar{c}}] && \sim \lambda^{\frac{7}{2}}
\end{aligned} \tag{3.31}$$

Type- E operators containing four hc fields:

$$\begin{aligned}
O_1^E &= \frac{\bar{n} \cdot v}{(\bar{n} \cdot \mathcal{P}_{hc})^2} (\bar{\mathcal{X}}_{hc[y_1]}^{(u)} \mathcal{A}_{hc[y_2]}^\perp \not{n} P_R b_v) (\bar{\mathcal{X}}_{hc}^{(\ell)} \mathcal{A}_{hc[y_3]}^\perp P_L \nu_{\bar{c}}) && \sim \lambda^{\frac{7}{2}} \\
O_2^E &= \frac{\bar{n} \cdot v}{(\bar{n} \cdot \mathcal{P}_{hc})^2} (\bar{\mathcal{X}}_{hc[y_1]}^{(u)} \mathcal{G}_{hc[y_2]}^\perp \not{n} P_R b_v) (\bar{\mathcal{X}}_{hc}^{(\ell)} \mathcal{A}_{hc[y_3]}^\perp P_L \nu_{\bar{c}}) && \sim \lambda^{\frac{7}{2}} \\
O_3^E &= \frac{\bar{n} \cdot v}{(\bar{n} \cdot \mathcal{P}_{hc})^2} (\bar{\mathcal{X}}_{hc[y_1]}^{(u)} \mathcal{G}_{hc[y_2]}^{\perp\alpha} \mathcal{G}_{hc[y_3]}^\perp \not{n} P_R b_v) (\bar{\mathcal{X}}_{hc}^{(\ell)} \gamma_\alpha^\perp P_L \nu_{\bar{c}}) && \sim \lambda^{\frac{7}{2}} \\
O_4^E &= \frac{\bar{n} \cdot v}{(\bar{n} \cdot \mathcal{P}_{hc})^2} (\bar{\mathcal{X}}_{hc[y_1]}^{(u)} \mathcal{G}_{hc[y_2]}^{\perp\alpha,a} \mathcal{G}_{hc[y_3]}^{\perp,a} \not{n} P_R b_v) (\bar{\mathcal{X}}_{hc}^{(\ell)} \gamma_\alpha^\perp P_L \nu_{\bar{c}}) && \sim \lambda^{\frac{7}{2}}
\end{aligned} \tag{3.32}$$

Type- F operator containing a soft lepton field:

$$O_1^F = (\bar{\mathcal{X}}_{hc}^{(u)} \not{n} P_L b_v) (\bar{\ell}_s \not{n} P_L \nu_{\bar{c}}) \sim \lambda^{\frac{7}{2}} \tag{3.33}$$

After renormalization, the charged-lepton mass appearing in the definition of some of the operators is defined as the running mass $m_\ell(\mu)$ in the $\overline{\text{MS}}$ scheme. It will later be converted into the physical pole mass (see Section 4.8).

The label operator $\bar{n} \cdot \mathcal{P}_{hc}$ projects out the large component of the total hard-collinear momentum carried by an operator, which in our case evaluates to $\bar{n} \cdot p_\ell$. As mentioned earlier, when an operator contains two or more hard-collinear fields, one needs to indicate how these fields share the large component of the total hard-collinear momentum. For type- B operators

we assign the momentum fraction y to the gauge field, which implies that the lepton field carries the momentum fraction $(1 - y)$. Similarly, for type- C operators we assign the momentum fraction y to the hard-collinear quark field. For type- D operators the large component of the total hard-collinear momentum is shared among three fields. We assign momentum the fractions y_1 and y_2 to the up-quark field and the gauge field, respectively, which implies that the charged lepton carries the momentum fraction $(1 - y_1 - y_2)$. For type- E operators, finally, the large component of the total hard-collinear momentum is shared among four fields as indicated, and the charged lepton carries momentum fraction $(1 - y_1 - y_2 - y_3)$.

After each operator, we give its power counting with the expansion parameters λ_ℓ and λ . Using the above rules, one finds that these operators match onto SCET-2 operators scaling (at least) as $\lambda_\ell^2 \lambda^3$ and thus potentially can give leading contributions to the $B^- \rightarrow \ell^- \bar{\nu}_\ell$ decay amplitude in the SM. There are five exceptions, namely

$$O_1^C, \quad O_3^C, \quad O_4^C, \quad O_3^D, \quad O_4^D, \quad (3.34)$$

which naively appear to give “super-leading” contributions scaling as $\lambda_\ell \lambda^{\frac{7}{2}}$ in SCET-2. However, for these operators an additional power-suppressed Lagrangian insertion of $\mathcal{O}(\lambda^{\frac{1}{2}})$ is needed to perform the matching onto SCET-2.

Some comments are in order concerning the construction of the operators in the different classes:

- Operators containing a transverse derivative acting on the (non-interacting) neutrino field can be omitted, since with our choice of reference frame $p_\nu^\perp = 0$.
- In general, Dirac structures in the quark and lepton bilinears involving γ_\perp^α matrices can be simplified using the identities (3.23) and (3.25). For all other operators containing a pair of contracted transverse Lorentz indices, relation (3.23) implies that contracting the two indices with $\epsilon_\perp^{\mu\nu}$ rather than $g_\perp^{\mu\nu}$ yields nothing new. This statement applies to all other operators with a pair of contracted transverse indices.
- There is no need to include type- A or type- B operators in which the quark current has the form $\bar{u}_s P_R b_v$. Using that $\not{v} b_v = b_v$, it is straightforward to show that (with $v^2 = n \cdot v \bar{n} \cdot v = 1$)

$$\bar{u}_s P_R b_v = \frac{n \cdot v}{2} \bar{u}_s \not{n} P_L b_v + \frac{\bar{n} \cdot v}{2} \bar{u}_s \not{\bar{n}} P_L b_v, \quad (3.35)$$

which implies that any such operator can be reduced to our basis operators.

- Several of the basis operators of type- C , D and E contain a transverse Dirac matrix in both the quark and the lepton current. The first relation in (3.24) implies that

$$(\bar{\mathcal{X}}_{hc}^{(u)} \gamma_\perp^\mu P_L \Gamma b_v) (\bar{\mathcal{X}}_{hc}^{(\ell)} \gamma_{\perp\mu} P_L \nu_{\bar{c}}) = 0, \quad (3.36)$$

where Γ can be an arbitrary Dirac structure. We will refer to this equality as the “magic identity”. Setting $\Gamma = \gamma_\perp^\alpha \gamma_\perp^\beta$, and using that in $d = 4$ spacetime dimensions

$$\gamma_\perp^\mu \gamma_\perp^\alpha \gamma_\perp^\beta = \gamma_\perp^\mu g_\perp^{\alpha\beta} + \gamma_\perp^\beta g_\perp^{\mu\alpha} - \gamma_\perp^\alpha g_\perp^{\mu\beta}, \quad (3.37)$$

we find the identity

$$(\bar{\mathcal{X}}_{hc}^{(u)} \gamma_{\perp}^{\alpha} P_L b_v) (\bar{\mathcal{X}}_{hc}^{(\ell)} \gamma_{\perp}^{\beta} P_L \nu_{\bar{c}}) = (\bar{\mathcal{X}}_{hc}^{(u)} \gamma_{\perp}^{\beta} P_L b_v) (\bar{\mathcal{X}}_{hc}^{(\ell)} \gamma_{\perp}^{\alpha} P_L \nu_{\bar{c}}). \quad (3.38)$$

- Operators containing two hard-collinear transverse objects with Lorentz indices α and β , i.e. O_5^C , $O_{5,6,7,8}^D$ and $O_{1,2,3,4}^E$, need to involve the Dirac structure

$$\gamma_{\perp}^{\alpha} P_L \otimes \gamma_{\perp}^{\beta} P_L. \quad (3.39)$$

If we contract this with $g_{\alpha\beta}^{\perp}$ or $\epsilon_{\alpha\beta}^{\perp}$, the result vanishes by the magic identity (3.36). Hence, each index must be contracted with one of the transverse objects. Relation (3.38) allows us to exchange the indices α and β in order to reduce the set of operators. Using this freedom, the operators

$$\begin{aligned} \frac{\bar{n} \cdot v}{(\bar{n} \cdot \mathcal{P}_{hc})^2} [\bar{\mathcal{X}}_{hc[y_1]}^{(u)} (-i \overleftarrow{\partial}_{\perp}^{\alpha}) \mathcal{A}_{hc[y_2]}^{\perp} \not{n} P_R b_v] (\bar{\mathcal{X}}_{hc}^{(\ell)} \gamma_{\alpha}^{\perp} P_L \nu_{\bar{c}}) &= O_5^D, \\ \frac{\bar{n} \cdot v}{(\bar{n} \cdot \mathcal{P}_{hc})^2} [\bar{\mathcal{X}}_{hc[y_1]}^{(u)} (-i \overleftarrow{\partial}_{\perp}^{\alpha}) \mathcal{G}_{hc[y_2]}^{\perp} \not{n} P_R b_v] (\bar{\mathcal{X}}_{hc}^{(\ell)} \gamma_{\alpha}^{\perp} P_L \nu_{\bar{c}}) &= O_6^D, \\ \frac{\bar{n} \cdot v}{(\bar{n} \cdot \mathcal{P}_{hc})^2} [\bar{\mathcal{X}}_{hc[y_1]}^{(u)} (i \not{\partial}_{\perp} \mathcal{A}_{hc[y_2]}^{\perp \alpha}) \not{n} P_R b_v] (\bar{\mathcal{X}}_{hc}^{(\ell)} \gamma_{\alpha}^{\perp} P_L \nu_{\bar{c}}) &= O_5^D + O_7^D + \mathcal{O}(\lambda^4), \\ \frac{\bar{n} \cdot v}{(\bar{n} \cdot \mathcal{P}_{hc})^2} [\bar{\mathcal{X}}_{hc[y_1]}^{(u)} (i \not{\partial}_{\perp} \mathcal{G}_{hc[y_2]}^{\perp \alpha}) \not{n} P_R b_v] (\bar{\mathcal{X}}_{hc}^{(\ell)} \gamma_{\alpha}^{\perp} P_L \nu_{\bar{c}}) &= O_6^D + O_8^D + \mathcal{O}(\lambda^4), \end{aligned} \quad (3.40)$$

as well as

$$\begin{aligned} \frac{\bar{n} \cdot v}{(\bar{n} \cdot \mathcal{P}_{hc})^2} (\bar{\mathcal{X}}_{hc[y_1]}^{(u)} \mathcal{A}_{hc[y_2]}^{\perp} \mathcal{G}_{hc[y_3]}^{\perp \alpha} \not{n} P_R b_v) (\bar{\mathcal{X}}_{hc}^{(\ell)} \gamma_{\alpha}^{\perp} P_L \nu_{\bar{c}}) &= O_2^E (y_2 \leftrightarrow y_3), \\ \frac{\bar{n} \cdot v}{(\bar{n} \cdot \mathcal{P}_{hc})^2} (\bar{\mathcal{X}}_{hc[y_1]}^{(u)} \mathcal{G}_{hc[y_2]}^{\perp} \mathcal{G}_{hc[y_3]}^{\perp \alpha} \not{n} P_R b_v) (\bar{\mathcal{X}}_{hc}^{(\ell)} \gamma_{\alpha}^{\perp} P_L \nu_{\bar{c}}) &= O_3^E \end{aligned} \quad (3.41)$$

can be removed from the basis. Moreover, it follows that

$$O_4^E = O_4^E (y_2 \leftrightarrow y_3), \quad (3.42)$$

implying that the coefficient H_4^E can be symmetrized in the variables y_2 and y_3 .

- The operators O_3^C and O_4^C , which involve the derivative $iD_{s\perp}^{\alpha} = i\partial_{\perp}^{\alpha} + g_s G_{s\perp}^{\alpha,a} t^a + Q_u e A_{s\perp}^{\alpha,a} t^a$ acting on the hard-collinear up-quark field, have inhomogeneous power counting, as indicated. As shown in [70, 89], it would be possible to rewrite them as sums of manifestly gauge-invariant operators with different (but homogeneous) power counting using field redefinitions. Here we keep the compact form in (3.30). An additional operator

$$\frac{1}{\bar{n} \cdot \mathcal{P}_{hc}} (\bar{\mathcal{X}}_{hc[y]}^{(u)} \not{n} P_L iD_{s\perp}^{\alpha} b_v) (\bar{\mathcal{X}}_{hc}^{(\ell)} \gamma_{\alpha}^{\perp} \nu_{\bar{c}}) = O_3^C + O_4^C \sim \lambda^{\frac{7}{2}} \quad (3.43)$$

can be reduced to O_3^C and O_4^C using an integration by parts (recall that we set the transverse momentum of the neutrino to be zero). The other possible single-derivative operator (recall that $iv \cdot D_s b_v = 0$ in HQET)

$$\frac{1}{\bar{n} \cdot \mathcal{P}_{hc}} (\bar{\mathcal{X}}_{hc[y]}^{(u)} \gamma_{\perp}^{\alpha} P_L i\bar{n} \cdot D_s b_v) (\bar{\mathcal{X}}_{hc}^{(\ell)} \gamma_{\alpha}^{\perp} \nu_{\bar{c}}) = 0 \quad (3.44)$$

vanishes due to the magic identity (3.36). The same is true for operators containing a derivative $in \cdot \partial$ acting on a hard-collinear field or the small component $n \cdot \mathcal{A}_{hc}$ or $n \cdot \mathcal{G}_{hc}$ of a hard-collinear gauge field.

3.3 Evanescent operators in SCET

In the matching from the LEFT to SCET-1 (and also from SCET-1 to SCET-2) several reducible Dirac structures appear. Their reduction in $d = 4 - 2\epsilon$ spacetime dimensions typically generates $O(\epsilon)$ remnants. When inserted into divergent loop integrals, these “evanescent” terms can yield finite contributions. To work with a physical basis containing only non-evanescent operators, such contributions must be computed and absorbed into the matching coefficients of the physical basis. The general procedure for how to do this consistently is well known [90–92] (see also [93] and references therein) and can be summarized as follows: Suppose an identity that is valid only in $d = 4$ is used to reduce a redundant operator R_i to O_i , i.e.

$$R_i \stackrel{d=4}{\equiv} O_i. \quad (3.45)$$

In $d \neq 4$ dimensions, the difference between the two operators must be retained,

$$R_i \stackrel{d \neq 4}{\equiv} O_i + (R_i - O_i) \equiv O_i + \tilde{O}_i. \quad (3.46)$$

By construction, the evanescent operator \tilde{O}_i has a vanishing tree-level matrix element. At loop order, however, it can yield finite contributions, which can be absorbed into shifts of the Wilson coefficients of the physical operators O_j . For example, at one-loop order we define

$$E_i^{\text{tree}} \langle \tilde{O}_i \rangle^{1\text{-loop}} \equiv \sum_j \delta H_j^{1\text{-loop}} \langle O_j \rangle^{\text{tree}}. \quad (3.47)$$

The explicit form of $\langle \tilde{O}_i \rangle$ depends on how the original reduction identity, valid only in $d = 4$ dimensions, is extended to $d = 4 - 2\epsilon$. The specific choice of this extension does not matter as long as it reduces to the original identity for $d = 4$, and it is applied consistently throughout the calculation. Some choices, however, are more convenient than others, as they may help to avoid the appearance of spurious intermediate contributions.

To define a consistent reduction scheme, the $O(\epsilon)$ terms can be chosen freely only for a set of linearly independent Dirac structures. We identify such structures by enforcing a canonical ordering on the transverse objects: slashed vectors always comes first, followed by repeated transverse Lorentz indices ordered alphabetically from left to right (i.e. μ, ν, ρ, σ). In the lepton current we always use the projector $\frac{1}{4} \not{n} \not{\bar{n}}$. With this ordering prescription, we define

our reduction scheme by imposing the validity of the $d = 4$ identities also in $d \neq 4$ dimensions for the canonically ordered Dirac structures, for instance

$$\begin{aligned} \frac{\not{n}}{2} \gamma_\mu^\perp \gamma_\nu^\perp P_L \otimes \frac{\not{n}\not{n}}{4} \gamma_\perp^\mu \gamma_\perp^\nu P_L &= 0, \\ \gamma_\mu^\perp \gamma_\nu^\perp \gamma_\rho^\perp P_L \otimes \frac{\not{n}\not{n}}{4} \gamma_\perp^\mu \gamma_\perp^\nu \gamma_\perp^\rho P_L &= 4 \gamma_\mu^\perp P_L \otimes \frac{\not{n}\not{n}}{4} \gamma_\perp^\mu P_L, \end{aligned} \quad (3.48)$$

where we omitted the explicit spinors for simplicity. The full list of reductions needed in our calculations is given in Appendix B. Structures that are not in canonical form can always be rewritten as combinations of those that are. Note that for the relation shown in (2.5) our scheme implies $\kappa = 0$, unlike the more common choice $\kappa = -4(1 + \epsilon)$ obtained using the ‘‘greek trick’’ [94]. Therefore, care needs to be taken to convert any literature result used here to our scheme choice.

Our ‘‘SCET-friendly’’ reduction scheme offers several advantages. First of all, it preserves the identities (3.24) also in $d = 4 - 2\epsilon$ dimensions, which greatly simplifies the construction of the evanescent operators and eliminates power-enhanced contributions at intermediate steps, including the LEFT to SCET-1 matching, the SCET-1 to SCET-2 matching, and the SCET-2 matrix elements. Such spurious power-enhanced contributions cancel out in the sum of all terms (see Appendix B for an explicit example), but avoiding them altogether is of great advantage. Second, with our scheme no evanescent shifts δJ arise in the SCET-1 to SCET-2 matching. Third, at one-loop order in QED, it is not necessary to consider contributions involving a soft lepton loop.

Already at tree level, the LEFT operator $O_\ell^{V,LL}$ matches onto several evanescent SCET-1 operators, whose one-loop matrix elements we need to consider. Among these, only operators of type- B , C and F can contribute to the $B^- \rightarrow \ell^- \bar{\nu}_\ell$ process at $\mathcal{O}(\alpha)$. They are

$$\begin{aligned} \tilde{O}_1^B &= \frac{1}{\bar{n} \cdot \mathcal{P}_{hc}} (\bar{u}_s \not{n} \gamma_\perp^\alpha \mathcal{A}_{hc[y]}^\perp P_L b_v) (\bar{\mathcal{X}}_{hc}^{(\ell)} \gamma_\alpha^\perp P_L \nu_{\bar{c}}) &\sim \lambda^4, \\ \tilde{O}_2^B &= \frac{(\bar{n} \cdot v)^2}{\bar{n} \cdot \mathcal{P}_{hc}} (\bar{u}_s \not{n} \mathcal{A}_{hc[y]}^\perp \gamma_\perp^\alpha P_L b_v) (\bar{\mathcal{X}}_{hc}^{(\ell)} \gamma_\alpha^\perp P_L \nu_{\bar{c}}) &\sim \lambda^4, \\ \tilde{O}_1^C &= (\bar{\mathcal{X}}_{hc[y]}^{(u)} \gamma_\perp^\alpha P_L b_v) (\bar{\mathcal{X}}_{hc}^{(\ell)} \gamma_\alpha^\perp P_L \nu_{\bar{c}}) &\sim \lambda^{\frac{5}{2}}, \\ \tilde{O}_2^C &= \frac{1}{\bar{n} \cdot \mathcal{P}_{hc}} [\bar{\mathcal{X}}_{hc[y]}^{(u)} \not{n} \gamma_\perp^\alpha (-i \overleftarrow{\not{\partial}}_\perp) P_L b_v] (\bar{\mathcal{X}}_{hc}^{(\ell)} \gamma_\alpha^\perp P_L \nu_{\bar{c}}) &\sim \lambda^3, \\ \tilde{O}_3^C &= \frac{1}{\bar{n} \cdot \mathcal{P}_{hc}} [\bar{\mathcal{X}}_{hc[y]}^{(u)} \not{n} \gamma_\perp^\alpha i \not{D}_s P_L b_v] (\bar{\mathcal{X}}_{hc}^{(\ell)} \gamma_\alpha^\perp P_L \nu_{\bar{c}}) &\sim \lambda^{\frac{7}{2}}, \\ \tilde{O}_1^F &= (\bar{\mathcal{X}}_{hc[y]}^{(u)} \gamma_\perp^\alpha P_L b_v) (\bar{l}_s \gamma_\alpha^\perp P_L \nu_{\bar{c}}) &\sim \lambda^{\frac{7}{2}}. \end{aligned} \quad (3.49)$$

Since by definition these operators have non-vanishing matrix elements only at loop order, it is sufficient for our purposes to compute their hard matching coefficients at tree level.

To account for the contributions from the evanescent operators, we compute the convolutions of their one-loop matrix elements with the corresponding tree-level matching coefficients, working with an off-shell lepton as an infrared regulator to ensure that only the ultraviolet

(UV) poles of the matrix elements contribute. We then match the results onto the physical SCET-1 operator basis constructed in Section 3.2. This yields a result of the form

$$\sum_i \int_0^1 dy E_i(y) \langle \tilde{O}_i(y) \rangle = \delta H_1^A \langle O_1^A \rangle + \delta H_2^A \langle O_2^A \rangle + \dots \quad (3.50)$$

At $\mathcal{O}(\alpha)$, we only need the evanescent shifts to the hard matching coefficients $H_{1,2}^A$, because only the operators $O_{1,2}^A$ give tree-level matrix elements for the $B^- \rightarrow \ell^- \bar{\nu}_\ell$ process. Applying the reduction scheme defined above, we obtain

$$\delta H_1^A = \frac{Q_\ell \alpha}{2\pi} \int_0^1 dy [2y E_1^B(y) + 4Q_u y(1-y) E_2^C(y)] = -Q_\ell Q_u \frac{\alpha}{\pi}, \quad (3.51)$$

and $\delta H_2^A = 0$, where we have used the tree-level expressions

$$E_1^B(y) = -\frac{Q_u}{2y} + \mathcal{O}(\alpha_s), \quad E_2^C(y) = -\frac{1}{2y} + \mathcal{O}(\alpha_s). \quad (3.52)$$

The contributions of evanescent operators other than \tilde{O}_1^B and \tilde{O}_2^C vanish in our projection scheme.

3.4 Results for the bare hard matching coefficients

Based on the operator basis constructed in Section 3.2, we write the SCET-1 representation for the operator $\mathcal{O}_\ell^{V,LL}$ in (3.1) in the form

$$\begin{aligned} \mathcal{O}_\ell^{V,LL} \rightarrow & \sum_{i=1}^4 H_i^A O_i^A + \int_0^1 dy \left[\sum_{i=1}^4 H_i^B(y) O_i^B(y) + \sum_{i=1}^5 H_i^C(y) O_i^C(y) \right] \\ & + \int_0^1 dy_1 \int_0^1 dy_2 \theta(1-y_1-y_2) \sum_{i=1}^8 H_i^D(y_1, y_2) O_i^D(y_1, y_2) \\ & + \int_0^1 dy_1 \int_0^1 dy_2 \int_0^1 dy_3 \theta(1-y_1-y_2-y_3) \sum_{i=1}^4 H_i^E(y_1, y_2, y_3) O_i^E(y_1, y_2, y_3) \\ & + H_1^F O_1^F, \end{aligned} \quad (3.53)$$

where for simplicity we suppress the dependence of the Wilson coefficients on the hard scales m_b and $\bar{n} \cdot \mathcal{P}_{hc}$. Without loss of generality, we evaluate all operators at the spacetime point $x = 0$. Otherwise, there would be a phase factor $e^{-im_b v \cdot x}$ in front of each term, and soft fields would need to be multipole expanded in interactions with hard-collinear fields [70, 89]. It is straightforward to calculate the tree-level matching conditions for the hard functions in (3.53) by performing the substitutions

$$b \rightarrow \left[1 - \frac{1}{m_b v \cdot n} \not{n} \left(Q_b \mathcal{A}_{hc}^\perp + \mathcal{G}_{hc}^\perp \right) + \left(\frac{i \not{D}_s}{2m_b} + \dots \right) + \mathcal{O}(\lambda^{3/2}) \right] b_v,$$

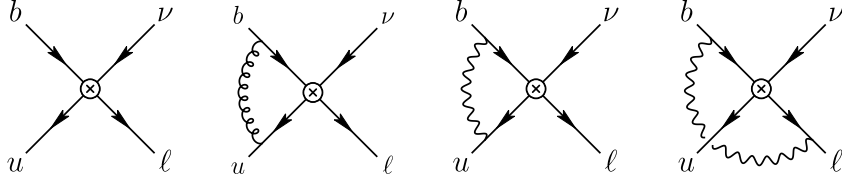


Figure 3: Tree-level and one-loop Feynman diagrams for the LEFT to SCET-1 matching for the type-*A* four-fermion operators. There is also a contribution from the wave-function renormalization of the *b* quark.

$$\begin{aligned}
u &\rightarrow \left[1 - \frac{1}{i\bar{n} \cdot \partial} \frac{\not{\bar{n}}}{2} (Q_u \mathcal{A}_{hc}^\perp + \mathcal{G}_{hc}^\perp) \right] u_s \\
&\quad + \left[1 - \frac{1}{i\bar{n} \cdot \partial} \frac{\not{\bar{n}}}{2} (i\mathcal{D}_s^\perp + Q_u \mathcal{A}_{hc}^\perp + \mathcal{G}_{hc}^\perp) \right] \mathcal{X}_{hc}^{(u)}, \\
\ell &\rightarrow \left[1 + \mathcal{O}(\lambda^{\frac{1}{2}}) \right] \ell_s + \left[1 - \frac{1}{i\bar{n} \cdot \partial} \frac{\not{\bar{n}}}{2} (i\mathcal{D}_s^\perp + Q_\ell \mathcal{A}_{hc}^\perp - m_\ell) \right] \mathcal{X}_{hc}^{(\ell)}, \\
\nu_\ell &\rightarrow \nu_{\bar{c}}
\end{aligned} \tag{3.54}$$

in the four-fermion operator $\mathcal{O}_\ell^{V,LL}$, where all fields are evaluated at $x = 0$. These replacements account for the hard matching corrections resulting from integrating out the small components of the heavy-quark spinor in HQET and the hard-collinear spinors in SCET-1. The contributions of hard-collinear gauge fields to the matching relations for the heavy-quark and up-quark fields have been derived in [70]. While the $\mathcal{O}(\lambda)$ corrections in the relation for the heavy-quark spinor give rise to SCET-1 operators that vanish by virtue of the magic identity (3.36), the term involving $i\mathcal{D}_s/2m_b$ is needed for the correct treatment of evanescent operators, see the operator \tilde{O}_3^C in (3.49). The dots refer to further $\mathcal{O}(\lambda)$ terms involving collinear gauge fields, which vanish in our reduction scheme at least to one-loop order. The $\mathcal{O}(\lambda^{\frac{1}{2}})$ corrections to the soft lepton field would give rise to power-suppressed SCET-1 operators.

For the type-*A* operators, it is possible to include the first-order QCD corrections using known results from the literature. For the case of the operators O_1^A and O_2^A , it is necessary to also include the one-loop QED corrections, which we compute here for the first time. The relevant diagrams are shown in Figure 3. For all other operators, a photon loop is required when performing the matching onto SCET-2, and hence we give their coefficients at zeroth order in α . Working in dimensional regularization with $d = 4 - 2\epsilon$ spacetime dimensions, we obtain the bare expressions

$$\begin{aligned}
H_1^A &= C_1^{\text{HQET}} + \frac{1}{2} C_2^{\text{HQET}} - \frac{Q_b \alpha}{4\pi} \left\{ Q_\ell \left[\frac{1}{\epsilon^2} + \frac{L}{\epsilon} - \frac{1}{\epsilon} + \frac{L^2}{2} - L - \frac{z \ln z}{z-1} + 2\text{Li}_2(1-z) + 1 + \frac{\pi^2}{12} \right] \right. \\
&\quad \left. + Q_b \left(\frac{3}{2\epsilon} + \frac{3}{2} L_m + 2 \right) + Q_u \right\} \\
&\quad - Q_\ell (Q_b + Q_u) \frac{\alpha}{16\pi} \kappa + \delta H_1^A,
\end{aligned}$$

$$H_2^A = \frac{1}{2} \mathcal{C}_2^{\text{HQET}} + \frac{Q_b \alpha}{4\pi} \left[z Q_\ell \left(\frac{1}{\epsilon} + L + \ln z + \frac{z-1}{z} \right) + Q_u \right], \quad (3.55)$$

$$H_3^A = -\mathcal{C}_1^{\text{HQET}} - \frac{1}{2} \mathcal{C}_2^{\text{HQET}} + \mathcal{O}(\alpha),$$

$$H_4^A = -\frac{1}{2} \mathcal{C}_2^{\text{HQET}} + \mathcal{O}(\alpha),$$

where the scale μ is defined through dimensional transmutation in the $\overline{\text{MS}}$ scheme, and we have introduced

$$L = \ln \frac{\mu^2 (\bar{n} \cdot v)^2}{(\bar{n} \cdot \mathcal{P}_{hc})^2}, \quad L_m = \ln \frac{\mu^2}{m_b^2}, \quad z = \frac{\bar{n} \cdot \mathcal{P}_{hc}}{m_b \bar{n} \cdot v}. \quad (3.56)$$

The coefficients

$$\mathcal{C}_1^{\text{HQET}} = 1 + \frac{C_F \alpha_s}{4\pi} \left(-\frac{3}{2\epsilon} - \frac{3}{2} L_m - 4 \right) + \mathcal{O}(\alpha_s^2), \quad (3.57)$$

$$\mathcal{C}_2^{\text{HQET}} = \frac{C_F \alpha_s}{2\pi} + \mathcal{O}(\alpha_s^2).$$

appear in the leading-order matching relations for the heavy-light vector current in HQET [66, 95]. Note that the scheme-dependent terms proportional to κ cancel the κ -dependent terms in the matching coefficient K_{EW} in (2.4). The quantity δH_1^A is the remnant shift from eliminating evanescent operators and has been given in (3.51). For our process of interest, the variable z evaluates to $z = m_B/m_b$, where m_b denotes the pole mass of the b quark. This ratio equals 1 up to power corrections of $\mathcal{O}(\lambda)$, but we prefer to work with the general expressions given above.

The coefficients of the type- B operators take the form

$$H_1^B(y) = -Q_\ell \left(\mathcal{C}_1^{\text{HQET}} + \frac{1}{2} \mathcal{C}_2^{\text{HQET}} \right) + \left[\frac{Q_u}{y} + \mathcal{O}(\alpha_s) \right] = -Q_\ell + \frac{Q_u}{y} + \mathcal{O}(\alpha_s),$$

$$H_2^B(y) = -\frac{Q_\ell}{2} \mathcal{C}_2^{\text{HQET}} + [z Q_b + \mathcal{O}(\alpha_s)] = z Q_b + \mathcal{O}(\alpha_s), \quad (3.58)$$

$$H_3^B(y) = \frac{1}{y} + \mathcal{O}(\alpha_s),$$

$$H_4^B(y) = z + \mathcal{O}(\alpha_s),$$

where the QCD corrections proportional to Q_ℓ are again determined in terms of the coefficients in (3.57). The yet unknown QCD corrections are associated with the terms involving hard-collinear gauge fields in the $\mathcal{O}(\lambda)$ contribution to the matching relations for the b quark in (3.54) (marked by the dots). For two of the type- C operators one can use known expressions for the matching relations of heavy-light current operators in SCET-1 to derive the matching coefficients including QCD corrections. For the remaining coefficients only the tree-level expressions are known, because they can receive contributions from yet unknown second-order

($\sim \lambda$) power corrections to the SCET-1 heavy-light current operators. We find

$$\begin{aligned}
H_1^C(y) &= \frac{1}{1-y} \left[\mathcal{C}_1^A(y) + \frac{1}{2} \mathcal{C}_2^A(y) + \mathcal{C}_3^A(y) \right] = \frac{1}{1-y} + \mathcal{O}(\alpha_s), \\
H_2^C(y) &= -\frac{1}{y(1-y)} \left[\frac{1}{2} \mathcal{C}_2^A(y) + \mathcal{C}_3^A(y) \right] = \mathcal{O}(\alpha_s), \\
H_3^C(y) &= \frac{1}{y} + \mathcal{O}(\alpha_s), \\
H_4^C(y) &= -\frac{1}{1-y} + \mathcal{O}(\alpha_s), \\
H_5^C(y) &= \mathcal{O}(\alpha_s),
\end{aligned} \tag{3.59}$$

where [96, 97]

$$\begin{aligned}
\mathcal{C}_1^A(y) &= 1 + \frac{C_F \alpha_s}{4\pi} \left[-\frac{1}{\epsilon^2} - \frac{1}{\epsilon} L_y - \frac{5}{2\epsilon} - \frac{1}{2} L_y^2 - L_y - \frac{3}{2} L_m \right. \\
&\quad \left. - \frac{yz \ln yz}{1-yz} - 2\text{Li}_2(1-yz) - 6 - \frac{\pi^2}{12} \right] + \mathcal{O}(\alpha_s^2), \\
\mathcal{C}_2^A(y) &= \frac{C_F \alpha_s}{4\pi} \frac{2}{1-yz} \left(\frac{yz \ln yz}{1-yz} + 1 \right) + \mathcal{O}(\alpha_s^2), \\
\mathcal{C}_3^A(y) &= \frac{C_F \alpha_s}{4\pi} \frac{yz}{1-yz} \left(\frac{1-2yz}{1-yz} \ln yz - 1 \right) + \mathcal{O}(\alpha_s^2),
\end{aligned} \tag{3.60}$$

where

$$L_y = \ln \frac{\mu^2 (\bar{n} \cdot v)^2}{(y \bar{n} \cdot \mathcal{P}_{hc})^2}. \tag{3.61}$$

The coefficients of the remaining operators will only be needed at tree level. For the type- D operators, we obtain

$$\begin{aligned}
H_1^D(y_1, y_2) &= -\frac{z Q_b}{1-y_1-y_2} + \mathcal{O}(\alpha_s), \\
H_2^D(y_1, y_2) &= -\frac{z}{1-y_1-y_2} + \mathcal{O}(\alpha_s), \\
H_3^D(y_1, y_2) &= -\frac{Q_\ell}{1-y_1} + \frac{Q_u}{y_1+y_2} + \mathcal{O}(\alpha_s), \\
H_4^D(y_1, y_2) &= \frac{1}{y_1+y_2} + \mathcal{O}(\alpha_s), \\
H_5^D(y_1, y_2) &= -\frac{z Q_b}{y_1} + \mathcal{O}(\alpha_s),
\end{aligned} \tag{3.62}$$

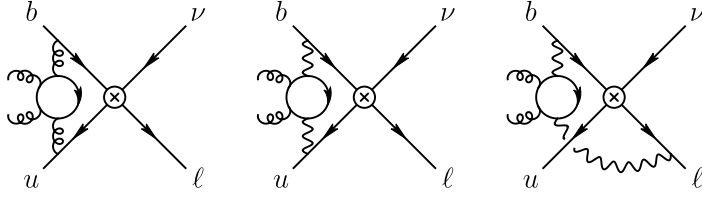


Figure 4: Hard two-loop diagrams which can generate the operator O_4^E in SCET-1. The light quark, the charged lepton and the external gluons carry hard-collinear momenta.

$$H_6^D(y_1, y_2) = -\frac{z}{y_1} + \mathcal{O}(\alpha_s),$$

$$H_7^D(y_1, y_2) = \frac{zQ_b}{1 - y_1 - y_2} + \mathcal{O}(\alpha_s),$$

$$H_8^D(y_1, y_2) = \frac{z}{1 - y_1 - y_2} + \mathcal{O}(\alpha_s).$$

At $\mathcal{O}(\alpha_s)$, these coefficients receive contributions from yet unknown higher-order power corrections to the heavy-light currents in SCET-1. For the coefficients of the type- E operators, we find

$$H_1^E(y_1, y_2, y_3) = \frac{zQ_\ell Q_b}{1 - y_1 - y_2} - \frac{zQ_b Q_u}{y_1 + y_3} + \mathcal{O}(\alpha_s),$$

$$H_2^E(y_1, y_2, y_3) = \frac{zQ_\ell}{1 - y_1 - y_2} - \frac{zQ_b}{y_1 + y_2} - \frac{zQ_u}{y_1 + y_3} + \mathcal{O}(\alpha_s), \quad (3.63)$$

$$H_3^E(y_1, y_2, y_3) = -\frac{z}{y_1 + y_2} + \mathcal{O}(\alpha_s),$$

$$H_4^E(y_1, y_2, y_3) = \mathcal{O}(\alpha_s^2, \alpha\alpha_s).$$

The coefficient H_4^E can first be generated at two-loop order from diagrams such as those shown in Figure 4. For the coefficient of the type- F operator, we get

$$H_1^F(\mu) = \frac{1}{2} + \mathcal{O}(\alpha_s). \quad (3.64)$$

Finally, we list the tree-level matching coefficients for the evanescent operators defined in (3.49). We obtain

$$E_1^B(y) = -\frac{Q_u}{2y} + \mathcal{O}(\alpha_s),$$

$$E_2^B(y) = -\frac{zQ_b}{2} + \mathcal{O}(\alpha_s),$$

$$E_1^C(y) = 1 + \mathcal{O}(\alpha_s),$$

$$E_2^C(y) = -\frac{1}{2y} + \mathcal{O}(\alpha_s), \quad (3.65)$$

$$E_3^C(y) = \frac{z}{4} + \mathcal{O}(\alpha_s),$$

$$E_1^F(y) = 1 + \mathcal{O}(\alpha_s).$$

Two of these relations have already been given in (3.52).

3.5 Simplifications arising at $\mathcal{O}(\alpha)$ in perturbation theory

While the detailed matching onto SCET-2 will be discussed in Section 4, a simple inspection of the relevant Feynman graphs can be used to deduce at which order in the couplings α_s and α a given basis operator might contribute to the $B^- \rightarrow \ell^- \bar{\nu}_\ell$ decay amplitude (in some cases these contributions may still turn out to be zero upon explicit calculation). The results of such an analysis are shown in Table 1. When QED corrections are neglected, only the operators O_1^A and O_2^A contribute to the decay amplitude, and to all orders in QCD perturbation theory the sum of their contributions can be expressed in terms of the B -meson decay constant f_B defined in QCD. In the approximation where one works consistently at first order in α or α_s , but neglects two-loop mixed QCD–QED corrections, the operators $O_{1,2}^A$, $O_{1,2}^B$, and $O_{1,3,4}^C$ need to be retained. When the goal is to work consistently up to $\mathcal{O}(\alpha\alpha_s)$, in addition the type- C operator O_2^C and the type- D operators $O_{2,4,6,8}^D$ need to be included. The remaining type- D operators and the type- F operator could first contribute at $\mathcal{O}(\alpha^2)$, while the leading type- E operator O_3^E could first enter at $\mathcal{O}(\alpha\alpha_s^2)$. For all practical purposes, these latter three contributions will play no role for the foreseeable future.

In Section 4, we will construct the most general SCET-2 operator basis, so that the analysis of the $B^- \rightarrow \mu^- \bar{\nu}_\mu$ decay amplitude can in principle be performed at any order in perturbation theory. For practical applications, we will then limit ourselves to $\mathcal{O}(\alpha)$ accuracy, including however the leading logarithmic QCD and QED corrections to all orders in perturbation theory.

3.6 Renormalization of the hard functions

We now discuss the renormalization of the hard functions H_i^X at one-loop order in both QCD and QED. From the discussion in the previous section we know that in this approximation the operator basis can be restricted to the operators $O_{1,2}^A$, $O_{1,2}^B$, and O_i^C , where the type- B and C operators depend on the momentum variable y . Only the type- A hard functions contain divergences from QED, as exhibited in (3.55) (type- B and type- C hard functions are only needed at tree level).

In general, the SCET-1 operators with the same quantum numbers and mass dimension can mix with each other under renormalization. We define renormalization factors $Z_{ij}^{XX'}$ via the renormalization condition

$$O_i^X(\mu) = \sum_{j,X'} Z_{ij}^{XX'}(\mu) \otimes O_j^{X'}, \quad (3.66)$$

which relates the renormalized (and scale-dependent) operators $O_i^X(\mu)$ to the bare operators $O_j^{X'}$. The labels X and X' refer to the operator type (A , B or C), and the symbol \otimes means an integration over the momentum variables shared by the quantities $Z_{ij}^{XX'}$ and $O_j^{X'}$. Since we

Operator	Hard function	Jet function*	Contribution to decay amplitude			
Perturbative approximation:			$\mathcal{O}(\alpha^0)$	$\mathcal{O}(\alpha)$	$\mathcal{O}(\alpha\alpha_s)$	$\mathcal{O}(\alpha\alpha_s^2, \alpha^2)$
O_1^A	1	1	✓	✓	✓	✓
O_2^A	α_s	1	✓	✓	✓	✓
O_3^A	1	0	—	—	—	—
O_4^A	α_s	0	—	—	—	—
$O_{1,2}^B$	1	α	—	✓	✓	✓
$O_{3,4}^B$	1	0	—	—	—	—
$O_{1,3,4}^C$	1	α	—	✓	✓	✓
O_2^C	α_s	α	—	—	✓	✓
O_5^C	α_s	α^\dagger	—	—	—	—
$O_{1,3,5,7}^D$	1	α^2	—	—	—	✓
$O_{2,4,6,8}^D$	1	$\alpha\alpha_s$	—	—	✓	✓
O_1^E	1	α^3	—	—	—	—
O_2^E	1	$\alpha^2\alpha_s$	—	—	—	—
O_3^E	1	$\alpha\alpha_s^2$	—	—	—	✓
O_4^E	α_s^2	$\alpha\alpha_s^2$	—	—	—	—
O_1^F	1	α^\dagger	—	—	—	✓

Table 1: Perturbative scaling of the hard functions of the SCET-1 basis operators defined in Section 3.2, and of the jet functions arising in their matching onto SCET-2. The star indicates that for the type-*B*, *D* and *E* operators the indicated order refers to the product of the jet function and the low-energy matrix element, as in some cases the low-energy matrix element may include a collinear photon loop. The product of the entries in the first two columns gives the (largest possible) scaling behavior of the corresponding contributions to the $B^- \rightarrow \mu^- \bar{\nu}_\mu$ decay amplitude. Entries in the third column marked with a dagger are naively of the given order, but vanish at that order upon explicit calculation.

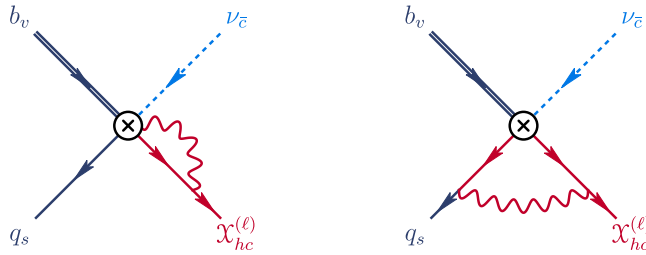


Figure 5: Left: One-loop diagrams leading to a mixing of the operators O_i^B and O_i^A (with $i = 1, 2$). The lepton mass insertion is not shown explicitly. Right: One-loop diagram leading to a mixing of the operators O_i^C and O_i^A (with $i = 1, 2$). Here and in later figures, red lines refer to hard-collinear fields, gray lines to soft fields, and light blue lines to collinear or anti-collinear fields. The soft heavy-quark is represented by a double line.

are working with a basis of subleading-power operators, there can be mixing of operators with different scaling dimensions. Specifically, the time-ordered products of the type-*B* operators ($\sim \lambda^4$) with the power-suppressed lepton mass term ($\sim \lambda_\ell/\lambda^{\frac{1}{2}}$) in the SCET-1 Lagrangian can mix with the type-*A* operators ($\sim \lambda_\ell \lambda^{\frac{7}{2}}$). Calculating the UV divergences of the one-loop diagram on the left in Figure 5, we find that the corresponding off-diagonal renormalization factors are

$$Z_{11}^{BA}(y, \mu) = Z_{22}^{BA}(y, \mu) = Q_\ell \frac{\alpha}{2\pi\epsilon} y, \quad (3.67)$$

while the remaining entries Z_{ij}^{BA} vanish. The scale dependence of the renormalization factors arises via dimensional transmutation, since the dimensionless bare coupling $\alpha \propto \mu^{-2\epsilon}$. Similarly, the time-ordered products of some of the type-*C* operators with the power-suppressed Lagrangian $\mathcal{L}_{\xi q}^{(1/2)}$ [70], which converts a hard-collinear to a soft quark, can mix with the type-*A* operators. Calculating the UV divergences of the diagram shown on the right in Figure 5, we obtain for the off-diagonal renormalization factors at one-loop order

$$Z_{11}^{CA}(y, \mu) = Q_\ell Q_u \frac{\alpha}{2\pi} (1-y) \left[\frac{1}{y^{1+\epsilon}} \left(\frac{1}{\epsilon} + \ln \frac{\mu^2}{\bar{n} \cdot \mathcal{P}_{hc} n \cdot l_s} + 1 \right) + \frac{1}{\epsilon} \right]_{\text{poles}}, \quad (3.68)$$

$$Z_{22}^{CA}(y, \mu) = -Q_\ell Q_u \frac{\alpha}{2\pi} y(1-y)^2 \left[\frac{1}{y^{1+\epsilon}} \left(\frac{1}{\epsilon} + \ln \frac{\mu^2}{\bar{n} \cdot \mathcal{P}_{hc} n \cdot l_s} \right) \right]_{\text{poles}}.$$

The remaining entries Z_{ij}^{CA} vanish. Due to the appearance of a singularity for $y \rightarrow 0$, we have kept some subleading terms. One may be tempted to replace

$$\frac{1}{y^{1+\epsilon}} = -\frac{1}{\epsilon} \delta(y) + \left[\frac{1}{y} \right]_+ + \mathcal{O}(\epsilon), \quad (3.69)$$

in which case all of the terms shown above would give rise to $1/\epsilon^n$ poles. However, as we will soon see, things are actually a bit more subtle, because these renormalization factors will be multiplied by hard functions which are themselves singular at $y = 0$. The appearance of the incoming soft momentum of the \bar{u} quark in the expression for Z_{11}^{CA} is a bit worrisome, since

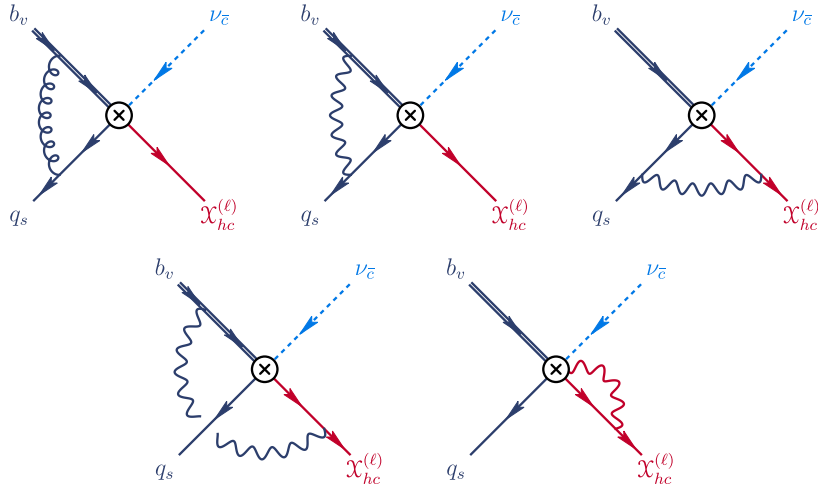


Figure 6: One-loop diagrams needed for the calculation of the diagonal renormalization factors Z_{ii}^{AA} . These graphs need to be supplemented by wave-function renormalization.

this is an IR scale in SCET-1. We will see later how this puzzle is resolved. At $\mathcal{O}(\alpha)$ there is also a mixing of the type- C operators with the type- B operators, but the corresponding contributions to our process of interest would only appear at $\mathcal{O}(\alpha^2)$, so we can ignore them.

Renormalization is also required within each class of operators. For the operators $O_{1,2}^A$, the corresponding renormalization factors are obtained from the UV poles of the diagrams shown in Figure 6, supplemented by wave-function renormalization and the renormalization of the charged-lepton mass. To regularize IR divergences, we keep the soft external momenta of the quarks off shell and assign an off-shell collinear momentum to the charged lepton. The scale $(-p_\ell^2)$ enters the expressions for the last three diagrams as an infrared (IR) regulator, but it cancels out in their sum. We find that (for $i = 1, 2$)

$$Z_{ii}^{AA}(\mu) = 1 + \frac{C_F \alpha_s}{4\pi} \left(-\frac{3}{2\epsilon} \right) \quad (3.70)$$

$$+ \frac{\alpha}{4\pi} \left[-Q_\ell Q_b \left(\frac{1}{\epsilon^2} + \frac{L}{\epsilon} + \frac{1}{\epsilon} \right) + Q_\ell Q_u \left(\frac{2}{\epsilon^2} + \frac{2}{\epsilon} \ln \frac{\mu^2}{\bar{n} \cdot \mathcal{P}_{hc} n \cdot l_s} \right) + \frac{3}{2\epsilon} (Q_\ell^2 - Q_u^2) \right].$$

Note that a dependence on the incoming soft momentum l_s of the \bar{u} quark remains in this expression.

From (3.66) it is straightforward to derive the renormalization condition for the hard functions. At one-loop order, we obtain for the coefficients of the type- A operators (with $i = 1, 2$)

$$H_i^A(\mu) = Z_{EW}(\mu) [Z_{ii}^{AA}(\mu)]^{-1} H_i^A - \int_0^1 dy Z_{ii}^{BA}(y, \mu) H_i^B(y) - \int_0^1 dy Z_{ii}^{CA}(y, \mu) H_i^C(y), \quad (3.71)$$

where

$$Z_{EW}(\mu) = 1 + 3Q_\ell Q_u \frac{\alpha}{4\pi\epsilon}. \quad (3.72)$$

While the first two terms on the right-hand side of (3.71) are straightforward to evaluate, the last term is problematic, since both functions in the integrand are singular in the limit $y \rightarrow 0$. For $i = 1$, the renormalization factor $Z_{11}^{CA}(y) \propto y^{-1-n\epsilon}$ at n -loop order, while the bare coefficient $H_1^C(y) \propto y^{-n'\epsilon}$ at n' loops. For $i = 2$, one finds $Z_{22}^{CA}(y) \propto y^{-n\epsilon}$ and $H_2^C(y) \propto y^{-1-n'\epsilon}$. In either case, the endpoint behavior of the product is $y^{-1-(n+n')\epsilon}$, where the strength of the singularity is determined by the loop order of the product of the two functions. We therefore cannot interpret Z_{11}^{CA} in the distribution sense, as indicated in (3.69), and the same is true for Z_{22}^{CA} . Instead, we perform a plus-type subtraction of the integrand and rewrite the integral in the form

$$\begin{aligned} \int_0^1 dy Z_{ii}^{CA}(y) H_i^C(y) &= \int_0^1 dy \left[Z_{ii}^{CA}(y) H_i^C(y) - \llbracket Z_{ii}^{CA}(y) \rrbracket \llbracket H_i^C(y) \rrbracket \right] \\ &+ \int_0^1 dy \llbracket Z_{ii}^{CA}(y) \rrbracket \llbracket H_i^C(y) \rrbracket, \end{aligned} \quad (3.73)$$

where the notation $\llbracket f(y) \rrbracket$ indicates that one must only keep the leading terms of the function $f(y)$ in the limit $y \rightarrow 0$. In the first integral on the right-hand side, the leading terms for $y \rightarrow 0$ cancel out, so that the integral is convergent and can be evaluated using the naive ϵ expansions

$$\begin{aligned} Z_{11}^{CA} &= Q_\ell Q_u \frac{\alpha}{2\pi\epsilon} \frac{1-y^2}{y}, & \llbracket Z_{11}^{CA} \rrbracket &= Q_\ell Q_u \frac{\alpha}{2\pi\epsilon} \frac{1}{y} \\ Z_{22}^{CA} &= -Q_\ell Q_u \frac{\alpha}{2\pi\epsilon} (1-y)^2, & \llbracket Z_{22}^{CA} \rrbracket &= -Q_\ell Q_u \frac{\alpha}{2\pi\epsilon}, \end{aligned} \quad (3.74)$$

along with

$$\llbracket H_1^C(y) \rrbracket = 1 + \mathcal{O}(\alpha_s), \quad \llbracket H_2^C(y) \rrbracket = \mathcal{O}(\alpha_s). \quad (3.75)$$

For the last term, it is necessary to keep the full expressions in (3.68), consider the singularities of the product of the two functions *together*, and evaluate the integral in dimensional regularization. In order for the result to fit the structure of a renormalization condition, it must be possible to factorize the integral into one of the hard functions already present in our operator basis and a renormalization factor [51, 54]. This is ensured by the exact d -dimensional refactorization conditions

$$\begin{aligned} \llbracket H_1^C(y) \rrbracket &= H_1^A S_1^C \left(\frac{y\bar{n} \cdot \mathcal{P}_{hc}}{\bar{n} \cdot v} \right), \\ \llbracket H_2^C(y) \rrbracket &= -\frac{H_2^A}{y} S_2^C \left(\frac{y\bar{n} \cdot \mathcal{P}_{hc}}{\bar{n} \cdot v} \right), \end{aligned} \quad (3.76)$$

which must hold to all orders of perturbation theory. Here $H_{1,2}^A$ are the bare hard matching coefficient of the type- A operators $O_{1,2}^A$, and $S_{1,2}^C = 1 + \mathcal{O}(\alpha_s)$ are functions of the indicated combination of momentum variables, which becomes soft in the region $y \rightarrow 0$. For example, performing a region analysis of the function $\llbracket H_1^C \rrbracket$ at one-loop order in QCD, we find

$$S_1^C(\bar{\omega}) = 1 - \frac{C_F \alpha_s}{4\pi} \left(\frac{\mu^2}{\bar{\omega}^2} \right)^\epsilon \left[\frac{1}{\epsilon^2} + \frac{1}{\epsilon} + 2 + \frac{5\pi^2}{12} + \mathcal{O}(\epsilon) \right]. \quad (3.77)$$

Evaluating the last integral in (3.73) using the expressions (3.68) and (3.76), we obtain

$$\begin{aligned} \int_0^1 dy \llbracket Z_{11}^{CA}(y) \rrbracket \llbracket H_1^C(y) \rrbracket &= -H_1^A Q_\ell Q_u \frac{\alpha}{2\pi} \left(\frac{1}{\epsilon^2} + \frac{1}{\epsilon} \ln \frac{\mu^2}{\bar{n} \cdot \mathcal{P}_{hc} n \cdot l_s} + \frac{1}{\epsilon} \right) + \mathcal{O}(\alpha\alpha_s), \\ \int_0^1 dy \llbracket Z_{22}^{CA}(y) \rrbracket \llbracket H_2^C(y) \rrbracket &= -H_2^A Q_\ell Q_u \frac{\alpha}{2\pi} \left(\frac{1}{\epsilon^2} + \frac{1}{\epsilon} \ln \frac{\mu^2}{\bar{n} \cdot \mathcal{P}_{hc} n \cdot l_s} \right) + \mathcal{O}(\alpha\alpha_s). \end{aligned} \quad (3.78)$$

This contribution can be combined with the first term on the right-hand side of (3.71) and has the effect of canceling a corresponding term in $[Z_{ii}^A]^{-1}$. In the refactorization-based subtraction (RBS) scheme [51, 52, 54, 55] employed here, we find at one-loop order⁴

$$\begin{aligned} H_1^A(\mu) &= \left\{ 1 + \frac{C_F \alpha_s}{4\pi} \left(\frac{3}{2\epsilon} \right) \right. \\ &\quad \left. + \frac{\alpha}{4\pi} \left[Q_\ell Q_b \left(\frac{1}{\epsilon^2} + \frac{L}{\epsilon} + \frac{1}{\epsilon} \right) - \frac{3}{\epsilon} Q_\ell^2 + \frac{3}{2\epsilon} Q_b^2 + \frac{2}{\epsilon} Q_\ell Q_u \right] \right\} H_1^A \\ &\quad - \int_0^1 dy Z_{11}^{BA}(y) H_1^B(y) - \int_0^1 dy \left[Z_{11}^{CA}(y) H_1^C(y) - \llbracket Z_{11}^{CA}(y) \rrbracket \llbracket H_1^C(y) \rrbracket \right] \\ &= H_1^A + \frac{C_F \alpha_s}{4\pi} \left(\frac{3}{2\epsilon} \right) + \frac{\alpha}{4\pi} \left[Q_\ell Q_b \left(\frac{1}{\epsilon^2} + \frac{L}{\epsilon} - \frac{1}{\epsilon} \right) + \frac{3}{2\epsilon} Q_b^2 \right], \end{aligned} \quad (3.79)$$

and

$$\begin{aligned} H_2^A(\mu) &= \left\{ 1 + \frac{C_F \alpha_s}{4\pi} \left(\frac{3}{2\epsilon} \right) + \frac{\alpha}{4\pi} \left[Q_\ell Q_b \left(\frac{1}{\epsilon^2} + \frac{L}{\epsilon} + \frac{1}{\epsilon} \right) - \frac{3}{\epsilon} Q_\ell^2 + \frac{3}{2\epsilon} Q_b^2 \right] \right\} H_2^A \\ &\quad - \int_0^1 dy Z_{22}^{BA}(y) H_2^B(y) - \int_0^1 dy \left[Z_{22}^{CA}(y) H_2^C(y) - \llbracket Z_{22}^{CA}(y) \rrbracket \llbracket H_2^C(y) \rrbracket \right] \\ &= H_2^A - z Q_\ell Q_b \frac{\alpha}{4\pi\epsilon}. \end{aligned} \quad (3.80)$$

These are precisely the correct counterterms to remove the divergences in the bare functions H_i^A in (3.55). Note that the troublesome terms involving the IR scale $n \cdot l_s$ have disappeared.

The appearance of the soft momentum $n \cdot l_s$ in the expressions for the renormalization factors in (3.68) and (3.70) suggests that one should redefine the operator basis. This will be discussed in more detail in Section 4.

3.7 RG evolution equations

We now discuss the scale evolution of the renormalized hard functions and the resummation of the leading large logarithmic corrections in both QCD and QED. The evolution equations governing the scale dependence of the hard functions take the form

$$\frac{d}{d \ln \mu} H_i^X(\mu) = -\gamma_{EW} H_i^X(\mu) + \sum_{j, X'} \Gamma_{ij}^{XX'}(\mu) \otimes H_j^{X'}(\mu), \quad (3.81)$$

⁴This result is analogous to expression (4.29) in [54], where the RBS scheme was first applied to a subleading-power observable in SCET.

where the anomalous dimensions are related to the renormalization factors by [98]

$$\Gamma_{ij}^{XX'} = 2 \left(\alpha_s \frac{\partial}{\partial \alpha_s} + \alpha \frac{\partial}{\partial \alpha} \right) Z_{ij}^{XX'[1]}, \quad (3.82)$$

where $Z_{ij}^{XX'[1]}$ denotes the coefficient of the single $1/\epsilon$ pole term. The quantity γ_{EW} has been given in (2.6). The symbol \otimes means an integration over the momentum variables shared by $\Gamma_{ij}^{XX'}$ and $H_j^{X'}$. From (3.79), we obtain at one-loop order in QED

$$\begin{aligned} \frac{d}{d \ln \mu} H_1^A(\mu) &= \left\{ \gamma_{\text{hl}}(\alpha_s) - \frac{\alpha}{2\pi} \left[Q_\ell Q_b \left(\ln \frac{\mu^2}{m_B^2} + 1 \right) - 3Q_\ell^2 + \frac{3}{2} Q_b^2 + 2Q_\ell Q_u \right] \right\} H_1^A(\mu) \\ &\quad + Q_\ell \frac{\alpha}{\pi} \int_0^1 dy y H_1^B(y, \mu) + Q_\ell Q_u \frac{\alpha}{\pi} \int_0^1 \frac{dy}{y} \left[(1-y)^2 H_1^C(y, \mu) - \llbracket H_1^C(y, \mu) \rrbracket \right], \\ \frac{d}{d \ln \mu} H_2^A(\mu) &= \left\{ \gamma_{\text{hl}}(\alpha_s) - \frac{\alpha}{2\pi} \left[Q_\ell Q_b \left(\ln \frac{\mu^2}{m_B^2} + 1 \right) - 3Q_\ell^2 + \frac{3}{2} Q_b^2 \right] \right\} H_2^A(\mu) \\ &\quad + Q_\ell \frac{\alpha}{\pi} \int_0^1 dy y H_2^B(y, \mu) - Q_\ell Q_u \frac{\alpha}{\pi} \int_0^1 dy \left[(1-y)^2 H_2^C(y, \mu) - \llbracket H_2^C(y, \mu) \rrbracket \right], \end{aligned} \quad (3.83)$$

where we have used that $\bar{n} \cdot \mathcal{P}_{hc} / \bar{n} \cdot v = m_B$ in our case to simplify the notation. The evolution in pure QCD is governed by the universal anomalous dimension of heavy-light current operators in HQET. Its two-loop expression reads [95]

$$\gamma_{\text{hl}}(\alpha_s) = -3C_F \frac{\alpha_s}{4\pi} - \left(\frac{254}{9} + \frac{56\pi^2}{27} - \frac{20}{9} n_f \right) \left(\frac{\alpha_s}{4\pi} \right)^2 + \mathcal{O}(\alpha_s^3), \quad (3.84)$$

where $n_f = 4$ is the appropriate number of active quark flavors below the scale m_B , and the two-loop coefficient has been evaluated for $N_c = 3$.

The remaining hard functions give contributions to the $B^- \rightarrow \ell^- \bar{\nu}_\ell$ decay amplitude that are suppressed by a power of either α_s or α . For these cases, an approximate treatment of QED evolution effects will be sufficient, especially since we will evolve the hard functions over a rather narrow scale interval, from $\mu_h \sim m_B$ to $\mu_{hc} \sim \sqrt{m_B \Lambda_{\text{QCD}}}$. It is then a good approximation to treat QCD evolution effects exactly (to the order in which they are needed), while for QED we only keep the terms in the anomalous dimension giving rise to Sudakov double logarithms, which can be derived using the results of [99]. In this approximation, the relevant RG equations are diagonal and given by

$$\begin{aligned} \frac{d}{d \ln \mu} H_i^B(y, \mu) &= \left[\gamma_{\text{hl}}(\alpha_s) - \frac{\alpha}{2\pi} \left(Q_\ell Q_b \ln \frac{\mu^2}{m_B^2} + \dots \right) \right] H_i^B(y, \mu); \quad i = 1, 2, \\ \frac{d}{d \ln \mu} H_i^C(y, \mu) &= \left[\gamma^A(y, \alpha_s) - \frac{\alpha}{2\pi} \left(Q_\ell Q_b \ln \frac{\mu^2}{(1-y)^2 m_B^2} + Q_b Q_u \ln \frac{\mu^2}{y^2 m_B^2} + \dots \right) \right] H_i^C(y, \mu), \end{aligned} \quad (3.85)$$

where the dots indicate the neglected, non-logarithmic QED contributions. The QCD evolution of the type- C hard functions is governed by the universal anomalous dimension $\gamma^A(\alpha_s)$

of heavy-light current operators in SCET [96, 97, 100, 101],⁵ which takes the general form

$$\gamma^A(y, \alpha_s) = -\frac{C_F}{2} \gamma_{\text{cusp}}(\alpha_s) \ln \frac{\mu^2}{y^2 m_B^2} + \tilde{\gamma}(\alpha_s). \quad (3.86)$$

Here

$$\gamma_{\text{cusp}}(\alpha_s) = \frac{\alpha_s}{\pi} + \left(\frac{268}{3} - 4\pi^2 - \frac{9}{40} n_f \right) \left(\frac{\alpha_s}{4\pi} \right)^2 + \mathcal{O}(\alpha_s^3) \quad (3.87)$$

denotes the light-like cusp anomalous dimension [102, 103], where again we have set $N_c = 3$ in the two-loop coefficient, and

$$\tilde{\gamma}(\alpha_s) = -5C_F \frac{\alpha_s}{4\pi} + \mathcal{O}(\alpha_s^2). \quad (3.88)$$

Note that the QED Sudakov evolution of the type- C hard functions is different from that of the type- A and type- B hard functions.

The solutions to the (approximate) evolution equations for the type- B coefficients in (3.85) reads

$$\begin{aligned} H_1^B(y, \mu) &= U_{\text{hl}}(\mu, m_B) \exp \left[-Q_\ell Q_b \frac{\alpha}{8\pi} \ln^2 \frac{\mu^2}{m_B^2} \right] \left(\frac{Q_u}{y} - Q_\ell \right), \\ H_2^B(y, \mu) &= U_{\text{hl}}(\mu, m_B) \exp \left[-Q_\ell Q_b \frac{\alpha}{8\pi} \ln^2 \frac{\mu^2}{m_B^2} \right] z Q_b, \end{aligned} \quad (3.89)$$

where

$$U_{\text{hl}}(\mu, m_B) = \left(\frac{\alpha_s(\mu)}{\alpha_s(m_B)} \right)^{-\frac{\gamma_0^{\text{hl}}}{2\beta_0}} \left[1 - \frac{\gamma_1^{\text{hl}} \beta_0 - \gamma_0^{\text{hl}} \beta_1}{2\beta_0^2} \frac{\alpha_s(\mu) - \alpha_s(m_B)}{4\pi} + \dots \right] \quad (3.90)$$

encodes the QCD evolution at NLO in RG-improved perturbation theory. The one- and two-loop coefficients $\gamma_0^{\text{hl}}, \gamma_1^{\text{hl}}$ of the anomalous dimension (expanded in powers of $\alpha_s/4\pi$) can be read off from (3.84), and β_0, β_1 denote the one- and two-loop coefficients of the QCD β -function. Corrections to the above solutions arise first at order α_s or $\alpha \ln(\mu^2/m_B^2)$ times the terms of order $[\alpha_s \ln(\mu^2/m_B^2)]^n$ and $[\alpha \ln^2(\mu^2/m_B^2)]^n$, which we have resummed to all orders, and hence it is consistent to drop the two-loop terms in (3.90).

For the solutions to the (approximate) evolution equations for the relevant type- C coefficients, we find

$$\begin{aligned} H_1^C(y, \mu) &= \frac{U_C(\mu, m_B, y)}{1-y} \exp \left[-Q_b^2 \frac{\alpha}{8\pi} \ln^2 \frac{\mu^2}{m_B^2} \right], \\ H_3^C(y, \mu) &= \frac{U_C(\mu, m_B, y)}{y} \exp \left[-Q_b^2 \frac{\alpha}{8\pi} \ln^2 \frac{\mu^2}{m_B^2} \right], \\ H_4^C(y, \mu) &= -\frac{U_C(\mu, m_B, y)}{1-y} \exp \left[-Q_b^2 \frac{\alpha}{8\pi} \ln^2 \frac{\mu^2}{m_B^2} \right], \end{aligned} \quad (3.91)$$

⁵Specifically, the quark current appearing in the operators $O_{1,4}^C$ can be related to $\bar{n}_\mu J_{V1}^{A\mu}$, the quark current appearing in the operators $O_{2,5}^C$ can be related to J_S^A and $\bar{n}_\mu J_{V2}^{A\mu}$, and the quark current appearing in the operator O_3^C can be related to the operator $g_{\perp\mu}^\alpha J_{V3}^{A\mu}$ in the notation of [101].

where

$$U_C(\mu, m_B, y) = \exp \left[C_F S_{\gamma_{\text{cusp}}}(m_B, \mu) - \frac{C_F \gamma_0 \ln y + \tilde{\gamma}_0}{2\beta_0} \ln \frac{\alpha_s(\mu)}{\alpha_s(m_B)} \right]. \quad (3.92)$$

The Sudakov exponent [104]

$$S_{\gamma_{\text{cusp}}}(m_B, \mu) = \frac{\gamma_0}{4\beta_0^2} \left[\frac{4\pi}{\alpha_s(m_B)} \left(1 - \frac{1}{r} - \ln r \right) + \left(\frac{\gamma_1}{\gamma_0} - \frac{\beta_1}{\beta_0} \right) (1 - r + \ln r) + \frac{\beta_1}{2\beta_0^2} \ln^2 r + \dots \right] \quad (3.93)$$

with $r = \alpha_s(\mu)/\alpha_s(m_B)$ encodes the QCD evolution at LO in RG-improved perturbation theory. The one- and two-loop coefficients γ_0 and γ_1 of the cusp anomalous dimension can be read off from (3.87) and the one-loop coefficient $\tilde{\gamma}_0$ from (3.88). We have neglected the y dependence of the QED Sudakov logarithms, which is an effect beyond our accuracy. Note the interesting fact that, for $\mu < m_B$, QCD resummation leads to a power-like divergence of the evolution function for $y \rightarrow 0$, such that

$$U_C(\mu, m_B, y) = U_C(\mu, m_B) y^{-\delta(\mu)}, \quad \text{with} \quad \delta(\mu) = \frac{C_F \gamma_0}{2\beta_0} \ln \frac{\alpha_s(\mu)}{\alpha_s(m_B)}, \quad (3.94)$$

where $U_C(\mu, m_B) \equiv U_C(\mu, m_B, 1)$. Once again, corrections to the above solutions arise first at order α_s or $\alpha \ln(\mu^2/m_B^2)$ times the terms resummed in the exponentials in (3.92) and (3.93).

As indicated in Table 1, the contributions of the type- B and type- C operators to the $B^- \rightarrow \ell^- \bar{\nu}_\ell$ decay amplitude receive an additional $\mathcal{O}(\alpha)$ suppression from (hard-)collinear photon loops, implying that these contributions are determined up to higher-order terms scaling as $\alpha\alpha_s$ or $\alpha^2 \ln(\mu^2/m_B^2)$ times the exponentiated terms. We emphasize that the solutions in (3.91) are derived under the assumption that the dimensionless variable y can be treated as an $\mathcal{O}(1)$ quantity. In cases where the functions $H_i^C(y, \mu)$ enter convolution integrals in which the region $y \ll 1$ is unsuppressed, it will be necessary to generalize these solutions (see Section 4.6 below).

We now turn to the solution of the evolution equations (3.83), which with the explicit results for the RG-evolved hard functions H_i^B and H_i^C take the form

$$\begin{aligned} \frac{d}{d \ln \mu} H_1^A(\mu) &= \gamma_{\text{hl}}(\alpha_s) H_1^A(\mu) - \frac{\alpha}{2\pi} \left[Q_\ell Q_b \ln \frac{\mu^2}{m_B^2} - 2Q_\ell^2 + \frac{3}{2} Q_b^2 + 3Q_\ell Q_u \right] H_1^A(\mu) \\ &\quad + Q_\ell (2Q_u - Q_\ell) \frac{\alpha}{2\pi} U_{\text{hl}}(\mu, m_B) \exp \left[-Q_\ell Q_b \frac{\alpha}{8\pi} \ln^2 \frac{\mu^2}{m_B^2} \right] \\ &\quad + Q_\ell Q_u \frac{\alpha}{\pi} \frac{U_C(\mu, m_B)}{1 - \delta(\mu)} \exp \left[-Q_b^2 \frac{\alpha}{8\pi} \ln^2 \frac{\mu^2}{m_B^2} \right], \end{aligned} \quad (3.95)$$

$$\begin{aligned} \frac{d}{d \ln \mu} H_2^A(\mu) &= \gamma_{\text{hl}}(\alpha_s) H_2^A(\mu) - \frac{\alpha}{2\pi} \left[Q_\ell Q_b \ln \frac{\mu^2}{m_B^2} \right] H_2^A(\mu) \\ &\quad + z Q_\ell Q_b \frac{\alpha}{2\pi} U_{\text{hl}}(\mu, m_B) \exp \left[-Q_\ell Q_b \frac{\alpha}{8\pi} \ln^2 \frac{\mu^2}{m_B^2} \right]. \end{aligned}$$

In the inhomogeneous terms of these equations, we are able to include the leading logarithmic QCD corrections to the terms multiplying α , as encoded in the evolution functions $U_{\text{hl}}(\mu, m_B)$

and $U_C(\mu, m_B)$. Unfortunately, the corresponding corrections to the homogeneous terms in the first line of each equation are not yet known. They would require a two-loop calculation of the contributions to the anomalous dimensions Γ_{ii}^{AA} of $\mathcal{O}(\alpha\alpha_s)$. In Section 4.9, we will be able to bootstrap the leading higher-order terms from the requirement of RG invariance.

Given the accuracy of the expressions for the type- B and C hard functions indicated above, the solutions for H_i^A obtained from these equations will (at most) be accurate up to, but not including, corrections of order α_s^2 , $\alpha\alpha_s \ln(\mu^2/m_B^2)$, or $\alpha^2 \ln^2(\mu^2/m_B^2)$ times the exponentiated terms. Explicitly, the solutions are

$$\begin{aligned}
H_1^A(\mu) &= U_{\text{hl}}(\mu, m_B) \exp \left[-Q_\ell Q_b \frac{\alpha}{8\pi} \ln^2 \frac{\mu^2}{m_B^2} \right] \\
&\quad \times \left[H_1^A(m_B) + \frac{\alpha}{4\pi} \left(Q_\ell^2 - \frac{3}{2} Q_b^2 - Q_\ell Q_u \right) \ln \frac{\mu^2}{m_B^2} + Q_\ell Q_u \frac{\alpha}{\pi} \int_{m_B}^{\mu} \frac{d\mu'}{\mu'} \frac{\tilde{U}_C(\mu', m_B)}{1 - \delta(\mu')} \right], \\
H_2^A(\mu) &= U_{\text{hl}}(\mu, m_B) \exp \left[-Q_\ell Q_b \frac{\alpha}{8\pi} \ln^2 \frac{\mu^2}{m_B^2} \right] \left[H_2^A(m_B) + z Q_\ell Q_b \frac{\alpha}{4\pi} \ln \frac{\mu^2}{m_B^2} \right],
\end{aligned} \tag{3.96}$$

where

$$\tilde{U}_C(\mu, m_B) \equiv \frac{U_C(\mu, m_B)}{U_{\text{hl}}(\mu, m_B)} \exp \left[-Q_b Q_u \frac{\alpha}{8\pi} \ln^2 \frac{\mu^2}{m_B^2} \right], \tag{3.97}$$

and we have expanded out the single-logarithmic QED corrections in the exponent of the first result. The initial conditions at the scale m_B are given by

$$\begin{aligned}
H_1^A(m_B) &= 1 - 3C_F \frac{\alpha_s(m_B)}{4\pi} (1 + \ln z) \\
&\quad - \frac{Q_b \alpha}{4\pi} \left\{ Q_\ell \left[-\frac{z \ln z}{z-1} + 2\text{Li}_2(1-z) + 1 + \frac{\pi^2}{12} \right] + Q_b (2 + 3 \ln z) + Q_u \right\} \\
&\quad - Q_\ell Q_u \frac{\alpha}{\pi} - Q_\ell (Q_b + Q_u) \frac{\alpha}{16\pi} \kappa, \\
H_2^A(m_B) &= C_F \frac{\alpha_s(m_B)}{4\pi} + \frac{Q_b \alpha}{4\pi} \left[Q_u + z Q_\ell \left(\ln z + \frac{z-1}{z} \right) \right].
\end{aligned} \tag{3.98}$$

In (3.96), we neglect the running of α , which is a tiny effect in the scale window between m_B and a typical hard-collinear scale. Since the hard function H_1^A starts at tree level, we must keep the two-loop coefficient in (3.90) for consistency in the first equation.

4 Matching to SCET-2

At a hard-collinear scale $\mu_{hc} \sim \sqrt{m_B \Lambda_{\text{QCD}}}$, the SCET-1 basis operators listed in Section 3.2 are matched onto operators in SCET-2, consisting of soft and collinear fields with virtualities of order Λ_{QCD} and m_ℓ , respectively, and momenta scaling as

$$p_s^\mu \sim m_B (\lambda, \lambda, \lambda), \quad p_c^\mu \sim m_B (\lambda_\ell^2, 1, \lambda_\ell). \quad (4.1)$$

Soft and collinear fields do not interact with one another in SCET-2, since such interactions would violate momentum conservation. The sum of a soft momentum and a collinear momentum produces an off-shell momentum with hard-collinear scaling $(p_s^\mu + p_c^\mu) \sim (\lambda, 1, \dots)$, where the perpendicular component scales like λ or λ_ℓ , whichever is larger. Such hard-collinear fluctuations are integrated out in the matching from SCET-1 onto SCET-2. This argument holds irrespectively of whether the charged lepton is a muon, for which $\lambda_\ell \sim \lambda$, or an electron, for which $\lambda_\ell \ll \lambda$.

The operators in SCET-2 can be conveniently written in terms of gauge-invariant building blocks of fields, which are invariant under soft and collinear gauge transformations [69, 86]. The soft quark and gluon fields can be grouped into hadronic current operators, whereas the collinear lepton and photon fields, along with the anti-collinear neutrino field, can be grouped into leptonic currents. The two currents are decoupled from each other and do not interact.

Already in SCET-1, the interactions coupling hard-collinear to soft fields can be removed from the leading-order effective Lagrangian by means of the field redefinitions [68]

$$\begin{aligned} \bar{\mathcal{X}}_{hc}^{(\ell)}(x + t\bar{n}) &\rightarrow \bar{\mathcal{X}}_{hc}^{(\ell),(0)}(x + t\bar{n}) Y_n^{(\ell)\dagger}(x_-), \\ \bar{\mathcal{X}}_{hc}^{(u)}(x + t\bar{n}) &\rightarrow \bar{\mathcal{X}}_{hc}^{(u),(0)}(x + t\bar{n}) \bar{Y}_n^{(u)\dagger}(x_-), \\ \mathcal{A}_{hc}^{(f)\perp}(x + t\bar{n}) &\rightarrow \mathcal{A}_{hc}^{(f)\perp,(0)}(x + t\bar{n}), \\ \mathcal{G}_{hc}^\perp(x + t\bar{n}) &\rightarrow \bar{Y}_n(x_-) \mathcal{G}_{hc}^{\perp,(0)}(x + t\bar{n}) \bar{Y}_n^\dagger(x_-), \end{aligned} \quad (4.2)$$

with $f = \ell, u, b$ denoting the charged fermions. Following [23, 105–107], we define the QCD soft Wilson lines for initial-state hard-collinear particles as

$$\begin{aligned} \bar{Y}_n(x) &= \mathbf{P} \exp \left[+i g_s t^a \int_{-\infty}^0 ds n \cdot G_s^a(x + sn) e^{-\epsilon|s|} \right], \\ \bar{Y}_n^\dagger(x) &= \bar{\mathbf{P}} \exp \left[-i g_s t^a \int_{-\infty}^0 ds n \cdot G_s^a(x + sn) e^{-\epsilon|s|} \right], \end{aligned} \quad (4.3)$$

where the path ordering \mathbf{P} is such that fields are ordered from left to right according to decreasing values of s , and $\bar{\mathbf{P}}$ denotes the opposite ordering. The regulator $\epsilon > 0$ ensures that the integrals converge at infinity. The soft Wilson lines including QED effects for the initial-state anti-quark and the final-state charged lepton are given by

$$\begin{aligned} \bar{Y}_n^{(u)\dagger}(x) &= \exp \left[-i Q_u e \int_{-\infty}^0 ds n \cdot A_s(x + sn) e^{-\epsilon|s|} \right] \bar{Y}_n^\dagger(x), \\ Y_n^{(\ell)\dagger}(x) &= \exp \left[+i Q_\ell e \int_0^\infty ds n \cdot A_s(x + sn) e^{-\epsilon|s|} \right]. \end{aligned} \quad (4.4)$$

In SCET-1, soft fields and Wilson lines interacting with hard-collinear fields need to be multipole-expanded in such a way that only the $n \cdot k_s$ component of soft momenta enter the interaction vertices [70, 89]. The soft Wilson lines and gauge fields must therefore be evaluated at the spacetime point $x_-^\mu \equiv \frac{\bar{n} \cdot x}{2} n^\mu$ rather than at x^μ . Note that the displacement vector $t\bar{n}$ in the argument of the hard-collinear fields does not contribute to x_- . The superscript “(0)” on the fields appearing on the right-hand side of (4.2) indicates that the new hard-collinear fields are decoupled from leading-order soft interactions. Importantly, interactions among hard-collinear and soft fields are still allowed at subleading order in power counting. In the matching to SCET-2, the off-shell hard-collinear fields are integrated out, leaving effective operators built out of decoupled soft and collinear fields [80–82].

For the operators $O_{3,4}^C$, one further needs the relations

$$\begin{aligned} \bar{\mathcal{X}}_{hc}^{(u)}(x+t\bar{n})(-i\overleftarrow{D}_{s\perp}^\alpha) &\rightarrow \bar{\mathcal{X}}_{hc}^{(u),(0)}(x+t\bar{n})(-i\overleftarrow{\partial}_{s\perp}^\alpha + \mathcal{G}_{s\perp}^\alpha(x_-) + Q_u \mathcal{A}_{s\perp}^\alpha(x_-)) \bar{Y}_n^{(u)\dagger}(x_-), \\ \bar{\mathcal{X}}_{hc}^{(\ell)}(x+t\bar{n})(-i\overleftarrow{\mathcal{D}}_{s\perp}) &\rightarrow \bar{\mathcal{X}}_{hc}^{(\ell),(0)}(x+t\bar{n})(-i\overleftarrow{\phi}_s^\perp + Q_\ell \mathcal{A}_s^\perp(x_-)) Y_n^{(\ell)\dagger}(x_-), \end{aligned} \quad (4.5)$$

where the gauge-invariant building blocks for the soft gauge fields are defined as [86]

$$\begin{aligned} \mathcal{G}_s^\mu(x) &= \bar{Y}_n^\dagger(x) [iD_s^\mu \bar{Y}_n(x)] = g_s \int_{-\infty}^0 ds n_\alpha [\bar{Y}_n^\dagger G_s^{\alpha\mu} \bar{Y}_n](x+sn) \equiv t^a \mathcal{G}_s^{\mu,a}(x), \\ \mathcal{A}_s^\mu(x) &= \frac{1}{Q_\ell} Y_n^{(\ell)\dagger}(x) [iD_s^\mu Y_n^{(\ell)}(x)] = e \int_{-\infty}^0 ds n_\alpha F_s^{\alpha\mu}(x+sn). \end{aligned} \quad (4.6)$$

For the abelian gauge field, the soft Wilson lines commute with $F_s^{\alpha\mu}$ and cancel out.

4.1 Systematics of the SCET-1 \rightarrow SCET-2 matching

At tree level, the SCET-1 to SCET-2 matching relations for hard-collinear fields have been studied in detail in [81, 82]. Besides the trivial possibility, in which the decoupled hard-collinear fields with superscript “(0)” in (4.2) are simply replaced by the corresponding collinear fields, we note the relation

$$\bar{\mathcal{X}}_{hc}^{(u),(0)}(x+t\bar{n}) \rightarrow -\frac{Q_u}{2} (\bar{u}_s \bar{Y}_n^{(u)})(x_-) \frac{\not{n}}{in \cdot \overleftarrow{\partial}_s} (\mathcal{G}_c^\perp(x+t\bar{n}) + Q_u \mathcal{A}_c^\perp(x+t\bar{n})) + \dots, \quad (4.7)$$

in which a hard-collinear fermion splits into a soft quark and a collinear gauge field. The dots represent terms with higher power suppression. These tree-level matching relations are summarized in Table 2. The virtuality of collinear fields in SCET-2 is set by the mass of the charged lepton, and hence the power-counting rules for the collinear fields are

$$\mathcal{X}_c^{(\ell)} \sim \lambda_\ell, \quad \mathcal{A}_c^\perp \sim \lambda_\ell, \quad (4.8)$$

with $\lambda_\ell \sim m_\ell/m_B$. Integrating out hard-collinear propagators can introduce inverse soft derivatives $(in \cdot \overleftarrow{\partial}_s)^{-1} \sim \lambda^{-1}$ in the SCET-2 operators, as shown in (4.7). This has the effect of delocalizing the soft fields along the n light-cone, i.e., the direction of motion of

SCET-1 field	power counting	SCET-2 field	power counting	cost factor
$\bar{\mathcal{X}}_{hc}^{(\ell)}$	$\lambda^{\frac{1}{2}}$	$\bar{\mathcal{X}}_c^{(\ell)}$	λ_ℓ	$\lambda_\ell \lambda^{-\frac{1}{2}}$
\mathcal{A}_{hc}^\perp	$\lambda^{\frac{1}{2}}$	\mathcal{A}_c^\perp	λ_ℓ	$\lambda_\ell \lambda^{-\frac{1}{2}}$
$\bar{\mathcal{X}}_{hc}^{(u)}$	$\lambda^{\frac{1}{2}}$	$\bar{u}_s \mathcal{A}_c^\perp$	$\lambda_\ell \lambda^{\frac{1}{2}}$	λ_ℓ
$\bar{\mathcal{X}}_{hc}^{(\ell)}$	$\lambda^{\frac{1}{2}}$	$\bar{\mathcal{X}}_c^{(\ell)} \mathcal{A}_s^\perp$	λ_ℓ^2	$\lambda_\ell^2 \lambda^{-\frac{1}{2}}$

Table 2: Relevant tree-level matching relations for hard-collinear fields splitting into collinear and soft fields in SCET-2. Here \mathcal{A}_{hc}^\perp and \mathcal{A}_c^\perp refer to generic gauge bosons (gluons or photons). Additional soft gauge fields are contained in the SCET-2 Wilson lines (not shown). In all cases, adding extra fields implies a higher-order scaling with λ and λ_ℓ .

the charged lepton. The inverse derivative lifts the power-suppression of the soft quark field $\bar{u}_s \sim \lambda^{\frac{3}{2}}$ relative to the hard-collinear quark field $\bar{\mathcal{X}}_{hc}^{(u)} \sim \lambda^{\frac{1}{2}}$. At first sight, it would seem that multiple inverse soft derivatives could upset the power counting in SCET-2. However, reparameterization invariance forces every inverse factor of $in \cdot \partial_s$ to be compensated by a power of n in the numerator. The fact that $n^2 = 0$ then restricts the number of operators and ensures that SCET-2 operators are always power-suppressed relative to the SCET-1 operators they descend from [82].

We will now study in detail which SCET-2 operators can descend from the operators contained in the SCET-1 operator basis constructed in Section 3.2. For the operators of type-*A* and the type-*B* operators $O_{1,2}^B$ in the SCET-1 basis, there is no hard-collinear momentum flow between the quark and lepton currents. This implies that all hard-collinear loop diagrams are scaleless and vanish in dimensional regularization. The tree-level matching relations discussed above are then all that is needed to derive the corresponding expressions for the SCET-2 operators, in which all hard-collinear fields are simply replaced by collinear fields times the appropriate soft Wilson lines. Using the rules given in Table 2, one finds that these operators scale like⁶ $\lambda_\ell^2 \lambda^3$. Adding additional fields or derivatives in the SCET-2 operators would give rise to additional power suppression. In particular, the transition $\bar{\mathcal{X}}_{hc}^{(\ell)} \rightarrow \bar{\mathcal{X}}_c^{(\ell)} \mathcal{A}_s^\perp$ produces a pair of SCET-2 fields with power counting λ_ℓ^2 , which implies a higher cost factor (see Table 2). The emission of the additional soft photon is thus a power-suppressed effect, which can be neglected. The descendants of the operators $O_{3,4}^A$ involve the leptonic current

$$\bar{\mathcal{X}}_{hc}^{(\ell)} (-i \overleftarrow{\partial}_\perp) P_L \nu_{\bar{c}} = \bar{\mathcal{X}}_{hc}^{(\ell)} (-i \overleftarrow{\partial}_\rho^\perp) \gamma_\perp^\rho P_L \nu_{\bar{c}}, \quad (4.9)$$

whose matrix element vanishes to all orders of perturbation theory, because we work in a reference frame where $p_\ell^\perp = 0$. Hence, these two operators can be omitted from the SCET-2 basis. The operators $O_{3,4}^B$ contain a hard-collinear gluon field, which needs to be converted into a hard-collinear photon field before the hard-collinear momentum can be transferred from the quark current to the lepton current. As shown in Figure 7, this conversion involves at

⁶Recall that the external *B*-meson and charged-lepton states have power counting $\lambda^{-\frac{3}{2}}$ and λ_ℓ^{-1} , respectively, so that the decay amplitude scales like $\lambda_\ell \lambda^{\frac{3}{2}}$, which is indeed the scaling of the product $m_\ell f_B$.

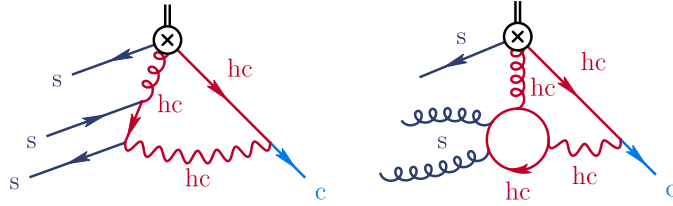


Figure 7: Representative hard-collinear loop diagrams for the matching of type- B SCET-1 operators onto SCET-2. Red (dark blue) lines represent hard-collinear (soft) propagators and external states. Light blue lines represent collinear external states. The double line at the vertex represents the b -quark and neutrino fields.

least two power-suppressed interactions, yielding SCET-2 operators which are suppressed by (at least) a factor λ with respect to $O_{1,2}^B$. In other words, the descendants of the operators $O_{3,4}^B$ do not match onto the leading-power SCET-2 operator basis.

For the remaining operators in the SCET-1 basis, it is straightforward to check that using the tree-level matching relations one obtains SCET-2 operators that are either power suppressed beyond $\mathcal{O}(\lambda_\ell^2 \lambda^3)$ or have a vanishing projection onto the B meson. The only non-trivial case is the operator O_3^C , for which the application of the tree-level matching relation (4.7) yields the SCET-2 operator (omitting spacetime arguments)

$$O_3^C \rightarrow -\frac{Q_u}{2} \frac{1}{\bar{n} \cdot \mathcal{P}_c} (\bar{u}_s \bar{Y}_n^{(u)}) \frac{\not{n}}{in \cdot \partial_s} \gamma_\perp^\beta (-i \overleftarrow{\partial}_{s\perp}^\alpha + \mathcal{G}_{s\perp}^\alpha + Q_u \mathcal{A}_{s\perp}^\alpha) \not{n} P_L Y_n^{(\ell)\dagger} \bar{Y}_n^{(u)\dagger} b_\nu \times \bar{X}_c^{(\ell)} \mathcal{A}_{c,\beta[y]}^\perp \gamma_\alpha^\perp P_L \nu_{\bar{c}}, \quad (4.10)$$

which indeed exhibits the correct scaling $\lambda_\ell^2 \lambda^3$. We can now use the fact that the external B -meson and lepton states have vanishing transverse momenta. Lorentz invariance then requires that the B -meson matrix element of the quark operator in the first line of this expression, and the lepton matrix element of the fermion bilinear in the second line, each contain two components multiplying $g_\perp^{\alpha\beta}$ and $i\epsilon_\perp^{\alpha\beta}$. Performing appropriate contractions of these matrix elements and using the relations (3.23), it is straightforward to show that the hadronic matrix element is proportional to $\Pi_+^{\alpha\beta}$ and the leptonic one to $\Pi_{-\beta\alpha}$, where

$$\Pi_\pm^{\alpha\beta} \equiv \frac{g_\perp^{\alpha\beta} \pm i\epsilon_\perp^{\alpha\beta}}{2}. \quad (4.11)$$

The fact that $\Pi_+^{\alpha\beta} \Pi_-^{\beta\alpha} = 0$ implies that the tree-level matching relation for the operator O_3^C indeed vanishes when projected onto the B meson.

It is therefore necessary to extend the matching beyond the tree approximation. The present work is one of the first where the SCET-1 \rightarrow SCET-2 matching relations are calculated at one-loop order. In this case, one needs to consider the matching relations for products of hard-collinear fields rather than individual fields. These relations involve loop diagrams, in which the exchange of a hard-collinear photon transfers the hard-collinear momentum from the quark current to the lepton current, as illustrated in Figure 8. This matching can be formalized by introducing an intermediate effective theory containing (off-shell) hard-collinear

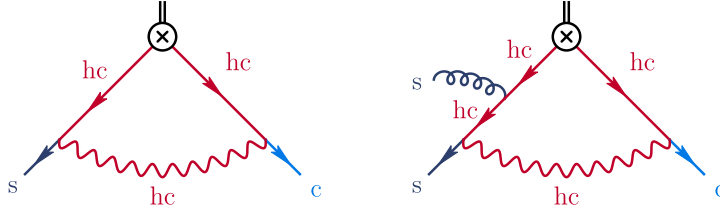


Figure 8: One-loop exchange of a hard-collinear photon, converting a hard-collinear to a soft quark. Red (dark blue) lines represent hard-collinear (soft) propagators and external states. Light blue lines represent collinear external states.

fields along with (on-shell) collinear fields and soft fields, and then integrating out the off-shell collinear fields [81, 82]. Here we use symmetry arguments to constrain the form of the resulting operators, based on the following observations:

1. Every SCET-1 \rightarrow SCET-2 matching relation must contain at least one collinear and one soft field on the right-hand side to conserve momentum, where the soft field can also appear in the form of a soft Wilson line.
2. The matching relation for a hard-collinear fermion field must vanish when multiplied with \not{n} .
3. The matching relation for a massless hard-collinear fermion field must preserve chirality.
4. The matching relation for a collection of hard-collinear fields must preserve the total mass dimension of the fields.
5. The B -meson 4-velocity v^μ does not appear in SCET-1 \rightarrow SCET-2 matching relations.

The latter condition follows from the fact that the effective b -quark field b_v solely participates in soft interactions, while only hard-collinear interactions contribute to the matching. It ensures that there can be at most one inverse soft derivative, since the reparameterization-invariant combination $n \cdot v / (in \cdot \overleftarrow{\partial}_s)$ cannot appear.

Conditions 2 and 3 imply that, to all orders of perturbation theory, a matching relation for a massless hard-collinear quark field onto a soft quark field must be of the form⁷

$$\bar{\chi}_{hc}^{(u),(0)} \dots \rightarrow (\bar{u}_s \bar{Y}_n^{(u)}) \frac{\not{n}}{in \cdot \overleftarrow{\partial}_s} \gamma_\perp^\rho \dots \quad \text{or} \quad \bar{\chi}_{hc}^{(u),(0)} \dots \rightarrow (\bar{u}_s \bar{Y}_n^{(u)}) \frac{\not{n} \not{n}}{4} \dots, \quad (4.12)$$

where in the first case the mass dimension is lowered by one unit and an open transverse Lorentz index appears. In the SCET-1 basis, operators involving hard-collinear quark and leptons fields can have up to two additional transverse hard-collinear objects (derivatives or gauge fields), which also carry mass dimension and transverse Lorentz indices. The 17 basis

⁷Beyond one-loop order additional pairs of transverse Dirac matrices can appear, but they can be reduced to the expressions shown above using the relations (3.23) and (3.25), apart from evanescent structures that do not appear in the physical operator basis.

operators involving hard-collinear quark and leptons fields can be written as collections of hard-collinear fields times one of the following four Dirac structures:

$$\begin{aligned}
S_1 : & \quad \not{n} P_L b_v \otimes P_L \nu_{\bar{e}} && (\text{operator } O_1^C) \\
S_2 : & \quad \gamma_{\perp}^{\alpha} \not{n} P_R b_v \otimes P_L \nu_{\bar{e}} && (\text{operators } O_2^C, O_{1,2}^D) \\
S_3 : & \quad \not{n} P_L b_v \otimes \gamma_{\perp}^{\alpha} P_L \nu_{\bar{e}} && (\text{operators } O_{3,4}^C, O_{3,4}^D) \\
S_4 : & \quad \gamma_{\perp}^{\alpha} \not{n} P_R b_v \otimes \gamma_{\perp}^{\beta} P_L \nu_{\bar{e}} && (\text{operators } O_5^C, O_{5,6,7,8}^D, O_{1,2,3,4}^E)
\end{aligned} \tag{4.13}$$

where the indices α, β are those of hard-collinear derivatives or gauge fields entering the loop function. Since neither the b quark nor the neutrino participate in the matching, these structures can only be modified from their left-hand sides in each current. Matching the hard-collinear quark field to a soft quark field yields one of the two structures in (4.12). For the hard-collinear lepton field, the possible matching relations are

$$\bar{\mathcal{X}}_{hc}^{(\ell),(0)} \dots \rightarrow \bar{\mathcal{X}}_c^{(\ell)} \dots \quad \text{or} \quad \bar{\mathcal{X}}_{hc}^{(\ell),(0)} \dots \rightarrow m_{\ell} \bar{\mathcal{X}}_c^{(\ell)} \gamma_{\perp}^{\sigma} \dots, \tag{4.14}$$

where the factor of the lepton mass in the second relation requires a chirality flip and hence an extra Dirac matrix. The hard-collinear loop functions carry the open transverse Lorentz indices in such a way that in the end all indices are contracted.

It is now a simple matter to combine the various possibilities in (4.12) and (4.14) with the four structures in (4.13) in such a way that the overall mass dimension is preserved and the quark current does not contain an odd number of open transverse indices, since otherwise it would have a vanishing projection onto the B meson. The resulting structures are summarized in Table 3, omitting the fermion fields and soft Wilson lines. Extra derivatives, gauge fields and factors of the lepton mass needed to obtain the correct mass dimension and a non-zero projection onto the B -meson and lepton states are colored in blue. When there are two options a and b , they are given in the form of a list as (a, b) . In the second line of each expression, we show the results obtained after projection onto the B -meson and lepton matrix elements. A few comments are in order:

- The transverse index ρ in the first structure for S_1 can in principle be contracted with a transverse derivative, a transverse soft or collinear gauge field, or an extra Dirac matrix in the lepton current, which changes the chirality and comes along with a factor m_{ℓ} . However, in order to obtain a non-zero projection onto the B meson, only a soft derivative or a soft gauge field are allowed.
- In an analogous way, the first structure for S_3 requires an extra soft derivative or a soft gauge field for a non-zero projection on the B meson, In addition, one needs an additional mass insertion or a collinear gauge field to ensure a non-zero leptonic matrix element.
- In the case of the structures S_2 and S_4 , it is possible to add a factor of the hard-collinear virtuality $\bar{n} \cdot \mathcal{P}_c \text{in} \cdot \overleftarrow{\partial}_s$ with mass dimension 2 in the numerator and still obtain a non-vanishing projection onto the B meson. Compared to this, insertions of two transverse objects would yield power-suppressed corrections.

	$\frac{\not{n}}{in \cdot \overleftarrow{\partial}_s} \gamma_\perp^\rho \dots$	$\frac{\not{n} \not{n}}{4} \dots$
S_1	$(i\overleftarrow{\partial}_{s\perp}^\sigma, \mathcal{G}_{s\perp}^\sigma) \frac{\not{n}}{in \cdot \overleftarrow{\partial}_s} \gamma_\perp^\rho \not{n} P_L \otimes P_L$ $\rightarrow -\Pi_-^{\rho\sigma} \frac{\not{n} \not{n}}{in \cdot \overleftarrow{\partial}_s} (i\overleftarrow{\partial}_s^\perp, \mathcal{G}_s^\perp) P_L \otimes P_L$	$\not{n} P_L \otimes P_L$
S_2	$\bar{n} \cdot \mathcal{P}_c in \cdot \overleftarrow{\partial}_s \frac{\not{n}}{in \cdot \overleftarrow{\partial}_s} \gamma_\perp^\rho \gamma_\perp^\alpha \not{n} P_R \otimes P_L$ $\rightarrow \Pi_-^{\rho\alpha} \bar{n} \cdot \mathcal{P}_c \not{n} \not{n} P_R \otimes P_L$	–
S_3	$(i\overleftarrow{\partial}_{s\perp}^\sigma, \mathcal{G}_{s\perp}^\sigma) \frac{\not{n}}{in \cdot \overleftarrow{\partial}_s} \gamma_\perp^\rho \not{n} P_L \otimes (m_\ell \gamma_\perp^\gamma, \mathcal{A}_{c\perp}^\gamma) \gamma_\perp^\alpha P_L$ $\rightarrow -\Pi_-^{\rho\sigma} \Pi_+^{\alpha\gamma} \frac{\not{n} \not{n}}{in \cdot \overleftarrow{\partial}_s} (i\overleftarrow{\partial}_s^\perp, \mathcal{G}_s^\perp) P_L \otimes (m_\ell, \mathcal{A}_c^\perp) P_L$	$\not{n} P_L \otimes (m_\ell \gamma_\perp^\gamma, \mathcal{A}_{c\perp}^\gamma) \gamma_\perp^\alpha P_L$ $\rightarrow \Pi_+^{\alpha\gamma} \not{n} P_L \otimes (m_\ell, \mathcal{A}_c^\perp) P_L$
S_4	$\bar{n} \cdot \mathcal{P}_c in \cdot \overleftarrow{\partial}_s \frac{\not{n}}{in \cdot \overleftarrow{\partial}_s} \gamma_\perp^\rho \gamma_\perp^\alpha \not{n} P_R \otimes (m_\ell \gamma_\perp^\gamma, \mathcal{A}_{c\perp}^\gamma) \gamma_\perp^\beta P_L$ $\rightarrow \Pi_-^{\rho\alpha} \Pi_+^{\beta\gamma} \bar{n} \cdot \mathcal{P}_c \not{n} \not{n} P_R \otimes (m_\ell, \mathcal{A}_c^\perp) P_L$	–
S_5	$\frac{1}{\bar{n} \cdot \mathcal{P}_c} (i\overleftarrow{\partial}_{s\perp}^\sigma, \mathcal{G}_{s\perp}^\sigma) \frac{\not{n}}{in \cdot \overleftarrow{\partial}_s} \gamma_\perp^\rho \not{n} P_L \otimes m_\ell P_L$ $\rightarrow -\frac{\Pi_-^{\rho\sigma}}{\bar{n} \cdot \mathcal{P}_c} \frac{\not{n} \not{n}}{in \cdot \overleftarrow{\partial}_s} (i\overleftarrow{\partial}_s^\perp, \mathcal{G}_s^\perp) P_L \otimes m_\ell P_L$	$\frac{1}{\bar{n} \cdot \mathcal{P}_c} \not{n} P_L \otimes m_\ell P_L$

Table 3: Structures arising in the matching of the SCET-1 basis operators onto SCET-2. The two columns correspond to the two options for the matching of the hard-collinear quark field shown in (4.12). The fermion fields and soft Wilson lines are not shown for brevity. A gluon field can also be replaced by a photon field. Open Lorentz indices are contracted with those of the hard-collinear loop functions.

- The open transverse Lorentz indices in the obtained structures are contracted with open indices in the loop functions. In some cases, like in (4.7), this can give rise to vanishing results, because

$$\Pi_\pm^{\alpha\beta} g_{\beta\gamma}^\perp \Pi_\mp^{\gamma\delta} = 0. \quad (4.15)$$

We finally consider the case of the soft-lepton operator O_1^F in (3.33), which comes with the Dirac structure:

$$S_5 : \not{n} P_L b_v \otimes \not{n} P_L \nu_{\bar{c}} \quad (\text{operator } O_1^F) \quad (4.16)$$

For the hard-collinear quark field, the two options for the matching are those shown in (4.12). For the soft lepton field, on the other hand, the only option is

$$\bar{\ell}_s \dots \rightarrow m_\ell Y_n^{(\ell)\dagger} \bar{X}_c^{(\ell)} \frac{\not{n}}{\bar{n} \cdot \mathcal{P}_c} \dots \quad (4.17)$$

The presence of \not{n} is required in order to get a non-vanishing result, given the structure of S_5 . The lepton mass is generated from soft dynamics. Its presence requires a chirality flip and

hence a single additional Dirac matrix. Combining the two bilinears, and adding gauge fields or derivatives to ensure the correct mass dimension and non-zero B meson and lepton matrix elements, we find the options shown in the lowest row of Table 3.

4.2 Construction of the SCET-2 operator basis

We are now in a position to write down the complete SCET-2 operator basis for our problem, consisting of operators scaling as $\lambda_\ell^2 \lambda^3$ with a non-zero projection onto the B meson. The type- A and type- B operators $O_{1,2}^A$ and $O_{1,2}^B$ match trivially onto the corresponding SCET-2 operators

$$\begin{aligned}
Q_1^A &= \frac{m_\ell \bar{n} \cdot v}{\bar{n} \cdot \mathcal{P}_c} \left(\bar{u}_s \frac{\not{n}}{\bar{n} \cdot v} P_L b_v Y_n^{(\ell)\dagger} \right) \left(\bar{\chi}_c^{(\ell)} P_L \nu_{\bar{c}} \right), \\
Q_2^A &= \frac{m_\ell \bar{n} \cdot v}{\bar{n} \cdot \mathcal{P}_c} \left(\bar{u}_s \frac{\not{n}}{n \cdot v} P_L b_v Y_n^{(\ell)\dagger} \right) \left(\bar{\chi}_c^{(\ell)} P_L \nu_{\bar{c}} \right), \\
Q_1^B &= \frac{\bar{n} \cdot v}{\bar{n} \cdot \mathcal{P}_c} \left(\bar{u}_s \frac{\not{n}}{\bar{n} \cdot v} P_L b_v Y_n^{(\ell)\dagger} \right) \left(\bar{\chi}_c^{(\ell)} \mathcal{A}_{c[x]}^\perp P_L \nu_{\bar{c}} \right), \\
Q_2^B &= \frac{\bar{n} \cdot v}{\bar{n} \cdot \mathcal{P}_c} \left(\bar{u}_s \frac{\not{n}}{n \cdot v} P_L b_v Y_n^{(\ell)\dagger} \right) \left(\bar{\chi}_c^{(\ell)} \mathcal{A}_{c[x]}^\perp P_L \nu_{\bar{c}} \right).
\end{aligned} \tag{4.18}$$

No hard-collinear momentum transfer from the quark to the lepton side is involved in this matching. We refer to these operators as “local”, since all fermion fields are evaluated at the same spacetime point. Nonetheless, these operators still contain soft and collinear Wilson lines, which are non-local objects.

Before writing down the remaining basis operators, which result from the matching of the SCET-1 operators of type- C , D , E , and F containing a hard-collinear quark field, we need to discuss one more subtlety. When a SCET-1 operator is matched onto SCET-2 and hard-collinear propagators are integrated out, the presence of inverse soft derivatives implies that the soft fields (but not the heavy-quark field b_v) in the SCET-2 operators can be smeared out along the light-like direction n . According to Table 3, we find operators containing a soft anti-quark field $\bar{u}_s(x + sn)$ and up to one soft gauge field $\mathcal{A}_s(x + s'n)$. In analogy to the discussion in Section 3.1, we can write for a generic soft field

$$\phi_s^{(i)}(x + s_i n) = e^{-is_i n \cdot \mathcal{P}_s^{(i)}} \phi_s^{(i)}(x) = \int d\omega_i e^{-is_i n \cdot v \omega_i} \phi_{s[\omega_i]}^{(i)}(x). \tag{4.19}$$

where

$$\phi_{s[\omega_i]}^{(i)}(x) \equiv \delta\left(\omega_i - \frac{n \cdot \mathcal{P}_s^{(i)}}{n \cdot v}\right) \phi_s^{(i)}(x). \tag{4.20}$$

The operator $\mathcal{P}_s^{(i)}$ projects out the incoming momentum of the initial-state soft field. The auxiliary integration over ω_i is introduced to turn this operator into a light-cone momentum variable. The position-space jet functions arising as Wilson coefficients in the matching onto SCET-2 depend on the variables s_i , in the same way in which the position-space hard functions in (3.14) depend on the variables t_i . Performing the Fourier integrals over the displacements

s_i , one obtains the momentum-space jet functions $J_{O_i^X \rightarrow Q_j^{X'}}$ in the matching relations

$$O_i^X(\{\underline{y}\}, \mu) = \sum_{j, X'} J_{O_i^X \rightarrow Q_j^{X'}}(\{\underline{y}\}, \{\underline{x}\}, \{\underline{\omega}\}, \mu) \otimes Q_j^{X'}(\{\underline{x}\}, \{\underline{\omega}\}, \mu), \quad (4.21)$$

which now depend on the momentum variables ω_i conjugate to s_i . We use the notation $\{\underline{y}\} = \{y_1, \dots, y_n\}$ etc. for the lists of relevant momentum fractions y_i , x_i and momentum variables ω_i . The symbol \otimes implies an integration over the common variables $\{\underline{x}\}$ and $\{\underline{\omega}\}$ shared by the jet functions and the SCET-2 operators, where the variables x_i denote the collinear momentum fractions in case a SCET-2 operator contains more than one collinear field.

To construct the “non-local” SCET-2 basis operators for our problem, in which the various soft fields live at different spacetime points, we introduce gauge-invariant building blocks for the soft quark fields, defined as [18, 19]

$$\bar{Q}_s(x) = (\bar{u}_s \bar{Y}_n^{(u)})(x), \quad \mathcal{H}_v(x) = (Y_n^{(\ell)\dagger} \bar{Y}_n^{(u)\dagger} b_v)(x). \quad (4.22)$$

Note that the gauge-invariant building block for the heavy-quark field contains the soft Wilson lines arising from the field redefinitions of the hard-collinear fermion fields in (4.2). This ensures that \mathcal{H}_v is indeed invariant under QCD and QED gauge transformations, since $Q_\ell + Q_u = Q_b$. With these definitions, we find that the remaining SCET-1 operators of type- C , D , E and F match onto the operators

$$\begin{aligned} Q_1^C &= \frac{m_\ell \bar{n} \cdot v}{\bar{n} \cdot \mathcal{P}_c} (\bar{Q}_{s[\omega]} \frac{\not{n}}{\bar{n} \cdot v} P_L \mathcal{H}_v) (\bar{\mathcal{X}}_c^{(\ell)} P_L \nu_{\bar{c}}), \\ Q_2^C &= \frac{m_\ell \bar{n} \cdot v}{\bar{n} \cdot \mathcal{P}_c} (\bar{Q}_{s[\omega]} \frac{\not{n}}{n \cdot v} P_L \mathcal{H}_v) (\bar{\mathcal{X}}_c^{(\ell)} P_L \nu_{\bar{c}}), \\ Q_1^D &= \frac{\bar{n} \cdot v}{\bar{n} \cdot \mathcal{P}_c} (\bar{Q}_{s[\omega]} \frac{\not{n}}{\bar{n} \cdot v} P_L \mathcal{H}_v) (\bar{\mathcal{X}}_c^{(\ell)} \mathcal{A}_{c[x]}^\perp P_L \nu_{\bar{c}}), \\ Q_2^D &= \frac{\bar{n} \cdot v}{\bar{n} \cdot \mathcal{P}_c} (\bar{Q}_{s[\omega]} \frac{\not{n}}{n \cdot v} P_L \mathcal{H}_v) (\bar{\mathcal{X}}_c^{(\ell)} \mathcal{A}_{c[x]}^\perp P_L \nu_{\bar{c}}), \\ Q_1^E &= \frac{m_\ell \bar{n} \cdot v}{\omega \bar{n} \cdot \mathcal{P}_c} (\bar{Q}_{s[\omega]} \mathcal{A}_{s[\omega_g]}^\perp \frac{\not{n}}{n \cdot v} P_R \mathcal{H}_v) (\bar{\mathcal{X}}_c^{(\ell)} P_L \nu_{\bar{c}}), \\ Q_2^E &= \frac{m_\ell \bar{n} \cdot v}{\omega \bar{n} \cdot \mathcal{P}_c} (\bar{Q}_{s[\omega]} \mathcal{G}_{s[\omega_g]}^\perp \frac{\not{n}}{n \cdot v} P_R \mathcal{H}_v) (\bar{\mathcal{X}}_c^{(\ell)} P_L \nu_{\bar{c}}), \\ Q_1^F &= \frac{\bar{n} \cdot v}{\omega \bar{n} \cdot \mathcal{P}_c} (\bar{Q}_{s[\omega]} \mathcal{A}_{s[\omega_g]}^\perp \frac{\not{n}}{n \cdot v} P_R \mathcal{H}_v) (\bar{\mathcal{X}}_c^{(\ell)} \mathcal{A}_{c[x]}^\perp P_L \nu_{\bar{c}}), \\ Q_2^F &= \frac{\bar{n} \cdot v}{\omega \bar{n} \cdot \mathcal{P}_c} (\bar{Q}_{s[\omega]} \mathcal{G}_{s[\omega_g]}^\perp \frac{\not{n}}{n \cdot v} P_R \mathcal{H}_v) (\bar{\mathcal{X}}_c^{(\ell)} \mathcal{A}_{c[x]}^\perp P_L \nu_{\bar{c}}), \end{aligned} \quad (4.23)$$

whose structure can be readily inferred from Table 3. The non-locality of the operators is reflected in the fact that they depend on the light-cone momentum variables ω and ω_g

corresponding to the (incoming) components $n \cdot l_s/n \cdot v$ and $n \cdot q_s/n \cdot v$ of the soft spectator anti-quark and a soft gluon or photon in the B meson, respectively. In the last four operators we have pulled out an inverse power of ω to obtain the correct mass dimension. We see that the SCET-2 basis operators depend on at most two ω_i variables and at most one x variable.

The results shown in Table 3 suggest that one needs additional two operators containing a soft derivative $i\overleftarrow{\partial}_s^\perp$ acting on the soft quark field $\bar{Q}_{s[\omega]}$, but they turn out to be redundant and can be eliminated using the equation of motion $i\overleftarrow{\mathcal{D}}_s u_s = 0$ of the massless quark field. When converted into gauge-invariant building blocks, this relation implies

$$\frac{\not{n} \not{q}_s}{4} \frac{i\overleftarrow{\partial}_s^\perp}{in \cdot \partial_s} Q_{s[\omega]} = -\frac{\not{n}}{2} Q_{s[\omega]} - \frac{\bar{n} \cdot v}{\omega} \frac{\not{n} \not{q}_s}{4} \int d\omega' \int d\omega_g \delta(\omega - \omega' - \omega_g) \left(\mathcal{G}_{s[\omega_g]}^\perp + Q_u \mathcal{A}_{s[\omega_g]}^\perp \right) Q_{s[\omega']}. \quad (4.24)$$

Using the hermitian conjugate of this identity, we find

$$\begin{aligned} & \frac{m_\ell \bar{n} \cdot v}{\bar{n} \cdot \mathcal{P}_c} \left(\bar{Q}_{s[\omega]} \frac{i\overleftarrow{\partial}_s^\perp}{in \cdot \overleftarrow{\partial}_s} \not{n} P_R \mathcal{H}_v \right) (\bar{X}_c^{(\ell)} P_L \nu_{\bar{c}}) \\ &= -Q_1^C(\omega) - \int d\omega' \int d\omega_g \delta(\omega - \omega' - \omega_g) \left[Q_u Q_1^E(\omega', \omega_g) + Q_2^E(\omega', \omega_g) \right], \\ & \frac{\bar{n} \cdot v}{\bar{n} \cdot \mathcal{P}_c} \left(\bar{Q}_{s[\omega]} \frac{i\overleftarrow{\partial}_s^\perp}{in \cdot \overleftarrow{\partial}_s} \not{n} P_R \mathcal{H}_v \right) (\bar{X}_c^{(\ell)} \mathcal{A}_{c[x]}^\perp P_L \nu_{\bar{c}}) \\ &= -Q_1^D(x, \omega) - \int d\omega' \int d\omega_g \delta(\omega - \omega' - \omega_g) \left[Q_u Q_1^F(x, \omega', \omega_g) + Q_2^F(x, \omega', \omega_g) \right], \end{aligned} \quad (4.25)$$

which shows that these two operators can be omitted from the basis.

Table 4 shows the SCET-2 basis operators onto which the various SCET-1 basis operators can be matched and at which order of perturbation theory the corresponding jet functions can first arise. We do not exclude the possibility that some matching coefficients can be zero. As indicated by the symbol α^\dagger , the one-loop jet functions in fact disappear in the cases of O_5^C and O_1^F . For the SCET-2 operators of type- B , D and F , the presence of the collinear photon field implies that their matrix elements involve a collinear photon loop and hence will be suppressed by a power of α . Consequently, the type- D and type- F SCET-2 operators are only needed to calculate the decay amplitude $B^- \rightarrow \ell^- \bar{\nu}_\ell$ in $\mathcal{O}(\alpha^2)$, which is beyond the scope of the present work.

4.3 Results for the bare jet functions

We now present the relevant jet functions arising in the matching of the SCET-1 basis operators O_i^X onto the SCET-2 basis operators defined in (4.18) and (4.23). As always in this paper, we restrict ourselves to terms contributing at $\mathcal{O}(\alpha)$ to the $B^- \rightarrow \ell^- \bar{\nu}_\ell$ decay amplitude.

SCET-1 operator	SCET-2 operators	Jet function*
O_1^A	Q_1^A	1
O_2^A	Q_2^A	1
$O_{3,4}^A$	–	–
O_1^B	Q_1^B	1
O_2^B	Q_2^B	1
$O_{3,4}^B$	–	–
O_1^C	Q_1^C, Q_1^E, Q_2^E	α
O_2^C	Q_2^C	α
$O_{3,4}^C$	$Q_1^C, Q_1^D, Q_1^E, Q_2^E, Q_1^F, Q_2^F$	α
O_5^C	Q_2^C, Q_2^D	α^\dagger
O_1^D	Q_2^C	α^2
O_2^D	Q_2^C	$\alpha\alpha_s$
O_3^D	$Q_1^C, Q_1^D, Q_1^E, Q_2^E, Q_1^F, Q_2^F$	α^2
O_4^D	$Q_1^C, Q_1^D, Q_1^E, Q_2^E, Q_1^F, Q_2^F$	$\alpha\alpha_s$
$O_{5,7}^D$	Q_2^C, Q_2^D	α^2
$O_{6,8}^D$	Q_2^C, Q_2^D	$\alpha\alpha_s$
O_1^E	Q_2^C, Q_2^D	α^3
O_2^E	Q_2^C, Q_2^D	$\alpha^2\alpha_s$
$O_{3,4}^E$	Q_2^C, Q_2^D	$\alpha\alpha_s^2$
O_1^F	Q_1^C, Q_1^E, Q_2^E	α^\dagger

Table 4: Pattern of SCET-1 \rightarrow SCET-2 matching relations, showing the set of SCET-2 operators onto which a given SCET-1 basis operator can be matched. The last column indicates at which order in perturbation theory this matching can first occur. This is the minimum perturbative suppression of the corresponding jet functions (times the low-energy matrix elements, if they contain a photon loop). It is not excluded that jet functions vanish upon explicit calculations. Indeed, for the cases marked with a dagger, we have explicitly shown that the jet functions vanish at the indicated order.

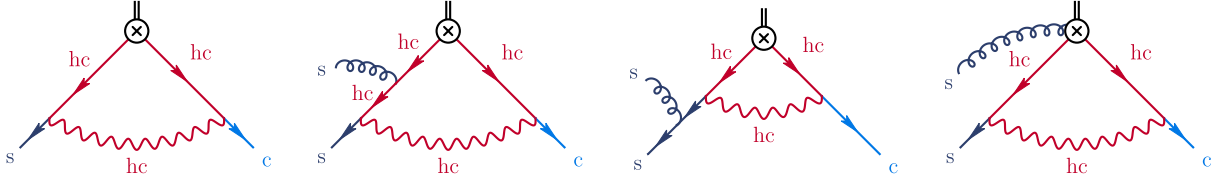


Figure 9: Representative hard-collinear loop diagrams for the matching of the type- C SCET-1 operators onto SCET-2. Red (dark blue) lines represent hard-collinear (soft) propagators and external states. Light blue lines represent collinear external states. The double line at the vertex represents the b -quark and neutrino fields.

Type- A and type- B SCET-1 operators

For these operators we find the non-zero matching relations

$$\begin{aligned} J_{O_1^A \rightarrow Q_1^A} &= J_{O_2^A \rightarrow Q_2^A} = 1, \\ J_{O_1^B \rightarrow Q_1^B}(y, x) &= J_{O_2^B \rightarrow Q_2^B}(y, x) = \delta(x - y). \end{aligned} \quad (4.26)$$

Both relations hold to all orders of perturbation theory.

Type- C SCET-1 operators

For the type- C operators, the jet functions start at one-loop order in QED and are obtained by calculating the diagrams shown in Figure 9. Starting with the matching onto type- C SCET-2 operators (first diagram), we find for the non-vanishing jet functions in $d = 4 - 2\epsilon$ spacetime dimensions (with $0 \leq y \leq 1$)

$$\begin{aligned} J_{O_1^C \rightarrow Q_1^C}(y, \omega) &= -Q_\ell Q_u \frac{\alpha}{2\pi} \frac{e^{\epsilon\gamma_E} \Gamma(\epsilon)}{1 - \epsilon} \left(\frac{\mu^2 \bar{n} \cdot v}{y(1-y) \bar{n} \cdot \mathcal{P}_c \omega} \right)^\epsilon (1-y) \left(\frac{1}{y} + 1 - \epsilon \right), \\ J_{O_2^C \rightarrow Q_2^C}(y, \omega) &= Q_\ell Q_u \frac{\alpha}{2\pi} e^{\epsilon\gamma_E} \Gamma(\epsilon) \left(\frac{\mu^2 \bar{n} \cdot v}{y(1-y) \bar{n} \cdot \mathcal{P}_c \omega} \right)^\epsilon (1-y)^2, \\ J_{O_3^C \rightarrow Q_1^C}(y, \omega) &= Q_\ell Q_u \frac{\alpha}{2\pi} \frac{e^{\epsilon\gamma_E} \Gamma(1 + \epsilon)}{1 - \epsilon} \left(\frac{\mu^2 \bar{n} \cdot v}{y(1-y) \bar{n} \cdot \mathcal{P}_c \omega} \right)^\epsilon y(1-y), \\ J_{O_4^C \rightarrow Q_1^C}(y, \omega) &= -Q_\ell Q_u \frac{\alpha}{2\pi} \frac{e^{\epsilon\gamma_E} \Gamma(1 + \epsilon)}{1 - \epsilon} \left(\frac{\mu^2 \bar{n} \cdot v}{y(1-y) \bar{n} \cdot \mathcal{P}_c \omega} \right)^\epsilon y(1-y). \end{aligned} \quad (4.27)$$

Despite appearance, these bare expressions are independent of the scale μ , since the dimensionless bare coupling $\alpha \propto \mu^{-2\epsilon}$. In the SCET-friendly projection scheme defined in Section 3.3, there are no evanescent contributions to these expressions. Note that the SCET-1 operator O_5^C does not match onto the SCET-2 basis operators at one-loop order. Its contributions vanish by virtue of the magic identity (3.36). We do not compute the jet functions arising in the matching relations onto the type- D SCET-2 operators, because their matrix elements bring in a second factor of α and hence are beyond our accuracy.

The calculation of the jet functions for the matching onto SCET-2 operators of type- E (remaining diagrams in Figure 9) is subtle and deserves a more detailed discussion. If we denote the incoming soft gluon momentum by q_s and its polarization vector by $\varepsilon^a(q_s)$, the calculation gives rise to the three structures

$$g_s t^a \varepsilon_\mu^a(q_s) \left[A_1(n \cdot q_s) \gamma_\perp^\mu + A_2(n \cdot q_s) \frac{\not{q}_s^\perp}{n \cdot q_s} n^\mu + A_3(n \cdot q_s) \not{n} n^\mu \right] \quad (4.28)$$

sandwiched between the quark spinors, where the coefficient functions can also depend on $n \cdot l_s$, with l_s the incoming momentum of the anti-up quark. Gauge invariance requires that $A_2(n \cdot q_s) = -A_1(n \cdot q_s)$, so that the first two terms combine to give the Feynman rule for the gauge-invariant field \mathcal{G}_s^\perp contained in the operator Q_2^E in (4.23).⁸ In a general projection scheme, it is essential to include the last diagram in Figure 9 in order for this relation to be satisfied. It is also important to consider the third diagram, in which the soft gluon is emitted off the soft \bar{u} quark. While naively this graph involves a soft propagator and thus would not contribute to the matching, closer inspection shows that it contains a “short-distance” contribution, in which the soft propagator $1/(\not{l}_s + \not{q}_s)$ is canceled by a factor of $(\not{l}_s + \not{q}_s)$ in the numerator.⁹ Only this short-distance piece contributes to the matching calculation. In our SCET-friendly projection scheme, only the SCET-1 operator O_1^C has a non-trivial matching onto SCET-2 operators of type- E . We consider the case of the operator Q_2^E here, which contains a soft gluon field inside the B meson. The analogous operator Q_1^E containing a soft photon in the B meson is suppressed, relative to the former one, by a factor of α/α_s . Also, we do not compute the matching onto type- F operators containing a collinear photon field, because their matrix elements bring in a second factor of α . Evaluating the last three diagrams in Figure 9, we obtain the bare jet function

$$J_{O_1^C \rightarrow Q_2^E}(y, \omega, \omega_g) = Q_\ell Q_u \frac{\alpha}{2\pi} \frac{e^{\epsilon\gamma_E} \Gamma(\epsilon)}{1 - \epsilon} \frac{\omega}{\omega_g} \left(\frac{\mu^2 \bar{n} \cdot v}{y(1-y) \bar{n} \cdot \mathcal{P}_c \omega} \right)^\epsilon \frac{(1-y)^2}{y} \times \left[\left(1 + \epsilon \frac{\omega_g}{\omega + \omega_g} \right) \left(\frac{\omega + \omega_g}{\omega} \right)^{-\epsilon} - 1 \right]. \quad (4.29)$$

Note that this expression is regular in the limit $\omega_g \rightarrow 0$.

Type- D and type- E SCET-1 operators

The jet functions arising from the SCET-1 operators of type- D and type- E are not needed for our purposes. As shown in Figure 10, they require at least two loops for type- D (upper graphs) and three loops for type- E operators (lower graphs). If the resulting SCET-2 operator contains a collinear photon field, the jet function starts one loop lower, but the matrix element

⁸The third structure corresponds to soft gluon emission from one of the soft Wilson lines contained in the operators $Q_{1,2}^C$ and can be ignored for this matching calculation.

⁹Alternatively, one could work with a Green’s basis containing the redundant operator shown in the first relation of (4.25), match its coefficient, and then use the given relation to convert the result into a contribution to the SCET-2 operator Q_2^E .

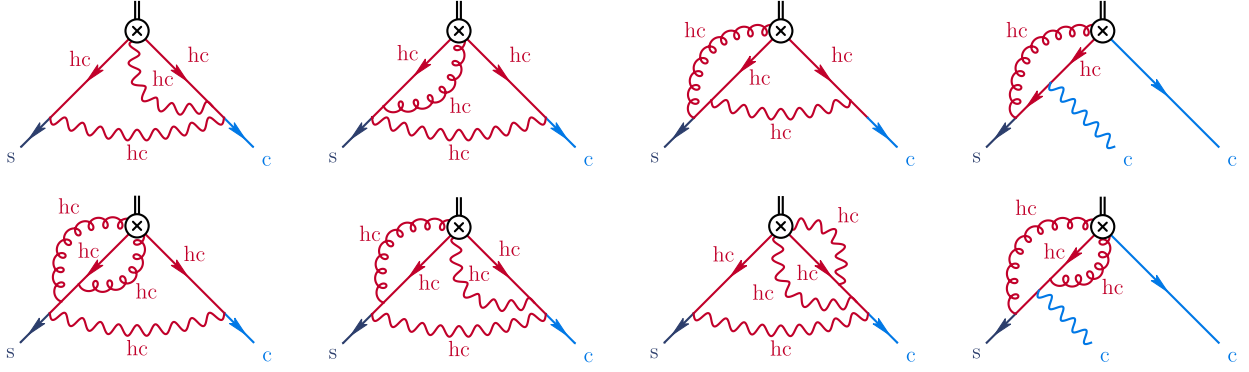


Figure 10: Representative hard-collinear loop diagrams for the matching of type-*D* SCET-1 operators (upper row) and type-*E* SCET-1 operators (lower row) onto SCET-2. Red (dark blue) lines represent hard-collinear (soft) propagators and external states. Light blue lines represent collinear external states.

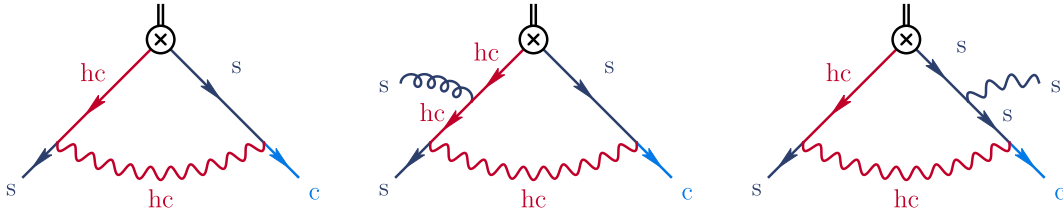


Figure 11: Representative hard-collinear loop diagrams for the matching of type-*F* SCET-1 operators onto SCET-2. Red (dark blue) lines represent hard-collinear (soft) propagators and external states. Light blue lines represent collinear external states.

of the operator contains a photon loop. Note that in each case the hard-collinear photon exchange between the up quark and the charged lepton is needed to transfer the hard-collinear momentum from the quark to the lepton side. For type-*D* operators, we find that the $\mathcal{O}(\alpha\alpha_s)$ jet functions for $O_{6,8}^D$ vanish in our projection scheme.

Type-*F* SCET-1 operator

The one-loop diagrams relevant for the matching of the type-*F* operator O_1^F onto our SCET-2 operator basis are depicted in Figure 11. As before, we only focus on the SCET-2 operators Q_i^C and Q_i^E , because the matrix elements of operators involving a collinear photon field come with an extra factor of α . The one-loop diagram for the matching onto type-*C* operators (first graph) requires an analytic regulator to be well defined but then turns out to be scaleless. Hence this contribution vanishes. The one-loop diagrams for the matching onto type-*E* operators have a non-vanishing loop integral, but their Dirac structure vanishes by virtue of the magic identity (3.36). As a result, the operator O_1^F does not contribute to the $B^- \rightarrow \ell^- \bar{\nu}_\ell$ decay amplitude at $\mathcal{O}(\alpha)$.

4.4 Endpoint divergent convolution integrals

Two of the jet functions calculated in (4.27) and (4.29), namely $J_{O_1^C \rightarrow Q_1^C}$ and $J_{O_1^C \rightarrow Q_2^E}$, exhibit a singular behavior $\sim y^{-1-\epsilon}$ in the limit where $y \rightarrow 0$. One might be tempted to interpret this singularity in the sense of distributions, using the familiar relation

$$y^{-1-\epsilon} = -\frac{1}{\epsilon} \delta(y) + \left[\frac{1}{y} \right]_+ + \mathcal{O}(\epsilon), \quad (4.30)$$

which would be valid if the two jet functions were convoluted with a function that is regular near $y = 0$. But this condition is not satisfied in the case at hand, because the hard matching coefficient $H_1^C(y, \mu)$ in (3.59) is logarithmically divergent for $y \rightarrow 0$. The corresponding bare coefficient contains terms proportional to $y^{-\epsilon}$ at one-loop order. This causes a major problem, because the $1/\epsilon$ poles of the convolutions

$$\int_0^1 dy H_1^C(y) J_{O_1^C \rightarrow Q_1^C}(y, \omega) \quad \text{and} \quad \int_0^1 dy H_1^C(y) J_{O_1^C \rightarrow Q_2^E}(y, \omega) \quad (4.31)$$

cannot be removed by individually removing the poles of the hard and jet functions.

The appearance of such endpoint-divergent convolution integrals is a generic feature of SCET factorization theorems at subleading power in λ [45–56, 58, 59]. The “refactorization-based subtraction (RBS) scheme” introduced in [51, 54] offers a systematic method for dealing with this problem. It consists of two steps: One first removes the singularities of the integrals by performing plus-type subtractions of the integrands, e.g.

$$\int_0^1 dy H_1^C(y) J_{O_1^C \rightarrow Q_1^C}(y, \omega) \rightarrow \int_0^1 dy \left[H_1^C(y) J_{O_1^C \rightarrow Q_1^C}(y, \omega) - \theta(\eta - y) \llbracket H_1^C(y) \rrbracket \llbracket J_{O_1^C \rightarrow Q_1^C}(y, \omega) \rrbracket \right] \quad (4.32)$$

with $0 < \eta \leq 1$, and analogously for the second integral. This subtraction is similar to (3.73), but following [55] we have introduced an auxiliary parameter η in its definition. As before, the notation $\llbracket f(y) \rrbracket$ means that one retains only the leading terms of the function $f(y)$ in the limit $y \rightarrow 0$. In the second step, the subtraction terms need to be added back and combined with other terms in the factorization theorem for the process of interest. Exact d -dimensional refactorization conditions ensure that this is always possible, i.e., that the subtraction terms have the required form.

What is the physical meaning of the subtraction performed above? Note that $y\bar{n} \cdot p_\ell$ denotes the large momentum component of the hard-collinear anti-quark field, which for generic y is of order the hard scale m_B . In the limit $y \rightarrow 0$, specifically in the region where $y \sim \lambda$ or smaller, this momentum component becomes soft, and the hard-collinear field in the operator O_1^C should more appropriately be replaced by a soft field. To cut away the soft region from the integral, the parameter η should scale like a soft parameter, $\eta = \mathcal{O}(\lambda)$, but it will be necessary to choose it sufficiently large that the soft scale $\Lambda \equiv \eta m_B$ is in the perturbative domain. In other words, we require that

$$\lambda \ll \eta \ll 1, \quad (4.33)$$

or equivalently $\Lambda_{\text{QCD}} \ll \Lambda \ll m_B$. Based on the argument just presented, we expect that the subtraction term is structurally connected with the operator O_1^A , which is the analogue of O_1^C

containing a soft quark field. Indeed, the first relation in (3.76) shows that

$$\llbracket H_1^C(y) \rrbracket = H_1^A S_1^C(\bar{\omega}), \quad (4.34)$$

where H_1^A is the (bare) hard matching coefficient of the operator O_1^A , and we have defined $\bar{\omega} \equiv y \bar{n} \cdot p_\ell / \bar{n} \cdot v$. The new (bare) soft function $S_1^C(\bar{\omega})$ has been given at one-loop order in (3.77). Moreover, from (4.27) and (4.29) we obtain

$$\llbracket J_{O_1^C \rightarrow Q_1^C}(y, \omega) \rrbracket dy = S_{O_1^C \rightarrow Q_1^C}(\bar{\omega}, \omega) \frac{d\bar{\omega}}{\bar{\omega}} \quad (4.35)$$

and analogously for $J_{O_1^C \rightarrow Q_2^E}$, with the (bare) soft functions

$$\begin{aligned} S_{O_1^C \rightarrow Q_1^C}(\bar{\omega}, \omega) &= -Q_\ell Q_u \frac{\alpha}{2\pi} \frac{e^{\epsilon\gamma_E} \Gamma(\epsilon)}{1-\epsilon} \left(\frac{\bar{\omega}\omega}{\mu^2} \right)^{-\epsilon} + \mathcal{O}(\alpha\alpha_s), \\ S_{O_1^C \rightarrow Q_2^E}(\bar{\omega}, \omega) &= Q_\ell Q_u \frac{\alpha}{2\pi} \frac{e^{\epsilon\gamma_E} \Gamma(\epsilon)}{1-\epsilon} \frac{\omega}{\omega_g} \left(\frac{\bar{\omega}\omega}{\mu^2} \right)^{-\epsilon} \\ &\quad \times \left[\left(1 + \epsilon \frac{\omega_g}{\omega + \omega_g} \right) \left(\frac{\omega + \omega_g}{\omega} \right)^{-\epsilon} - 1 \right] + \mathcal{O}(\alpha\alpha_s). \end{aligned} \quad (4.36)$$

This allows us to rewrite the subtraction terms in the form

$$\begin{aligned} \int_0^\eta dy \llbracket H_1^C(y) \rrbracket \llbracket J_{O_1^C \rightarrow Q_1^C}(y, \omega) \rrbracket &= H_1^A \int_0^\Lambda \frac{d\bar{\omega}}{\bar{\omega}} S_1^C(\bar{\omega}) S_{O_1^C \rightarrow Q_1^C}(\bar{\omega}, \omega) \\ &= -H_1^A \int_\Lambda^\infty \frac{d\bar{\omega}}{\bar{\omega}} S_1^C(\bar{\omega}) S_{O_1^C \rightarrow Q_1^C}(\bar{\omega}, \omega), \end{aligned} \quad (4.37)$$

and similarly for the second term, where we have defined $\Lambda \equiv \eta \bar{n} \cdot \mathcal{P}_{hc} / \bar{n} \cdot v$. In the last step, we have used that the difference between the last two expressions is a scaleless integral, which vanishes in dimensional regularization. Performing the integral over $\bar{\omega}$, we find

$$\begin{aligned} \int_\Lambda^\infty \frac{d\bar{\omega}}{\bar{\omega}} S_1^C(\bar{\omega}) S_{O_1^C \rightarrow Q_1^C}(\bar{\omega}, \omega) &= -Q_\ell Q_u \frac{\alpha}{2\pi} \frac{e^{\epsilon\gamma_E} \Gamma(\epsilon)}{\epsilon(1-\epsilon)} \left(\frac{\Lambda\omega}{\mu^2} \right)^{-\epsilon} + \mathcal{O}(\alpha\alpha_s), \\ \int_\Lambda^\infty \frac{d\bar{\omega}}{\bar{\omega}} S_1^C(\bar{\omega}) S_{O_1^C \rightarrow Q_2^E}(\bar{\omega}, \omega, \omega_g) &= Q_\ell Q_u \frac{\alpha}{2\pi} \frac{e^{\epsilon\gamma_E} \Gamma(\epsilon)}{\epsilon(1-\epsilon)} \frac{\omega}{\omega_g} \left(\frac{\Lambda\omega}{\mu^2} \right)^{-\epsilon} \\ &\quad \times \left[\left(1 + \epsilon \frac{\omega_g}{\omega + \omega_g} \right) \left(\frac{\omega + \omega_g}{\omega} \right)^{-\epsilon} - 1 \right] + \mathcal{O}(\alpha\alpha_s). \end{aligned} \quad (4.38)$$

In previous applications of the RBS scheme, in which the matrix elements of the operators containing soft fields were calculable in perturbation theory, adding back the subtraction term had the effect of imposing a cutoff on a convolution integral multiplying the hard function remaining after taking the endpoint limit, i.e. H_1^A in our case (see e.g. [51, 54, 55, 58, 59]).

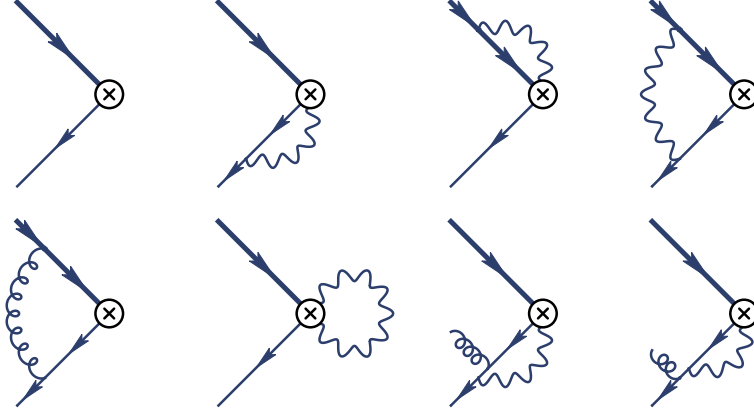


Figure 12: Tree-level and one-loop diagrams contributing to the perturbative calculation of the matrix element in (4.41) in the region where $\Lambda \gg \Lambda_{\text{QCD}}$. The tree diagram vanishes in this region. Diagrams in which a gluon is emitted from the current (not shown) give vanishing contributions.

We find that something analogous happens also in the present case, in which the soft matrix elements are non-perturbative hadronic functions (see Section 4.8). Concretely, the convolutions of the above expressions with the corresponding SCET-2 operators yield a new operator related closely to the operator Q_1^A , namely

$$\begin{aligned}
& \int_{\Lambda}^{\infty} \frac{d\bar{\omega}}{\bar{\omega}} S_1^C(\bar{\omega}) \left[\int d\omega S_{O_1^C \rightarrow Q_1^C}(\bar{\omega}, \omega) Q_1^C(\omega) + \int d\omega \int d\omega_g S_{O_1^C \rightarrow Q_2^E}(\bar{\omega}, \omega, \omega_g) Q_2^E(\omega, \omega_g) \right] \\
&= \frac{m_\ell}{\bar{n} \cdot \mathcal{P}_c} \left[\bar{u}_s \theta_T \left(\frac{-i\bar{n} \cdot \overleftarrow{D}_s}{\bar{n} \cdot v} - \Lambda \right) \not{n} P_L b_v Y_n^{(\ell)\dagger} \right] (\bar{\mathcal{X}}_c^{(\ell)} P_L \nu_{\bar{c}}) \\
&= \frac{m_\ell}{\bar{n} \cdot \mathcal{P}_c} \left[(\bar{u}_s \bar{Y}_{\bar{n}}^{(u)}) \theta_T \left(\frac{-i\bar{n} \cdot \overleftarrow{\partial}_s}{\bar{n} \cdot v} - \Lambda \right) \not{n} P_L (Y_n^{(\ell)\dagger} \bar{Y}_{\bar{n}}^{(u)\dagger} b_v) \right] (\bar{\mathcal{X}}_c^{(\ell)} P_L \nu_{\bar{c}}).
\end{aligned} \tag{4.39}$$

In the last step, we have converted the covariant derivative into a regular one using soft Wilson lines along the direction \bar{n} . We then encounter gauge-invariant building blocks for the quark fields, which are defined in analogy with the definitions in (4.22), but with soft Wilson lines $\bar{Y}_{\bar{n}}^{(u)}$ instead of $\bar{Y}_n^{(u)}$. The θ_T function restricts the component $\bar{n} \cdot l_s / \bar{n} \cdot v$ of the incoming anti-quark momentum to be negative and less than $-\Lambda$, which is only possible if QED effects are taken into account [21]. The subscript “ T ” indicates that in evaluating the matrix elements of this operator one needs to perform a Taylor expansion, treating $\Lambda \gg \Lambda_{\text{QCD}}$ as parametrically larger than all soft QCD scales.

To prove the above relation at one-loop order, we first rewrite the θ_T functions as an integral over a δ -distribution (with the same Taylor expansion prescription)

$$\theta_T \left(\frac{-i\bar{n} \cdot \overleftarrow{\partial}_s}{\bar{n} \cdot v} - \Lambda \right) = \int_{\Lambda}^{\infty} d\bar{\omega} \delta_T \left(\frac{-i\bar{n} \cdot \overleftarrow{\partial}_s}{\bar{n} \cdot v} - \bar{\omega} \right). \tag{4.40}$$

We then evaluate the one-loop diagrams shown in Figure 12 for external quark and gluon states with incoming soft momentum l_s for the \bar{u} quark, incoming residual momentum k_s for

the b quark, and incoming momentum q_s for the gluon (if present). Since $\bar{\omega} \geq \Lambda \gg \Lambda_{\text{QCD}}$, we perform a systematic expansion in the ratios of the soft scales over $\bar{\omega}$ and keep the leading terms only. Photon fields in the operator originate from the three Wilson lines. Focusing first on the diagrams without external gluons, we find that the tree diagrams vanish, because the argument of the δ_T distribution is always negative for $\Lambda \gg \Lambda_{\text{QCD}}$. The two diagrams in which the photon (or a gluon) is attached to the heavy quark vanish by residues. The photon tadpole graph is scaleless and vanishes in dimensional regularization. This leaves the second diagram, which gives rise to a non-vanishing contribution. Focusing next on the three-particle contributions, we find again that only diagrams with a photon emitted from the operator and attached to the \bar{u} quark are non-vanishing. Allowing for an arbitrary Dirac structure Γ , we obtain

$$\begin{aligned}
& \left\langle (\bar{u}_s \bar{Y}_{\bar{n}}^{(u)}) \theta_T \left(\frac{-i\bar{n} \cdot \overleftarrow{D}_s}{\bar{n} \cdot v} - \Lambda \right) \Gamma (Y_n^{(\ell)\dagger} \bar{Y}_{\bar{n}}^{(u)\dagger} b_v) \right\rangle \\
&= -Q_\ell Q_u \frac{\alpha}{2\pi} \frac{e^{\epsilon\gamma_E} \Gamma(\epsilon)}{\epsilon} \int d\omega \left(\frac{\Lambda\omega}{\mu^2} \right)^{-\epsilon} \left\langle \bar{Q}_{s[\omega]} \left(1 + \frac{\epsilon}{1-\epsilon} \frac{\not{n} \not{\omega}}{4} \right) \Gamma \mathcal{H}_v \right\rangle \\
&+ Q_\ell Q_u \frac{\alpha}{4\pi} \frac{e^{\epsilon\gamma_E} \Gamma(\epsilon)}{\epsilon(1-\epsilon)} \int d\omega \int d\omega_g \frac{1}{\omega_g} \left(\frac{\Lambda\omega}{\mu^2} \right)^{-\epsilon} \left[\left(1 + \epsilon \frac{\omega_g}{\omega + \omega_g} \right) \left(\frac{\omega + \omega_g}{\omega} \right)^{-\epsilon} - 1 \right] \\
&\times \left\langle \bar{Q}_{s[\omega]} \mathcal{G}_{s[\omega_g]}^\perp \frac{\not{\omega}}{\bar{n} \cdot v} \Gamma \mathcal{H}_v \right\rangle.
\end{aligned} \tag{4.41}$$

Setting $\Gamma = \not{n} P_L$, we recover relations (4.38) and (4.39). We stress that, while hadronic matrix elements of quark and gluon operators are non-perturbative quantities, which cannot be calculated in perturbation theory, the dependence of the matrix elements of the θ_T operator on the scale $\Lambda \gg \Lambda_{\text{QCD}}$ can be calculated as long as Λ is in the perturbative domain. In the following, we assume that the identification of the subtraction term with the matrix element of the θ_T operator holds to all orders of perturbation theory.

The outcome of this analysis is that removing the endpoint divergences as shown in (4.32) leads to a redefinition of the operator O_1^A in the SCET-2, to which we add back the subtraction term to obtain the new operator

$$Q_{1,\theta}^A = \frac{m_\ell}{\bar{n} \cdot \mathcal{P}_c} \left(\bar{u}_s \left[1 - \theta_T \left(\frac{-i\bar{n} \cdot \overleftarrow{D}_s}{\bar{n} \cdot v} - \Lambda \right) \right] \not{n} P_L b_v Y_n^{(\ell)\dagger} \right) (\bar{\chi}_c^{(\ell)} P_L \nu_{\bar{c}}). \tag{4.42}$$

Due to the T symbol in the Heaviside function, it is not legitimate to replace the terms inside the square brackets by a Heaviside function with the opposite-sign argument. In higher orders of perturbation theory, an analogous redefinition would need to be performed for the operators Q_2^A , Q_1^B and Q_2^B . The result (4.42) has a nice physical interpretation: In the same way that the subtraction in (4.32) has removed the soft component in the integral over y , the Heaviside function in (4.42) removes the momentum modes of the soft \bar{u} quark that would correspond to a *hard-collinear* momentum, with $\bar{n} \cdot (-l_s) > \Lambda \gg \Lambda_{\text{QCD}}$.

4.5 Renormalized jet functions

Once the endpoint divergences have been removed from the convolution integrals as shown in (4.32), the hard and jet functions can be renormalized in the $\overline{\text{MS}}$ scheme without paying special attention to the singularities at $y = 0$. The non-vanishing jet functions that are non-trivial (i.e. different from unity) are those shown in (4.27) and (4.29), of which only $J_{O_1^C \rightarrow Q_1^C}$ and $J_{O_2^C \rightarrow Q_2^C}$ require renormalization at one-loop order. From (3.66), it follows that after matching to SCET-2 the renormalized operators $O_i^C(\mu)$ with $i = 1, 2$ can be written as

$$O_i(y, \mu) = \int dx \int d\omega Z_{ii}^{CC}(y, x, \mu) J_{O_i^C \rightarrow Q_i^C}(x, \omega) Q_i^C(\omega) + Z_{ii}^{CA}(y, \mu) J_{O_i^A \rightarrow Q_i^A} Q_i^A, \quad (4.43)$$

where the bare jet functions $J_{O_i^C \rightarrow Q_i^C}(x)$ and the renormalization factors $Z_{ii}^{CA}(y, \mu)$ start at $\mathcal{O}(\alpha)$ and have been given in (4.27) and (3.73), respectively, while $J_{O_i^A \rightarrow Q_i^A} = 1$ and $Z_{ii}^{CC}(y, x, \mu) = \delta(y - x) + \mathcal{O}(\alpha)$. We now split up the bare functions in their $1/\epsilon$ pole terms, which are independent of the variable ω , and finite remainders,

$$J_{O_i^C \rightarrow Q_i^C}(x, \omega) \equiv J_{O_i^C \rightarrow Q_i^C}^{\text{poles}}(x) + J_{O_i^C \rightarrow Q_i^C}^{\text{fin}}(x, \omega). \quad (4.44)$$

Next, we use the fact that the bare operators satisfy the exact relations

$$\int d\omega Q_i^C(\omega) = Q_i^A. \quad (4.45)$$

At first order in α , this leads to

$$O_i(y, \mu) = \left[J_{O_i^C \rightarrow Q_i^C}^{\text{poles}}(y) + Z_{ii}^{CA}(y, \mu) \right] Q_i^A + \int d\omega J_{O_i^C \rightarrow Q_i^C}^{\text{fin}}(y, \omega) Q_i^C(\omega). \quad (4.46)$$

It is easy to check from the explicit expressions that the two terms inside the rectangular brackets cancel each other, and only the second term remains. In the last step, we define renormalization factors for the SCET-2 operators via the condition

$$Q_i^X(\mu) = \sum_{j, X'} \mathcal{Z}_{ij}^{XX'}(\mu) \otimes Q_j^{X'}, \quad (4.47)$$

which relates the renormalized (and scale-dependent) operators $Q_i^X(\mu)$ to the bare operators $Q_j^{X'}$. As before, the labels X and X' refer to the operator type (A through F), and the symbol \otimes means an integration over the momentum variables shared by the quantities $\mathcal{Z}_{ij}^{XX'}$ and $Q_j^{X'}$. To the order we are working, we only need this relation at tree level, where $\mathcal{Z}_{ij}^{XX'}(\mu)$ is the unity operator and hence diagonal in i, j and X, X' . This leads to the final result

$$O_i(y, \mu) = \int d\omega J_{O_i^C \rightarrow Q_i^C}^{\text{fin}}(y, \omega) Q_i^C(\omega, \mu) + \mathcal{O}(\alpha\alpha_s). \quad (4.48)$$

Using again that $\bar{n} \cdot \mathcal{P}_{hc}/\bar{n} \cdot v = m_B$ in our case to simplify the notation, we thus obtain the renormalized jet functions

$$\begin{aligned}
J_{O_1^C \rightarrow Q_1^C}(y, \omega, \mu) &= -Q_\ell Q_u \frac{\alpha}{2\pi} \frac{1-y}{y} \left[(1+y) \ln \frac{\mu^2}{y(1-y)m_B \omega} + 1 \right], \\
J_{O_2^C \rightarrow Q_2^C}(y, \omega) &= Q_\ell Q_u \frac{\alpha}{2\pi} (1-y)^2 \ln \frac{\mu^2}{y(1-y)m_B \omega}, \\
J_{O_3^C \rightarrow Q_1^C}(y, \omega) &= Q_\ell Q_u \frac{\alpha}{2\pi} y(1-y), \\
J_{O_4^C \rightarrow Q_1^C}(y, \omega) &= -Q_\ell Q_u \frac{\alpha}{2\pi} y(1-y),
\end{aligned} \tag{4.49}$$

and

$$J_{O_1^C \rightarrow Q_2^E}(y, \omega, \omega_g) = -Q_\ell Q_u \frac{\alpha}{2\pi} \frac{(1-y)^2}{y} \left(\frac{\omega}{\omega_g} \ln \frac{\omega + \omega_g}{\omega} - \frac{\omega}{\omega + \omega_g} \right). \tag{4.50}$$

For performing the subtracted convolution integrals in (4.32), we also need the expressions

$$\begin{aligned}
\llbracket J_{O_1^C \rightarrow Q_1^C}(y, \omega, \mu) \rrbracket &= -Q_\ell Q_u \frac{\alpha}{2\pi} \frac{1}{y} \left(\ln \frac{\mu^2}{ym_B \omega} + 1 \right), \\
\llbracket J_{O_1^C \rightarrow Q_2^E}(y, \omega, \omega_g) \rrbracket &= -Q_\ell Q_u \frac{\alpha}{2\pi} \frac{1}{y} \left(\frac{\omega}{\omega_g} \ln \frac{\omega + \omega_g}{\omega} - \frac{\omega}{\omega + \omega_g} \right).
\end{aligned} \tag{4.51}$$

4.6 Two-scale RG evolution of the hard function H_1^C

Let us return to the subtracted convolution integral in (4.32), now expressed in terms of renormalized functions, i.e.¹⁰

$$\begin{aligned}
&\int_0^1 dy \left[H_1^C(y, \mu) J_{O_1^C \rightarrow Q_1^C}(y, \omega, \mu) - \theta(\eta - y) \llbracket H_1^C(y, \mu) \rrbracket \llbracket J_{O_1^C \rightarrow Q_1^C}(y, \omega, \mu) \rrbracket \right] \\
&= \int_0^1 dy \left[H_1^C(y, \mu) J_{O_1^C \rightarrow Q_1^C}(y, \omega, \mu) - \llbracket H_1^C(y, \mu) \rrbracket \llbracket J_{O_1^C \rightarrow Q_1^C}(y, \omega, \mu) \rrbracket \right] \\
&\quad + \int_\eta^1 dy \llbracket H_1^C(y, \mu) \rrbracket \llbracket J_{O_1^C \rightarrow Q_1^C}(y, \omega, \mu) \rrbracket.
\end{aligned} \tag{4.52}$$

As mentioned earlier, from the point of view of subtracting the soft contribution from the integral, which involves hard and hard-collinear functions, one should require that $\lambda \ll \eta \ll 1$ is a parametrically small quantity separating the $\bar{n} \cdot p$ components of soft and hard-collinear

¹⁰In general, moving the cutoff η from an integral over bare functions over to a corresponding integral of renormalized functions can give rise to additional correction terms, which must be calculated and properly accounted for [54, 58]. In our case, these terms could only arise from the renormalization of the jet functions, which as discussed in the previous section is a higher-order effect.

modes. In this case the convolution integral leads to large logarithms, which need to be resummed.¹¹

The solutions (3.91) have been derived under the implicit assumption that the dimensionless variable y can be treated as an $\mathcal{O}(1)$ quantity. This assumption is justified for the first integral on the right-hand side of (4.52), in which the $1/y$ -enhanced terms of the integrand are removed and hence the region $y \ll 1$ gives a power-suppressed contribution. However, the assumption is invalidated for the second integral, which receives a leading contribution from the region where y takes parametrically small values. We therefore need to construct an RG-improved expression for the hard function $H_1^C(y, \mu)$ that is simultaneously valid for both large and small y values.¹² Our explicit expression for the hard function H_1^C in (3.59) shows that it depends on two different hard scales, $m_b \sim m_B = \bar{n} \cdot \mathcal{P}_{hc} / \bar{n} \cdot v$ and ym_B . For $y = \mathcal{O}(1)$ these scales are of the same order, but they are hierarchically separated for $y \ll 1$. The first refactorization condition in (3.76) suggests that we define a new function \tilde{H}_1^C via

$$H_1^C(y, \mu) \equiv \frac{H_1^A(\mu)}{1-y} \tilde{H}_1^C(y, \mu). \quad (4.53)$$

At one-loop order in QCD, we obtain (with $\bar{n} \cdot \mathcal{P}_{hc} / \bar{n} \cdot v = m_B$)

$$\begin{aligned} \tilde{H}_1^C(y, \mu) = 1 + \frac{C_F \alpha_s(\mu)}{4\pi} & \left[-\frac{1}{2} \ln^2 \frac{\mu^2}{(ym_B)^2} - \ln \frac{\mu^2}{(ym_B)^2} - 2 - \frac{5\pi^2}{12} \right. \\ & \left. + 2\text{Li}_2(yz) + 2 \ln yz \ln(1-yz) + \frac{yz \ln yz}{1-yz} \right], \end{aligned} \quad (4.54)$$

where the terms in the second line are of $\mathcal{O}(y)$. From the RG equations of the hard functions H_1^C and H_1^A in (3.83) and (3.85), it follows that in our approximation

$$\begin{aligned} \frac{d}{d \ln \mu} \tilde{H}_1^C(y, \mu) &= \left\{ \gamma^A(y, \alpha_s) - \gamma_{\text{hl}}(\alpha_s) - \frac{\alpha}{2\pi} \left[Q_b Q_u \ln \frac{\mu^2}{(ym_B)^2} - 2Q_l Q_b \ln(1-y) \right] \right\} \tilde{H}_1^C(y, \mu) \\ &= \left[-\frac{C_F}{2} \gamma_{\text{cusp}}(\alpha_s) \ln \frac{\mu^2}{(ym_B)^2} - \frac{C_F \alpha_s}{2\pi} - Q_b Q_u \frac{\alpha}{2\pi} \ln \frac{\mu^2}{(ym_B)^2} + \dots \right] \tilde{H}_1^C(y, \mu), \end{aligned} \quad (4.55)$$

where in the second line we have neglected the QED correction proportional to $\ln(1-y)$, which is beyond our approximation. Solving this equation yields

$$\begin{aligned} \tilde{H}_1^C(y, \mu) &= \exp \left[C_F S_{\text{cusp}}(ym_B, \mu) + \frac{C_F}{\beta_0} \ln \frac{\alpha_s(\mu)}{\alpha_s(ym_B)} - Q_b Q_u \frac{\alpha}{8\pi} \ln^2 \frac{\mu^2}{(ym_B)^2} \right] \tilde{H}_1^C(y, ym_B) \\ &= \tilde{U}_C(\mu, ym_B) \tilde{H}_1^C(y, ym_B), \end{aligned} \quad (4.56)$$

¹¹Alternatively, we could choose $\eta \sim 1$ in order to avoid these large logarithms, but then the matrix element of the soft operator contains large logarithms involving the hard scale m_B , which need to be resummed. This option will be discussed in Section 4.8.

¹²In principle the same is true for the jet functions. However, as mentioned earlier, in our case the jet functions are free of large logarithms for any reasonable choice of η .

where

$$\tilde{U}_C(\mu, ym_B) \equiv \frac{U_C(\mu, ym_B)}{U_{\text{hl}}(\mu, ym_B)} \exp \left[-Q_b Q_u \frac{\alpha}{8\pi} \ln^2 \frac{\mu^2}{(ym_B)^2} \right], \quad (4.57)$$

and the matching condition

$$\tilde{H}_1^C(y, ym_B) = 1 + \frac{C_F \alpha_s(ym_B)}{4\pi} \left[-2 - \frac{5\pi^2}{12} + 2\text{Li}_2(yz) + 2 \ln yz \ln(1 - yz) + \frac{yz \ln yz}{1 - yz} \right] \quad (4.58)$$

is free of large logarithms. With these results, the RG-improved expression for H_1^C reads

$$H_1^C(y, \mu) = U_{\text{hl}}(\mu, m_B) H_1^A(m_B) \exp \left[-Q_l Q_b \frac{\alpha}{8\pi} \ln^2 \frac{\mu^2}{m_B^2} \right] \tilde{U}_C(\mu, ym_B) \frac{\tilde{H}_1^C(y, ym_B)}{1 - y}. \quad (4.59)$$

It is valid for any relation between the hard scales m_B and ym_B and thus can be used to evaluate the last convolution integral in (4.52) in a consistent way. In particular, we find that $H_1^C(y, \mu)$ smoothly approaches the function

$$\begin{aligned} \llbracket H_1^C(y, \mu) \rrbracket &= U_{\text{hl}}(\mu, m_B) H_1^A(m_B) \exp \left[-Q_l Q_b \frac{\alpha}{8\pi} \ln^2 \frac{\mu^2}{m_B^2} \right] \\ &\times \tilde{U}_C(\mu, ym_B) \left\{ 1 + \frac{C_F \alpha_s(ym_B)}{4\pi} \left[-2 - \frac{5\pi^2}{12} \right] \right\} \end{aligned} \quad (4.60)$$

in the limit where y approaches small values. The fact that the solution (4.59) involves the running coupling $\alpha_s(ym_B)$ does not pose any conceptual problem, because the last integral in (4.52) does not run below the scale $\eta m_B = \Lambda$, which by assumption is above the Landau pole of the running coupling $\alpha_s(\mu)$.

It is instructive to consider a further generalization of the result (4.59), obtained by introducing flexible matching scales $\mu_h \sim m_B$ and $\bar{\mu}_h \sim ym_B$. This leads to (neglecting single-logarithmic QED effects)

$$H_1^C(y, \mu) = U_{\text{hl}}(\mu, \mu_h) H_1^A(\mu_h) \exp \left[-Q_l Q_b \frac{\alpha}{8\pi} \ln^2 \frac{\mu^2}{\mu_h^2} \right] \tilde{U}_C(\mu, \bar{\mu}_h) \frac{\tilde{H}_1^C(y, \bar{\mu}_h)}{1 - y} \left(\frac{ym_B}{\bar{\mu}_h} \right)^{-\delta(\mu, \bar{\mu}_h)}, \quad (4.61)$$

where

$$\delta(\mu, \bar{\mu}_h) \equiv \frac{C_F \gamma_0}{2\beta_0} \ln \frac{\alpha_s(\mu)}{\alpha_s(\bar{\mu}_h)}. \quad (4.62)$$

Setting $\mu_h = \bar{\mu}_h = m_B$, one would reproduce the result for H_1^C given in (3.91). However, in this case the matching condition $\tilde{H}_1^C(y, m_B)$ contains terms proportional to $\ln^n y$ with $n = 1, 2$, which become large for $y \ll 1$. This approximation is therefore only justified for y values of $\mathcal{O}(1)$.

4.7 RG evolution in SCET-2

The SCET-2 basis operators in (4.18) and (4.23) consist of products of a hadronic current, composed of soft fields, and a leptonic current, composed of collinear fields and the (sterile)

neutrino. Importantly, soft and collinear fields do not interact with each other, so the two currents can be treated separately. The hadronic currents include the two-particle operators

$$\begin{aligned}
j_1^{\text{had}}(\Lambda, \mu) &= \bar{u}_s \left[1 - \theta_T \left(\frac{-i\bar{n} \cdot \overleftarrow{D}_s}{\bar{n} \cdot v} - \Lambda \right) \right] \frac{\overleftarrow{\not{n}}}{\bar{n} \cdot v} P_L b_v Y_n^{(\ell)\dagger}, \\
j_2^{\text{had}}(\Lambda, \mu) &= \bar{u}_s \left[1 - \theta_T \left(\frac{-i\bar{n} \cdot \overleftarrow{D}_s}{\bar{n} \cdot v} - \Lambda \right) \right] \frac{\not{n}}{n \cdot v} P_L b_v Y_n^{(\ell)\dagger}, \\
j_3^{\text{had}}(\omega, \mu) &= \bar{Q}_{s[\omega]} \frac{\overleftarrow{\not{n}}}{\bar{n} \cdot v} P_L \mathcal{H}_v, \\
j_4^{\text{had}}(\omega, \mu) &= \bar{Q}_{s[\omega]} \frac{\not{n}}{n \cdot v} P_L \mathcal{H}_v,
\end{aligned} \tag{4.63}$$

and the three-particle operators

$$\begin{aligned}
j_5^{\text{had}}(\omega, \omega_g, \mu) &= \frac{1}{\omega} \bar{Q}_{s[\omega]} \mathcal{G}_{s[\omega_g]}^\perp \frac{\not{n}}{n \cdot v} P_R \mathcal{H}_v, \\
j_6^{\text{had}}(\omega, \omega_g, \mu) &= \frac{1}{\omega} \bar{Q}_{s[\omega]} \mathcal{A}_{s[\omega_g]}^\perp \frac{\not{n}}{n \cdot v} P_R \mathcal{H}_v.
\end{aligned} \tag{4.64}$$

The leptonic currents are

$$\begin{aligned}
j_1^{\text{lep}}(\mu) &= m_\ell \bar{\mathcal{X}}_c^{(\ell)} P_L \nu_{\bar{c}}, \\
j_2^{\text{lep}}(x, \mu) &= \bar{\mathcal{X}}_c^{(\ell)} \mathcal{A}_{c[x]}^\perp P_L \nu_{\bar{c}},
\end{aligned} \tag{4.65}$$

where m_ℓ still is the running lepton mass in the $\overline{\text{MS}}$ scheme.

The scale dependence of these currents is controlled by RG evolution equations. Matrix elements of the hadronic currents can be expressed in terms of HQET decay constants and LCDAs of the B -meson, as will be discussed in Section 4.8. These objects should be evolved from the hard-collinear matching scale $\mu_{hc} \sim \sqrt{m_B \Lambda_{\text{QCD}}}$ to a hadronic scale $\mu_0 \sim$ several times Λ_{QCD} , which should still be in the perturbative domain. With $\Lambda_{\text{QCD}} \sim 500 \text{ MeV}$, a typical value of the hard-collinear scale is $\mu_{hc} \approx 1.6 \text{ GeV}$, which is approximately $3 \times \Lambda_{\text{QCD}}$. Hence, in practice there is little room for this scale evolution, and hence no need to resum logarithms in the jet functions. We will simply perform the matching to SCET-2 at the scale $\mu_0 \approx \mu_{hc}$. Let us mention an interesting observation at this point. While the ‘‘local’’ current operators $\bar{u}_s \Gamma b_v Y_n^{(\ell)\dagger}$ with $\Gamma = \overleftarrow{\not{n}} P_L$ or $\not{n} P_L$ are gauge invariant, they exhibit a peculiar behavior under scale evolution when QED effects are taken into account. As we will show in Section 4.8, these currents mix with the ‘‘non-local’’ currents j_i^{had} with $i = 3, 4, 5, 6$ under renormalization. This is an unexpected phenomenon, which does not occur when QED is switched off. Interestingly, we find that with the inclusion of the θ_T operator in the definitions of j_1^{had} and j_2^{had} , this mixing disappears and the two currents evolve multiplicatively (at least to one-loop order). In essence, the θ_T operator removes contributions to the matrix elements of the currents from large negative values of the light-cone momentum $n \cdot l_s$ of the light spectator quark. These large negative momenta seem to be responsible for the mixing with the non-local operators.

Matrix elements of the leptonic currents should be evolved from the scale of the charged-lepton mass up to the matching scale μ_0 , thereby resumming large QED logarithms of the ratio

(μ_0^2/m_ℓ^2) , which is larger than 200 in the muon case. At one-loop order, the RG equations satisfied by the leptonic currents j_1^{lep} and j_2^{lep} are

$$\begin{aligned}\frac{d}{d \ln \mu} j_1^{\text{lep}}(\mu) &= Q_\ell^2 \frac{\alpha}{\pi} \left(\ln \frac{\mu}{m_\ell} - \frac{5}{4} \right) j_1^{\text{lep}}(\mu), \\ \frac{d}{d \ln \mu} j_2^{\text{lep}}(x, \mu) &= -Q_\ell \frac{\alpha}{\pi} x j_1^{\text{lep}}(\mu) + Q_\ell^2 \frac{\alpha}{\pi} \int_0^1 dx' \left[\ln \frac{\mu}{m_\ell} \delta(x-x') + \gamma_{22}(x, x') \right] j_2^{\text{lep}}(x', \mu),\end{aligned}\tag{4.66}$$

where the form of γ_{22} is unknown.¹³ The first equation can be solved to give (again neglecting the scale dependence of α)

$$j_1^{\text{lep}}(\mu) = \exp \left[Q_\ell^2 \frac{\alpha}{2\pi} \left(\ln^2 \frac{\mu}{m_\ell} - \frac{5}{2} \ln \frac{\mu}{m_\ell} \right) \right] j_1^{\text{lep}}(m_\ell).\tag{4.67}$$

For the second current, it will be sufficient to have the solution in the leading double-logarithmic approximation, since its matrix element starts at $\mathcal{O}(\alpha)$. This leads to

$$j_2^{\text{lep}}(x, \mu) = \exp \left(Q_\ell^2 \frac{\alpha}{2\pi} \ln^2 \frac{\mu}{m_\ell} \right) \left[j_2^{\text{lep}}(x, m_\ell) - Q_\ell \frac{\alpha}{\pi} x \ln \frac{\mu}{m_\ell} j_1^{\text{lep}}(m_\ell) \right] + \dots,\tag{4.68}$$

where the dots represent terms of subleading logarithmic order.

4.8 SCET-2 matrix elements

We now study the matrix elements of the SCET-2 operators between on-shell meson and lepton states and in the absence of photons emitted into the final state. In Section 5 below, we will construct a low-energy effective theory for the emission of very soft photons with energies much below the scale Λ_{QCD} . In such a theory, the B meson can be described as a point-like meson, and the charged lepton as a highly boosted heavy particle. We will find that the soft and collinear matrix elements considered below will play the role of the Wilson coefficients arising in the (non-perturbative) matching of SCET-2 onto this low-energy effective theory.

We begin with the matrix elements of the leptonic currents defined in (4.65) and define collinear functions $K_i(\mu)$ via ($i = 1, 2$)

$$\langle \ell(p_\ell) \bar{\nu}(p_\nu) | j_i^{\text{lep}}(x, \mu) | 0 \rangle = m_\ell^{\text{phys}} K_i(x, \mu) \bar{u}(v_\ell) P_L v(p_\nu),\tag{4.69}$$

where the on-shell lepton spinors satisfy $\psi_\ell u(v_\ell) = u(v_\ell)$ and $\not{p}_\nu v(p_\nu) = 0$. The variable x is only present for the case $i = 2$. We express these matrix elements in terms of the physical (pole) mass of the charged lepton, which is related to the running mass in the $\overline{\text{MS}}$ scheme by

$$m_\ell^{\text{phys}} = m_\ell(\mu) \left[1 + Q_\ell^2 \frac{\alpha}{2\pi} \left(3 \ln \frac{\mu}{m_\ell} + 2 \right) \right],\tag{4.70}$$

¹³Analogous equations for leptonic currents formed out of two charged muons were derived in [23]. In equation (A.43) of this paper, the quantity analogous to our γ_{22} has been calculated at one-loop order.

where the superscript “phys” is dropped in the following. After a straightforward calculation, including the contribution from on-shell wave-function renormalization, we obtain at one-loop order

$$K_1(\mu) = 1 + Q_\ell^2 \frac{\alpha}{2\pi} \left(\ln^2 \frac{\mu}{m_\ell} - \frac{5}{2} \ln \frac{\mu}{m_\ell} + \frac{\pi^2}{24} - 1 \right),$$

$$K_2(x, \mu) = -Q_\ell \frac{\alpha}{\pi} x \left(\ln \frac{\mu}{m_\ell} - \ln x - \frac{1}{2} \right).$$
(4.71)

For $\mu \gg m_\ell$, we can use the relations (4.67) and (4.68) to resum the large logarithmic corrections of these expressions, obtaining

$$K_1(\mu) = \exp \left[Q_\ell^2 \frac{\alpha}{2\pi} \left(\ln^2 \frac{\mu}{m_\ell} - \frac{5}{2} \ln \frac{\mu}{m_\ell} \right) \right] \left[1 + Q_\ell^2 \frac{\alpha}{2\pi} \left(\frac{\pi^2}{24} - 1 \right) \right],$$

$$K_2(x, \mu) = -Q_\ell \frac{\alpha}{\pi} x \exp \left(Q_\ell^2 \frac{\alpha}{2\pi} \ln^2 \frac{\mu}{m_\ell} \right) \left(\ln \frac{\mu}{m_\ell} - \ln x - \frac{1}{2} \right),$$
(4.72)

where in the second relation only the double-logarithmic corrections are resummed.

We now turn to the matrix elements of the hadronic currents defined in (4.63) and (4.64). It has been shown in [18, 23] that, in the presence of QED effects, these matrix elements contain an overlap contribution from the soft and collinear regions, which is in conflict with factorization. It is necessary to eliminate this contribution by dividing the hadronic currents by the vacuum matrix element of two soft Wilson lines corresponding to the B^- meson and the charged lepton,

$$R^{(\ell, B)} \equiv \langle 0 | Y_n^{(\ell)\dagger} \bar{Y}_v^{(B)} | 0 \rangle. \quad (4.73)$$

Only when this is done, the hadronic matrix elements become independent of unphysical IR regulators (see Appendix C for a detailed discussion).

Preliminary definitions

We will define reduced matrix elements using the trace formalism of HQET [66, 72]. Starting with the “local” current operators without the θ_T operator included, we define

$$\begin{aligned} & \frac{1}{R^{(\ell, B)}} \langle 0 | \bar{u}_s \Gamma b_v Y_n^{(\ell)\dagger} | B^-(v) \rangle \\ &= -\frac{i}{2} \sqrt{m_B} \text{Tr} \left\{ \left[F_+(\mu) - \frac{\not{n}}{2n \cdot v} (F_-(\mu) - F_+(\mu)) \right] \Gamma \frac{1 + \not{v}}{2} \gamma_5 \right\} \\ &= \frac{i}{2} \sqrt{m_B} \text{Tr} \left\{ \left[\frac{\not{\bar{n}}}{2\bar{n} \cdot v} F_+(\mu) + \frac{\not{n}}{2n \cdot v} F_-(\mu) \right] \Gamma \frac{1 + \not{v}}{2} \gamma_5 \right\}, \end{aligned} \quad (4.74)$$

where F_\pm are referred to as HQET decay constants, and Γ can be an arbitrary Dirac structure. Due to the presence of the soft Wilson line $Y_n^{(\ell)\dagger}$, the matrix element “knows” about the direction n of the charged lepton, and this allows for the presence of a second structure proportional to $(F_- - F_+)$, which is absent in pure QCD. It follows that

$$F_\pm(\mu) = F_{\text{QCD}}(\mu) + \mathcal{O}(\alpha), \quad (4.75)$$

where F_{QCD} is the decay constant defined in QCD without electromagnetic effects. In an analogous way, we can express the matrix elements of the “non-local” currents j_3^{had} and j_4^{had} in terms of functions $\phi_{\pm}^B(\omega, \mu)$ defined via [108]

$$\begin{aligned} & \frac{1}{R^{(\ell, B)}} \langle 0 | \bar{Q}_s(z) \Gamma \mathcal{H}_v(0) | B^-(v) \rangle \\ &= \frac{i}{2} \sqrt{m_B} \int d\omega e^{-i\omega\tau} \text{Tr} \left\{ \left[\frac{\not{n}}{2\bar{n} \cdot v} F_+(\mu) \phi_+^B(\omega, \mu) + \frac{\not{n}}{2n \cdot v} F_-(\mu) \phi_-^B(\omega, \mu) \right] \Gamma \frac{1+\not{v}}{2} \gamma_5 \right\}, \end{aligned} \quad (4.76)$$

where $\tau = v \cdot z$, and $z \parallel n$ with $z^2 = 0$. Here ϕ_+^B and ϕ_-^B are the leading-twist and subleading-twist two-particle LCDAs of the B meson. This definition implies

$$\int d\omega \phi_{\pm}^B(\omega, \mu) = 1. \quad (4.77)$$

Strictly speaking, this relation holds only for the bare LCDAs prior to the subtraction of UV pole terms. When corrections of $\mathcal{O}(\alpha_s)$ are included, the LCDAs develop a radiative tail, so that these integrals no longer converge at infinity [108–110]. One then needs to refactorize these integrals in the region where $\Lambda_{\text{QCD}} \ll \omega \ll m_b$ and match them onto the B -meson LCDAs defined in full QCD [110, 111]. For the purposes of our discussion in this work, where corrections of $\mathcal{O}(\alpha_s)$ are neglected, we can ignore these subtleties and assume that relation (4.77) holds for the renormalized LCDAs, too.

Final definitions

After refactorization, we have seen that the “local” currents get modified by the presence of the θ_T operator, which introduces the scale Λ . We thus need to generalize the definition (4.74) to account for this effect, which we do by writing

$$\begin{aligned} & \frac{1}{R^{(\ell, B)}} \langle 0 | \bar{u}_s \left[1 - \theta_T \left(\frac{-i\bar{n} \cdot \overleftarrow{D}_s}{\bar{n} \cdot v} - \Lambda \right) \right] \Gamma b_v Y_n^{(\ell)\dagger} | B^-(v) \rangle \\ &= \frac{i}{2} \sqrt{m_B} \text{Tr} \left\{ \left[\frac{\not{n}}{2\bar{n} \cdot v} F_+(\Lambda, \mu) + \frac{\not{n}}{2n \cdot v} F_-(\Lambda, \mu) \right] \Gamma \frac{1+\not{v}}{2} \gamma_5 \right\}, \end{aligned} \quad (4.78)$$

where as before

$$F_{\pm}(\Lambda, \mu) = F_{\text{QCD}}(\mu) + \mathcal{O}(\alpha). \quad (4.79)$$

But now the definitions (4.78) and (4.76) involve different F_{\pm} parameters, and hence the normalization condition (4.77) no longer holds. One may therefore adopt a different definition, employed in [21], in which all QED effects are absorbed into the LCDAs, i.e.

$$\begin{aligned} & \frac{1}{R^{(\ell, B)}} \langle 0 | \bar{Q}_s(z) \Gamma \mathcal{H}_v(0) | B^-(v) \rangle \\ &= \frac{i}{2} \sqrt{m_B} F_{\text{QCD}}(\mu) \int d\omega e^{-i\omega\tau} \text{Tr} \left\{ \left[\frac{\not{n}}{2\bar{n} \cdot v} \phi_+^B(\omega, \mu) + \frac{\not{n}}{2n \cdot v} \phi_-^B(\omega, \mu) \right] \Gamma \frac{1+\not{v}}{2} \gamma_5 \right\}, \end{aligned} \quad (4.80)$$

with

$$\int d\omega \phi_{\pm}^B(\omega, \mu) = 1 + \mathcal{O}(\alpha). \quad (4.81)$$

With these definitions, we obtain

$$\begin{aligned} S_1 &= \frac{\langle 0 | j_1^{\text{had}}(\Lambda, \mu) | B^- \rangle}{R^{(\ell, B)}} = -\frac{i}{2} \sqrt{m_B} F_-(\Lambda, \mu), \\ S_2 &= \frac{\langle 0 | j_2^{\text{had}}(\Lambda, \mu) | B^- \rangle}{R^{(\ell, B)}} = -\frac{i}{2} \sqrt{m_B} F_+(\Lambda, \mu), \\ S_3 &= \frac{\langle 0 | j_3^{\text{had}}(\omega, \mu) | B^- \rangle}{R^{(\ell, B)}} = -\frac{i}{2} \sqrt{m_B} F_{\text{QCD}}(\mu) \phi_-^B(\omega, \mu), \\ S_4 &= \frac{\langle 0 | j_4^{\text{had}}(\omega, \mu) | B^- \rangle}{R^{(\ell, B)}} = -\frac{i}{2} \sqrt{m_B} F_{\text{QCD}}(\mu) \phi_+^B(\omega, \mu). \end{aligned} \quad (4.82)$$

The remaining hadronic matrix elements can be expressed in terms of three-particle LCDAs of the B meson, corresponding to the Fock state with an extra gluon or photon. Generalizing the definitions in [112, 113] to include QED effects, we define

$$\begin{aligned} S_5 &= \frac{\langle 0 | j_5^{\text{had}}(\omega, \omega_g, \mu) | B^- \rangle}{R^{(\ell, B)}} = i \sqrt{m_B} F_{\text{QCD}}(\mu) \frac{\phi_{3g}^B(\omega, \omega_g, \mu)}{\omega}, \\ S_6 &= \frac{\langle 0 | j_6^{\text{had}}(\omega, \omega_g, \mu) | B^- \rangle}{R^{(\ell, B)}} = i \sqrt{m_B} F_{\text{QCD}}(\mu) \frac{\phi_{3\gamma}^B(\omega, \omega_g, \mu)}{\omega}. \end{aligned} \quad (4.83)$$

Our 3-particle LCDA ϕ_{3g}^B is related to the definitions in used in these references by

$$\phi_{3g}^B(\omega, \omega_g, \mu) = \frac{\psi_A(\omega, \omega_g, \mu) - \psi_V(\omega, \omega_g, \mu)}{\omega_g} = \frac{\phi_3(\omega, \omega_g, \mu)}{\omega_g}, \quad (4.84)$$

and the 3-particle LCDA $\phi_{3\gamma}^B$ is the analogous object defined with an electromagnetic gauge field. This latter function is suppressed relative to ϕ_{3g}^B by a factor α/α_s . It would contribute to the $B^- \rightarrow \ell^- \bar{\nu}_\ell$ process starting at $\mathcal{O}(\alpha^2)$, but can be ignored for our purposes. In the limit of very large μ , the asymptotic behavior of the LCDAs for small values of the momentum variables is dictated by conformal symmetry. One finds [113]

$$\phi_+^B(\omega, \mu) \sim \omega, \quad \phi_-^B(\omega, \mu) \sim 1, \quad \phi_{3g, 3\gamma}^B(\omega, \omega_g, \mu) \sim \omega \omega_g. \quad (4.85)$$

Evolution equations for the parameters $F_{\pm}(\Lambda, \mu)$

By carefully computing the UV divergences of the hadronic currents $j_{1,2}^{\text{had}}$ defined in (4.63), we find that the parameters $F_{\pm}(\Lambda, \mu)$ satisfy the RG evolution equations

$$\frac{d}{d \ln \mu} F_{\mp}(\Lambda, \mu) = -\gamma_{F_{\mp}}(\Lambda, \mu) F_{\mp}(\Lambda, \mu), \quad (4.86)$$

with

$$\begin{aligned}\gamma_{F_-}(\Lambda, \mu) &= \gamma_{\text{hl}}(\alpha_s) + \frac{\alpha}{4\pi} \left(3Q_\ell^2 - 3Q_b^2 - 2Q_\ell Q_u \ln \frac{\mu^2}{\Lambda^2} \right) + \mathcal{O}(\alpha\alpha_s), \\ \gamma_{F_+}(\Lambda, \mu) &= \gamma_{\text{hl}}(\alpha_s) + \frac{\alpha}{4\pi} \left(-Q_\ell^2 - 3Q_b^2 + 4Q_\ell Q_b - 2Q_\ell Q_u \ln \frac{\mu^2}{\Lambda^2} \right) + \mathcal{O}(\alpha\alpha_s),\end{aligned}\tag{4.87}$$

where the QCD anomalous dimension has been given in (3.84). The two results can be simplified using charge conservation and combined into

$$\gamma_{F_\mp}(\Lambda, \mu) = \gamma_{\text{hl}}(\alpha_s) + \frac{Q_u \alpha}{4\pi} \left(-(4 \pm 2)Q_\ell - 3Q_u - 2Q_\ell \ln \frac{\mu^2}{\Lambda^2} \right) + \mathcal{O}(\alpha\alpha_s).\tag{4.88}$$

The technical details of this calculation are presented in Appendix C. For the case of F_- , the above result was first derived in [24].

The fact that the Λ -dependent decay constants satisfy multiplicative evolution equations is non-trivial. Without refactorization, the parameters $F_\pm(\mu)$ introduced in (4.74) would exhibit an off-diagonal mixing with the matrix elements of non-local operators, such that

$$\begin{aligned}\frac{d}{d \ln \mu} F_\mp(\mu) &= - \left[\gamma_{\text{hl}}(\alpha_s) + \frac{Q_u \alpha}{4\pi} (-2Q_\ell - 3Q_u) \right] F_\mp(\mu) \\ &\quad - \frac{\alpha}{2\pi} Q_\ell Q_u F_{\text{QCD}}(\mu) \int_0^\infty d\omega \phi_\mp^B(\omega, \mu) \ln \frac{\mu^2}{\omega^2}.\end{aligned}\tag{4.89}$$

The anomalous dimensions in this result follow directly from (3.70).

The Λ dependence of the parameters $F_\mp(\Lambda, \mu)$ is compensated by an equal and opposite cutoff dependence of the RBS-subtracted convolution integrals of the hard and jet functions to render the final result independent of the cutoff scale. It is entirely determined by the subtraction terms derived from (4.41). Taking a derivative with respect to $\ln \Lambda$, and subtracting the $1/\epsilon$ pole terms in the $\overline{\text{MS}}$ scheme, we find the Λ evolution equations¹⁴

$$\begin{aligned}\frac{d}{d \ln \Lambda} \frac{F_-(\Lambda, \mu)}{F_{\text{QCD}}(\mu)} &= -Q_\ell Q_u \frac{\alpha}{2\pi} \left[\int_0^\infty d\omega \phi_-^B(\omega, \mu) \left(\ln \frac{\mu^2}{\Lambda\omega} + 1 \right) \right. \\ &\quad \left. - 2 \int_0^\infty d\omega \int_0^\infty d\omega_g \phi_{3g}^B(\omega, \omega_g, \mu) \left(\frac{1}{\omega_g} \ln \frac{\omega + \omega_g}{\omega} - \frac{1}{\omega + \omega_g} \right) \right], \\ \frac{d}{d \ln \Lambda} \frac{F_+(\Lambda, \mu)}{F_{\text{QCD}}(\mu)} &= -Q_\ell Q_u \frac{\alpha}{2\pi} \int_0^\infty d\omega \phi_+^B(\omega, \mu) \ln \frac{\mu^2}{\Lambda\omega},\end{aligned}\tag{4.90}$$

which are valid at one-loop order.

It is possible to include the leading-logarithmic QCD corrections to these results, which become important if $\Lambda \gg \mu_0$ (whereas $\sqrt{\Lambda\Lambda_{\text{QCD}}} \sim \mu_0$ even for the extreme choice $\Lambda = m_B$).

¹⁴The right-hand sides of these relations can be related to the negative tails of the QED-corrected LCDAs of the B meson, as defined in [21]. This connection will be studied elsewhere.

We will discuss the case of the parameter F_- for concreteness. So far, we have derived the dependence of F_- on Λ by starting from the bare expressions in (4.41) and extracting the one-loop anomalous dimension γ_{F_-} from the $1/\epsilon$ pole terms. We can alternatively derive the Λ dependence of the renormalized function $F_-(\Lambda, \mu)$ using that the renormalized SCET-2 operator $Q_{1,\theta}^A(\mu)$ contains the integral (only the upper integration limit matters)

$$Q_{1,\theta}^A(\mu) \ni \int^\eta dy \llbracket \tilde{H}_1^C(y, \mu) \rrbracket \left[\int d\omega \llbracket J_{O_1^C \rightarrow Q_1^C}(y, \omega, \mu) \rrbracket Q_1^C(\omega, \mu) + \int d\omega \int d\omega_g \llbracket J_{O_1^C \rightarrow Q_2^E}(y, \omega, \mu) \rrbracket Q_2^E(\omega, \omega_g, \mu) \right], \quad (4.91)$$

where

$$\begin{aligned} \llbracket \tilde{H}_1^C(y, \mu) \rrbracket &= \tilde{U}_C(\mu, \bar{\omega}) \left[1 + \mathcal{O}(\alpha_s) \right], \\ \llbracket J_{O_1^C \rightarrow Q_1^C}(y, \omega, \mu) \rrbracket &= -Q_\ell Q_u \frac{\alpha}{2\pi} \frac{1}{y} \left[\left(\ln \frac{\mu^2}{\bar{\omega}\omega} + 1 \right) + \mathcal{O}(\alpha_s) \right], \\ \llbracket J_{O_1^C \rightarrow Q_2^E}(y, \omega, \omega_g, \mu) \rrbracket &= -Q_\ell Q_u \frac{\alpha}{2\pi} \frac{1}{y} \left[\left(\frac{\omega}{\omega_g} \ln \frac{\omega + \omega_g}{\omega} - \frac{\omega}{\omega + \omega_g} \right) + \mathcal{O}(\alpha_s) \right], \end{aligned} \quad (4.92)$$

with $\bar{\omega} \equiv y m_B$, and $\mathcal{O}(\alpha_s)$ corrections that are free of large logarithms even for $\Lambda \lesssim m_B$. The first relation follows from (4.56) by taking the limit of small y , and the one-loop expressions for the renormalized jet functions have been given in (4.49) and (4.50). Taking the matrix elements of the operators involved, we then obtain

$$\begin{aligned} \frac{d}{d \ln \Lambda} \frac{F_-(\Lambda, \mu)}{F_{\text{QCD}}(\mu)} &= -Q_l Q_u \frac{\alpha}{2\pi} \tilde{U}_C(\mu, \Lambda) \left[\int_0^\infty d\omega \phi_-^B(\omega, \mu) \left(\ln \frac{\mu^2}{\Lambda\omega} + 1 \right) \right. \\ &\quad \left. - 2 \int_0^\infty d\omega \int_0^\infty d\omega_g \left(\frac{1}{\omega_g} \ln \frac{\omega + \omega_g}{\omega} - \frac{1}{\omega + \omega_g} \right) \phi_{3g}^B(\omega, \omega_g, \mu) + \mathcal{O}(\alpha_s) \right], \end{aligned} \quad (4.93)$$

and similarly

$$\frac{d}{d \ln \Lambda} \frac{F_+(\Lambda, \mu)}{F_{\text{QCD}}(\mu)} = -Q_l Q_u \frac{\alpha}{2\pi} \tilde{U}_C(\mu, \Lambda) \int_0^\infty d\omega \phi_+^B(\omega, \mu) \ln \frac{\mu^2}{\Lambda\omega}. \quad (4.94)$$

These result differ from those in (4.90) by the Sudakov factor $\tilde{U}_C(\mu, \Lambda)$ on the right-hand side, which becomes relevant if Λ is significantly different from the scale μ . The first equation can be solved to give

$$\begin{aligned} \frac{F_-(m_B, \mu)}{F_{\text{QCD}}(\mu)} &= \frac{F_-(\Lambda, \mu)}{F_{\text{QCD}}(\mu)} - Q_l Q_u \frac{\alpha}{2\pi} \int_\Lambda^{m_B} \frac{d\bar{\omega}}{\bar{\omega}} \tilde{U}_C(\mu, \bar{\omega}) \left[\int_0^\infty d\omega \phi_-^B(\omega, \mu) \left(\ln \frac{\mu^2}{\bar{\omega}\omega} + 1 \right) \right. \\ &\quad \left. - 2 \int_0^\infty d\omega \int_0^\infty d\omega_g \left(\frac{1}{\omega_g} \ln \frac{\omega + \omega_g}{\omega} - \frac{1}{\omega + \omega_g} \right) \phi_{3g}^B(\omega, \omega_g, \mu) + \mathcal{O}(\alpha_s) \right], \end{aligned} \quad (4.95)$$

which can be used to calculate the parameter $F_-(m_B, \mu)$ in terms of $F_-(\Lambda, \mu)$ in leading logarithmic approximation.

Given these results, it is straightforward to show that¹⁵

$$\frac{d}{d \ln \mu} \frac{d}{d \ln \Lambda} \frac{F_{\mp}(\Lambda, \mu)}{F_{\text{QCD}}(\mu)} = -Q_l Q_u \frac{\alpha}{\pi} \tilde{U}_C(\mu, \Lambda) \left[1 + \mathcal{O}\left(\alpha_s \ln \frac{\mu^2}{\Lambda^2}\right) \right], \quad (4.96)$$

where the leading, single-logarithmic corrections arise from the μ -derivative of $\tilde{U}_C(\mu, \Lambda)$. It follows that the anomalous dimensions $\gamma_{F_{\mp}}$ in (4.88) must be generalized to

$$\gamma_{F_{\mp}}(\Lambda, \mu) = \gamma_{\text{hl}}(\alpha_s) + \frac{Q_u \alpha}{4\pi} \left[-(4 \pm 2) Q_\ell - 3 Q_u - 4 Q_\ell \int_\Lambda^\mu \frac{d\bar{\omega}}{\bar{\omega}} \tilde{U}_C(\mu, \bar{\omega}) \right] + \mathcal{O}\left(\alpha \alpha_s \ln^2 \frac{\mu^2}{\Lambda^2}\right). \quad (4.97)$$

The fact that this anomalous dimension is beyond the Sudakov type, as it involves a non-linear function of $\ln(\mu^2/\Lambda^2)$ and needs to be resummed if the two scales Λ and μ are of different order, appears to be a generic feature of SCET factorization problems at next-to-leading power (see e.g. [114, 115] and the Introduction of [52], as well as [54, 58]). It deserves further exploration.

4.9 The virtual $B^- \rightarrow \ell^- \bar{\nu}_\ell$ amplitude

We are now in a position to combine our results to obtain the factorized and RG-improved expression for the $B^- \rightarrow \ell^- \bar{\nu}_\ell$ decay amplitude without additional soft photon emission. We eliminate the HQET parameter F_{QCD} in terms of the B -meson decay constant f_B defined in pure QCD, which can be calculated with high accuracy using lattice QCD. The relevant relation is

$$\sqrt{m_B} f_B = [H_1^A(\mu) + H_2^A(\mu)]_{\text{QCD}} F_{\text{QCD}}(\mu), \quad (4.98)$$

which holds up to power corrections of $\mathcal{O}(\Lambda_{\text{QCD}}/m_b)$ [116]. The subscript ‘‘QCD’’ on the hard functions indicates that they must be evaluated setting $\alpha \rightarrow 0$. We then write the decay amplitude in the form

$$\mathcal{M}(B^- \rightarrow \ell^- \bar{\nu}_\ell) = i\sqrt{2} G_F^{(\mu)} V_{ub} m_\ell f_B \bar{u}(v_\ell) P_L v(p_\nu) \sum_{i,X} T_i^X, \quad (4.99)$$

where we have used that the vacuum matrix element $\langle 0 | R^{(\ell,B)} | 0 \rangle = 1$ is scaleless without emitted photons and hence equals unity. The contributions T_i^X result from the matrix elements of the relevant SCET-1 operators O_i^X , matched onto SCET-2 as described in this section. In full generality, we obtain

$$\begin{aligned} T_{1,2}^A &= K_{\text{EW}}(\mu) \frac{H_{1,2}^A(\mu)}{[H_1^A(\mu) + H_2^A(\mu)]_{\text{QCD}}} K_1(\mu) \frac{F_{-,+}(\Lambda, \mu)}{F_{\text{QCD}}(\mu)}, \\ T_{1,2}^B &= K_{\text{EW}}(\mu) \int_0^1 dy \frac{H_{1,2}^B(y, \mu)}{[H_1^A(\mu) + H_2^A(\mu)]_{\text{QCD}}} K_2(y, \mu) \frac{F_{-,+}(\Lambda, \mu)}{F_{\text{QCD}}(\mu)}, \end{aligned} \quad (4.100)$$

¹⁵When QCD corrections to the jet functions are included, there will be additional contributions to the right-hand side, which we expect to be numerically subdominant.

and

$$\begin{aligned}
T_1^C &= K_{\text{EW}}(\mu) K_1(\mu) \int_0^1 dy \frac{1}{[H_1^A(\mu) + H_2^A(\mu)]_{\text{QCD}}} \\
&\times \int_0^\infty d\omega \left\{ \left[H_1^C(y, \mu) J_{O_1^C \rightarrow Q_1^C}(y, \omega, \mu) - \theta(\eta - y) \llbracket H_1^C(y, \mu) \rrbracket \llbracket J_{O_1^C \rightarrow Q_1^C}(y, \omega, \mu) \rrbracket \right] \phi_-^B(\omega, \mu) \right. \\
&\quad \left. - 2 \int_0^\infty \frac{d\omega_g}{\omega} \left[H_1^C(y, \mu) J_{O_1^C \rightarrow Q_2^E}(y, \omega, \omega_g, \mu) \right. \right. \\
&\quad \quad \left. \left. - \theta(\eta - y) \llbracket H_1^C(y, \mu) \rrbracket \llbracket J_{O_1^C \rightarrow Q_2^E}(y, \omega, \omega_g, \mu) \rrbracket \right] \phi_{3g}^B(\omega, \omega_g, \mu) \right\}, \\
T_{3,4}^C &= K_{\text{EW}}(\mu) K_1(\mu) \int_0^1 dy \int_0^\infty d\omega \frac{H_{3,4}^C(y, \mu)}{[H_1^A(\mu) + H_2^A(\mu)]_{\text{QCD}}} J_{O_{3,4}^C \rightarrow Q_1^C}(y, \omega, \mu) \phi_-^B(\omega, \mu).
\end{aligned} \tag{4.101}$$

The dependence on the cutoff $\Lambda = \eta m_B$ cancels between the the parameters $F_\mp(\Lambda, \mu)$ in (4.100) and the η -dependent terms in (4.101). As mentioned earlier, we will evaluate the quantities T_i^X at a hadronic scale $\mu = \mu_0$, which is still in the perturbative domain. In our numerical work, we will take $\mu_0 = 1.5 \text{ GeV}$ as default value, and estimate scale uncertainties by varying μ_0 up and down by a factor $\sqrt{2}$.

For the sum of the type-*A* and type-*B* contributions, we find in our approximation scheme

$$\begin{aligned}
T_{1+2}^{A+B} &= U_{\text{EW}}(m_B, m_Z) \exp \left[\frac{\alpha}{8\pi} \left(Q_\ell^2 \ln^2 \frac{\mu_0^2}{m_\ell^2} - Q_\ell Q_b \ln^2 \frac{\mu_0^2}{m_B^2} \right) \right] \frac{F_-(\Lambda, \mu_0)}{F_{\text{QCD}}(\mu_0)} \\
&\times \left\{ \left[H_1^A(m_B) + H_2^A(m_B) \right]_{\text{QED}}^{\kappa=0} \right. \\
&\quad + \frac{\alpha}{4\pi} \left[\left(Q_\ell Q_u + (1+z) Q_\ell Q_b - \frac{3}{2} Q_b^2 \right) \ln \frac{\mu_0^2}{m_B^2} \right. \\
&\quad \quad \left. - \left(2Q_\ell Q_u + \frac{3}{2} Q_\ell^2 + z Q_\ell Q_b \right) \ln \frac{\mu_0^2}{m_\ell^2} + \frac{31}{2} Q_\ell Q_u + Q_\ell Q_b + \left(\frac{\pi^2}{12} - 2 \right) Q_\ell^2 \right. \\
&\quad \quad \left. \left. + 4Q_\ell Q_u \int_{m_B}^{\mu_0} \frac{d\mu'}{\mu'} \frac{\tilde{U}_C(\mu', m_B)}{1 - \delta(\mu')} \right] \right\},
\end{aligned} \tag{4.102}$$

where $U_{\text{EW}}(m_B, m_Z)$ has been given in (2.10). We have used that the quantity F_+ appears only in the one-loop QED corrections, so it is sufficient to keeps its double-logarithmic terms, which are the same as those of F_- . In the matching conditions for the hard functions $H_{1,2}^A(m_B)$, given explicitly in (3.98), we only keep the QED contributions and set $\kappa = 0$. At one-loop order, the κ -dependent corrections cancel between K_{EW} and H_1^A . We further obtain for the

sum of the type- C contributions

$$\begin{aligned}
T_{1+3+4}^C &= -U_{\text{EW}}(m_B, m_Z) \exp \left[\frac{\alpha}{8\pi} \left(Q_\ell^2 \ln^2 \frac{\mu_0^2}{m_\ell^2} - Q_\ell Q_b \ln^2 \frac{\mu_0^2}{m_B^2} \right) \right] \\
&\times Q_\ell Q_u \frac{\alpha}{2\pi} \left\{ \left[\frac{1}{1 - \delta(\mu_0)} \ln \frac{\mu_0^2}{m_B \omega_-(\mu_0)} - h_1(\delta(\mu_0)) \right] \tilde{U}_C(\mu_0, m_B) \right. \\
&\quad + \int_\Lambda^{m_B} \frac{d\bar{\omega}}{\bar{\omega}} \left(\ln \frac{\mu_0^2}{\bar{\omega} \omega_-(\mu_0)} + 1 \right) \tilde{U}_C(\mu_0, \bar{\omega}) \\
&\quad + 2 \left[\frac{\tilde{U}_C(\mu_0, m_B)}{1 - \delta(\mu_0)} - \int_\Lambda^{m_B} \frac{d\bar{\omega}}{\bar{\omega}} \tilde{U}_C(\mu_0, \bar{\omega}) \right] \\
&\quad \left. \times \int_0^\infty d\omega \int_0^\infty d\omega_g \phi_{3g}^B(\omega, \omega_g, \mu_0) \left[\frac{1}{\omega_g} \ln \frac{\omega + \omega_g}{\omega} - \frac{1}{\omega + \omega_g} \right] \right\}, \tag{4.103}
\end{aligned}$$

where

$$h_1(\delta) = \frac{H(-\delta)}{\delta} - \frac{H(1-\delta)}{1-\delta} - \frac{\delta}{(1-\delta)^2}, \tag{4.104}$$

and $H(x) = \psi(1+x) + \gamma_E$ is the harmonic-number function. The parameter ω_- is defined as the logarithmic moment of the B -meson LCDA,

$$\ln \frac{\omega_-(\mu)}{\nu} = \int_0^\infty d\omega \phi_-^B(\omega, \mu) \ln \frac{\omega}{\nu}. \tag{4.105}$$

where ν is an arbitrary reference scale introduced to render the arguments of the logarithms dimensionless. Note that $\omega_-(\mu)$ is scale dependent, but this dependence is beyond our accuracy. The same is true for $\delta(\mu)$.

Given the above results, it is straightforward to show that, at one-loop order,

$$\begin{aligned}
\frac{d}{d \ln \mu_0} \ln \sum_{i,X} T_i^X &= \gamma_{\text{soft}}(\alpha) + Q_\ell Q_u \frac{\alpha}{2\pi} \left(2 \int_{m_B}^{\mu_0} \frac{d\bar{\omega}}{\bar{\omega}} \tilde{U}_C(\mu_0, \bar{\omega}) - \ln \frac{\mu_0^2}{m_B^2} \right) \\
&+ \left[\frac{d}{d \ln \mu_0} \ln \frac{F_-(\Lambda, \mu_0)}{F_{\text{QCD}}(\mu_0)} + \frac{\alpha}{4\pi} \left(3Q_\ell^2 - 3Q_b^2 - 4Q_\ell Q_u \int_\Lambda^{\mu_0} \frac{d\bar{\omega}}{\bar{\omega}} \tilde{U}_C(\mu_0, \bar{\omega}) \right) \right], \tag{4.106}
\end{aligned}$$

where the first term on the right-hand side is the soft anomalous dimension

$$\gamma_{\text{soft}} = Q_\ell^2 \frac{\alpha}{2\pi} \left(\ln \frac{m_B^2}{m_\ell^2} - 2 \right), \tag{4.107}$$

which cancels the scale dependence of the real-photon emission contributions calculated in a low-energy effective theory in Section 5. The quantity γ_{soft} is closely related to the velocity-dependent anomalous dimension of a QED current in heavy-particle effective theory, consisting

of a charged B -meson field with 4-velocity $v \equiv v_B$ and a soft lepton field with 4-velocity v_ℓ , which reads [72]

$$\gamma_{\text{soft}}(v_\ell \cdot v_B, \alpha) = Q_\ell Q_B \frac{\alpha}{\pi} \left[\frac{w}{\sqrt{w^2 - 1}} \ln \left(w + \sqrt{w^2 - 1} \right) - 1 \right], \quad w = v_\ell \cdot v_B. \quad (4.108)$$

With $w = (m_B^2 + m_\ell^2)/(2m_B m_\ell)$, cf. (3.4), one finds

$$\gamma_{\text{soft}}(v_\ell \cdot v_B, \alpha) = Q_\ell Q_B \frac{\alpha}{\pi} \left(\frac{m_B^2 + m_\ell^2}{m_B^2 - m_\ell^2} \ln \frac{m_B}{m_\ell} - 1 \right), \quad (4.109)$$

which reduces to the result (4.107) in the limit $m_\ell \ll m_B$.

The term in brackets in the second line of (4.106) vanishes due to the scale dependence of the ratio $F_-(\Lambda, \mu)/F_{\text{QCD}}(\mu)$ obtained from (4.97). This leaves the second term in the first line, which differs from 1 by terms of order $\alpha \ln(\mu_0^2/m_B^2) [\alpha_s \ln^2(\mu_0^2/m_B^2)]^n$ with $n \in \mathbb{N}$. These leading-logarithmic QCD corrections are, however, within our accuracy goal. The fact that they do not cancel out is related to the missing two-loop terms of $\mathcal{O}(\alpha\alpha_s)$ in the RG evolution equations for the hard functions $H_{1,2}^A$ in (3.95). To fix the problem, we must replace

$$Q_\ell Q_b \ln \frac{\mu^2}{m_B^2} \rightarrow Q_\ell^2 \ln \frac{\mu^2}{m_B^2} + 2Q_\ell Q_u \int_{m_B}^\mu \frac{d\bar{\omega}}{\bar{\omega}} \tilde{U}_C(\mu, \bar{\omega}) \quad (4.110)$$

in the homogeneous terms shown in the first line of each equation. When this is done, the QED Sudakov exponent in (4.102) and (4.103) is replaced by

$$Q_\ell^2 \frac{\alpha}{8\pi} \left(\ln^2 \frac{\mu_0^2}{m_\ell^2} - \ln^2 \frac{\mu_0^2}{m_B^2} \right) - Q_\ell Q_u \frac{\alpha}{\pi} \int_{m_B}^{\mu_0} \frac{d\mu'}{\mu'} \int_{m_B}^{\mu'} \frac{d\bar{\omega}}{\bar{\omega}} \tilde{U}_C(\mu', \bar{\omega}), \quad (4.111)$$

and the extra terms in the first line of (4.106) vanish.

We now rearrange the QED double and single logarithms in such a way that we factor out

$$\exp \left[Q_\ell^2 \frac{\alpha}{8\pi} \left(\ln^2 \frac{\mu^2}{m_\ell^2} - \ln^2 \frac{\mu^2}{m_B^2} - 2 \ln \frac{\mu^2}{m_\ell^2} - 2 \ln \frac{\mu^2}{m_B^2} \right) \right] = \left(\frac{\mu^2}{m_B m_\ell} \right)^{\gamma_{\text{soft}}/2}. \quad (4.112)$$

We then define a scale-invariant quantity $\mathcal{R}_{\text{virt}}$ by

$$\sum_{i,X} T_i^X = \left(\frac{\alpha(m_Z)}{\alpha(m_B)} \right)^{\frac{9}{40}} \left(\frac{\mu_0^2}{m_B m_\ell} \right)^{\gamma_{\text{soft}}/2} \mathcal{R}_{\text{virt}}. \quad (4.113)$$

Within our approximations, it is given by

$$\begin{aligned}
\mathcal{R}_{\text{virt}} = & \exp \left[- Q_\ell Q_u \frac{\alpha}{\pi} \int_{m_B}^{\mu_0} \frac{d\mu'}{\mu'} \int_{m_B}^{\mu'} \frac{d\bar{\omega}}{\bar{\omega}} \tilde{U}_C(\mu', \bar{\omega}) \right] \frac{F_-(\Lambda, \mu_0)}{F_{\text{QCD}}(\mu_0)} \\
& \times \left\{ 1 + \frac{\alpha}{4\pi} \left[\frac{3}{2} Q_\ell^2 \ln \frac{\mu_0^2}{m_\ell^2} - \frac{3}{2} Q_b^2 \ln \frac{\mu_0^2}{m_B^2} - (2+z) Q_\ell Q_b \ln \frac{m_B^2}{m_\ell^2} + \left(\frac{\pi^2}{12} - \frac{27}{2} \right) Q_\ell^2 \right. \right. \\
& \quad \left. \left. + \left(\frac{21}{2} + \frac{z^2 \ln z}{z-1} + z - 2\text{Li}_2(1-z) - \frac{\pi^2}{12} \right) Q_\ell Q_b - (2+3 \ln z) Q_b^2 \right] \right. \\
& + Q_\ell Q_u \frac{\alpha}{\pi} \int_{m_B}^{\mu_0} \frac{d\mu'}{\mu'} \frac{\tilde{U}_C(\mu', m_B)}{1 - \delta(\mu')} \\
& - Q_\ell Q_u \frac{\alpha}{2\pi} \left[\left[\frac{1}{1 - \delta(\mu_0)} \ln \frac{\mu_0^2}{m_B \omega_-(\mu_0)} - h_1(\delta(\mu_0)) \right] \tilde{U}_C(\mu_0, m_B) \right. \\
& \quad \left. + \int_\Lambda^{m_B} \frac{d\bar{\omega}}{\bar{\omega}} \left(\ln \frac{\mu_0^2}{\bar{\omega} \omega_-(\mu_0)} + 1 \right) \tilde{U}_C(\mu_0, \bar{\omega}) \right] \\
& - Q_\ell Q_u \frac{\alpha}{\pi} \left[\frac{\tilde{U}_C(\mu_0, m_B)}{1 - \delta(\mu_0)} - \int_\Lambda^{m_B} \frac{d\bar{\omega}}{\bar{\omega}} \tilde{U}_C(\mu_0, \bar{\omega}) \right] \\
& \left. \times \int_0^\infty d\omega \int_0^\infty d\omega_g \phi_{3g}^B(\omega, \omega_g, \mu_0) \left[\frac{1}{\omega_g} \ln \frac{\omega + \omega_g}{\omega} - \frac{1}{\omega + \omega_g} \right] \right\}. \tag{4.114}
\end{aligned}$$

This expression is the main result of our paper up to now, and it constitutes the RG-improved expression of a result presented in [24]. Using the result (4.93), we obtain

$$\frac{d\mathcal{R}_{\text{virt}}}{d \ln \Lambda} = 0, \tag{4.115}$$

up to terms that are beyond our approximation. A particularly simple form of the result is

obtained by setting $\Lambda = m_B$, in which case

$$\begin{aligned}
\mathcal{R}_{\text{virt}} = & \exp \left[-Q_\ell Q_u \frac{\alpha}{\pi} \int_{m_B}^{\mu_0} \frac{d\mu'}{\mu'} \int_{m_B}^{\mu'} \frac{d\bar{\omega}}{\bar{\omega}} \tilde{U}_C(\mu', \bar{\omega}) \right] \frac{F_-(m_B, \mu_0)}{F_{\text{QCD}}(\mu_0)} \\
& \times \left\{ 1 + \frac{\alpha}{4\pi} \left[\frac{3}{2} Q_\ell^2 \ln \frac{\mu_0^2}{m_\ell^2} - \frac{3}{2} Q_b^2 \ln \frac{\mu_0^2}{m_B^2} - (2+z) Q_\ell Q_b \ln \frac{m_B^2}{m_\ell^2} + \left(\frac{\pi^2}{12} - \frac{27}{2} \right) Q_\ell^2 \right. \right. \\
& \quad \left. \left. + \left(\frac{21}{2} + \frac{z^2 \ln z}{z-1} + z - 2\text{Li}_2(1-z) - \frac{\pi^2}{12} \right) Q_\ell Q_b - (2+3 \ln z) Q_b^2 \right] \right. \\
& + Q_\ell Q_u \frac{\alpha}{\pi} \int_{m_B}^{\mu_0} \frac{d\mu'}{\mu'} \frac{\tilde{U}_C(\mu', m_B)}{1-\delta(\mu')} \\
& - Q_\ell Q_u \frac{\alpha}{2\pi} \left[\frac{1}{1-\delta(\mu_0)} \ln \frac{\mu_0^2}{m_B \omega_-(\mu_0)} - h_1(\delta(\mu_0)) \right] \tilde{U}_C(\mu_0, m_B) \\
& \left. - Q_\ell Q_u \frac{\alpha}{\pi} \frac{\tilde{U}_C(\mu_0, m_B)}{1-\delta(\mu_0)} \int_0^\infty d\omega \int_0^\infty d\omega_g \phi_{3g}^B(\omega, \omega_g, \mu_0) \left[\frac{1}{\omega_g} \ln \frac{\omega + \omega_g}{\omega} - \frac{1}{\omega + \omega_g} \right] \right\}. \tag{4.116}
\end{aligned}$$

The choice $\Lambda = m_B$ (corresponding to $\eta = 1$) lies outside the window indicated in (4.33), but since our result is explicitly Λ -independent, we are free to take this choice. The large logarithms associated with the parameter η are then entirely contained in the parameter $F_-(m_B, \mu_0)$, which now depends on the hadronic B -meson mass. With the help of relation (4.95), we can related this parameter to a parameter $F_-(\Lambda, \mu_0)$ with a different choice of Λ .

Let us finally estimate the perturbative uncertainty of the above result based on its residual scale dependence. We find that

$$\frac{d}{d \ln \mu_0} \ln \mathcal{R}_{\text{virt}} = \mathcal{O} \left(\alpha \alpha_s \ln \frac{\mu_0^2}{m_B^2}, \alpha^2 \ln^2 \frac{\mu_0^2}{m_B^2} \right), \tag{4.117}$$

where the former arise from the residual scale dependence of the terms involving $\tilde{U}_c(\mu_0, m_B)$, while the latter are due to our restriction to the leading QED double logarithms at two-loop order and beyond. The discussion preceding the results (3.96) shows that these ambiguities are consistent with our approximation scheme.¹⁶

4.10 Power-enhanced QED corrections from new physics

The decay $B_s \rightarrow \ell^+ \ell^-$ shares several similarities with the $B^- \rightarrow \ell^- \bar{\nu}_\ell$ process considered here, in particular it is also chirally suppressed, i.e., its decay amplitude is proportional to the charged-lepton mass m_ℓ . It has been shown in [22] that some of the QED corrections to the

¹⁶Relation (4.97) suggests that the scale ambiguity of the ratio $F_-(m_B, \mu_0)/F_{\text{QCD}}(\mu_0)$ starts at order $\alpha \alpha_s \ln^2(\mu_0^2/m_B^2)$, which is one power of logarithm higher than what we found here. Since the remaining terms in the expression for $\mathcal{R}_{\text{virt}}$ do not exhibit a corresponding scale ambiguity, we conclude that the true scale ambiguity in (4.97) is reduced to $\mathcal{O}(\alpha \alpha_s \ln(\mu^2/m_B^2))$ when higher-order QCD corrections are included.

$B_s \rightarrow \ell^+ \ell^-$ decay rate are enhanced by a factor of $\mathcal{O}(m_B/\Lambda_{\text{QCD}})$ relative to the leading-order rate. For $B^- \rightarrow \ell^- \bar{\nu}_\ell$ in the SM, on the other hand, we have shown in Section 3.2 that such power-enhanced QED corrections are absent – a fact that was also noted in [22]. This is a direct consequence of the $(V - A) \otimes (V - A)$ structure of the effective four-fermion operator mediating this decay.

In the presence of new physics, this conclusion can be changed. Consider as an example the operator with structure $(V + A) \otimes (V - A)$ multiplying the Wilson coefficient $L_\ell^{V,LR}$ in the effective Lagrangian (2.1). When matching this operator onto SCET-1, one encounters the operator

$$(\bar{\mathcal{X}}_{hc}^{(u)} \gamma_\perp^\alpha P_R b_v) (\bar{\mathcal{X}}_{hc}^{(\ell)} \gamma_\alpha^\perp P_L \nu_{\bar{c}}) \sim \lambda^{\frac{5}{2}}. \quad (4.118)$$

Matching this operator onto SCET-2, using the same rules as in the previous section, one finds the operators

$$\begin{aligned} & \left(\bar{u}_s \frac{\not{n}}{in \cdot \partial_s} \gamma_\perp^\rho \gamma_\perp^\alpha P_R b_v \right) (\bar{\mathcal{X}}_c^{(\ell)} \{m_\ell \gamma_\rho^\perp, \mathcal{A}_{c\rho}^\perp\} \gamma_\alpha^\perp P_L \nu_{\bar{c}}) \\ & \rightarrow \left(\bar{u}_s \frac{\not{n}}{in \cdot \partial_s} P_R b_v \right) (\bar{\mathcal{X}}_c^{(\ell)} \{m_\ell, \mathcal{A}_c^\perp\} P_L \nu_{\bar{c}}) \sim \lambda_\ell^2 \lambda^2, \end{aligned} \quad (4.119)$$

which are enhanced by a factor $1/\lambda$ compared with the leading-order type- A and type- B operators

$$\frac{1}{\bar{n} \cdot \mathcal{P}_c} (\bar{u}_s \not{n} P_R b_v) (\bar{\mathcal{X}}_c^{(\ell)} \{m_\ell, \mathcal{A}_c^\perp\} P_L \nu_{\bar{c}}) \sim \lambda_\ell^2 \lambda^3 \quad (4.120)$$

encountered in the absence of QED corrections. This is completely analogous to what happens in the case of the $B_s \rightarrow \ell^+ \ell^-$ process, which in the SM is mediated by operators with equal or opposite chirality. In the presence of new physics, the naive magnitude $\sim \alpha/\pi$ of QED corrections may thus be boosted by a factor m_B/m_ℓ , which is about 50 for the case of the muon. Such an enhancement could bring QED corrections to similar size as perturbative QCD effects.

5 Low-energy description and real corrections

We now outline the construction of the effective theory valid below the QCD confinement scale $\Lambda_c \approx 500$ MeV. In this regime, the B meson can be described as a point-like object. Our primary focus is the dynamics of photons with total energy below an experimentally imposed cut $E_\gamma^{\text{tot}} \leq E_{\text{cut}} \ll \Lambda_c$. These very soft photons see the B meson and the charged lepton as static sources of electric charge, allowing for an HQET-like description of both particles. However, it is important to include the possibility of the photon-induced excitation of the B meson into the B^* vector meson, whose leptonic weak decay is not chirally suppressed. The dynamics of other light degrees of freedom, specifically the light pseudoscalar mesons, can be included within the framework of heavy-hadron chiral perturbation theory (HH χ PT) [74–76]. For the lepton, the appropriate theory is boosted heavy-lepton effective theory (bHLET) [117, 118]. The ingredients of these EFT constructions will be presented below.

5.1 Heavy-particle effective theory

Which mass and energy scales should an effective theory valid below the scale of QCD confinement capture? A first relevant scale is set by E_{cut} , the maximal energy allowed for final-state radiation. Another important scale is the mass splitting between the B meson and its first excited state, the B^* , which vanishes in the limit $m_b \rightarrow \infty$ due to heavy-quark spin symmetry. The associated parameter $(m_{B^*} - m_B) \sim \Lambda_c^2/m_b$ is parametrically smaller than Λ_c . Finally, the light pseudoscalar mesons π, K, η associated with spontaneous chiral symmetry breaking in QCD are parametrically lighter than all other QCD resonances. Their masses squared are proportional to the light-quark masses, $m_{\pi, K, \eta}^2 \sim m_q \Lambda_c$, with $m_u, m_d, m_s \ll \Lambda_c$. We begin with a discussion of the first two scales and will later include the dynamics of the light pseudoscalar mesons.

Figure 13 shows the different topologies for the real emission of low-energy photons in the effective description of point-like particles. A region analysis reveals that the relevant momentum modes are either “ultrasoft” (us) or “ultrasoft-collinear” (usc), scaling as

$$\begin{aligned} p_{us} &\sim E_{\text{cut}} \equiv \Lambda_c (\zeta, \zeta, \zeta), \\ p_{usc} &\sim E_{\text{cut}} \left(\frac{m_\ell^2}{m_B^2}, 1, \frac{m_\ell}{m_B} \right) = \Lambda_c \zeta (\lambda_\ell^2, 1, \lambda_\ell), \end{aligned} \tag{5.1}$$

where $\zeta \equiv E_{\text{cut}}/\Lambda_c$ is the expansion parameter of the low-energy theory. The ultrasoft-collinear photons obey the homogeneous scaling $p' \sim \frac{E_{\text{cut}} m_\ell}{m_B} (1, 1, 1)$ when boosted to the rest frame of the charged lepton. Hence, in their respective rest frames, both modes are a factor $E_{\text{cut}}/m_B = \lambda \zeta$ softer than the masses of the B meson and the charged lepton. The physical reason for the appearance of the ultrasoft-collinear mode is that its energy is of order E_{cut} in the B -meson rest frame, where the measurement is performed.

The real-emission corrections come from two different mechanisms: one involving the emission of a photon off the charged external particles, and one where the B meson emits a photon by transitioning into a virtual excited state X_b containing a b quark, which subsequently decays into the lepton pair. In the literature, these two topologies are commonly referred to as

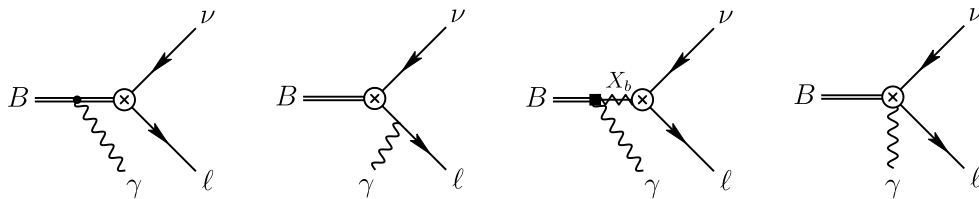


Figure 13: Decay topologies describing the $B^- \rightarrow \ell^- \bar{\nu}_\ell \gamma$ process at energies far below Λ_c . The photon energy is restricted to be less than $E_{\text{cut}} \ll \Lambda_c$ in the B -meson rest frame. The crossed circle indicates the weak interaction vertex. In the third graph, the B meson transitions to an excited meson X_b via the emission of a photon. The black square indicates that the corresponding vertex is a power-suppressed interaction.

“inner bremsstrahlung” and “structure-dependent” contributions, respectively. This nomenclature, introduced for leptonic decays of light mesons [119, 120] and then adopted also for B -meson decays [8, 27], is somewhat misleading, since, as we have shown in the previous sections, also the inner bremsstrahlung contribution contains structure dependence through the weak vertex. We therefore choose to refer to the two contributions as the “direct” and “indirect” ones, where in the latter case the weak decay occurs through an excited state of the B meson. In principle, an additional topology exists (last graph in Figure 13), in which the photon is emitted from a local effective $B\ell\bar{\nu}_\ell\gamma$ interaction vertex [121], which can arise e.g. from ρ -meson exchange [122]. We will show below that this contribution is further power suppressed by a factor of $\mathcal{O}(\zeta^2)$, and will therefore be neglected in our analysis.

For the indirect contribution, heavy-quark spin symmetry implies that only the state $X_b = B^*$ needs to be included as an intermediate state as long as $E_{\text{cut}} \ll \Lambda_c$. To see this, it is instructive to examine the propagator of the intermediate state X_b . In the rest frame of the B meson, we have

$$\frac{1}{(p_B - k_\gamma)^2 - m_X^2} = -\frac{1}{2m_B(E_\gamma + \delta_{X_b})}; \quad \text{with} \quad \delta_{X_b} = \frac{m_X^2 - m_B^2}{2m_B}, \quad (5.2)$$

indicating that only states satisfying $\delta_{X_b} \lesssim E_{\text{cut}}$ contribute at leading power in $\zeta = E_{\text{cut}}/\Lambda_c$. In the heavy-quark limit, one finds that $m_B^* - m_B \rightarrow 0$ due to heavy-quark symmetry, whereas $m_{X_b} - m_B = \mathcal{O}(\Lambda_c)$ [66] for all other excited states, such that

$$\delta_{X_b} \sim \begin{cases} \frac{\Lambda_c^2}{m_B}; & \text{for } X_b = B^*, \\ \Lambda_c; & \text{for } X_b \neq B^*. \end{cases} \quad (5.3)$$

Numerically, one finds $\delta_{B^*} \simeq 45.4 \text{ MeV}$ for the B^{*-} meson, and $\delta_{B_1} \simeq 465.5 \text{ MeV}$ for the next excited state $B_1(5721)$. A significant number of excited B states with masses below 6 GeV are known [34], for which $\delta_{X_b} < 770 \text{ MeV}$. For the validity of the low-energy effective theory it is therefore essential to impose the condition $E_{\text{cut}} \ll \Lambda_c$. Choosing a larger value $E_{\text{cut}} \gtrsim \Lambda_c$ would require including the full tower of excited hadronic states or, equivalently, knowing the two form factors parameterizing the $B^- \rightarrow \ell^- \bar{\nu}_\ell \gamma$ transition for arbitrary photon

energy (see e.g. [123]). It would then not be possible to integrate out the scale Λ_c , and both real and virtual photon corrections would contribute in the low-energy theory at the QCD scale. For $E_{\text{cut}} \ll \Lambda_c$, these form factors simplify and are controlled by the product of two non-perturbative parameters, the $BB^*\gamma$ coupling and the decay constant f_{B^*} .

Leptonic sector

We begin with the construction of the effective description of the charged lepton (the neutrino is trivially described by $\nu_{\bar{c}}$ at all scales). For $\mu \ll m_\ell$, the charged lepton can be treated as a heavy field in the spirit of HQET. Ultrasoft radiation in the lepton rest frame appears boosted in the rest frame of the decaying B meson, giving rise to the ultrasoft-collinear scaling in (5.1). To describe these fluctuations we adopt the bHLET framework [111, 117, 118]. The lepton momentum is decomposed as

$$p_\ell^\mu = m_\ell v_\ell^\mu + k_\ell^\mu, \quad (5.4)$$

where v_ℓ is the 4-velocity of the lepton, and k_ℓ denotes its residual (ultrasoft-collinear) momentum. In the B -meson rest frame, the components of v_ℓ are given by

$$(n \cdot v_\ell, \bar{n} \cdot v_\ell, v_{\ell\perp}^\mu) = \left(\frac{m_\ell}{m_B}, \frac{m_B}{m_\ell}, 0 \right) \sim (\lambda_\ell, \lambda_\ell^{-1}, 0). \quad (5.5)$$

Following the standard HQET construction, we define a rephased lepton field

$$\ell(x) = e^{-im_\ell v_\ell \cdot x} [h_{v_\ell}(x) + H_{v_\ell}(x)], \quad (5.6)$$

where $\not{v}_\ell h_{v_\ell} = h_{v_\ell}$ and $\not{v}_\ell H_{v_\ell} = -H_{v_\ell}$. The field h_{v_ℓ} describes ultrasoft-collinear fluctuations with virtuality of order $\frac{E_{\text{cut}} m_\ell}{m_B} \sim \lambda \zeta m_\ell$ of the lepton about its mass shell, whereas H_{v_ℓ} describes fluctuations with virtuality of order m_ℓ . The latter are integrated out in bHLET and give rise to power-suppressed terms. This leads to the effective Lagrangian

$$\mathcal{L}_\ell = \mathcal{L}_{\text{bHLET}} = \bar{h}_{v_\ell} i v_\ell \cdot D h_{v_\ell} + \dots, \quad (5.7)$$

where the terms not shown are multiplied by powers of $1/m_\ell$ and are suppressed, relative to the leading term, by powers of $\lambda \zeta \sim E_{\text{cut}}/m_B$.

In the low-energy theory, the charged lepton couples only to ultrasoft-collinear radiations, because soft radiations have already been decoupled in SCET-2. These interactions can be decoupled in the bHLET Lagrangian via the field redefinition

$$h_{v_\ell}(x) = C_{v_\ell}^{(\ell)}(x) h_{v_\ell}^{(0)}(x), \quad (5.8)$$

where we have defined the ultrasoft-collinear Wilson line

$$C_{v_\ell}^{(\ell)}(x) = \exp \left[-i Q_\ell e \int_0^\infty ds n \cdot A_{usc}(x + s v_\ell) e^{-\epsilon|s|} \right]. \quad (5.9)$$

In terms of the decoupled field $h_{v_\ell}^{(0)}$, the leading-order effective Lagrangian (5.7) becomes that of a free theory.

For the collinear charged-lepton field in SCET-2, the above field redefinition implies

$$\bar{\chi}_c^{(\ell)}(x) = e^{im_\ell v_\ell \cdot x} C_{v_\ell}^{(\ell)\dagger}(x) \bar{h}_{v_\ell}^{(0)}(x) \frac{\not{n} \not{v}_\ell}{4} + \dots \quad (5.10)$$

In the leptonic current, the SCET projector can be absorbed in the neutrino field. At leading power in bHLET, we thus obtain for the $(V - A)$ weak lepton current in the low-energy theory

$$J_{\text{lep}}^\mu(x) = \bar{\ell} \gamma^\mu P_L \nu_\ell \rightarrow e^{im_\ell v_\ell \cdot x} C_{v_\ell}^{(\ell)\dagger}(x) \left[\bar{h}_{v_\ell}^{(0)} \gamma_\perp^\mu P_L \nu_{\bar{c}} + \frac{m_\ell}{\bar{n} \cdot p_\ell} \bar{n}^\mu \bar{h}_{v_\ell}^{(0)} P_L \nu_{\bar{c}} \right], \quad (5.11)$$

up to $\mathcal{O}(\lambda\zeta)$ power corrections.

Hadronic sector

In the heavy-quark limit, the ground-state mesons containing a heavy quark Q and a light antiquark \bar{q} form a doublet under the heavy-quark spin symmetry and a triplet under $SU(3)_V$, containing pseudoscalar meson field φ_v and vector meson field ρ_v (with $v \cdot \rho_v = 0$), which are degenerate in mass. For the case $Q = b$ and $q = u$ these are the B^- and B^{*-} mesons. To construct the heavy-meson effective theory (HMET) describing the interactions of these particles with photons, it is convenient to define the superfield

$$\Phi_B = \frac{e^{-i\bar{m}_B v \cdot x}}{\sqrt{2\bar{m}_B}} H, \quad \text{with} \quad H = \frac{1 + \not{v}}{2} (\not{\phi}_v - \varphi_v \gamma_5), \quad (5.12)$$

where $\not{v} H = H = -H \not{v}$.¹⁷ We denote by $\bar{m}_B = m_b + \Lambda_c$ the common mass of the B and B^* states in the heavy-quark limit. The field H describes ultrasoft fluctuations about the mass shell of these states.

The leading-order Lagrangian of the H field can be written in the compact form

$$\mathcal{L}_{\text{HMET}} = -\frac{1}{2} \text{Tr}[\bar{H} i v \cdot D H] = \varphi_v^\dagger i v \cdot D \varphi_v - \rho_{v,\mu}^\dagger i v \cdot D \rho_v^\mu, \quad (5.13)$$

where $\bar{H} = \gamma^0 H^\dagger \gamma^0$. Momentum conservation allows these fields to interact with both ultrasoft and ultrasoft-collinear photons. The corresponding covariant derivative reads

$$iD^\mu = i\partial^\mu + Q_B e A_{us}^\mu(x) + Q_B e \frac{n^\mu}{2} \bar{n} \cdot A_{usc}(x_+), \quad (5.14)$$

where $Q_B = -1$ is the charge of the B^- meson, and we have multipole expanded the ultrasoft-collinear gauge field about the point x_+ . This ensures that only the large momentum component $\bar{n} \cdot k_{usc} \sim E_{\text{cut}}$ is kept at the interaction vertices and smaller components are expanded out. In analogy with the discussion of the lepton sector, the leading-power interactions of the H field can be decoupled at the Lagrangian level via the field redefinition

$$H(x) = \bar{Y}_v^{(B)}(x) \bar{C}_{\bar{n}}^{(B)}(x_+) H^{(0)}(x), \quad (5.15)$$

¹⁷The meson field H is not to be confused with the field H_{v_ℓ} introduced earlier.

where we define the ultrasoft and ultrasoft-collinear Wilson lines

$$\begin{aligned}\bar{Y}_v^{(B)}(x) &= \exp \left[i Q_B e \int_{-\infty}^0 ds v \cdot A_{us}(x + sv) e^{-\epsilon|s|} \right], \\ \bar{C}_{\bar{n}}^{(B)}(x_+) &= \exp \left[i Q_B e \int_{-\infty}^0 ds \bar{n} \cdot A_{usc}(x_+ + s\bar{n}) e^{-\epsilon|s|} \right].\end{aligned}\tag{5.16}$$

Written in terms of the field $H^{(0)}$, the leading-order Lagrangian (5.13) describes a free theory.

The effective field H has mass dimension $D = \frac{3}{2}$ and EFT power counting $(\Lambda_c \zeta)^{\frac{3}{2}}$, hence the leading-order Lagrangian (5.13) has scaling $(\Lambda_c \zeta)^4 \sim E_{\text{cut}}^4$, which compensates the scaling of the measure $d^4 x_{us} \sim E_{\text{cut}}^{-4}$ to give unsuppressed contributions to the action. It will be necessary for our analysis to include some subleading terms in the hadronic sector. At mass dimension $D = 5$, the only relevant subleading operator is [124]

$$c_{\text{dip}}^{\text{HMET}} \frac{Q_u e}{8\Lambda_c} \text{Tr} [\sigma_{\mu\nu} \bar{H}^{(0)} H^{(0)}] F_{us}^{\mu\nu},\tag{5.17}$$

with a non-perturbative low-energy constant $c_{\text{dip}}^{\text{HMET}} = \mathcal{O}(1)$. This operator conserves $SU(2)_v$ and yields contributions to the action suppressed by one power of $\zeta = E_{\text{cut}}/\Lambda_c$. It can be understood as arising from dipole interactions of the light spectator quark inside the heavy mesons [125], which is why we have included the charge Q_u in the normalization of this operator. The analogous operator with ultrasoft-collinear photons is further power-suppressed by a factor m_ℓ/m_B and can be safely neglected. In order to account for the small mass splitting between the B and B^* mesons, it will also be necessary to include the leading corrections to the heavy-quark limit $m_b \rightarrow \infty$, which are best identified at the parton level and incorporated into the EFT via spurions. In the HQET Lagrangian, the leading power corrections are given by [66]

$$C_{\text{kin}} \frac{1}{2m_b} \bar{b}_v (iD_{\perp v})^2 b_v + C_{\text{mag}}(\mu) \frac{g_s}{4m_b} \bar{b}_v \sigma_{\mu\nu} G_{us}^{\mu\nu} b_v + \dots,\tag{5.18}$$

where the symbol \perp_v projects out the components of a vector orthogonal to v (i.e. $v_\mu D_{\perp v}^\mu = 0$), $G_{us}^{\mu\nu}$ denotes the ultrasoft gluon field-strength tensor, and the dots refer to terms suppressed by at least two powers of $1/m_b$. The Wilson coefficient of the kinetic operator satisfies $C_{\text{kin}} = 1$ to all orders of perturbation theory [126], while the expression for the coefficient C_{mag} at NLO in RG-improved perturbation theory has been derived in [127]. The terms shown here are suppressed relative to the leading-order terms by a factor $\zeta \Lambda_c/m_b \sim \lambda \zeta$. From this we can read off the spurions

$$\Sigma_{\text{kin}} = C_{\text{kin}} = 1, \quad \Sigma_{\text{mag}}^{\mu\nu} = C_{\text{mag}}(\mu) \sigma^{\mu\nu},\tag{5.19}$$

both of which transform as triplets under $SU(2)_v$. It is now a straightforward matter to construct the relevant power-suppressed corrections to the effective Lagrangian (5.13). We obtain

$$\begin{aligned}\mathcal{L}_H &= -\frac{1}{2} \text{Tr} [\bar{H}^{(0)} i v \cdot \partial H^{(0)}] - \frac{1}{4m_B} \text{Tr} [\bar{H}^{(0)} (iD_{\perp v})^2 H^{(0)}] + c_{\text{dip}}^{\text{HMET}} \frac{Q_u e}{8\Lambda_c} \text{Tr} [\sigma_{\mu\nu} \bar{H}^{(0)} H^{(0)}] F_{us}^{\mu\nu} \\ &\quad - \frac{\lambda_1}{4m_b} \text{Tr} [\bar{H}^{(0)} H^{(0)}] - \frac{\lambda_2(\mu)}{8m_b} \text{Tr} [\bar{H}^{(0)} \Sigma_{\text{mag}}^{\mu\nu} H^{(0)} \sigma_{\mu\nu}] + \dots,\end{aligned}\tag{5.20}$$

where the second term in the first line arises as a consequence of the field redefinition in (5.12) and plays no role for our analysis. It is suppressed relative to the leading term by $E_{\text{cut}}/m_B \sim \lambda\zeta$. As mentioned earlier, the third operator is suppressed by ζ . The operators shown in the second line scale like $\Lambda_c^2/(m_B E_{\text{cut}}) \sim \lambda/\zeta$ relative to the leading term. They are suppressed for $E_{\text{cut}} \gg \Lambda_c^2/m_B$ but become of leading order for $E_{\text{cut}} \sim \delta_{B^*}$. Further operators not shown are suppressed by at least two powers of ζ or λ^2/ζ . The quantities $\lambda_{1,2} \sim \Lambda_c^2$ are well-known hadronic matrix elements defined in HQET, and the product $C_{\text{mag}}\lambda_2 \approx 0.12 \text{ GeV}^2$ is scale independent [128]. Written out in component fields, we find

$$\begin{aligned} \mathcal{L}_H = & \varphi_v^{\dagger(0)} i v \cdot \partial \varphi_v^{(0)} - \delta m_B \varphi_v^{\dagger(0)} \varphi_v^{(0)} - \rho_{v,\mu}^{\dagger(0)} i v \cdot \partial \rho_v^{\mu(0)} + \delta m_{B^*} \rho_{v,\mu}^{\dagger(0)} \rho_v^{\mu(0)} \\ & + \frac{e c_{BB^*\gamma}}{2\Lambda_c} \left(v^\mu \rho_v^{\dagger\nu(0)} \varphi_v^{(0)} \tilde{F}_{\mu\nu}^{us} + \text{h.c.} \right) - \frac{i e c_{B^*B^*\gamma}}{2\Lambda_c} \rho_v^{\dagger\mu(0)} \rho_v^{\nu(0)} F_{\mu\nu}^{us} + \dots, \end{aligned} \quad (5.21)$$

with $\tilde{F}_{\mu\nu}^{us} = \frac{1}{2} \epsilon_{\mu\nu\rho\sigma} F_{\rho\sigma}^{us}$ being the dual field-strength tensor, and the dipole couplings

$$c_{BB^*\gamma} = c_{B^*B^*\gamma} = Q_u c_{\text{dip}}^{\text{HMET}}. \quad (5.22)$$

Our coupling $c_{BB^*\gamma}$ is related to the parameter $g_{BB^*\gamma}$ defined in [27] via $c_{BB^*\gamma}/\Lambda_c = g_{BB^*\gamma}$. The corrections to the meson masses arising at first order in $1/m_b$ are [128]

$$\delta m_B = -\frac{\lambda_1 + 3C_{\text{mag}}(\mu)\lambda_2(\mu)}{2m_b}, \quad \delta m_{B^*} = -\frac{\lambda_1 - C_{\text{mag}}(\mu)\lambda_2(\mu)}{2m_b}, \quad (5.23)$$

from which we obtain

$$\delta_{B^*} = \frac{m_{B^*}^2 - m_B^2}{2m_B} = C_{\text{mag}}(\mu) \frac{2\lambda_2(\mu)}{m_b} + \dots, \quad (5.24)$$

up to terms of order $1/m_b^2$ and higher. The physical masses of the B and B^* mesons are given by $m_{B^{(*)}} = \bar{m}_B + \delta m_{B^{(*)}}$. Since we have used the parameter \bar{m}_B in the field redefinition (5.12), the propagators of $B^{(*)}$ mesons with residual momentum q in HMET are given by $i/(v \cdot q - \delta m_{B^{(*)}} + i0)$. External states for on-shell $B^{(*)}$ mesons carry the residual momentum $q^\mu = \delta m_{B^{(*)}} v^\mu$.

We now discuss the representation of the flavor-changing quark current $\bar{u}\gamma^\mu P_L b$ in the low-energy theory. In this discussion we neglect QED corrections, because we will consider real-photon emission topologies, whose rate is already suppressed by a power of α . Including short-distance QCD corrections, the relevant weak current is of the form [66]

$$J_{\text{had}}^\mu(x) = e^{-im_B v \cdot x} Y_n^{(\ell)\dagger}(x_-) \left[\mathcal{C}_1^{\text{HQET}}(\mu) \bar{u} \gamma^\mu P_L b_v + \mathcal{C}_2^{\text{HQET}}(\mu) \bar{u} v^\mu P_R b_v \right], \quad (5.25)$$

where the soft Wilson line $Y_n^{(\ell)\dagger}$ is inherited from the lepton current, see relation (4.2), and the Wilson coefficients have been given at one-loop order in (3.57). These currents introduce sources of $SU(2)_v$ -breaking, which can be captured in HMET via the spurion

$$\Gamma_{\text{weak}}^\mu = \mathcal{C}_1^{\text{HQET}}(\mu) \gamma^\mu P_L + \mathcal{C}_2^{\text{HQET}}(\mu) v^\mu P_R. \quad (5.26)$$

There is no need to introduce two spurions, because heavy-quark spin ensures that the combination of the two terms remains unchanged in the matching to the low-energy theory. The representation of the weak current in HMET is obtained as

$$J_{\text{had}}^\mu(x) \rightarrow e^{-im_B v \cdot x} \bar{Y}_v^{(B)}(x) \bar{C}_{\bar{n}}^{(B)}(x_+) Y_n^{(\ell)\dagger}(x_-) \frac{i\mathcal{F}_{\text{HMET}}(\mu)}{2\sqrt{2}} \text{Tr}[\Gamma_{\text{weak}}^\mu H^{(0)}], \quad (5.27)$$

where $\mathcal{F}_{\text{HMET}}$ is a non-perturbative parameter. In components, we find

$$\text{Tr}[\Gamma_{\text{weak}}^\mu H^{(0)}] = - \left[\mathcal{C}_1^{\text{HQET}}(\mu) + \mathcal{C}_2^{\text{HQET}}(\mu) \right] v^\mu \varphi_v^{(0)} + \mathcal{C}_1^{\text{HQET}}(\mu) \rho_v^\mu{}^{(0)}. \quad (5.28)$$

The normalization of the fields φ_v and ρ_v^μ is such that

$$\langle 0 | \varphi_v | B(v) \rangle = \sqrt{2m_B}, \quad \langle 0 | \rho_v^\mu | B^*(v) \rangle = \sqrt{2m_{B^*}} \epsilon^\mu(v). \quad (5.29)$$

where for convenience we normalize the states to the physical masses of the B and B^* mesons. Matching (5.27) to the usual definition of the meson decay constants,

$$\langle 0 | \bar{u} \gamma^\mu P_L b | B(v) \rangle = -\frac{i}{2} m_B f_B v^\mu, \quad \langle 0 | \bar{u} \gamma^\mu P_L b | B^*(v) \rangle = \frac{i}{2} m_{B^*} f_{B^*} \epsilon^\mu, \quad (5.30)$$

we obtain

$$\begin{aligned} m_B f_B^{\text{QCD}} &= \left[\mathcal{C}_1^{\text{HQET}}(\mu) + \mathcal{C}_2^{\text{HQET}}(\mu) \right] \sqrt{m_B} \mathcal{F}_{\text{HMET}}(\mu), \\ m_{B^*} f_{B^*}^{\text{QCD}} &= \mathcal{C}_1^{\text{HQET}}(\mu) \sqrt{m_{B^*}} \mathcal{F}_{\text{HMET}}(\mu), \end{aligned} \quad (5.31)$$

valid at leading power in $1/m_b$. From these relations, we can identify $\mathcal{F}_{\text{HMET}}(\mu)$ with the HQET decay constant $F_{\text{QCD}}(\mu)$ introduced in (4.98), taking into account that $\mathcal{C}_1^{\text{HQET}} + \mathcal{C}_2^{\text{HQET}} = H_1^A + H_2^A$.

Effective weak interactions

Contracting the representation of the weak flavor-changing quark current with the representation of the lepton current in (5.11), the effective weak interaction in the low-energy theory (cf. (2.1)) takes the form (we set $x = 0$ for simplicity)

$$\begin{aligned} \mathcal{L}_{H\ell} &= i\sqrt{2} G_F^{(\mu)} V_{ub} \bar{Y}_v^{(B)} \bar{C}_{\bar{n}}^{(B)} Y_n^{(\ell)\dagger} C_{v_\ell}^{(\ell)\dagger} \\ &\times \left\{ \frac{f_B^{\text{QCD}} m_\ell}{\sqrt{2m_B}} \varphi_v^{(0)} \bar{h}_{v_\ell}^{(0)} P_L \nu_{\bar{c}} - \frac{f_{B^*}^{\text{QCD}} m_{B^*}}{\sqrt{2m_{B^*}}} \left[\bar{h}_{v_\ell}^{(0)} \not{v}^\perp{}^{(0)} P_L \nu_{\bar{c}} + \frac{m_\ell}{m_{B^*}} \frac{\bar{n} \cdot \rho_v^{(0)}}{\bar{n} \cdot v} \bar{h}_{v_\ell}^{(0)} P_L \nu_{\bar{c}} \right] \right\}. \end{aligned} \quad (5.32)$$

As a last step, we need to account for QED radiative corrections. This is accomplished by multiplying the terms in (5.32) with factors y_B (for φ_v) and $y_{B^*}^{\perp, \parallel}$ (for ρ_v^\perp and $\bar{n} \cdot \rho_v$). For the case of the B^* meson, it will be sufficient to work with the lowest-order approximation $y_{B^*}^{\perp, \parallel} = 1 + \mathcal{O}(\alpha)$, since a real photon is involved in converting the B meson into a B^* meson, and the rate for this process is already suppressed by one power of α . For the B meson, however, we need to perform a consistent matching of SCET-2 onto the low-energy effective

theory to determine y_B including perturbative and non-perturbative QED effects. This will be discussed in Section 5.4.

According to Low's theorem [129], the emissions of very soft photons – i.e. with energies below all relevant masses and excitation thresholds – can be obtained, for our process, from the squared matrix element of the product of soft QED Wilson lines $S_{v_\ell}^{(\ell)\dagger}(x)\bar{S}_v^{(B)}(x)$, where $v \equiv v_B$ denotes the 4-velocity of the B meson. It is interesting to ask how this product of two Wilson lines is related to the product of four Wilson lines appearing in (5.32). The answer is simple: after integrating over the photon phase space, the squared matrix element of $S_{v_\ell}^{(\ell)\dagger}\bar{S}_v^{(B)}$ can only depend on the Lorentz invariants $v^2 = v_\ell^2 = 1$ and $v \cdot v_\ell$. For the $B^- \rightarrow \ell^- \bar{\nu}_\ell$ process with $\ell = \mu, e$, the latter is parametrically large,

$$v \cdot v_\ell = \frac{m_B^2 + m_\ell^2}{2m_B m_\ell} \approx \frac{m_B}{2m_\ell} \gg 1. \quad (5.33)$$

A region analysis shows that, in this limit, two different momentum modes contribute to the squared matrix element arising from Low's theorem, corresponding to the ultrasoft and ultrasoft-collinear regions identified earlier. In the spirit of asymptotic expansions, one finds that

$$S_{v_\ell}^{(\ell)\dagger}\bar{S}_v^{(B)} = \left[Y_n^{(\ell)\dagger} \bar{Y}_v^{(B)} \right] \left[C_{v_\ell}^{(\ell)\dagger} \bar{C}_{\bar{n}}^{(B)} \right] + \mathcal{O}\left(\frac{m_\ell}{m_B}\right). \quad (5.34)$$

Combining all ingredients, at this stage the low-energy effective Lagrangian reads

$$\mathcal{L}_{\text{low-}E} = \mathcal{L}_\ell + \mathcal{L}_H + \mathcal{L}_{H\ell}. \quad (5.35)$$

From this construction, the direct and indirect real-emission contributions introduced earlier can be clearly identified. They are shown in the first two graphs in Figure 14. For the direct contribution, the B meson couples to the leptons via the m_ℓ/m_B -suppressed weak interaction of the pseudoscalar meson in $\mathcal{L}_{H\ell}$, see (5.32), with photons emitted from the Wilson lines (first diagram). Effective $B\ell\bar{\nu}_\ell\gamma$ interactions beyond those induced by photon emission from the Wilson lines, represented by the last graph in Figure 13, would require the insertion of an ultrasoft (or ultrasoft-collinear) field-strength tensor $F_{us}^{\mu\nu}$ (or $F_{usc}^{\mu\nu}$) in the weak-interaction operators shown in (5.32), which costs an additional power suppression of order $\zeta^2 \sim (E_{\text{cut}}/\Lambda_c)^2$ (or $(\lambda\zeta)^2 \sim (E_{\text{cut}}/m_B)^2$). In the indirect contribution, the B meson transitions to a B^* through the emission of a photon via the E_{cut}/Λ_c -suppressed dipole interaction in \mathcal{L}_H , see (5.21). The intermediate B^* meson then couples to the leptonic current with the leading-power interaction in $\mathcal{L}_{H\ell}$ (second diagram). The relative importance of these two contributions depends on the experimental cut on the photon energy. Naively, the indirect contribution becomes relevant for $E_{\text{cut}}/m_\ell \gtrsim \Lambda_c/m_B$, which yields $E_{\text{cut}} > 10$ MeV for the muon channel and $E_{\text{cut}} > 50$ keV for the electron case (for $\Lambda_c \approx 500$ MeV). However, as we will show later, the onset of the indirect contribution is pushed to larger values of E_{cut} by an additional suppression factor $\sim (E_{\text{cut}}/\delta_{B^*})^2$, with $\delta_{B^*} \simeq 45$ MeV. From these estimates, one can infer that for $\ell = e$ the decay is dominated by the $B \rightarrow B^*\gamma \rightarrow e\bar{\nu}_e\gamma$ contribution, while for $\ell = \mu$ the direct and indirect channels compete for low values of E_{cut} .

The last two graphs in Figure 14 show the virtual QED corrections to the $B^- \rightarrow \ell^- \bar{\nu}_\ell$ process in the low-energy theory as discussed so far. In principle, they must be added to

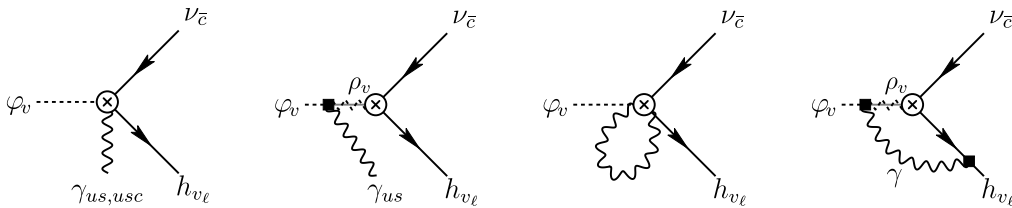


Figure 14: Feynman diagrams describing QCD corrections to the $B^- \rightarrow \ell^- \bar{\nu}_\ell$ process at $\mathcal{O}(\alpha)$ in the heavy-particle effective theory. For clarity, we label the lines by the corresponding EFT fields. A crossed circle indicates the weak interaction vertex, while a black square denotes a power-suppressed interaction. In the first and third graphs the photons are emitted from the Wilson lines contained in the effective weak Lagrangian (5.32).

the virtual corrections arising from scales above Λ_{QCD} , which, as we will show in Section 5.4, are accounted for by the coupling y_B discussed below (5.32). Virtual corrections arising from photons emitted from Wilson lines (third graph) are scaleless and vanish in dimensional regularization.¹⁸ The last diagram is *a priori* not scaleless, since the B^* propagator in the loop contains the mass parameter δ_{B^*} defined in (5.24). By angular momentum conservation, all these diagrams feature the chiral suppression $\sim m_\ell/m_B$ of the tree-level $B^- \rightarrow \ell^- \bar{\nu}_\ell$ decay amplitude. Upon explicit calculation, we find that the fourth diagram vanishes when the leading-order couplings of the photon to the Wilson lines are used. A non-zero result is obtained if the photon couples to an effective $B\ell\bar{\nu}_\ell\gamma$ interaction not induced by photon emission from the Wilson lines, which, as we have discussed above, costs an additional power suppression of order $\zeta^2 \sim (E_{\text{cut}}/\Lambda_c)^2$. Alternatively, the photon can couple to the charged lepton through a power-suppressed dipole interaction

$$\frac{Q_\ell e}{4m_\ell} \bar{h}_{\nu_\ell} \sigma_{\mu\nu} F_{usc}^{\mu\nu} h_{\nu_\ell}, \quad (5.36)$$

which can be added to the bHLET Lagrangian in (5.7). The corresponding contribution is suppressed, relative to the leading-order $B^- \rightarrow \ell^- \bar{\nu}_\ell$ amplitude, by a factor of order $(\lambda\zeta)^2 = (E_{\text{cut}}/m_B)^2$. We conclude that, at leading order in the heavy-particle effective theory discussed in this section, all virtual QED corrections are accounted for by the coupling y_B .

5.2 Heavy-hadron chiral effective theory

In our discussion so far we have ignored the fact that below the scale Λ_c the point-like mesons can interact not only with electromagnetic radiation, but also with the pseudo-Nambu-Goldstone bosons associated with the breaking of the chiral symmetry $SU(3)_L \times SU(3)_R \rightarrow SU(3)_V$, i.e., the light pseudoscalar mesons π , K and η . To include these interactions, we need to generalize the HMET to heavy-hadron chiral perturbation theory (HH χ PT) in the low-energy theory, following [74–76]. To this end, we promote the effective ground-state heavy-

¹⁸These virtual graphs have the effect of replacing the IR $1/\epsilon$ poles in the real-emission contributions by UV poles, which are removed by renormalization of the operators in the low-energy theory.

hadron field H to a triplet (with $a = 1, 2, 3$)

$$H_a = \frac{1 + \psi}{2} (\phi_{v,a} - \varphi_{v,a} \gamma_5) \quad (5.37)$$

transforming as a $\bar{3}$ under flavor $SU(3)$. It describes the pseudoscalar mesons ($B^-, \bar{B}^0, \bar{B}_s^0$) and their vector partners ($B^{*-}, \bar{B}^{*0}, \bar{B}_s^{*0}$). We then couple these fields to the octet of the light pseudoscalar mesons (π, K, η) using a chiral Lagrangian. Below the scale of chiral symmetry breaking, (π, K, η) are collected in the unitary field

$$\Sigma = \exp \left[\frac{i\sqrt{2} \pi^a \lambda^a}{f} \right], \quad \text{with} \quad \frac{\pi^a \lambda^a}{\sqrt{2}} = \begin{pmatrix} \frac{1}{\sqrt{2}} \pi^0 + \frac{1}{\sqrt{6}} \eta_8 & \pi^+ & K^+ \\ \pi^- & -\frac{1}{\sqrt{2}} \pi^0 + \frac{1}{\sqrt{6}} \eta_8 & K^0 \\ K^- & \bar{K}^0 & -\sqrt{\frac{2}{3}} \eta_8 \end{pmatrix}, \quad (5.38)$$

where the matrices λ^a satisfy $\text{tr}[\lambda^a \lambda^b] = 2\delta^{ab}$, and $f \simeq f_\pi = 130.2 \text{ MeV}$ is related to the pion decay constant. This field transforms as $\Sigma \rightarrow L \Sigma R^\dagger$ under chiral $SU(3)_L \times SU(3)_R$ transformations. Next, we define a new unitary field ξ via $\xi^2 = \Sigma$. It transforms as $\xi \rightarrow L \xi U^\dagger = U \xi R^\dagger$, where in general the special unitary matrix U is a complicated nonlinear function of L, R and the pseudo-Nambu-Goldstone boson fields [130]. The heavy-meson field H transforms as $H \rightarrow H U^\dagger$.

The leading-order HH χ PT Lagrangian reads [74–76]

$$\begin{aligned} \mathcal{L}_{\text{HH}\chi\text{PT}} = & -\frac{1}{2} \text{Tr}[\bar{H} i v \cdot D H] + \frac{1}{2} \text{Tr}[\bar{H} H v \cdot \mathcal{V}] + \frac{g}{2} \text{Tr}[\bar{H} H \mathcal{A} \gamma_5] \\ & + \varrho_1 \text{Tr}[\bar{H} H m_q^\xi] + \varrho_2 \text{Tr}[\bar{H} H] \text{tr}[m_q^\xi] + \varrho_3 Q_b \alpha \text{Tr}[\bar{H} H Q^\xi] \\ & + \frac{f^2}{8} \text{tr}[(D^\mu \Sigma)(D_\mu \Sigma^\dagger)] + \frac{f^2}{4} B_0 \text{tr}[m_q \Sigma^\dagger + \Sigma m_q^\dagger], \end{aligned} \quad (5.39)$$

where here and below the symbol “Tr” implies a combined trace over Dirac and flavor indices, while “tr” refers to a flavor trace. Note that $(\bar{H} H)_{ab} = \bar{H}_a H_b$ are the components of a 3×3 matrix in flavor space. The light pseudoscalar mesons couple to the heavy mesons through the vector and axial currents

$$\mathcal{V}_\mu = \frac{i}{2} (\xi^\dagger D_\mu \xi + \xi D_\mu \xi^\dagger), \quad \mathcal{A}_\mu = \frac{i}{2} (\xi^\dagger D_\mu \xi - \xi D_\mu \xi^\dagger). \quad (5.40)$$

The covariant derivative acting on a field $\psi(x)$ is defined as

$$iD^\mu \psi(x) = i\partial^\mu \psi(x) + e \left[A_{us}^\mu(x) + \frac{n^\mu}{2} \bar{n} \cdot A_{usc}^\mu(x_+) \right] [Q, \psi(x)], \quad (5.41)$$

where $Q = \text{diag}(Q_u, Q_d, Q_s)$ contains the light-quark charges. For the heavy-hadron field, we define

$$[Q, H] \equiv Q' H - H Q = H Q_B, \quad (5.42)$$

where $Q' = Q_b \mathbb{1}$ gives the charge of the b quark, and $Q_B = \text{diag}(-1, 0, 0)$ contains the charges of the three mesons described by H_a . Under the chiral symmetry, the spurions $m_q =$

$\text{diag}(m_u, m_d, m_s)$ and Q transform as $m_q \rightarrow L m_q R^\dagger$ and $Q \rightarrow L Q L^\dagger$ or $Q \rightarrow R Q R^\dagger$, and we have defined related quantities

$$m^\xi = \frac{1}{2} (\xi^\dagger m_q \xi^\dagger + \xi m_q^\dagger \xi), \quad Q^\xi = \frac{1}{2} (\xi^\dagger Q \xi + \xi Q \xi^\dagger), \quad (5.43)$$

which transform as $m_q^\xi \rightarrow U m_q^\xi U^\dagger$ and $Q^\xi \rightarrow U Q^\xi U^\dagger$. The first term in (5.39) contains $\text{Tr}[\bar{H}_a H_b Q_{ba}]$ from the covariant derivative acting on H , and this expression is not invariant under $SU(3)_L \times SU(3)_R$ transformations. The second term contains the same expression arising from the covariant derivatives inside $v \cdot \mathcal{V}$. The condition that the two terms cancel each other fixes the coefficient of the second term to be $+\frac{1}{2}$.

The coupling g in (5.39) is proportional (at lowest order) to the $BB^*\pi$ coupling constant. The parameter B_0 is defined such that, at leading order in the chiral expansion, $m_\pi^2 = B_0(m_u + m_d)$, and similarly for the other mesons. The parameter ϱ_1 governs the mass splittings between the components of the triplet H , whereas ϱ_2 leads to an overall mass shift of the three meson masses proportional to the sum of the quark masses [74]. The parameter ϱ_3 yields an electromagnetic correction to the masses of the heavy mesons from the Coulomb interaction between their constituent quarks. At the lowest order in the chiral expansion, we can identify

$$\begin{aligned} m_{B_s} - m_{B_d} &= 2\varrho_1(\mu) [m_s(\mu) - m_d(\mu)] \stackrel{!}{\simeq} 87.2 \text{ MeV}, \\ m_{B_d} - m_{B_u} &= 2\varrho_1(\mu) [m_d(\mu) - m_u(\mu)] + \frac{2\alpha}{3} \varrho_3 \stackrel{!}{\simeq} 0.31 \text{ MeV}, \end{aligned} \quad (5.44)$$

where the scale dependence cancels out. With $(m_s - m_d) \simeq 88.8 \text{ MeV}$ and $(m_d - m_u) \simeq 2.54 \text{ MeV}$ at $\mu = 2 \text{ GeV}$ [34], we obtain $\varrho_1(2 \text{ GeV}) \simeq 0.49$ and $\varrho_3 \simeq -436 \text{ MeV}$. It is natural to expect that the coefficient ϱ_2 takes an $\mathcal{O}(1)$ value, but this value cannot be determined from spectroscopy. In the presence of the parameters ϱ_i , the shifts of the meson masses in (5.23) must be generalized to

$$\begin{aligned} \delta m_{B_q} &= 2\varrho_1 m_q + 2\varrho_2(m_u + m_d + m_s) + 2\varrho_3 Q_b Q_q \alpha - \frac{\lambda_1 + 3C_{\text{mag}}(\mu)\lambda_2(\mu)}{2m_b}, \\ \delta m_{B_q^*} &= 2\varrho_1 m_q + 2\varrho_2(m_u + m_d + m_s) + 2\varrho_3 Q_b Q_q \alpha - \frac{\lambda_1 - C_{\text{mag}}(\mu)\lambda_2(\mu)}{2m_b}. \end{aligned} \quad (5.45)$$

The generalization of the remaining operators proceeds in an analogous way. In HH χ PT, the electromagnetic dipole operator in (5.17) is generalized to

$$\frac{c_{\text{dip}} e}{8\Lambda_c} \text{Tr}[\sigma_{\mu\nu} \bar{H} H Q^\xi] F_{us}^{\mu\nu}, \quad (5.46)$$

while the two operators describing the $1/m_b$ corrections in (5.20) remain unchanged. Finally, the representation of the left-handed, flavor-changing quark current (5.27) appearing in the weak interactions is generalized to

$$J_{\text{had},a}^\mu(x) = e^{-im_B v \cdot x} Y_n^{(\ell)\dagger}(x_-) \frac{i\mathcal{F}}{2\sqrt{2}} \text{tr}[\Gamma_{\text{weak}}^\mu (H \xi^\dagger)_a]. \quad (5.47)$$

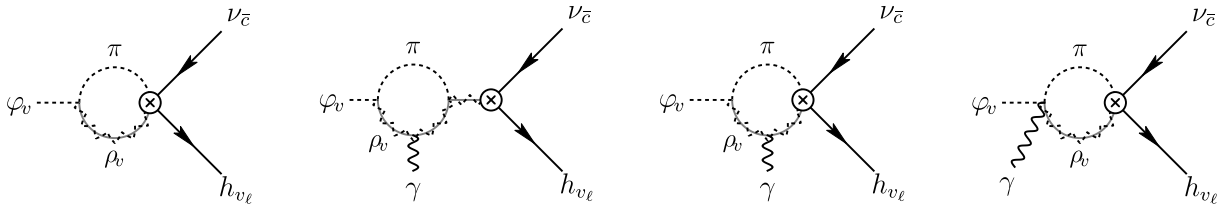


Figure 15: Representative one-loop diagrams in HH χ PT giving rise to higher-order corrections to the heavy-meson decay constant F_{QCD} (first graph) and the $BB^*\gamma$ coupling (second graph), and “genuine” one-loop corrections to the $B^- \rightarrow \ell^- \bar{\nu}_\ell \gamma$ decay amplitude (last two diagrams). Contributions from local higher-order operators in HH χ PT, which are needed as counterterms for these diagrams, exist but are not shown. A crossed circle indicates the weak interaction vertex. Photons are not yet decoupled from the hadrons, and we do not distinguish between leading-order and power-suppressed vertices. Instead of pions, other pseudoscalar mesons can also propagate in the loops.

Only the charged current (with $a = 1$) enters the effective weak Lagrangian (5.32) relevant to our process. Contracting it with the lepton current in (5.11), we obtain for the effective weak Lagrangian including pseudoscalar mesons

$$\mathcal{L}_{H\ell} = -2\sqrt{2}G_F^{(\mu)} V_{ub} g_{\mu\nu} J_{\text{had},1}^\mu J_{\text{lep}}^\nu. \quad (5.48)$$

In (5.47), the parameter \mathcal{F} denotes the leading-order term in the chiral expansion of the HQET decay constant $F_{\text{QCD}}(\mu)$. Higher-order corrections arise from chiral loops and local higher-order interactions in HH χ PT. At one-loop order, chiral logarithms in these corrections have been calculated in [131, 132], and a more complete expression including also (some) finite terms has been derived in [121]. A representative contribution is shown in the first graph of Figure 15. Likewise, the dipole coupling c_{dip} in (5.46), which determines the effective $BB^*\gamma$ and $B^*B^*\gamma$ couplings according to (5.22), receives higher-order corrections, which have been studied at leading logarithmic order in [133] and including finite terms in [134]. A representative contribution is shown in the second graph. For our purposes, it is sufficient to simply substitute the “physical” values of F_{QCD} and $c_{BB^*\gamma}$ for the leading-order parameters. Finally, there are also “genuine” chiral loop corrections to the $B^- \rightarrow \ell^- \bar{\nu}_\ell \gamma$ decay amplitude, illustrated in the last two diagrams in Figure 15. These diagrams scale like m_P^2/Λ_χ^2 (with $P = \pi, K, \eta_8$) relative to the tree-level real-emission contributions, and they involve loop functions depending on dimensionless ratios of the light-meson masses, the parameter δ_{B^*} , and the photon-energy cut E_{cut} . *A priori*, one would expect a rather complicated result from the sum of all graphs. However, we will now show that the genuine chiral loop corrections to the $B^- \rightarrow \ell^- \bar{\nu}_\ell(\gamma)$ process vanish identically.

Reorganizing HH χ PT

We can further simplify the HH χ PT Lagrangian by means of a non-linear field redefinition, using $H' \equiv H\xi^\dagger$ rather than the original H as the interpolating field for the heavy hadrons. The equation $H' = H [1 + \mathcal{O}(\pi^a/f)]$ shows that this is a legitimate choice. The new field transforms as $H' \rightarrow H'L^\dagger$ under $SU(3)_L \times SU(3)_R$. We then obtain the leading-order Lagrangian

(dropping the prime on the fields for convenience)

$$\begin{aligned}
\mathcal{L}_{\text{HH}\chi\text{PT}} = & -\frac{1}{2} \text{Tr}[\bar{H} i v \cdot D H] + \frac{1}{4} \text{Tr}[\bar{H} H v \cdot L] - \frac{g}{4} \text{Tr}[\bar{H} H \not{v} \gamma_5] \\
& + \frac{\varrho_1}{2} \text{Tr}[\bar{H} H S] + \frac{\varrho_2}{2} \text{Tr}[\bar{H} H] \text{tr}[S] + \frac{\varrho_3}{2} Q_b \alpha \text{Tr}[\bar{H} H (Q + \Sigma Q \Sigma^\dagger)] \\
& + \frac{f^2}{8} \text{tr}[L^2] + \frac{f^2}{4} B_0 \text{tr}[S],
\end{aligned} \tag{5.49}$$

where we have used the standard definitions of the “left-handed” meson current L^μ and the scalar density S , defined as

$$L^\mu = \Sigma i D^\mu \Sigma^\dagger, \quad S = m_q \Sigma^\dagger + \Sigma m_q^\dagger. \tag{5.50}$$

In deriving the structure multiplying the coupling g , we have used the identity

$$\xi (\xi^\dagger i D_\mu \xi - \xi i D_\mu \xi^\dagger) \xi^\dagger = -\Sigma i D^\mu \Sigma^\dagger, \tag{5.51}$$

which follows from $(i D_\mu \xi) \xi^\dagger + \xi (i D_\mu \xi^\dagger) = 0$. The power-suppressed terms relevant to our analysis include the dipole interaction and the $1/m_b$ corrections to the heavy-meson masses. They take the form

$$\begin{aligned}
\mathcal{L}_{\text{HH}\chi\text{PT}}^{\text{power}} = & \frac{c_{\text{dip}} e}{16 \Lambda_c} \text{Tr}[\sigma_{\mu\nu} \bar{H} H (Q + \Sigma Q \Sigma^\dagger)] F_{us}^{\mu\nu} \\
& - \frac{\lambda_1}{4 m_b} \text{Tr}[\bar{H} H] - \frac{\lambda_2}{8 m_b} \text{Tr}[\bar{H} \Sigma_{\text{mag}}^{\mu\nu} H \sigma_{\mu\nu}] + \dots
\end{aligned} \tag{5.52}$$

Finally, after the field redefinition, the flavor-changing quark current reads

$$J_{\text{had},a}^\mu(x) = e^{-i m_B v \cdot x} Y_n^{(\ell)\dagger}(x_-) \frac{i \mathcal{F}}{2\sqrt{2}} \text{Tr}[\Gamma_{\text{weak}}^\mu H'_a]. \tag{5.53}$$

Importantly, the pion fields have disappeared from the weak current, and they appear in the leading-order HH χ PT Lagrangian through objects defined in terms of the field Σ .

At this point, the photon interactions in the leading-order HH χ PT Lagrangian can be decoupled via the field redefinition

$$H(x) = H^{(0)}(x) \mathcal{R}(x), \quad \text{with} \quad \mathcal{R}(x) = \text{diag}[\bar{Y}_v^{(B)}(x) \bar{C}_{\bar{n}}^{(B)}(x_+), 1, 1]. \tag{5.54}$$

This replaces the covariant derivative in the first term of (5.49) by an ordinary derivative, $i v \cdot \partial$. However, most of the terms in the effective Lagrangian containing the pseudoscalar fields are not invariant under this field redefinition. For instance, the second term in (5.49) transforms into

$$\frac{1}{4} \text{Tr}[\bar{H}^{(0)} H^{(0)} \mathcal{R} v \cdot L \mathcal{R}^\dagger], \tag{5.55}$$

and the same applies to the operators multiplying the couplings g , ϱ_1 , ϱ_3 , and c_{dip} . After decoupling, the flavor-changing hadronic current takes the final form (for $a = 1$)

$$J_{\text{had},1}^\mu(x) = e^{-i m_B v \cdot x} \bar{Y}_v^{(B)}(x) \bar{C}_{\bar{n}}^{(B)}(x_+) Y_n^{(\ell)\dagger}(x_-) \frac{i \mathcal{F}}{2\sqrt{2}} \text{Tr}[\Gamma_{\text{weak}}^\mu H_1^{(0)}]. \tag{5.56}$$

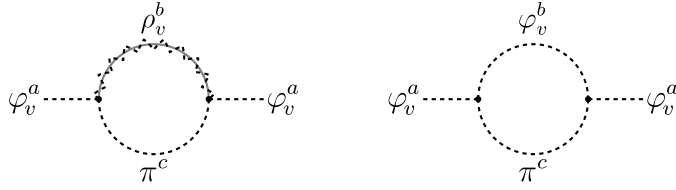


Figure 16: One-loop diagrams contributing to the wave-function renormalization of the pseudo-scalar heavy-meson fields φ_v^a (additional tadpole graphs contribute to the self-energy but not to the wave-function renormalization). The label π^c represents the pseudoscalar mesons π, K, η_8 , while ρ_v^b and φ_v^b represent B^* and B mesons of different flavors.

This result is identical to the corresponding expression obtained in heavy-particle effective theory, see (5.27), and thus the effective weak Lagrangian $\mathcal{L}_{H\ell}$ in (5.32) remains valid. Moreover, all terms in (5.20) are still present in the HH χ PT Lagrangians (5.49) and (5.52) (where we have omitted the irrelevant kinetic operator proportional to $1/m_B$). The additional interactions of the heavy hadrons with the pseudoscalar mesons present in HH χ PT renormalize the parameters and fields in the Lagrangian, but apart from the wave-function renormalization of the field $H^{(0)}$ they do not connect to the weak vertex. This implies that from the loop diagrams shown in Figure 15, only the second one is present after the field redefinition $H \rightarrow H'$. In general, the only chiral loop corrections contributing to our process are those renormalizing the B -meson wave function and the $BB^*\gamma$ coupling. In particular, the only corrections to the coupling \mathcal{F} come from wave-function renormalization.

Figure 16 shows the Feynman diagrams contributing at one-loop order to the wave-function renormalization constant of the B_q mesons in HH χ PT, where several terms in the leading-order Lagrangian (5.49) contribute to the vertices. Working in the isospin limit $m_u = m_d$ and ignoring QED effects, we find

$$\begin{aligned}
Z_{B^-} = 1 + \frac{1}{(4\pi f)^2} & \left\{ \frac{3m_\pi^2}{2} L_\pi + \frac{m_{\eta_8}^2}{6} L_{\eta_8} + m_K^2 L_K \right. \\
& + \frac{3g^2}{2} \left[m_\pi^2 (3L_\pi - 2) - 2\delta_{B^*}^2 \left(3L_\pi + 1 - 6f_1 \left(\frac{\delta_{B^*}}{m_\pi} \right) \right) \right] \\
& + \frac{g^2}{6} \left[m_{\eta_8}^2 (3L_{\eta_8} - 2) - 2\delta_{B^*}^2 \left(3L_{\eta_8} + 1 - 6f_1 \left(\frac{\delta_{B^*}}{m_{\eta_8}} \right) \right) \right] \\
& \left. + g^2 \left[m_K^2 (3L_K - 2) - 2\delta_{B_s^*}^2 \left(3L_K + 1 - 6f_1 \left(\frac{\delta_{B_s^*}}{m_K} \right) \right) \right] + \text{CTs} \right\}, \tag{5.57}
\end{aligned}$$

where

$$L_P = \left(\frac{1}{\epsilon} + 1 \right) + \ln \frac{\mu^2}{m_P^2} \xrightarrow{\text{renorm}} \ln \frac{\mu^2}{m_P^2} \tag{5.58}$$

are the chiral logarithms including the divergent $1/\epsilon$ UV poles obtained in dimensional regularization. These poles (along with the $+1$, as is conventional in χ PT [135, 136]) are removed

by counterterms (CTs) in the HH χ PT Lagrangian at NLO in the chiral expansion, whose explicit construction has been discussed in [121, 131], leaving behind a pure logarithm after renormalization, as indicated above. At leading order in the chiral Lagrangian, the mass of the η_8 meson is determined by the Gell-Mann–Okubo mass relation $m_{\eta_8}^2 = (4m_K^2 - m_\pi^2)/3$, and for simplicity we neglected the effects of π^0 – η – η' mixing. The values of the relevant δ_{X_b} parameters are $\delta_{B^*} \simeq 45.4$ MeV and $\delta_{B_s^*} \simeq 137.7$ MeV. The loop functions $f_i(x)$ are defined as (for $0 < x < 1$)

$$f_1(x) = \frac{\sqrt{1-x^2}}{x} \left[\arctan\left(\frac{x}{\sqrt{1-x^2}}\right) - \frac{\pi}{2} \right], \quad f_2(x) = \frac{x^2}{1-x^2} f_1(x). \quad (5.59)$$

The diagram with a pseudoscalar B_s meson and a charged kaon in the loop (second graph in Figure 16) receives contributions involving the $B^- \rightarrow B_s K^-$ vertices from the second and fourth operators in the effective Lagrangian (5.49). Using the relation $2\varrho_1(m_s - m_u) \approx \delta_{B_s}$, which is valid up to power corrections, we find that the sum of these contributions vanishes.

The “effective” decay constant of the B^- meson in HH χ PT is now obtained as

$$F_B = \sqrt{Z_{B^-}} \mathcal{F} + \mathcal{O}\left(\frac{1}{m_b}\right). \quad (5.60)$$

It is interesting to compare our results (5.57) and (5.60) with corresponding expressions available in the literature. Setting the parameters δ_{X_b} and ϱ_1 to zero, we find that the chiral logarithms L_P agree with the findings of [131]. In [121] a more complete expression was derived for the chiral loop corrections to the decay constant of neutral B and B^* mesons. It includes finite terms but neglects corrections proportional to m_π^2 . Also, for the mass of the η_8 meson the relation $m_{\eta_8}^2 = \frac{4}{3} m_K^2$ is used. In the isospin limit, we can compare our result (5.60) with their expression for the decay constant of the B^0 meson. We find agreement with the terms proportional to m_K^2 , $m_{\eta_8}^2$ and $\delta_{B_s^*}^2$ including all finite terms.¹⁹ The terms proportional to $\delta_{B^*}^2$ in the second and third line of (5.57) were dropped in [121], because $\delta_{B^*}^2$ is formally of $\mathcal{O}(\Lambda_c^2/m_b^2)$ in the heavy-quark limit and the authors worked consistently to first order in Λ_c/m_b . Our agreement of the NLO corrections to the B -meson decay constant in HH χ PT with existing results provides a non-trivial cross check of our rewriting of the HH χ PT Lagrangian. Using the original Lagrangian, the decay constant would receive loop corrections from wave-function renormalization and vertex corrections, the latter of which are absent in our scheme. The expression for the wave-function renormalization factor Z_{B^-} obtained from the traditional HH χ PT Lagrangian differs from our result (5.57) [134], but the sum of all corrections agrees with our result (5.60).

5.3 Integrating out the pseudoscalar mesons

After decoupling the pseudoscalar mesons from the weak vertex using a field redefinition, we have seen that chiral loop corrections plus higher-order counterterms have the effect of

¹⁹The only exception is the term involving $\ln(4/3)$ from L_{η_8} in the first line of (5.57), which appears to be missing in [121], in conflict with the findings of [131].

correcting the parameters \mathcal{F} , c_{dip} and g in the $\text{HH}\chi\text{PT}$ Lagrangian to their “physical” values, e.g.

$$\begin{aligned} F_{\text{QCD}}(\mu_0) &= \sqrt{Z_B} \mathcal{F} = \mathcal{F} + \mathcal{O}\left(\frac{m_P^2}{(4\pi f)^2}\right), \\ c_{BB^*\gamma} &= c_{\text{dip}} + \mathcal{O}\left(\frac{m_P^2}{(4\pi f)^2}\right), \\ g_{BB^*\pi} &= g + \mathcal{O}\left(\frac{m_P^2}{(4\pi f)^2}\right), \end{aligned} \quad (5.61)$$

and similarly for the meson decay constants and masses, but they do not give rise to genuinely new effects. The question then arises whether, for processes without pseudoscalar mesons in the external states, one can integrate out these modes to obtain a heavy-meson effective Lagrangian involving the B and B^* mesons, in analogy with the treatment in Section 5.1. This can indeed be done, but as we will see later there is one important subtlety that needs to be taken into account.

In the interactions of the B and B^* mesons with photons, the neutral pion and its diphoton decay can play a crucial role. The terms in the effective Lagrangian (5.49) producing a single π^0 are

$$\mathcal{L}_{\text{HH}\chi\text{PT}}^{(\pi^0)} = \frac{1}{2\sqrt{2}f_\pi} \text{Tr}[\bar{H}Ht^3] v \cdot \partial\pi^0 - \frac{g_{BB^*\pi}}{2\sqrt{2}f_\pi} \text{Tr}[\bar{H}Ht^3\gamma_\mu\gamma_5] \partial^\mu\pi^0, \quad (5.62)$$

where $t^3 = \text{diag}(1, -1, 0)$, and we neglect effects of $\mathcal{O}(\alpha)$.²⁰ The $\pi^0 \rightarrow \gamma\gamma$ decay is mediated by the axial anomaly. It can be described in the context of the chiral Lagrangian by adding a Wess–Zumino–Witten term [136–138]. The corresponding decay amplitude can be expressed as the matrix element of the operator

$$\mathcal{L}_{\text{eff}}^{\text{WZW}} = \frac{\alpha}{4\pi f_\pi} \pi^0 F_{\alpha\beta}^{us} \tilde{F}_{us}^{\alpha\beta}. \quad (5.63)$$

Combining the two expressions above, we obtain the effective Lagrangian for the coupling of two heavy mesons to two photons,

$$\mathcal{L}_{\text{eff}}^{\gamma\gamma}(x) = T \left\{ \mathcal{L}_{\text{HH}\chi\text{PT}}^{(\pi^0)}(x), i \int d^4y \mathcal{L}_{\text{eff}}^{\text{WZW}}(y) \right\}, \quad (5.64)$$

where T stands for time ordering. Integrating out the pion fields amounts to calculating the full pion propagator

$$\langle 0 | T \{ \pi^0(x), \pi^0(y) \} | 0 \rangle = \int \frac{d^4p}{(2\pi)^4} \frac{i e^{ip \cdot (x-y)}}{p^2 - m_\pi^2 + im_\pi \Gamma_\pi} = -\frac{i}{\square + m_\pi^2 - im_\pi \Gamma_\pi} \delta^{(4)}(x-y). \quad (5.65)$$

²⁰As written, these couplings are only present for $B^{(*)-}$ and $B_d^{(*)}$ mesons. When π^0 – η mixing is taken into account, also the $B_s^{(*)}$ states exhibit a coupling to the neutral pion, which is suppressed by $\sin\theta_{\pi\eta}$.

Here $\Gamma_\pi \simeq 7.8 \text{ eV}$ denotes the total width of the neutral pion, which to good approximation is given by

$$\Gamma_\pi \approx \Gamma(\pi^0 \rightarrow \gamma\gamma) \approx \frac{\alpha^2}{64\pi^3} \frac{m_\pi^3}{f_\pi^2}. \quad (5.66)$$

Using this result, we obtain

$$\mathcal{L}_{\text{eff}}^{\gamma\gamma} = \frac{1}{2\sqrt{2}f_\pi} \frac{\alpha}{4\pi f_\pi} \text{Tr}[\bar{H}H t^3 (v_\mu - g_{BB^*\pi} \gamma_\mu \gamma_5)] \frac{\partial^\mu}{\square + m_\pi^2 - im_\pi \Gamma_\pi} F_{\alpha\beta}^{us} \tilde{F}_{us}^{\alpha\beta}. \quad (5.67)$$

Since f_π and m_π are scales of the low-energy theory that are parametrically smaller than Λ_c , this Lagrangian describes leading-order interactions in the HMET, which should be added to the effective Lagrangian in (5.20). Despite appearances, these interactions are not suppressed by the QED coupling α . The squared momentum-space amplitude for a process involving one of these effective interactions contains the Breit–Wigner function

$$\frac{1}{(s_{\gamma\gamma} - m_\pi^2)^2 + (m_\pi \Gamma_\pi)^2} = \frac{\pi}{m_\pi \Gamma_\pi} \delta(s_{\gamma\gamma} - m_\pi^2) + \mathcal{O}((\Gamma_\pi)^0), \quad (5.68)$$

where $s_{\gamma\gamma}$ is the di-photon invariant mass squared. Keeping only the leading term in this expansion is an excellent approximation, since the neutral-pion width is seven orders of magnitude smaller than the pion mass. The decay amplitude squared obtained from the effective Lagrangian (5.20) scales like α^2 , but the factor $1/\Gamma_\pi$ scales like $1/\alpha^2$, so that the di-photon decay rate is in fact independent of the QED coupling (see Section 5.6 for details).

The δ -distribution on the right-hand side of (5.68) allows us to factorize the phase-space integration in a decay process mediated by the effective Lagrangian (5.67). Consider a decay of a particle with 4-momentum P into n particles with 4-momenta p_i , where the first two ($i = 1, 2$) refer to the photons produced by the effective interaction. When the n -particle phase-space integral is multiplied with $\delta((p_1 + p_2)^2 - m_\pi^2)$, we can insert a dummy integration over a 4-momentum $p_\pi \equiv p_1 + p_2$ to obtain

$$\begin{aligned} & \prod_{i=1}^n \int \frac{d^3 \mathbf{p}_i}{(2\pi)^3 2E_{\mathbf{p}_i}} \delta^{(4)}\left(\sum_{i=1}^n p_i - P\right) \frac{\pi}{m_\pi \Gamma_\pi} \delta((p_1 + p_2)^2 - m_\pi^2) \int \frac{d^4 p_\pi}{(2\pi)^4} (2\pi)^4 \delta^{(4)}(p_\pi - p_1 - p_2) \\ &= \frac{\pi}{m_\pi \Gamma_\pi} \int \frac{d^4 p_\pi}{(2\pi)^4} \theta(p_\pi^0) 2\pi \delta(p_\pi^2 - m_\pi^2) \prod_{i=3}^n \int \frac{d^3 \mathbf{p}_i}{(2\pi)^3 2E_{\mathbf{p}_i}} \delta^{(4)}\left(p_\pi + \sum_{i=3}^n p_i - P\right) \\ & \quad \times (2\pi)^3 \int \frac{d^3 \mathbf{p}_1}{(2\pi)^3 2E_{\mathbf{p}_1}} \int \frac{d^3 \mathbf{p}_2}{(2\pi)^3 2E_{\mathbf{p}_2}} \delta^{(4)}(p_\pi - p_1 - p_2) \quad (5.69) \\ &= \prod_{i=\pi,3}^n \int \frac{d^3 \mathbf{p}_i}{(2\pi)^3 2E_{\mathbf{p}_i}} \delta^{(4)}\left(p_\pi + \sum_{i=3}^n p_i - P\right) \\ & \quad \times \frac{1}{\Gamma_\pi} \frac{1}{2m_\pi} \int \frac{d^3 \mathbf{p}_1}{(2\pi)^3 2E_{\mathbf{p}_1}} \int \frac{d^3 \mathbf{p}_2}{(2\pi)^3 2E_{\mathbf{p}_2}} (2\pi)^4 \delta^{(4)}(p_\pi - p_1 - p_2). \end{aligned}$$

In the second step we have inserted $\theta(p_\pi^0) = 1$, which holds since p_1 and p_2 are the 4-momenta of on-shell particles with positive energies. The product in the last expression includes the $(n-1)$

particles with momenta p_π, p_3, \dots, p_n and masses m_π, m_3, \dots, m_n , whereas the expression in the last line contains the phase-space integral for the decay $\pi^0 \rightarrow \gamma\gamma$ (including the proper normalization $1/2m_\pi$, but not the symmetry factor $1/2$). The di-photon matrix element of the fields $F_{\alpha\beta}^{us} \tilde{F}_{us}^{\alpha\beta}$ in (5.20), when multiplied with $\frac{\alpha}{4\pi f_\pi}$, gives the $\pi^0 \rightarrow \gamma\gamma$ decay amplitude. Integrating the square of this amplitude over the di-photon phase-space (last line in (5.69)), taking into account a symmetry factor $1/2$, yields the corresponding decay rate, which gives the $\pi^0 \rightarrow \gamma\gamma$ branching ratio when divided by the total decay rate Γ_π .

5.4 Matching SCET-2 to HH χ PT

Having constructed the low-energy effective theory, we must now perform the matching of the results we obtained in SCET-2 to HH χ PT \otimes bHLET. Ignoring QED effects, we have already accomplished this task, since in Section 5.2 we have related the non-perturbative coupling parameter \mathcal{F} in (5.56) to the “physical” decay constant of the B meson. Since the heavy hadrons are treated in the heavy-quark limit in the effective theory below the scale m_B , this parameter equals the HQET parameter $F_{\text{QCD}}(\mu_0)$ at the scale where the matching onto HH χ PT is performed. This condition yields the non-perturbative matching condition

$$\mathcal{F} = \frac{F_{\text{QCD}}(\mu_0)}{\sqrt{Z_{B^-}}}. \quad (5.70)$$

On the other hand, we have seen earlier in Section 4 that the calculation of QED effects involves additional non-perturbative hadronic quantities, namely F_- and various B -meson LCDAs. We will now make contact between SCET-2 and the low-energy theory and study the non-perturbative matching of these theories in the presence of QED effects in detail.

In a first step, we need to address the fact that in our discussion of SCET-2 in Section 4 we have not explored the possible relevance of soft-collinear modes, with momentum scaling $p_{sc} \sim \lambda(\lambda_\ell^2, 1, \lambda_\ell)$. These modes have one momentum component of order $\lambda m_B = \Lambda_{\text{QCD}}$, but their virtuality $p_{sc}^2 \sim \lambda_\ell^2 \Lambda_{\text{QCD}}^2$ is far below the QCD confinement scale Λ_c , so one would expect that they are blind to the QCD dynamics inside hadrons. This is indeed the case, but it is nevertheless interesting to look at these modes in detail. The relevant quark currents in SCET-2 are of the form

$$\bar{u}_s(x) \Gamma b_v(x) Y_n^{(\ell)\dagger}(x_-) \quad \text{or} \quad \bar{Q}_s(x + sn) \Gamma \mathcal{H}_v(x) Y_n^{(\ell)\dagger}(x_-), \quad (5.71)$$

where the first form applies to the “local” operators in (4.18), and second one to the non-local operators in (4.23), some of which contain an additional soft gauge field $\mathcal{A}(x + s_g n)$. The interactions of soft-collinear gluons and photons interacting with soft fields are of eikonal form, and due to their momentum scaling, only the minus components of the soft-collinear momenta are transferred to the soft particles. The corresponding interaction term $\psi_s(x) i\bar{n} \cdot A_{sc}(x_+) \psi(x)$ can be decoupled via the field redefinition $\psi(x) \rightarrow \bar{C}_{\bar{n}}(x_+) \psi^{(0)}(x)$ for an initial-state soft field ψ . For both types of operators in (5.71) this produces the Wilson line (this is also true for operators containing an additional soft gauge field)

$$\bar{C}_{\bar{n}}^{(u)\dagger}(x_+) \bar{C}_{\bar{n}}^{(b)}(x_+) = \bar{C}_{\bar{n}}^{(B)}(x_+), \quad (5.72)$$

where the QCD parts of the Wilson lines cancel each other, and the QED parts add up to a combined Wilson line with the electric charge of the B meson, since $Q_b - Q_u = Q_B$. The result is the Wilson line for soft-collinear photon emission off a point-like B meson. This Wilson line is transmitted to the Wilson-line operator $R^{(\ell,B)}$ in (4.73), which we must then redefine as

$$R^{(\ell,B)} \equiv \langle 0 | Y_n^{(\ell)\dagger} \bar{Y}_v^{(B)} \bar{C}_{\bar{n}}^{(B)} | 0 \rangle. \quad (5.73)$$

In the definitions of the soft hadronic matrix elements S_i in terms of hadronic parameters and LCDAs in (4.82) and (4.83), the Wilson line $\bar{C}_{\bar{n}}^{(B)}$ cancels out between the numerator and denominator, and the hadronic quantities remain unchanged.

Let us now reconsider the definition of the leptonic functions K_i in (4.69). For performing the calculation of these functions, we have considered the simplest leptonic state consisting of a charged lepton and an anti-neutrino. What would change if we had allowed for the presence of soft-collinear photons in this calculation? The spinor product on the right-hand of the equation can trivially be rewritten in bHLET as

$$\bar{u}(v_\ell) P_L v(p_\nu) = \langle \ell(p_\ell) \bar{\nu}(p_\nu) | \bar{h}_{v_\ell} P_L \nu_{\bar{c}} | 0 \rangle, \quad (5.74)$$

where $\bar{u}(v_\ell) \not{v}_\ell = \bar{u}(v_\ell)$ obeys the same constraint as the field \bar{h}_{v_ℓ} , see (5.6). We can thus rewrite (4.69) as a matching relation connecting leptonic matrix elements in SCET-2 and bHLET, namely (for $i = 1, 2$)

$$\langle \ell(p_\ell) \bar{\nu}(p_\nu) | j_i^{\text{lep}}(x, \mu) | 0 \rangle = m_\ell^{\text{phys}} K_i(x, \mu) \langle \ell(p_\ell) \bar{\nu}(p_\nu) | \bar{h}_{v_\ell} P_L \nu_{\bar{c}} | 0 \rangle. \quad (5.75)$$

Since the matching of operators in two effective theories can be done using any choice of external states, we can allow for the presence of soft-collinear photons in the final state and generalize the relation to

$$\begin{aligned} \langle \ell \bar{\nu} + n \gamma_{sc} | j_i^{\text{lep}}(x, \mu) | 0 \rangle &= m_\ell^{\text{phys}} K_i(x, \mu) \langle \ell \bar{\nu} + n \gamma_{sc} | \bar{h}_{v_\ell} P_L \nu_{\bar{c}} | 0 \rangle \\ &= m_\ell^{\text{phys}} K_i(x, \mu) \langle \ell \bar{\nu} + n \gamma_{sc} | C_{v_\ell}^{(\ell)\dagger} \bar{h}_{v_\ell}^{(0)} P_L \nu_{\bar{c}} | 0 \rangle \\ &= m_\ell^{\text{phys}} K_i(x, \mu) \langle n \gamma_{sc} | C_{v_\ell}^{(\ell)\dagger} | 0 \rangle \bar{u}(p_\ell) P_L v(p_\nu), \end{aligned} \quad (5.76)$$

where the number n of photons is arbitrary, and in the last step we have applied the decoupling transformation (5.8) to the charged-lepton field. If bHLET is the correct low-energy theory in the leptonic sector, the functions K_i must be the same for all values of n . They are the Wilson coefficients associated with the matching of the two theories.

An analogous discussion applies for the hadronic sector, where we can rewrite the relations in (4.82) and (4.83) in the form (for $i = 1, \dots, 6$)

$$\begin{aligned} \langle 0 | j_i^{\text{had}}(\Lambda, \mu) | B^- \rangle &= S_i R^{(\ell,B)} = S_i \langle 0 | Y_n^{(\ell)\dagger} \bar{Y}_v^{(B)} \bar{C}_{\bar{n}}^{(B)} | 0 \rangle \\ &= \frac{S_i}{\sqrt{2m_B}} \langle 0 | Y_n^{(\ell)\dagger} \bar{Y}_v^{(B)} \bar{C}_{\bar{n}}^{(B)} \varphi_v^{(0)} | B^- \rangle, \end{aligned} \quad (5.77)$$

where in the last step we have reintroduced the decoupled initial-state B -meson field and used relation (5.29). This result again takes the form of a matching relation between two effective

theories, and we can generalize it by allowing for any number of soft or soft-collinear photons in the final state, i.e.

$$\langle n_s \gamma_s + n_{sc} \gamma_{sc} | j_i^{\text{had}}(\Lambda, \mu) | B^- \rangle = \frac{S_i}{\sqrt{2m_B}} \langle n_s \gamma_s + n_{sc} \gamma_{sc} | Y_n^{(\ell)\dagger} \bar{Y}_v^{(B)} \bar{C}_{\bar{n}}^{(B)} \varphi_v^{(0)} | B^- \rangle. \quad (5.78)$$

Once again, the SCET-2 hadronic matrix elements S_i appear as the Wilson coefficients of this matching relation, and they are the same for any numbers n_s and n_{sc} of photons if the low-energy theory is constructed in a consistent way.

It follows from these observations that the matrix elements of all SCET-2 operators can be written as a combination of a collinear function K_i (with $i = 1, 2$), a soft function S_i (with $i = 1, \dots, 6$), and the B -meson-to-leptons matrix element of the operator

$$\bar{Y}_v^{(B)} \bar{C}_{\bar{n}}^{(B)} Y_n^{(\ell)\dagger} C_{v_\ell}^{(\ell)\dagger} \frac{\varphi_v^{(0)}}{\sqrt{2m_B}} \bar{h}_{v_\ell}^{(0)} P_L \nu_{\bar{c}}, \quad (5.79)$$

with any number of soft or soft-collinear photons in the final state. Due to the experimental constraint that the energy of these photons should be less than a threshold value $E_{\text{cut}} \ll \Lambda_c$, we need to lower the scale of the soft and soft-collinear photons by a factor of $\zeta = E_{\text{cut}}/\Lambda_c$, turning them into ultrasoft and ultrasoft-collinear modes. With this in mind, we see that the operator in (5.79) is precisely the operator for the scalar heavy meson in (5.32). With this identification, and using the definitions in (4.99) and (4.113), we now obtain the matching coefficient

$$y_B(\mu_0) = \left(\frac{\alpha(m_Z)}{\alpha(m_B)} \right)^{\frac{9}{40}} \left(\frac{\mu_0^2}{m_B m_\ell} \right)^{\frac{\gamma_{\text{soft}}}{2}} \mathcal{R}_{\text{virt}}, \quad (5.80)$$

with the matching scale $\mu_0 = 1.5 \text{ GeV}$. The soft anomalous dimension γ_{soft} has been defined in (4.107), and the remaining virtual corrections contained in $\mathcal{R}_{\text{virt}}$ have been given in (4.116).

5.5 Direct contribution to the decay rate

We now compute the $B^- \rightarrow \ell^- \bar{\nu}_\ell(\gamma)$ decay rate for a photon-energy cut $E_{\text{cut}} \ll \Lambda_c$ at $\mathcal{O}(\alpha)$ in the low-energy theory. Here and below, the symbol “ (γ) ” refers to any form of electromagnetic radiation, from one or several low-energetic photons. The total decay rate can, to good approximation, be written as

$$\Gamma(E_{\text{cut}}) = \Gamma_{\text{dir}}(E_{\text{cut}}) + \Gamma_{\text{indir}}(E_{\text{cut}}). \quad (5.81)$$

The second term corresponds to the indirect contributions with an excited B^* resonance as an intermediate state. It will be discussed in detail in the next section, where we will also show that interference terms between the direct and indirect contributions are doubly power suppressed by factors of $(m_\ell/m_B)^2$ and $(E_{\text{cut}}/\Lambda_c)^2$, and thus can be safely neglected. The direct component factorizes into

$$\Gamma_{\text{dir}}(E_{\text{cut}}) = \Gamma_{\text{tree}} y_B^2(\mu_0) R(E_{\text{cut}}, \mu_0), \quad (5.82)$$

with the ‘‘tree-level’’ decay rate

$$\Gamma_{\text{tree}} = \frac{m_\ell^2 m_B}{8\pi} \left(G_F^{(\mu)} |V_{ub}| f_B^{\text{QCD}} \right)^2 \left(1 - \frac{m_\ell^2}{m_B^2} \right), \quad (5.83)$$

in which all QED corrections are omitted. The product $\Gamma_{\text{tree}} y_B^2$ is the non-radiative rate and $R(E_{\text{cut}}, \mu)$ is the radiation function. The former includes virtual QED corrections via the coupling $y_B(\mu)$ in (5.80), while the latter describes the real emission of ultrasoft or ultrasoft-collinear photons. At leading order in power counting, virtual corrections to the $B^- \rightarrow \ell^- \bar{\nu}_\ell$ process in the low-energy theory arise solely from the tadpole diagram shown by the third graph in Figure 14, which is scaleless and vanishes.

The radiation function is given by the convolution of the squared matrix elements of the ultrasoft and ultrasoft-collinear Wilson lines, integrated over phase space. We have

$$R(E_{\text{cut}}, \mu) = \int_0^\infty d\omega_{us} \int_0^\infty d\omega_{usc} \theta(E_{\text{cut}} - \omega_{us} - \omega_{usc}) W_{us}(\omega_{us}, \mu) W_{usc}(\omega_{usc}, \mu), \quad (5.84)$$

where ω_{us} and ω_{usc} are the total energies of ultrasoft and ultrasoft-collinear radiation (measured in the rest frame of the B meson), and the Heaviside function implements the cut on the total energy of all photons in the final state. The (bare) ultrasoft and ultrasoft-collinear functions W_{us} and W_{usc} are given by

$$\begin{aligned} W_{us}(\omega_{us}) &= \sum_{n=0}^\infty \left[\int \prod_{i=1}^n \frac{d^{d-1} \mathbf{q}_i}{(2\pi)^{d-1} 2E_i} \left| \langle \gamma_{us}^n | \bar{Y}_v^{(B)} Y_n^{(\ell)\dagger} | 0 \rangle \right|^2 \delta\left(\omega_{us} - \sum_{j=1}^n E_j\right) \right], \\ W_{usc}(\omega_{usc}) &= \sum_{n=0}^\infty \left[\int \prod_{i=1}^n \frac{d^{d-1} \mathbf{q}_i}{(2\pi)^{d-1} 2E_i} \left| \langle \gamma_{usc}^n | \bar{C}_{\bar{n}}^{(B)} C_{\nu_\ell}^{(\ell)\dagger} | 0 \rangle \right|^2 \delta\left(\omega_{usc} - \sum_{j=1}^n E_j\right) \right], \end{aligned} \quad (5.85)$$

where $\langle \gamma_i^n | = \langle \gamma_i(q_1) \dots \gamma_i(q_n) |$ with $i = us$ or $i = usc$ denotes the n -photon Fock state for ultrasoft or ultrasoft-collinear photons, respectively. At $\mathcal{O}(\alpha)$, we obtain in the $\overline{\text{MS}}$ scheme (with $q_+ \equiv \frac{n \cdot q}{n \cdot v}$ and $q_- \equiv \frac{\bar{n} \cdot q}{\bar{n} \cdot v}$)

$$\begin{aligned} W_{us}(\omega_{us}) &= \delta(\omega_{us}) + \frac{Q_\ell^2 \alpha}{\pi} \mu^{2\epsilon} \frac{e^{\epsilon\gamma_E}}{\Gamma(1-\epsilon)} \int_0^\infty dq_+ \int_0^\infty dq_- \frac{q_+^{-1-\epsilon} q_-^{1-\epsilon}}{(q_+ + q_-)^2} \delta\left(\omega_{us} - \frac{q_+ + q_-}{2}\right), \\ W_{usc}(\omega_{usc}) &= \delta(\omega_{usc}) + \frac{Q_\ell^2 \alpha}{\pi} \mu^{2\epsilon} \frac{e^{\epsilon\gamma_E}}{\Gamma(1-\epsilon)} \int_0^\infty dq_+ \int_0^\infty dq_- \frac{q_+^{1-\epsilon} q_-^{-1-\epsilon}}{\left(q_+ + \frac{m_\ell^2}{m_B^2} q_-\right)^2} \delta\left(\omega_{usc} - \frac{q_-}{2}\right), \end{aligned} \quad (5.86)$$

where we have used the relation

$$\int d^d q \delta(q^2) \theta(q^0) = \frac{1}{2} \int_0^\infty dq_+ \int_0^\infty dq_- \int d^{d-2} q_\perp \delta(q_+ q_- + q_\perp^2). \quad (5.87)$$

While the integrands of the two expressions in (5.86) coincide in the limit $m_\ell = m_B$, the integrals differ in the arguments of the δ -functions, since $q_+ \ll q_-$ for ultrasoft-collinear photons,

and hence the photon energy is equal to $q_-/2$ up to power-suppressed terms. Performing the integrations, we obtain

$$\begin{aligned}
W_{us}(\omega_{us}) &= \delta(\omega_{us}) + \frac{Q_\ell^2 \alpha}{\pi} \frac{1}{\omega_{us}} \left(\frac{\mu^2}{(2\omega_{us})^2} \right)^\epsilon e^{\epsilon\gamma_E} \frac{(1-\epsilon)\Gamma(-\epsilon)}{\Gamma(2-2\epsilon)} + \mathcal{O}(\alpha^2), \\
W_{usc}(\omega_{usc}) &= \delta(\omega_{usc}) + \frac{Q_\ell^2 \alpha}{\pi} \frac{1}{\omega_{usc}} \left(\frac{\mu^2 m_B^2}{(2\omega_{usc})^2 m_\ell^2} \right)^\epsilon e^{\epsilon\gamma_E} (1-\epsilon)\Gamma(\epsilon) + \mathcal{O}(\alpha^2).
\end{aligned} \tag{5.88}$$

Inserting these expressions into (5.84), performing the two energy integrals, and expanding the result in a Laurent series in ϵ , we obtain for the (bare) radiation function

$$R(E_{\text{cut}}) = 1 + \frac{Q_\ell^2 \alpha}{2\pi} \left[- \left(\frac{1}{\epsilon} + \ln \frac{\mu^2 m_B}{(2E_{\text{cut}})^2 m_\ell} \right) \left(\ln \frac{m_B^2}{m_\ell^2} - 2 \right) + 2 - \frac{\pi^2}{3} \right] + \mathcal{O}(\alpha^2). \tag{5.89}$$

A problematic feature of this derivation is the fact that the integrations in (5.84), when carried out with bare functions, produce additional $1/\epsilon$ poles not present in the functions W_{us} and W_{usc} . The result (5.89) thus does not provide a basis for a consistent scale separation and resummation of large logarithmic corrections. Instead, we should renormalize the ultrasoft and ultrasoft-collinear functions separately, and then perform the integrations over renormalized functions in (5.84). Due to their singular behavior at the origin, the functions W_{us} and W_{usc} must be treated as distributions and renormalized using convolutions, such that

$$W_{us}(\omega, \mu) = \int_0^\Omega d\omega' Z_{us}(\omega, \omega', \mu) W_{us}(\omega'), \tag{5.90}$$

and similarly for W_{usc} . Here Ω denotes the upper value of the interval on which the renormalized functions are defined, in our case $\Omega = E_{\text{cut}}$. To derive the renormalization factors, we regularize the bare functions in (5.88) using star distributions [97, 139], which are defined as

$$\begin{aligned}
\int_0^\Omega d\omega f(\omega) \left(\frac{1}{\omega} \right)_*^{[\mu/2]} &= \int_0^\Omega d\omega \frac{f(\omega) - f(0)}{\omega} + f(0) \ln \frac{2\Omega}{\mu}, \\
\int_0^\Omega d\omega f(\omega) \left(\frac{\ln \frac{2\omega}{\mu}}{\omega} \right)_*^{[\mu/2]} &= \int_0^\Omega d\omega \frac{f(\omega) - f(0)}{\omega} \ln \frac{2\omega}{\mu} + \frac{f(0)}{2} \ln^2 \frac{2\Omega}{\mu}.
\end{aligned} \tag{5.91}$$

Using the relation

$$\frac{1}{\omega} \left(\frac{\mu^2}{(2\omega)^2} \right)^\epsilon = -\frac{1}{2\epsilon} \delta(\omega) + \left(\frac{1}{\omega} \right)_*^{[\mu/2]} - 2\epsilon \left(\frac{\ln \frac{2\omega}{\mu}}{\omega} \right)_*^{[\mu/2]} + \mathcal{O}(\epsilon^2), \tag{5.92}$$

we find that

$$\begin{aligned}
W_{us}(\omega) &= \delta(\omega) \left[1 + \frac{Q_\ell^2 \alpha}{\pi} \left(\frac{1}{2\epsilon^2} + \frac{1}{2\epsilon} + 1 - \frac{\pi^2}{8} \right) \right] \\
&\quad + \frac{Q_\ell^2 \alpha}{\pi} \left[- \left(\frac{1}{\epsilon} + 1 \right) \left(\frac{1}{\omega} \right)_*^{[\mu/2]} + 2 \left(\frac{\ln \frac{2\omega}{\mu}}{\omega} \right)_*^{[\mu/2]} \right] + \mathcal{O}(\alpha^2), \\
W_{usc}(\omega) &= \delta(\omega) \left[1 + \frac{Q_\ell^2 \alpha}{\pi} \left(-\frac{1}{2\epsilon^2} + \frac{1}{2\epsilon} (1 - \ln r_\ell) - \frac{\pi^2}{24} + \frac{\ln r_\ell}{2} - \frac{\ln^2 r_\ell}{4} \right) \right] \\
&\quad + \frac{Q_\ell^2 \alpha}{\pi} \left[\left(\frac{1}{\epsilon} - 1 + \ln r_\ell \right) \left(\frac{1}{\omega} \right)_*^{[\mu/2]} - 2 \left(\frac{\ln \frac{2\omega}{\mu}}{\omega} \right)_*^{[\mu/2]} \right] + \mathcal{O}(\alpha^2),
\end{aligned} \tag{5.93}$$

where $r_\ell = m_B^2/m_\ell^2$. From these expressions we read off the renormalization factors

$$\begin{aligned}
Z_{us}(\omega, \omega', \mu) &= \delta(\omega - \omega') \left[1 - \frac{Q_\ell^2 \alpha}{2\pi} \left(\frac{1}{\epsilon^2} + \frac{1}{\epsilon} \right) \right] + \frac{Q_\ell^2 \alpha}{\pi} \frac{1}{\epsilon} \left(\frac{1}{\omega - \omega'} \right)_*^{[\mu/2]} + \mathcal{O}(\alpha^2), \\
Z_{usc}(\omega, \omega', \mu) &= \delta(\omega - \omega') \left[1 + \frac{Q_\ell^2 \alpha}{2\pi} \left(\frac{1}{\epsilon^2} - \frac{1}{\epsilon} (1 - \ln r_\ell) \right) \right] - \frac{Q_\ell^2 \alpha}{\pi} \frac{1}{\epsilon} \left(\frac{1}{\omega - \omega'} \right)_*^{[\mu/2]} + \mathcal{O}(\alpha^2),
\end{aligned} \tag{5.94}$$

and the renormalized functions

$$\begin{aligned}
W_{us}(\omega, \mu) &= \delta(\omega) \left[1 + \frac{Q_\ell^2 \alpha}{\pi} \left(1 - \frac{\pi^2}{8} \right) \right] + \frac{Q_\ell^2 \alpha}{\pi} \left[- \left(\frac{1}{\omega} \right)_*^{[\mu/2]} + 2 \left(\frac{\ln \frac{2\omega}{\mu}}{\omega} \right)_*^{[\mu/2]} \right] + \mathcal{O}(\alpha^2), \\
W_{usc}(\omega, \mu) &= \delta(\omega) \left[1 + \frac{Q_\ell^2 \alpha}{\pi} \left(-\frac{\pi^2}{24} + \frac{\ln r_\ell}{2} - \frac{\ln^2 r_\ell}{4} \right) \right] \\
&\quad + \frac{Q_\ell^2 \alpha}{\pi} \left[(\ln r_\ell - 1) \left(\frac{1}{\omega} \right)_*^{[\mu/2]} - 2 \left(\frac{\ln \frac{2\omega}{\mu}}{\omega} \right)_*^{[\mu/2]} \right] + \mathcal{O}(\alpha^2).
\end{aligned} \tag{5.95}$$

Using these distributions in (5.84), we find the renormalized expression

$$R(E_{\text{cut}}, \mu) = 1 + \frac{Q_\ell^2 \alpha}{2\pi} \left[-\ln \frac{\mu^2 m_B}{(2E_{\text{cut}})^2 m_\ell} \left(\ln \frac{m_B^2}{m_\ell^2} - 2 \right) + 2 - \frac{\pi^2}{3} \right] + \mathcal{O}(\alpha^2), \tag{5.96}$$

in which the $1/\epsilon$ pole present in (5.89) has been removed.

Resummation of large logarithmic corrections

The renormalized functions in (5.95) contain logarithms of the form $\ln(\mu/2\omega)$ and $\ln(m_B^2/m_\ell^2)$. This gives rise to ultrasoft and ultrasoft-collinear logarithms of the type $\ln(\mu/2E_{\text{cut}})$ and

$\ln(\mu m_B/2E_{\text{cut}}m_\ell)$ in the radiation function $R(E_{\text{cut}}, \mu)$, which cannot be simultaneously made small by an appropriate choice of the scale μ . Both types of logarithms can be resummed by solving the RG equations satisfied by the various functions. It follows from (5.90) that the renormalized ultrasoft and ultrasoft-collinear functions satisfy the evolution equations

$$\frac{d}{d \ln \mu} W_{us}(\omega, \mu) = \int_0^\Omega d\omega' \Gamma_{us}(\omega, \omega', \mu) W_{us}(\omega', \mu), \quad (5.97)$$

and similarly for W_{usc} , where the anomalous dimensions are obtained from the single $1/\epsilon$ pole terms of the renormalization factors in (5.94). They are

$$\begin{aligned} \Gamma_{us}(\omega, \omega', \mu) &= \frac{Q_\ell^2 \alpha}{\pi} \left[-\delta(\omega - \omega') + 2 \left(\frac{1}{\omega - \omega'} \right)_*^{[\mu/2]} \right] + \mathcal{O}(\alpha^2), \\ \Gamma_{usc}(\omega, \omega', \mu) &= \frac{Q_\ell^2 \alpha}{\pi} \left[\delta(\omega - \omega') \left(\ln \frac{m_B^2}{m_\ell^2} - 1 \right) - 2 \left(\frac{1}{\omega - \omega'} \right)_*^{[\mu/2]} \right] + \mathcal{O}(\alpha^2). \end{aligned} \quad (5.98)$$

The integro-differential evolution equation (5.97) has the same form as the RG equation for the B -meson shape function [140], which was obtained in [97, 141]. Its closed-form solution has been derived in [104] using a technique developed in [109]. For our purposes, it will however be more convenient to use a variant of the method formulated in Laplace space [142, 143], where the convolution in (5.84) turns into a product, i.e.

$$\widetilde{R}(s, \mu) = \int_0^\infty dE_{\text{cut}} e^{-sE_{\text{cut}}} R(E_{\text{cut}}, \mu) = \frac{\widetilde{W}_{us}(s, \mu) \widetilde{W}_{usc}(s, \mu)}{s}. \quad (5.99)$$

The Laplace transform

$$\widetilde{W}_{us}(s, \mu) = \int_0^\infty d\omega e^{-s\omega} W_{us}(\omega, \mu), \quad (5.100)$$

and similarly $\widetilde{W}_{usc}(s, \mu)$, cannot be derived using the distribution-valued expressions in (5.95), because the star distributions are defined for integrals with a finite upper cutoff $\omega \leq \Omega$, see (5.91). We thus need to go back to the expressions for the bare functions given in (5.88). Using the relation

$$\int_0^\infty d\omega e^{-s\omega} \omega^{-1+a} = \Gamma(a) s^{-a} \quad (5.101)$$

for $a = -2\epsilon$, we find for the bare ultrasoft and ultrasoft-collinear functions in Laplace space

$$\begin{aligned} \widetilde{W}_{us}(s) &= 1 + \frac{Q_\ell^2 \alpha}{2\pi} \left(\frac{1}{\epsilon^2} + \frac{1 + L_{us}}{\epsilon} + \frac{L_{us}^2}{2} + L_{us} + \frac{\pi^2}{12} + 2 \right) + \mathcal{O}(\alpha^2), \\ \widetilde{W}_{usc}(s) &= 1 + \frac{Q_\ell^2 \alpha}{2\pi} \left(-\frac{1}{\epsilon^2} + \frac{1 - L_{usc}}{\epsilon} - \frac{L_{usc}^2}{2} + L_{usc} - \frac{5\pi^2}{12} \right) + \mathcal{O}(\alpha^2), \end{aligned} \quad (5.102)$$

where all dependence on the Laplace variable s is contained in the logarithms

$$L_{us} = \ln \left(\frac{\mu^2 s^2 e^{2\gamma_E}}{4} \right), \quad L_{usc} = \ln \left(\frac{\mu^2 s^2 e^{2\gamma_E} m_B^2}{4m_\ell^2} \right). \quad (5.103)$$

The pole terms can now be subtracted locally, such that $\widetilde{W}_{us}(s, \mu) = Z_{us}(s, \mu) \widetilde{W}_{us}(s)$, and analogously for the ultrasoft-collinear function. The renormalized functions

$$\begin{aligned}\widetilde{W}_{us}(s, \mu) &= 1 + \frac{Q_\ell^2 \alpha}{2\pi} \left(\frac{L_{us}^2}{2} + L_{us} + \frac{\pi^2}{12} + 2 \right) + \mathcal{O}(\alpha^2), \\ \widetilde{W}_{usc}(s, \mu) &= 1 + \frac{Q_\ell^2 \alpha}{2\pi} \left(-\frac{L_{usc}^2}{2} + L_{usc} - \frac{5\pi^2}{12} \right) + \mathcal{O}(\alpha^2)\end{aligned}\tag{5.104}$$

obey local RG equations, e.g.

$$\frac{d}{d \ln \mu} \widetilde{W}_{us}(s, \mu) = \gamma_{us}(s, \mu) \widetilde{W}_{us}(s, \mu),\tag{5.105}$$

with anomalous dimensions

$$\begin{aligned}\gamma_{us}(s, \mu) &= \frac{Q_\ell^2 \alpha}{\pi} (L_{us} + 1) + \mathcal{O}(\alpha^2), \\ \gamma_{usc}(s, \mu) &= \frac{Q_\ell^2 \alpha}{\pi} (-L_{usc} + 1) + \mathcal{O}(\alpha^2).\end{aligned}\tag{5.106}$$

It is important for the resummation of large logarithms that, to all orders in perturbation theory, the anomalous dimensions contain only a single power of logarithms, whose coefficient is proportional to the light-like cusp anomalous dimension of QED [102, 103]. Note that

$$\gamma_{us} + \gamma_{usc} = -2\gamma_{\text{soft}},\tag{5.107}$$

where the soft anomalous dimension has been given in (4.107). This exact relation holds to all orders of perturbation theory. As we will see, it ensures that the direct contribution to the decay rate is RG invariant.

In general, the renormalized functions in (5.104) depend on the scale μ via the logarithms L_{us} and L_{usc} and the renormalized QED coupling $\alpha(\mu)$. In the approximation where the running of α is neglected, we can write

$$\widetilde{W}_{us}(s, \mu) \equiv \widetilde{W}_{us}(L_{us}), \quad \widetilde{W}_{usc}(s, \mu) \equiv \widetilde{W}_{usc}(L_{usc}).\tag{5.108}$$

The RG equations are then solved by

$$\begin{aligned}\widetilde{W}_{us}(L_{us}) &= \exp \left[\frac{Q_\ell^2 \alpha}{2\pi} \left(\frac{L_{us}^2}{2} + L_{us} \right) \right] \widetilde{W}_{us}(0), \\ \widetilde{W}_{usc}(L_{usc}) &= \exp \left[\frac{Q_\ell^2 \alpha}{2\pi} \left(-\frac{L_{usc}^2}{2} + L_{usc} \right) \right] \widetilde{W}_{usc}(0),\end{aligned}\tag{5.109}$$

where the matching scales are chosen such that $L_{us} = 0$ and $L_{usc} = 0$, respectively. Combining these solutions, we obtain the RG-improved expression

$$\widetilde{W}_{us}(s, \mu) \widetilde{W}_{usc}(s, \mu) = \left(\frac{\mu^2 s^2 e^{2\gamma_E} m_B}{4m_\ell} \right)^{-\gamma_{\text{soft}}} \left[1 + \frac{Q_\ell^2 \alpha}{2\pi} \left(2 - \frac{\pi^2}{3} \right) + \mathcal{O}(\alpha^2) \right].\tag{5.110}$$

Inserting this result in (5.99), and performing the inverse Laplace transformation using (5.101), we obtain for the RG-improved radiation function

$$R(E_{\text{cut}}, \mu) = \left(\frac{\mu^2 m_B}{(2E_{\text{cut}})^2 m_\ell} \right)^{-\gamma_{\text{soft}}} \frac{e^{-2\gamma_E \gamma_{\text{soft}}}}{\Gamma(1 + 2\gamma_{\text{soft}})} \left[1 + \frac{\alpha Q_\ell^2}{2\pi} \left(2 - \frac{\pi^2}{3} \right) + \mathcal{O}(\alpha^2) \right]. \quad (5.111)$$

In this result, the large rapidity logarithms contained in γ_{soft} are resummed to all orders. While in our derivation we have neglected the scale dependence of the QED coupling, the formalism developed in [143] allows one to include the effects of the running of α in a simple and systematic way. This is discussed in Appendix D.

From (5.80) and (5.82), we now obtain for the direct contribution to the $B^- \rightarrow \ell^- \bar{\nu}_\ell(\gamma)$ decay rate

$$\begin{aligned} \Gamma_{\text{dir}}(E_{\text{cut}}) &= \Gamma_{\text{tree}} y_B^2(\mu_0) R(E_{\text{cut}}, \mu_0) \\ &= \Gamma_{\text{tree}} \left(\frac{\alpha(m_Z)}{\alpha(m_B)} \right)^{\frac{9}{20}} \left(\frac{2E_{\text{cut}}}{m_B} \right)^{2\gamma_{\text{soft}}} \frac{e^{-2\gamma_E \gamma_{\text{soft}}}}{\Gamma(1 + 2\gamma_{\text{soft}})} \mathcal{R}_{\text{virt}}^2 \left[1 + \frac{Q_\ell^2 \alpha}{2\pi} \left(2 - \frac{\pi^2}{3} \right) + \mathcal{O}(\alpha^2) \right]. \end{aligned} \quad (5.112)$$

Note that the matching scale μ_0 has disappeared from the final result. Also, the lepton-mass dependence in the radiation function $R(E_{\text{cut}}, \mu_0)$ cancels against that of the prefactor in (5.80), ensuring that there are no double logarithms of the charged-lepton mass left in the physical decay rate.²¹

5.6 Indirect contributions to the decay rate

We now turn to the discussion of the indirect contributions to the $B^- \rightarrow \ell^- \bar{\nu}_\ell(\gamma)$ decay rate. They originate from the production of an off-shell B^{*-} resonance, which undergoes a weak $B^{*-} \rightarrow \ell^- \bar{\nu}_\ell$ decay. Analogous contributions of higher resonances are power suppressed in the limit of small photon energy. We split up the indirect rate into two contributions,

$$\Gamma_{\text{indir}}(E_{\text{cut}}) = \Gamma_{B^* \gamma}(E_{\text{cut}}) + \Gamma_{B^* \pi}(E_{\text{cut}}), \quad (5.113)$$

one in which a photon is produced in a $BB^* \gamma$ interaction, and one in which a neutral pion is produced in a $BB^* \pi^0$ interaction, which subsequently decays into electromagnetic radiation.

Contribution involving the $BB^* \gamma$ vertex

The low-energy effective theory allows for the process $B^- \rightarrow B^{*-} \gamma$ followed by the weak vector-meson decay $B^{*-} \rightarrow \ell^- \bar{\nu}_\ell$, which does not suffer the chiral suppression of the decay $B^- \rightarrow \ell^- \bar{\nu}_\ell$. The tree-level diagram for this process is shown in the first graph in Figure 17. The corresponding decay amplitude is given by

$$\mathcal{A}_{B^*}(B^- \rightarrow \ell^- \bar{\nu}_\ell \gamma) = \frac{G_F^{(\mu)} V_{ub}}{\sqrt{2}} f_{B^*} m_{B^*} \sqrt{\frac{m_B}{m_{B^*}}} \frac{e g_{BB^* \gamma}}{v \cdot q + \delta_{B^*}} \epsilon_{\mu\nu\rho\sigma} \varepsilon^{*\mu}(q) q^\nu v^\rho \bar{u}(v_\ell) \gamma_\perp^\sigma P_L v(p_\nu), \quad (5.114)$$

²¹The quantity $\mathcal{R}_{\text{virt}}$ in (4.116) contains single-logarithmic corrections involving m_ℓ . However, since the virtual decay rate is proportional to m_ℓ^2 due to its chiral suppression, the limit $m_\ell \rightarrow 0$ is smooth.

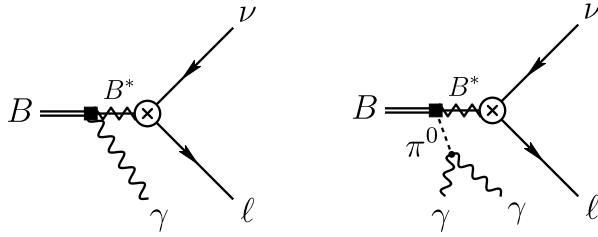


Figure 17: Indirect decay topologies contributing to $B^- \rightarrow \ell^- \bar{\nu}_\ell(\gamma)$ decay rate, which arise at leading order in the low-energy theory. In the first graph, a photon is emitted through the effective $BB^*\gamma$ coupling. In the second graph an on-shell pion is first emitted, which subsequently decays into two photons.

where q denotes the ultrasoft photon 4-momentum.²² The effective heavy-lepton spinor $u(v_\ell)$ is normalized to $\sqrt{2m_\ell}$, such that

$$\sum_{\text{pol}} u(v_\ell) \bar{u}(v_\ell) = 2m_\ell \frac{1 + \not{v}_\ell}{2} = \not{v}_\ell + m_\ell. \quad (5.115)$$

For the squared decay amplitude, summed over polarizations and normalized to the squared amplitude for the tree-level $B^- \rightarrow \ell^- \bar{\nu}_\ell$ process, we obtain (up to power-suppressed terms $\sim m_\ell^2/m_B^2$)

$$\frac{\sum_{\text{pol}} |\mathcal{A}_{B^*}(B^- \rightarrow \ell^- \bar{\nu}_\ell \gamma)|^2}{\sum_{\text{pol}} |\mathcal{A}_{\text{tree}}(B^- \rightarrow \ell^- \bar{\nu}_\ell)|^2} = \frac{m_B^2}{2m_\ell^2} \frac{f_{B^*}^2 m_{B^*}}{f_B^2 m_B} \left(\frac{e g_{BB^*\gamma}}{E_q + \delta_{B^*}} \right)^2 \mathbf{q}^2 \frac{1 + \cos^2 \theta}{2}, \quad (5.116)$$

where we have aligned the z -axis with the direction of the charged lepton, and $\theta = \angle(\mathbf{q}, \mathbf{v}_\ell)$ denotes the angle between the directions of the ultrasoft photon and the charged lepton in the B -meson rest frame. In the ultrasoft-photon limit $q \rightarrow 0$, the three-particle phase space integral factorizes into a two-particle phase-space times a phase-space integral of the emitted photon,

$$\int \frac{d^3 \mathbf{p}_\ell}{(2\pi)^3 2E_{\mathbf{p}_\ell}} \int \frac{d^3 \mathbf{p}_\nu}{(2\pi)^3 2E_{\mathbf{p}_\nu}} \int \frac{d^3 \mathbf{q}}{(2\pi)^3 2E_{\mathbf{q}}} (2\pi)^4 \delta^{(4)}(m_B v - p_\ell - p_\nu - q) \quad (5.117)$$

$$\stackrel{q \rightarrow 0}{=} \int \frac{d^3 \mathbf{p}_\ell}{(2\pi)^3 2E_{\mathbf{p}_\ell}} \int \frac{d^3 \mathbf{p}_\nu}{(2\pi)^3 2E_{\mathbf{p}_\nu}} (2\pi)^4 \delta^{(4)}(m_B v - p_\ell - p_\nu) \int \frac{d^3 \mathbf{q}}{(2\pi)^3 2E_{\mathbf{q}}}.$$

²²One may wonder whether there is another contribution to the amplitude in which photon has ultrasoft-collinear momentum scaling. In this case the phase-space measure $d^3 \mathbf{q}$ in (5.118) is suppressed by a factor of $\mathcal{O}(\lambda_\ell^2)$ relative to the measure for an ultrasoft photon, while the integrand obeys the same scaling on both cases. Hence the ultrasoft-collinear contribution is suppressed by a factor $\sim (m_\ell/m_B)^2$ and can be neglected.

It follows that (with $E_{\mathbf{q}} = |\mathbf{q}|$ for a real photon)

$$\begin{aligned} \frac{\Gamma_{B^*\gamma}(E_{\text{cut}})}{\Gamma_{\text{tree}}} &= \frac{m_B^2}{2m_\ell^2} \frac{f_{B^*}^2 m_{B^*}}{f_B^2 m_B} (e g_{BB^*\gamma})^2 \int_{E_{\mathbf{q}} \leq E_{\text{cut}}} \frac{d^3 \mathbf{q}}{(2\pi)^3 2E_{\mathbf{q}}} \frac{\mathbf{q}^2}{(E_{\mathbf{q}} + \delta_{B^*})^2} \frac{1 + \cos^2 \theta}{2} \\ &= \frac{m_B^2}{m_\ell^2} \frac{f_{B^*}^2 m_{B^*}}{f_B^2 m_B} \frac{\alpha}{6\pi} (g_{BB^*\gamma} E_{\text{cut}})^2 I\left(0, \frac{\delta_{B^*}}{E_{\text{cut}}}\right). \end{aligned} \quad (5.118)$$

The phase-space integral $I(0, z)$ is a special case of the function

$$I(y, z) = 2 \int_y^1 dx \frac{(x^2 - y^2)^{\frac{3}{2}}}{(x + z)^2}, \quad (5.119)$$

which is normalized such that $I(0, 0) = 1$. For $y = 0$, we find

$$I(0, z) = 3 - 6z - \frac{2}{1+z} + 6z^2 \ln \frac{1+z}{z} = 9 - 2r - \frac{6}{r} - \frac{6(1-r)^2}{r^2} \ln(1-r), \quad (5.120)$$

where in the second form we have substituted $r = \frac{1}{1+z} = E_{\text{cut}}/(E_{\text{cut}} + \delta_{B^*})$. This function approaches 1 for $E_{\text{cut}} \gg \delta_{B^*} \simeq 45 \text{ MeV}$, while for $E_{\text{cut}} \lesssim \delta_{B^*}$ it is given by a power series in $E_{\text{cut}}/\delta_{B^*}$ starting with $\frac{1}{2}(E_{\text{cut}}/\delta_{B^*})^2 - \frac{4}{5}(E_{\text{cut}}/\delta_{B^*})^3 \pm \dots$. The factor $m_{B^*}^2/m_\ell^2$ in (5.118) removes the chiral suppression of the tree-level rate and hence gives a strong enhancement of the indirect rate. However, the factor $(g_{BB^*\gamma} E_{\text{cut}})^2 \sim (E_{\text{cut}}/\Lambda_c)^2$ leads to a power suppression. In the limit $E_{\text{cut}} \rightarrow 0$, the indirect rate scales like E_{cut}^4 .

The amplitudes for the direct and indirect contributions to the $B^- \rightarrow \ell^- \bar{\nu}_\ell \gamma$ process can interfere. However, this requires right-handed lepton polarization in the indirect amplitude, which leads to an additional power suppression $\sim m_\ell/m_B$. As a result, the interference contribution to the decay rate carries a chiral suppression $\sim (m_\ell/m_B)^2$ in addition to the suppression $\sim (E_{\text{cut}}/\Lambda_c)^2$ from the dipole operator contributing to the indirect rate. This makes the interference term negligible.

In the literature of leptonic weak decays of pseudoscalar mesons, the indirect contributions are often expressed in terms of the meson-to-photon matrix element of the time-ordered product of the weak current and the electromagnetic current, which for an on-shell photon can be parametrized by a vector form factor $F_V(x_\gamma)$ and an axial-vector form factor $F_A(x_\gamma)$, with $x_\gamma = 2E_\gamma/m_B$ (see e.g. [27, 119, 120]). After integration over the charged-lepton energy $x_\ell = 2E_\ell/m_B$ over the interval (with $\lambda_\ell = m_\ell/m_B$)

$$1 - x_\gamma + \frac{\lambda_\ell^2}{1 - x_\gamma} \leq x_\ell \leq 1 + \lambda_\ell^2, \quad (5.121)$$

one finds that the differential decay rate $d\Gamma_{B^*}(B^- \rightarrow \ell^- \bar{\nu}_\ell \gamma)/dx_\gamma$ is proportional to the sum $|F_V(x_\gamma)|^2 + |F_A(x_\gamma)|^2$. Our results imply that in the soft-photon limit $x_\gamma \ll 1$

$$F_V(x_\gamma) = \frac{f_{B^*} m_{B^*}}{2} \frac{g_{BB^*\gamma}}{E_\gamma + \delta_{B^*}}, \quad F_A(x_\gamma) = 0, \quad (5.122)$$

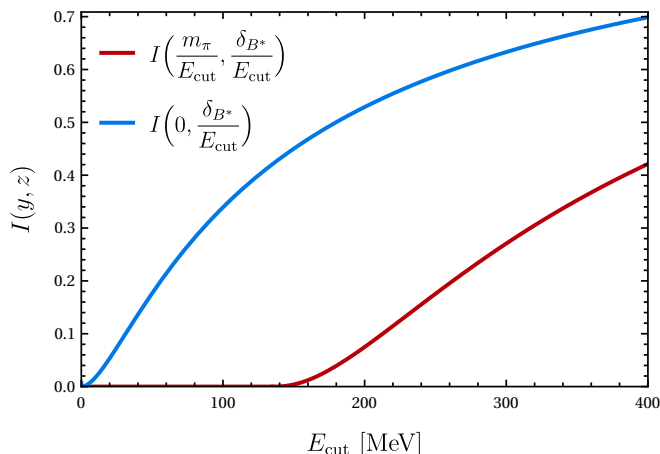


Figure 18: Dependence of the functions $I(0, \delta_{B^*}/E_{\text{cut}})$ (blue) and $I(m_\pi/E_{\text{cut}}, \delta_{B^*}/E_{\text{cut}})$ (red) on the photon energy cut. Both functions approach 1 from below in the limit $E_{\text{cut}} \rightarrow \infty$.

in agreement with [27]. Our HH χ PT construction thus corresponds to the first-vector pole approximation for the form factors. Corrections to these relations have energy denominators in which δ_{B^*} is replaced by $\delta_{X_b} \sim \Lambda_c$ and thus give contributions suppressed by E_γ/Λ_c for $E_\gamma > \delta_{B^*}$, and $\delta_{B^*}/\Lambda_c \sim \Lambda_c/m_B$ for $E_\gamma < \delta_{B^*}$. The first axial-vector resonance $B_1(5721)$, whose contribution was estimated in [27], therefore gives a power-suppressed contribution to the $B^- \rightarrow \ell^- \bar{\nu}_\ell \gamma$ decay rate suppressed by $(E_\gamma/\Lambda_c)^2$ or $(\Lambda_c/m_B)^2$, respectively, in the soft-pion limit. The first vector resonance with $J^P = 1^-$ and mass above the B^* mass would give contributions suppressed by E_γ/Λ_c or Λ_c/m_B , since it interferes with the B^* contribution. However, for orbitally excited states one expects reduced couplings to the weak current, because in quark models their decay constants probe the wave function at the origin.

Contribution involving the $BB^*\pi^0$ vertex

For values of E_{cut} below the pion mass, the $B^- \rightarrow B^{*-} \gamma \rightarrow \ell^- \bar{\nu}_\ell \gamma$ process is the dominant contribution to the indirect rate. However, experimental considerations might require raising the cutoff to values $E_{\text{cut}} \gtrsim m_\pi$. In this case, a second indirect contribution becomes kinematically allowed, and it turns out to be the dominant contribution by far. The low-energy effective theory allows for the transition $B^- \rightarrow B^{*-} \pi^0 \rightarrow \ell^- \bar{\nu}_\ell \pi^0$, shown in the right diagram in Figure 17. The ultrasoft π^0 meson decays promptly, within few 10^{-8} m from the production point, with branching fractions $\text{Br}(\pi^0 \rightarrow \gamma\gamma) \simeq 98.82\%$ and $\text{Br}(\pi^0 \rightarrow e^+e^-\gamma) \simeq 1.174\%$. Both signals are seen as “soft photons” in the electromagnetic calorimeter. We can thus reinterpret the associated final state as $B^- \rightarrow \ell^- \bar{\nu}_\ell \gamma\gamma$. Given that the width of the neutral pion is around 7.8 eV [34], this decay can only occur for an on-shell pion, which implies that the energy of the emitted electromagnetic radiation is bounded by $E_{\text{rad}} \geq m_{\pi^0} \simeq 135$ MeV. The decay amplitude for the $B^- \rightarrow \ell^- \bar{\nu}_\ell \pi^0$ process via an intermediate B^{*-} resonance is obtained

as

$$\mathcal{A}_{B^*}(B^- \rightarrow \ell^- \bar{\nu}_\ell \pi^0) = -\frac{G_F^{(\mu)} V_{ub}}{f_\pi} f_{B^*} m_{B^*} \sqrt{\frac{m_B}{m_{B^*}}} \frac{g_{BB^*\pi}}{v \cdot q + \delta_{B^*}} \bar{u}(v_\ell) \not{q}_\perp P_L v(p_\nu), \quad (5.123)$$

where now q denotes the 4-momentum of the pion. For the squared amplitude summed over polarizations, we find in this case (again up to power-suppressed terms $\sim (m_\ell/m_B)^2$)

$$\frac{\sum_{\text{pol}} |\mathcal{A}_{B^*}(B^- \rightarrow \ell^- \bar{\nu}_\ell \pi^0)|^2}{\sum_{\text{pol}} |\mathcal{A}_{\text{tree}}(B^- \rightarrow \ell^- \bar{\nu}_\ell)|^2} = \frac{m_B^2}{2m_\ell^2} \frac{f_{B^*}^2 m_{B^*}}{f_B^2 m_B} \left(\frac{g_{BB^*\pi}/f_\pi}{E_q + \delta_{B^*}} \right)^2 \mathbf{q}^2 (1 - \cos^2 \theta). \quad (5.124)$$

Compared with (5.116), we find $e g_{BB^*\gamma} \approx 0.44 \text{ GeV}^{-1}$ and $g_{BB^*\pi}/f_\pi \approx 4.3 \text{ GeV}^{-1}$ (see Table 5 in Section 6 for a discussion of our input parameter choices), so at the level of the squared decay amplitude the pion mode is enhanced by two orders of magnitude in the region $E_q > m_\pi$, where it is kinematically allowed. In the ultrasoft-pion limit, the three-particle decay rate can be approximated as (with $E_q = \sqrt{m_\pi^2 + \mathbf{q}^2}$)

$$\begin{aligned} \frac{\Gamma_{B^*}(B^- \rightarrow \ell^- \bar{\nu}_\ell \pi^0)}{\Gamma_{\text{tree}}} &= \frac{m_B^2}{2m_\ell^2} \frac{f_{B^*}^2 m_{B^*}}{f_B^2 m_B} \left(\frac{g_{BB^*\pi}}{f_\pi} \right)^2 \int_{m_\pi \leq E_q \leq E_{\text{cut}}} \frac{d^3 \mathbf{q}}{(2\pi)^3 2E_q} \frac{\mathbf{q}^2}{(E_q + \delta_{B^*})^2} (1 - \cos^2 \theta) \\ &= \frac{m_B^2}{m_\ell^2} \frac{f_{B^*}^2 m_{B^*}}{f_B^2 m_B} \frac{g_{BB^*\pi}^2}{24\pi^2} \left(\frac{E_{\text{cut}}}{f_\pi} \right)^2 I \left(\frac{m_\pi}{E_{\text{cut}}}, \frac{\delta_{B^*}}{E_{\text{cut}}} \right), \end{aligned} \quad (5.125)$$

where for $z < y < 1$

$$\begin{aligned} I(y, z) &= \frac{\sqrt{1-y^2}}{1+z} [1 + 2y^2 - 3z(1+2z)] - 3(y^2 - 2z^2) \operatorname{arctanh}(\sqrt{1-y^2}) \\ &\quad + 6z\sqrt{y^2 - z^2} \operatorname{arctan} \left(\frac{\sqrt{1-y^2}\sqrt{y^2 - z^2}}{y^2 + z} \right). \end{aligned} \quad (5.126)$$

Taking into account that the neutral pion decays electromagnetically and that energy is conserved in its decay, we obtain

$$\begin{aligned} \Gamma_{B^*\pi}(E_{\text{cut}}) &= \Gamma_{B^*\pi}(B^- \rightarrow \ell^- \bar{\nu}_\ell \gamma \gamma) \Big|_{E_{\gamma\gamma} \leq E_{\text{cut}}} + \Gamma_{B^*\pi}(B^- \rightarrow \ell^- \bar{\nu}_\ell \gamma e^+ e^-) \Big|_{E_{\gamma ee} \leq E_{\text{cut}}} \\ &= [\operatorname{Br}(\pi^0 \rightarrow \gamma\gamma) + \operatorname{Br}(\pi^0 \rightarrow \gamma e^+ e^-)] \Gamma(B^- \rightarrow \ell^- \bar{\nu}_\ell \pi^0) \Big|_{E_\pi \leq E_{\text{cut}}} \end{aligned} \quad (5.127)$$

to excellent approximation, because the two branching fractions add up to 99.997%. In Figure 18 we show the two phase-space integrals in (5.118) and (5.125) as functions of E_{cut} . The π^0 -induced decay mode opens up for $E_{\text{cut}} > m_{\pi^0} \simeq 135 \text{ MeV}$, and due to the strong enhancement of the squared amplitude for this process, it quickly becomes the dominant indirect decay mode. For $E_{\text{cut}} = 150 \text{ MeV}$ (200 MeV), we find $\Gamma_{B^*\pi}/\Gamma_{B^*\gamma} \approx 0.8$ (13).

Away from the soft-pion limit, the $B^- \rightarrow \ell^- \bar{\nu}_\ell \pi^0$ decay amplitude can be expressed in a model-independent way in terms of the scalar form factor $f_+^{B \rightarrow \pi}(q^2)$ (see e.g. [144]), where

$q^2 = (p_B - p_\pi)^2 = m_B^2 + m_\pi^2 - 2m_B v \cdot p_\pi$, where v denotes the 4-velocity of the B meson, and $v \cdot p_\pi = E_\pi$ in the B -meson rest frame. In the limit of vanishing lepton mass, one obtains the differential decay rate

$$\frac{d\Gamma(B^- \rightarrow \ell^- \bar{\nu}_\ell \pi^0)}{d(v \cdot p_\pi)} = \frac{G_F^2 m_B}{24\pi^3} |V_{ub}|^2 [(v \cdot p_\pi)^2 - m_\pi^2]^{\frac{3}{2}} |f_+(q^2)|^2. \quad (5.128)$$

A systematic analysis of the $B \rightarrow \pi$ form factors in the heavy quark expansion was performed in [145], where it was shown that in the soft-pion limit

$$\lim_{v \cdot p_\pi \rightarrow m_\pi} f_+(q^2) = \frac{f_{B^*} m_B}{2f_\pi} \frac{g_{BB^*\pi}}{v \cdot p_\pi + \delta_{B^*}}, \quad (5.129)$$

in agreement with [74–76]. Inserting this expression in (5.128) and integrating over the pion energy, we recover our previous result (5.125) times a factor $m_B/m_{B^*} = 1 + \mathcal{O}(1/m_b^2)$.

In the present work, we assume for simplicity that experimentally one measures the total energy of electromagnetic radiation, and that this energy is below the cutoff E_{cut} . The phenomenological results presented in Section 6 are obtained based on this assumption. Using a finely grained electromagnetic calorimeter, it is possible to measure further properties of the deposited electromagnetic showers. For example, in events with two (or more) final-state photons it may be possible to reconstruct the energies and directions of the photons individually. For a two-photon signature, one could then check whether the invariant mass of the photon pair is compatible with the pion mass, them being produced from the decay of a neutral pion (see e.g. [146]). Such an analysis, which typically uses modern tools of machine learning and deep neural networks, may allow one to veto against the indirect contribution $\Gamma_{B^*\pi}(E_{\text{cut}})$ which, as we will see below, turns out to be a significant background.

5.7 Electromagnetic radiation spectrum

Given the results derived in the previous two sections, it is possible to obtain the resummed differential decay rate for the $B^- \rightarrow \ell^- \bar{\nu}_\ell(\gamma)$ process with respect to the total energy of low-energy electromagnetic radiation. In the phase-space region where $E_{\text{rad}} \ll \Lambda_c$, we obtain

$$\frac{d\Gamma}{dE_{\text{rad}}} = \left. \frac{d\Gamma_{\text{dir}}(E_{\text{cut}})}{dE_{\text{cut}}} + \frac{d\Gamma_{\text{indir}}(E_{\text{cut}})}{dE_{\text{cut}}} \right|_{E_{\text{cut}}=E_{\text{rad}}}. \quad (5.130)$$

From the resummed expression (5.112) for the direct contribution, we deduce that

$$\frac{d\Gamma_{\text{dir}}}{dE_{\text{rad}}} = \frac{2\gamma_{\text{soft}}}{E_{\text{rad}}} \Gamma_{\text{dir}}(E_{\text{rad}}) \propto E_{\text{rad}}^{-1+2\gamma_{\text{soft}}}. \quad (5.131)$$

This contribution diverges for $E_{\text{rad}} \rightarrow 0$ but is integrable after RG resummation. The indirect contribution to the radiation spectrum vanishes for $E_{\text{rad}} \rightarrow 0$. It scales like E_{rad}^3 near the origin and is monotonically rising, exhibiting a linear behavior for values $E_{\text{rad}} \gg \delta_{B^*}$, with an abrupt change of the slope above the pion threshold.

6 Phenomenology

We are finally in a position to present our numerical predictions for the $B^- \rightarrow \mu^- \bar{\nu}_\mu(\gamma)$ decay rate. The input values for the parameters entering our calculation are collected in Table 5. The RG evolution of the strong coupling $\alpha_s(\mu)$ is provided by the `RunDec` package [147]. For the electromagnetic coupling, we perform the running between the weak scale and m_B at one-loop order.

6.1 Non-perturbative input parameters

A number of non-perturbative hadronic parameters are needed for our analysis. We determine them as follows.

Input for the BB^* couplings

For the coupling $g_{BB^*\gamma}$, neither experimental nor first-principle determinations are currently available. An experimental determination would require measuring the radiative decay $B^* \rightarrow B\gamma$ or the total B^* width, both of which are unlikely to be accessible in the foreseeable future. A first-principle result might eventually come from lattice QCD. Existing estimates based on quark models, HH χ PT, and light-cone sum rules (LCSR) span a wide range (see e.g. Table 7 of [148]). The central values of the two most recent calculations based on LCSRs are in good agreement with each other [148, 149]. To be conservative, we adopt the larger of the two quoted uncertainties.²³

Results for the $g_{BB^*\pi}$ coupling exist both from lattice QCD and LCSRs. Here we take as input the most recent lattice determination of the heavy-quark coupling g_b [150], which coincides with the coupling g in the HH χ PT Lagrangian up to $\mathcal{O}(1/m_b)$ corrections and thus with the physical coupling $g_{BB^*\pi}$ up to chiral corrections by virtue of (5.61). With this choice, the value of $g_{BB^*\pi}$ is approximately 30% larger than the LCSR determination [151, 152].

Modeling of the LCDAs

Another important set of non-perturbative ingredients are the light-cone distribution amplitudes (LCDAs) of the B meson, which encode information about its inner structure as probed in decays with highly energetic light final-state particles. For our analysis, the relevant LCDAs are the subleading-twist distribution amplitudes ϕ_-^B and ϕ_{3g}^B , which can be related to the leading-twist LCDA ϕ_+^B using equations of motion [112, 113]. In this way, one can derive the representations [158]

$$\begin{aligned} \phi_-^B(\omega, \mu) &= \int_\omega^\infty \frac{d\omega'}{\omega'} \phi_+^B(\omega', \mu) + \int_0^\infty ds J_0(2\sqrt{\omega s}) \eta_3^{(0)}(s, \mu), \\ \phi_{3g}^B(\omega, \omega_g, \mu) &= \int_0^\infty ds \left[\eta_3^{(0)}(s, \mu) Y_3^{(0)}(s|\omega, \omega_g) + \frac{1}{2} \int_{-\infty}^\infty dx \eta_3(s, x, \mu) Y_3(s, x|\omega, \omega_g) \right]. \end{aligned} \tag{6.1}$$

²³In principle, a theoretically clean determination of $g_{BB^*\gamma}$ could come from a measurement of the $B^- \rightarrow e^- \bar{\nu}_e$ branching ratio with a cut $E_{\text{cut}} \ll \Lambda_c$, because this channel is completely dominated by the indirect contribution $B \rightarrow B^* \gamma \rightarrow e^- \bar{\nu}_e \gamma$. The associated decay rate is thus proportional to $|g_{BB^*\gamma}|^2$.

Parameter	Value	Reference
$G_F^{(\mu)}$	$1.1663788(6) \cdot 10^{-5} \text{ GeV}^{-2}$	[34]
$\alpha(m_Z)^{-1}$	127.930(8)	[34]
$\alpha_s(m_Z)$	0.1180(9)	[34]
f_π	130.2 MeV	[153]
f_B	190.0(1.3) MeV	[153]
f_{B^*}/f_B	0.951(17)	[154, 155]
λ_E^2	0.03(2) GeV^2	[156]
λ_H^2	0.06(3) GeV^2	[156]
λ_B	0.383(153) GeV	[157]
$ g_{BB^*\gamma} $	1.45(27) GeV^{-1}	[148]
$ g_{BB^*\pi} $	0.56(8)	[150]

Table 5: Numerical input values for the relevant parameters. For the ratio f_{B^*}/f_B we use the average of the available $N_f = 2 + 1 + 1$ results, HPQCD [154] and ETMC [155].

In these expressions, the non-perturbative contributions are encoded in the functions $\eta_3^{(0)}$ and η_3 . The first one captures the subleading-twist contribution to the two-particle LCDA ϕ_-^B , while the second describes the genuine three-particle contribution to the three-particle LCDA ϕ_{3g}^B . These functions multiply the Bessel function J_0 and the eigenfunctions $Y_3^{(0)}$, Y_3 of the associated evolution equation (see [113] for details).

In our analysis, we assume the exponential model functions [108, 113]

$$\begin{aligned}
\phi_+^B(\omega, \mu_0) &= \frac{\omega}{\omega_0^2} e^{-\frac{\omega}{\omega_0}}, \\
\eta_3^{(0)}(s, \mu_0) &= -\frac{\lambda_E^2 - \lambda_H^2}{18} s^2 e^{-\omega_0 s}, \\
\phi_{3g}^B(\omega, \omega_g, \mu_0) &= \frac{\lambda_E^2 - \lambda_H^2}{6\omega_0^5} \omega \omega_g e^{-\frac{\omega + \omega_g}{\omega_0}},
\end{aligned} \tag{6.2}$$

from which we obtain

$$\phi_-^B(\omega, \mu_0) = \frac{1}{\omega_0} e^{-\frac{\omega}{\omega_0}} \left[1 - \frac{\lambda_E^2 - \lambda_H^2}{18\omega_0^2} \left(2 - \frac{4\omega}{\omega_0} + \frac{\omega^2}{\omega_0^2} \right) \right]. \tag{6.3}$$

Using these model functions, the relevant convolution integrals over the LCDAs in (4.105) and (4.116) become

$$\ln \frac{\omega_-(\mu_0)}{\omega_0} = \int_0^\infty d\omega \phi_-^B(\omega, \mu_0) \ln \frac{\omega}{\omega_0} = \frac{\lambda_E^2 - \lambda_H^2}{18\omega_0^2} - \gamma_E, \tag{6.4}$$

and

$$\int_0^\infty d\omega \int_0^\infty d\omega_g \phi_{3g}^B(\omega, \omega_g, \mu_0) \left(\frac{1}{\omega_g} \ln \frac{\omega + \omega_g}{\omega} - \frac{1}{\omega + \omega_g} \right) = \frac{\lambda_E^2 - \lambda_H^2}{36\omega_0^2}. \tag{6.5}$$

In practice, we fix ω_0 using a LCSR determination of the first inverse moment (λ_B) of the LCDA ϕ_+^B , which in our model is obtained as $\lambda_B = \omega_0$. For the remaining model parameters we use the values given in Table 5. Note that our model functions for the LCDAs neglect the perturbative radiative tails at large values of ω and ω_g [109, 110]. This is legitimate, since these tails would contribute to $B^- \rightarrow \ell^- \bar{\nu}_\ell$ decay starting at $\mathcal{O}(\alpha\alpha_s)$, which is beyond our accuracy goal in this work.

QED corrections to the B -meson decay constant

A central ingredient to the structure-dependent QED corrections is the QED-corrected HQET decay constant $F_-(\Lambda, \mu)$ defined in (4.78). This object is genuinely non-perturbative, since it results from the interplay between soft photons and the non-perturbative dynamics inside the B meson. Given that a reliable determination of F_- is unavailable at present, we parameterize it as a relative $\mathcal{O}(\alpha)$ correction to the HQET decay constant,

$$F_-(\Lambda, \mu) = F_{\text{QCD}}(\mu) \left[1 + \frac{\alpha}{\pi} f^{(1)}(\Lambda, \mu) + \mathcal{O}(\alpha^2) \right], \quad (6.6)$$

and treat $f^{(1)}$ evaluated at the low scales $\Lambda = \mu = \mu_0 = 1.5 \text{ GeV}$ as an unknown $\mathcal{O}(1)$ parameter by including it in the theoretical uncertainty,

$$f^{(1)}(\mu_0, \mu_0) = 0 \pm 1. \quad (6.7)$$

This scale choice avoids large logarithms inside $f^{(1)}$, so that this range seems reasonable. The evolution of F_- in Λ between μ_0 and m_B and is then accomplished using (4.95). It resums large logarithms of the ratio m_B/μ_0 . With our model LCDAs, we obtain the shift

$$\frac{F(m_B, \mu_0) - F(\mu_0, \mu_0)}{F_{\text{QCD}}(\mu_0)} = (2.32 \pm 0.51_{\phi_B}) \cdot 10^{-3}, \quad (6.8)$$

where the subscript “ ϕ_B ” indicates the uncertainty from the variation of the model parameters of the LCDAs.

6.2 Numerical estimates

We are now ready to present numerical estimates of our findings for the direct and indirect contributions to the QED-corrected $B^- \rightarrow \mu^- \bar{\nu}_\mu(\gamma)$ decay rate in (5.81). As mentioned earlier, the symbol “ (γ) ” stands for low-energetic electromagnetic radiation in the form of one or multiple photons. We begin with the direct contribution, whose explicit form is given in (5.112). In order to convey a sense of the numerical impact of the various ingredients in this formula, we consider them one by one. For the factor encoding short-distance electroweak corrections from the evolution between m_Z and m_B , we obtain

$$\left(\frac{\alpha(m_Z)}{\alpha(m_B)} \right)^{\frac{9}{20}} = 1.01406, \quad (6.9)$$

where the leading uncertainty comes from the determination of $\alpha^{-1}(m_Z)$ and can be safely neglected. Next, $\mathcal{R}_{\text{virt}}$ encodes QED and part of the mixed QED–QCD corrections from the evolution between m_B and Λ_c . As shown in Section 4.9, this quantity is scale-independent up to $\mathcal{O}(\alpha\alpha_s \ln \mu_0^2/m_B^2)$ terms, which are only partially included in our calculation. We estimate them by varying the scale μ_0 by a factor of $1/\sqrt{2}$ to $\sqrt{2}$ about its default value. Using the inputs in Table 5, we find

$$\mathcal{R}_{\text{virt}}^2 = 1 + (6.9 \pm 4.8_{f(1)} \pm 1.6_{\phi_B} \pm 1.1_{\mu_0}) \cdot 10^{-3}, \quad (6.10)$$

with the dominant error stemming from our estimate of the unknown QED effects in F_- , followed by the scale uncertainty and that on the LCDA parameters, which is largely driven by the uncertainty on λ_B . The scale uncertainty coming from the RG evolution of the LCDAs is neglected. Naively, one could expect $\mathcal{R}_{\text{virt}}^2 - 1$ to be at the few percent level, since it contains the large logarithms $\frac{\alpha}{\pi} \ln(m_B/m_\mu) \approx 1.9\%$ and $\frac{\alpha}{\pi} \ln^2(m_B/\Lambda_{\text{QCD}}) \sim (1.5-5.4)\%$ for $\Lambda_{\text{QCD}} \sim (0.5-1.5)$ GeV. In practice, accidental numerical cancellations between these logarithmic terms and the constant pieces suppress $\mathcal{R}_{\text{virt}}^2 - 1$ to the sub-percent level.

Moving to lower scales, the object

$$\Omega(E_{\text{cut}}) \equiv \left(\frac{2E_{\text{cut}}}{m_B} \right)^{2\gamma_{\text{soft}}} \quad (6.11)$$

encodes the dependence of the direct contribution to the decay rate on the experimental cut. For $E_{\text{cut}} = 25, 100$ and 200 MeV, we obtain

$$\begin{aligned} \Omega(25 \text{ MeV}) &= 1 - 62.6 \cdot 10^{-3}, \\ \Omega(100 \text{ MeV}) &= 1 - 44.4 \cdot 10^{-3}, \\ \Omega(200 \text{ MeV}) &= 1 - 35.2 \cdot 10^{-3}. \end{aligned} \quad (6.12)$$

For the factor

$$\mathcal{W} = \frac{e^{-2\gamma_E \gamma_{\text{soft}}}}{\Gamma(1 + 2\gamma_{\text{soft}})} \left[1 + \frac{Q_\ell^2 \alpha}{2\pi} \left(2 - \frac{\pi^2}{3} \right) \right], \quad (6.13)$$

which resums single logarithms of the boost factor m_B/m_ℓ , we find

$$\mathcal{W} = 1 - 1.69 \cdot 10^{-3}. \quad (6.14)$$

The resummation of large logarithms affects $\mathcal{R}_{\text{virt}}$, Ω , and \mathcal{W} numerically in the range from (1–20)%, with the largest impact in $\mathcal{R}_{\text{virt}}$ due to the presence of mixed QED–QCD effects.

In order to better elucidate the QED corrections to the individual contributions to the decay rate and their dependence on the cut parameter, we define

$$\Gamma(E_{\text{cut}}) = \Gamma_{\text{tree}} \left[1 + \Delta\Gamma_{\text{dir}}(E_{\text{cut}}) + \Delta\Gamma_{B^*\gamma}(E_{\text{cut}}) + \Delta\Gamma_{B^*\pi}(E_{\text{cut}}) \right]. \quad (6.15)$$

Combining the various ingredients above according to (5.112), the direct contribution for the three values of the cut chosen above is

$$\begin{aligned} \Delta\Gamma_{\text{dir}}(25 \text{ MeV}) &= (-44.4 \pm 4.5_{f(1)} \pm 1.5_{\phi_B} \pm 0.8_{\mu_0}) \cdot 10^{-3}, \\ \Delta\Gamma_{\text{dir}}(100 \text{ MeV}) &= (-25.9 \pm 4.6_{f(1)} \pm 1.5_{\phi_B} \pm 0.9_{\mu_0}) \cdot 10^{-3}, \\ \Delta\Gamma_{\text{dir}}(200 \text{ MeV}) &= (-16.5 \pm 4.7_{f(1)} \pm 1.5_{\phi_B} \pm 1.0_{\mu_0}) \cdot 10^{-3}. \end{aligned} \quad (6.16)$$

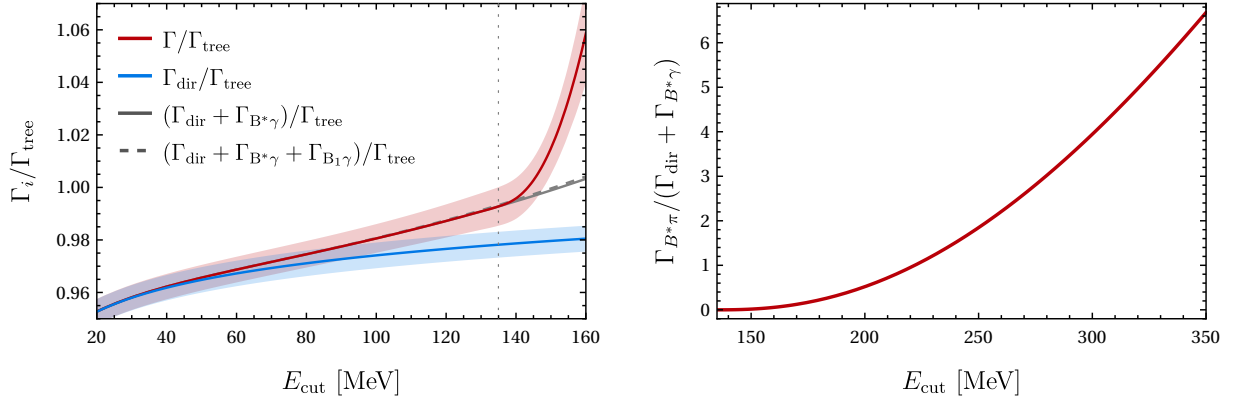


Figure 19: Left panel: The $B^- \rightarrow \mu^- \bar{\nu}_\mu$ decay rate including QED corrections and resummation effects, normalized to the leading-order rate. The red curve shows the full rate including the indirect contributions from $B \rightarrow B^*\gamma$ and $B \rightarrow B^*\pi^0$ transitions, while the blue curve shows only the direct contribution for comparison. Shaded areas indicate the combined uncertainties. The gray lines show the rate excluding the pion contribution, with the dashed line including an estimate of the next higher B resonance, the B_1 . Right panel: Size of the $BB^*\pi$ contribution relative to all other contributions as a function of E_{cut} .

The quoted uncertainties refer to the quantity $f^{(1)}$, the parameters of the LCDAs, and scale variations. In the left panel of Figure 19, the blue band shows the direct contribution to the decay rate as a function of E_{cut} .

We now turn to the indirect contributions to the decay rate, given by the difference between the red and blue bands in the figure. The contribution arising from the $BB^*\gamma$ interaction is negligible for $E_{\text{cut}} = 25$ MeV. It grows with the radiation veto and becomes sizable for $E_{\text{cut}} \gtrsim 50$ MeV. We find

$$\begin{aligned}
\Delta\Gamma_{B^*\gamma}(25 \text{ MeV}) &= (0.09 \pm 0.03_{g_{BB^*\gamma}}) \cdot 10^{-3}, \\
\Delta\Gamma_{B^*\gamma}(100 \text{ MeV}) &= (6.4 \pm 2.4_{g_{BB^*\gamma}} \pm 0.2_{f_{B^*}/f_B}) \cdot 10^{-3}, \\
\Delta\Gamma_{B^*\gamma}(200 \text{ MeV}) &= (40.2 \pm 15.0_{g_{BB^*\gamma}} \pm 1.44_{f_{B^*}/f_B}) \cdot 10^{-3}.
\end{aligned} \tag{6.17}$$

The growth continues for even larger values of the cut, but as discussed earlier the validity of our low-energy effective description requires $E_{\text{cut}} \ll \Lambda_c \approx 500$ MeV, hence we do not provide values of $\Delta\Gamma_{B^*\gamma}$ for E_{cut} larger than 200 MeV. The sum of this contribution plus the direct one is shown by the solid gray line in the left panel of Figure 19. For comparison, we also illustrate the approximate size of the contribution from the next excited B -meson state, the $B_1(5721)$. It can be obtained in a straightforward manner from (5.118) by replacing $(m_{B^*}, f_{B^*}^*, g_{BB^*\gamma}) \rightarrow (m_{B_1}, f_{B_1}, g_{BB_1\gamma})$. With $m_{B_1} = 5726$ MeV, and using $f_{B_1} = 248$ MeV and $g_{BB_1\gamma} = 0.73 \text{ GeV}^{-1}$ from [148], we obtain the dashed gray line for the sum of the direct contribution and the indirect contributions induced by the effective $BB^*\gamma$ and $BB_1\gamma$ interactions. The very small difference between the dashed and solid lines is the B_1 contribution, and it is negligible for values $E_{\text{cut}} < 160$ MeV.

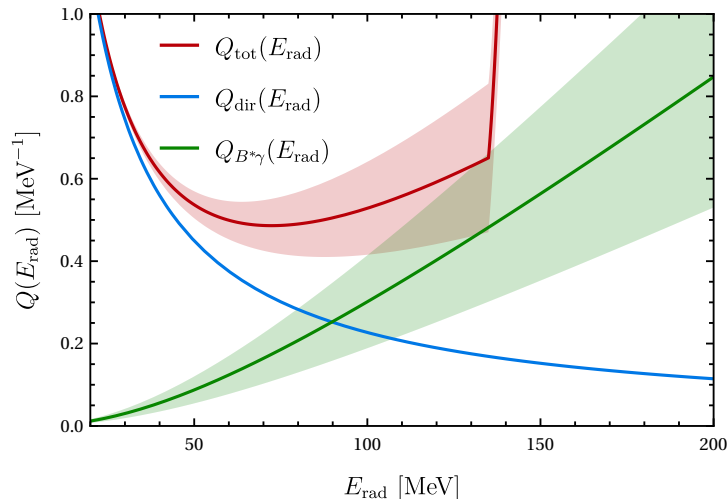


Figure 20: Different contributions to the radiation-energy spectrum $Q(E_{\text{rad}})$ as a function of the radiation energy. The three curves show the direct contribution (blue), the indirect $B^*\gamma$ contribution (green), and the full spectrum (red) including also the $B^*\pi$ contribution. Shaded areas denote the uncertainty.

The contribution from the $BB^*\pi$ interaction is absent for values of E_{cut} below the neutral pion mass, but then grows rapidly with E_{cut} above this threshold, quickly becoming the dominant contribution to the rate. For example, we find

$$\begin{aligned} \Delta\Gamma_{B^*\pi}(150 \text{ MeV}) &= (16.0 \pm 4.6 g_{BB^*\pi} \pm 0.6 f_{B^*}/f_B \pm 0.2 f_\pi) \cdot 10^{-3}, \\ \Delta\Gamma_{B^*\pi}(200 \text{ MeV}) &= 0.53 \pm 0.15 g_{BB^*\pi} \pm 0.02 f_{B^*}/f_B \pm 0.01 f_\pi. \end{aligned} \quad (6.18)$$

The sum of the direct contribution and the indirect contributions from the $BB^*\gamma$ and $BB^*\pi$ couplings is shown by the red band in the left panel of Figure 19. The pion-induced contribution is responsible for the sharp rise of the rate above $E_{\text{cut}} = 135 \text{ MeV}$. The right panel shows the size of just the pion contribution, $\Gamma_{B^*\pi} = \Gamma_{\text{tree}} \Delta\Gamma_{B^*\pi}$, without uncertainty, normalized to the other components for values of $E_{\text{cut}} > m_{\pi^0}$. We observe that the pion-induced contribution dominates all other contributions for $E_{\text{cut}} \gtrsim 220 \text{ MeV}$.

For completeness, Figure 20 displays the $B^- \rightarrow \mu^- \bar{\nu}_\mu(\gamma)$ radiation-energy spectrum, normalized as [8, 12]

$$Q(E_{\text{rad}}) \equiv \frac{4\pi}{\alpha} \frac{1}{\Gamma_{\text{tree}}} \frac{d\Gamma(E_{\text{rad}})}{dE_{\text{rad}}}. \quad (6.19)$$

The widths of the bands reflect the theoretical uncertainty in each contribution. Note that the absolute uncertainty in the direct contribution is much smaller than that of the indirect contributions, which is also true for the bands in Figure 19. The pion-induced contribution results in a cusp at $E_{\text{rad}} = m_{\pi^0}$, followed by a steep rise of the spectrum for larger values of E_{rad} (red band).

A few observations follow from Figure 19. First, QED effects induce a shift in the rate ranging from $-4.7(5)\%$ to $-0.7(7)\%$ for $E_{\text{cut}} \in [20 \text{ MeV}, m_{\pi^0}]$. The structure-dependent component of these corrections, encoded in the sum of its virtual piece, $\mathcal{R}_{\text{virt}}^2 - 1$, and its real one,

$\Delta\Gamma_{B^*\gamma}$, is always positive and varies between +0.7(5)% and +2.2(8)% in this range. While these QED effects are negligible at present, when only upper limits on the $B^- \rightarrow \mu^- \bar{\nu}_\mu$ decay rate exist, but they will become relevant by the end of the Belle II data taking (with 50 ab^{-1} of integrated luminosity), when a 5% precision on the $B^- \rightarrow \mu^- \bar{\nu}_\mu$ branching ratio is expected – and even more so at the FCC-ee, where a further four-fold improvement may be anticipated (based on statistics alone). Second, for $E_{\text{cut}} \lesssim 100 \text{ MeV}$, the uncertainty on the QED correction is entirely dominated by the one in $\mathcal{R}_{\text{virt}}^2$, which in turn is dominated by the unknown $\mathcal{O}(\alpha)$ correction $f^{(1)}$ entering F_- . For larger values of the cut it receives a comparable contribution from the uncertainty on $g_{BB^*\gamma}$. As soon as $E_{\text{cut}} \gtrsim m_\pi$, the pion channel turns on and $\Delta\Gamma_{B^*\pi}$ rapidly becomes the dominant contribution to the rate. Including radiation in this energy range, while still measuring $B^- \rightarrow \mu^- \bar{\nu}_\mu$ precisely, therefore requires a thorough understanding of the pion contribution. Its theory prediction is governed by $g_{BB^*\pi}$ or, more generally, the $B \rightarrow \pi$ form factor at small recoil, both of which are known with reasonable precision, so that this background can be quantified reliably. Indeed, the left panel of Figure 19 shows that the theory uncertainty band does not increase significantly for $E_{\text{cut}} > m_\pi$. The more critical limitation is instead the domain of validity of the HH χ PT framework, which as discussed requires $E_{\text{cut}} \ll \Lambda_c \approx 500 \text{ MeV}$. For this reason, we find it advisable to choose E_{cut} as low as possible, definitely not exceeding 200 MeV to remain on the conservative side – with the caveat that for $E_{\text{cut}} > m_\pi$ the pion contribution must be included in the signal model or subtracted as an explicit background.

When constructing the full rate from (6.15), one needs the tree-level rate Γ_{tree} , a pseudo observable defined in (5.83) as the $B^- \rightarrow \mu^- \bar{\nu}_\mu$ decay rate in a world where QED effects are absent. Note that this quantity is *not* equal to the rate in the limit $E_{\text{cut}} \rightarrow 0$. Indeed, the physical decay rate vanishes in this limit. Numerically, we find

$$\Gamma_{\text{tree}} = \left(\frac{|V_{ub}|}{3.6 \cdot 10^{-3}} \right)^2 \times (1.49 \pm 0.02_{f_B}) \cdot 10^{-19} \text{ GeV}, \quad (6.20)$$

where $|V_{ub}|$, which currently is the leading source of uncertainty, is left explicit and normalized to the central value from the latest FLAG global fit [153]. In the full rate, the QED-sourced uncertainty we have discussed above is subleading to the uncertainty in f_B for $E_{\text{cut}} \leq 150 \text{ MeV}$, and comparable between 150 and 200 MeV. It would become dominant for larger cuts because of the growing indirect contributions, however as discussed in this region our description ceases to be reliable. We therefore conclude that the QED corrections (and the dominant mixed QED–QCD corrections) to the $B^- \rightarrow \mu^- \bar{\nu}_\mu(\gamma)$ decay rate are well under theoretical control in the range of validity of our calculations.

The only result available in the literature for comparison was presented in [26], which missed the pion-induced contribution. A direct comparison of the remaining components is challenging due to the different methodology employed there. Indeed, without a strict separation of scales, the distinction between universal and structure-dependent corrections appears ambiguous. One can, however, compare the overall magnitude of the QED effects. Reading off the total QED correction $\Delta\Gamma_{\text{QED}}$ from Figure 5 of [26] (corresponding to our $\Delta\Gamma_{\text{dir}} + \Delta\Gamma_{B^*\gamma}$), we find a reasonably similar net effect at the level of central values over the range of E_{cut} considered. On the other hand, we disagree with the statement in this paper that “virtual structure-dependent” corrections amount to about a +5% relative effect. In

our framework, the virtual structure-dependent contribution is unambiguously identified with $\mathcal{R}_{\text{virt}}^2 - 1$, which we find to be much smaller, specifically $+0.7(5)\%$. This discrepancy can be traced to a different definition of “virtual structure-dependent”. Indeed, we believe that the authors’ definition of what classifies as such is misleading, since a distinction from universal contributions cannot be achieved by selecting graph topologies alone. Consequently, their “virtual structure-dependent” corrections are in large part universal, leading to a substantial overestimate of their magnitude. Furthermore, in [26] the theoretical uncertainty on the QED corrections appears to be essentially saturated by the B^* contribution. Our analysis instead shows that, for cuts $E_{\text{cut}} \leq 100$ MeV, the dominant uncertainty originates from the virtual structure-dependent term $\mathcal{R}_{\text{virt}}^2$ (through $f^{(1)}$ and the B -meson LCDAs).

Finally, an important aspect to consider is that existing measurements of the $B^- \rightarrow \mu^- \bar{\nu}_\mu(\gamma)$ process (see e.g. the measurement by the Belle collaboration in [159]) do not impose a photon-energy veto. Instead, they select events where the muon momentum in the B -meson rest frame is peaked around the two-body value, $|\mathbf{p}_\mu| = \frac{m_B^2 - m_\mu^2}{2m_B}$. This cut does not remove events with energetic photons (see e.g. the Dalitz plots in the (E_γ, E_μ) plane in [26, 27]). In order to cleanly isolate the $B^- \rightarrow \mu^- \bar{\nu}_\mu(\gamma)$ signal from the background, one should apply a cut on the photon energy as small as experimentally feasible. Relaxing the cut does not enhance the signal, but only the background. Moreover, if for experimental reasons it is not possible to lower the cut on the photon energy below 200 MeV, a meaningful comparison with theory is not possible at present. Such a comparison would require either a first-principle calculation of the $B^- \rightarrow \mu^- \bar{\nu}_\mu \gamma$ decay rate over a large range in photon energy, which could only come from the lattice.

7 Conclusions

We have derived a state-of-the-art prediction for the rate of the leptonic decay $B^- \rightarrow \mu^- \bar{\nu}_\mu(\gamma)$ at next-to-leading order in QED, including the resummation of the dominant logarithmic QED and QCD corrections. QED effects above the hadronic scale probe the internal structure of the B meson, rendering a point-like treatment of the meson insufficient to reach the percent accuracy needed to match the precision of future measurements. The central result of this work is a systematic and explicit characterization of the structure-dependent contributions in terms of perturbatively calculable functions and a well-defined set of non-perturbative input parameters. Due to the large number of scales involved, the chiral suppression of the process, and the non-perturbative dynamics involved, this has proven to be a technically challenging endeavor.

We have handled the multi-scale nature of the problem through a sequence of effective field theories, which we used to write the final rate in the form of a factorization theorem valid to all orders in QED \times QCD. Below the electroweak scale, the decay is described within the low-energy effective theory (LEFT). For scales below the B -meson mass, the relevant dynamics is captured by soft-collinear effective theory (SCET) and heavy-quark effective theory (HQET). We have constructed a complete basis of SCET operators at next-to-leading power for heavy-to-light quark currents coupled to weak leptonic currents. Corrections at the scale of the meson mass $\mu_h \sim m_B$ are encoded in hard functions, while interactions between the energetic charged lepton and the light spectator quark in the B meson introduce an intermediate hard-collinear scale $\mu_{hc}^2 \sim m_B \Lambda_{\text{QCD}}$. This is encoded in an additional matching step within SCET, giving rise to jet functions.

In this matching step, the hard and jet functions appear in convolutions that are generally endpoint divergent, as is characteristic for SCET factorization theorems at subleading power. We have treated these divergences using refactorization-based subtractions, which introduce a cutoff scale Λ . While physical predictions are independent of Λ , individual components carry logarithmic Λ dependence, and each component function has a different natural choice for which it is free of large logarithms involving this scale. For the first time, we derive the evolution equations associated with Λ and solve them to resum these large logarithms to all orders in perturbation theory. The resulting anomalous dimensions feature a non-linear dependence on $\ln(\mu^2/\Lambda^2)$, marking a qualitative departure from the more familiar single-scale Sudakov evolution problems. The final resummed prediction is obtained by solving coupled evolution equations in both the renormalization scale μ and the subtraction scale Λ . In practice, the perturbative ingredients entering the factorization formula are evaluated at the first non-trivial order in QED (and at the relevant order in QCD required for the logarithmic accuracy). After subtracting endpoint divergences, the relevant hadronic matrix elements include the known subleading-twist light-cone distribution amplitudes of the B meson, but in addition a new, genuinely non-perturbative parameter $F_-(\Lambda, \mu)$ appears, which generalizes the B -meson decay constant defined in HQET. Since a determination of this quantity from first principles is not yet available, we include it as a source of uncertainty in our error estimates.

For scales below Λ_{QCD} , we have performed a systematic, non-perturbative matching of SCET onto a low-energy description in the framework of heavy-hadron chiral perturbation theory (HH χ PT), treating the low-energy dynamics of the charged lepton in boosted heavy-

lepton effective theory (bHLET). In the hadronic sector, the relevant degrees of freedom of this low-energy theory include the (B, B^*) heavy spin doublet of meson states as well as the light pseudoscalar mesons π, K, η . In this regime, structure-dependent effects arise from two sources: the $B^- \rightarrow B^{*-}\gamma$ transition followed by the weak decay $B^{*-} \rightarrow \ell^- \bar{\nu}_\ell$ that is not chirally suppressed, and the transition $B^- \rightarrow B^{*-}\pi^0$ followed by an electromagnetic decay (almost always $\pi^0 \rightarrow \gamma\gamma$) by the on-shell pion, mediated by the chiral anomaly. This latter contribution arises as soon as $E_{\text{cut}} > m_{\pi^0}$ and becomes the dominant decay mode once the veto scale exceeds 220 MeV.

In our phenomenological analysis we have provided numerical estimates of the QED corrections to the $B^- \rightarrow \mu^- \bar{\nu}_\mu(\gamma)$ rate, showing that they amount to a relative correction of the order of a few percent (for veto energies below the pion mass), an effect that is relevant for Belle II and essential for FCC-ee. The structure-dependent component to these corrections is coincidentally modest for the process at hand, becoming relevant only at a future Tera- Z machine like FCC-ee. This conclusion however relies on numerical cancellations that are not obvious from the outset and should not be assumed to be generic for other decay channels.

The framework developed here applies straightforwardly to the electron mode as well. Because of the much stronger chiral suppression in this case, the $B^- \rightarrow e^- \bar{\nu}_e(\gamma)$ decay rate is completely dominated by the B^* contributions. The situation is qualitatively different for the tau channel: the mass of the tau lepton is not a particularly small parameter compared with m_B , and the appropriate effective field-theory setup for $B^- \rightarrow \tau^- \bar{\nu}_\tau(\gamma)$ decays is more closely related to heavy-to-heavy transitions, like $B \rightarrow D^{(*)}$ decays. A dedicated analysis is interesting in light of the projected future experimental accuracy, as the channel can serve as an exclusive extraction of $|V_{ub}|$ as well as a test of lepton flavor universality in conjunction with the muon channel. We leave this extension to future work.

Acknowledgements

We thank Florian Bernlochner, Philipp Böer, Matteo Di Carlo, Daniel Jacobi, and Enrico Lunghi for useful discussions, and Gino Isidori for encouraging us to engage in this project. This research has received funding from the Cluster of Excellence PRISMA⁺ (EXC 2118/1, Project ID 390831469) funded by the German Research Foundation (DFG) within the Germany Excellence Strategy, and from the European Research Council (ERC) under the European Union’s Horizon 2022 Research and Innovation Program (ERC Advanced Grant agreement No. 101097780, EFT4jets). Views and opinions expressed in this work are those of the authors only and do not necessarily reflect those of the European Union or the European Research Council Executive Agency. Neither the European Union nor the granting authority can be held responsible for them.

A SCET Lagrangians

Here we collect the relevant terms in the SCET Lagrangian including all necessary subleading interactions for the quark and the lepton, including the mass dependence of the latter. The leading-order Lagrangian of the hard-collinear lepton and quark fields is given by

$$\mathcal{L}_X = \sum_{f=\ell,u} \bar{\mathcal{X}}_{hc}^{(f)} \left(in \cdot \mathcal{D} + i\mathcal{D}_\perp \frac{1}{i\bar{n} \cdot \partial} i\mathcal{D}_\perp \right) \frac{\not{n}}{2} \mathcal{X}_{hc}^{(f)}, \quad (\text{A.1})$$

where we have defined

$$i\mathcal{D}^\mu \mathcal{X}_{hc}^{(f)} = (i\partial^\mu + Q_f \mathcal{A}_{hc}^\mu + \mathcal{G}_{hc}^{\mu,a} t_f^a) \mathcal{X}_{hc}^{(f)}, \quad (\text{A.2})$$

where t_f^a are the generators of the $SU(3)_c$ representation of the fermion f . For the lepton, the mass gives rise to power-suppressed interactions in SCET-1, described by the Lagrangians [160]

$$\mathcal{L}_{m_\ell}^{(1/2)} = \bar{\mathcal{X}}_{hc}^{(\ell)} \left[i\mathcal{D}_\perp, \frac{m_\ell}{i\bar{n} \cdot \partial} \right] \frac{\not{n}}{2} \mathcal{X}_{hc}^{(\ell)}, \quad \mathcal{L}_{m_\ell}^{(1)} = -m_\ell^2 \bar{\mathcal{X}}_{hc}^{(\ell)} \frac{\not{n}}{2} \frac{1}{i\bar{n} \cdot \partial} \mathcal{X}_{hc}^{(\ell)}. \quad (\text{A.3})$$

These terms generate subleading collinear interactions, responsible for introducing the lepton mass in matrix elements of SCET-1 operators of type- C , D and E that do not already contain m_ℓ .

Another class of important power-suppressed interactions for our calculations are those between soft and hard-collinear particles not contained in the covariant derivatives. They are contained in the subleading-power Lagrangians [70, 89]

$$\begin{aligned} \mathcal{L}_{\mathcal{X}q}^{(1/2)} &= \bar{q}_s \mathcal{A}_{hc}^\perp \mathcal{X}_{hc} + \text{h.c.}, \\ \mathcal{L}_{\mathcal{X}q}^{(1)} &= \bar{q}_s \left[n \cdot \mathcal{A}_{hc} + \mathcal{A}_{hc}^\perp \frac{1}{i\bar{n} \cdot \partial} (i\mathcal{D}_\perp + \mathcal{A}_{hc}^\perp) \right] \frac{\not{n}}{2} \mathcal{X}_{hc} + \bar{q}_s \overleftarrow{D}^\mu x_\mu^\perp \mathcal{A}_{hc}^\perp \mathcal{X}_{hc} + \text{h.c.}, \\ \mathcal{L}_{\mathcal{X}q}^{(3/2)} &= \bar{q}_s \overleftarrow{D}^\mu x_\mu^\perp \left[n \cdot \mathcal{A}_{hc} + \mathcal{A}_{hc}^\perp \frac{1}{i\bar{n} \cdot \partial} (i\mathcal{D}_\perp + \mathcal{A}_{hc}^\perp) \right] \frac{\not{n}}{2} \mathcal{X}_{hc} \\ &\quad + \bar{q}_s \bar{n} \cdot \overleftarrow{D} \frac{n \cdot x}{2} \mathcal{A}_{hc}^\perp \mathcal{X}_{hc} + \bar{q}_s \overleftarrow{D}^\mu \overleftarrow{D}^\nu \frac{x_\mu^\perp x_\nu^\perp}{2} \mathcal{A}_{hc}^\perp \mathcal{X}_{hc} + \text{h.c.}. \end{aligned} \quad (\text{A.4})$$

The soft field and its derivatives are evaluated at $x_-^\mu = \frac{n^\mu}{2} \bar{n} \cdot x$ in the usual way. The Feynman rules for interaction terms involving the coordinates x^μ explicitly implement the subleading terms in an expansion of the amplitude in the soft momentum, see Appendix A of [161] for a detailed discussion. For the three-particle contributions we also need the interactions between soft gluons and hard-collinear quarks to leading order. They follow from [70]

$$\mathcal{L}_x^{(1/2)} = \bar{\mathcal{X}}_{hc} x_\perp^\mu n^\nu F_{\mu\nu}^s \frac{\not{n}}{2} \mathcal{X}_{hc}, \quad (\text{A.5})$$

where the soft field-strength tensor must be evaluated at x_- .

In SCET-2, the lepton Lagrangian is structurally identical, but its power-counting changes because collinear derivatives and the lepton mass are of the same order in power counting. Then the leading-power collinear Lagrangian is of the form [160]

$$\mathcal{L}_x = \bar{\mathcal{X}}_{hc}^{(\ell)} \left[in \cdot \mathcal{D} + (i\mathcal{D}_\perp - m_\ell) \frac{1}{i\bar{n} \cdot \partial} (i\mathcal{D}_\perp + m_\ell) \right] \frac{\not{n}}{2} \mathcal{X}_{hc}^{(\ell)}. \quad (\text{A.6})$$

B Reduction of Dirac structures

Loop-level matching calculations produce Dirac structures beyond those included in our operator basis. While reducible in four spacetime dimensions, care needs to be taken when dimensional regularization is employed. Here we collect the relevant technical details and scheme choices applied to our calculations.

B.1 Scheme dependence and conversion

When extracting the Wilson coefficients of the LEFT from the literature, we need to ensure that our reduction scheme is consistent with the one used there, which amounts to applying the appropriate scheme conversion. In matching to the LEFT, the reduction identity

$$\gamma^\mu \gamma^\nu \gamma^\rho P_L \otimes \gamma_\mu \gamma_\nu \gamma_\rho P_L \rightarrow (16 + \kappa\epsilon) \gamma^\mu P_L \otimes \gamma_\mu P_L \quad (\text{B.1})$$

is used to remove redundant Dirac structures appearing beyond tree-level, where κ is a parameter representing the scheme choice. To find the scheme-conversion factor between different choices for κ , we note that this parameter cancels in the combination between matching coefficients and matrix elements of the effective theory. To obtain a scheme conversion, we thus compute the one-loop matrix elements in the LEFT and express them in terms of κ . Evaluating the $b \rightarrow u\ell^- \bar{\nu}_\ell$ amplitude at one-loop order, and keeping only terms involving the reducible structures, we find

$$i\mathcal{A}_{\text{LEFT}} = iC_L^{[\kappa]} \left[1 - Q_\ell(Q_b + Q_u) \frac{\alpha}{16\pi} \kappa \right] \gamma_\mu P_L \otimes \gamma^\mu P_L + \dots, \quad (\text{B.2})$$

where $C_L^{[\kappa]}$ is the LEFT matching coefficient with a specific choice of κ , and the dots refer to terms independent of it. Since the product of $C_L^{[\kappa]}$ with the factor multiplying it must be independent of κ , we find that the scheme-conversion factor at one-loop order is given by

$$C_L^{[\kappa']} = C_L^{[\kappa]} \left[1 - Q_\ell(Q_b + Q_u) \frac{\alpha}{16\pi} (\kappa - \kappa') \right]. \quad (\text{B.3})$$

As discussed in the main text, our reduction identities in SCET imply the choice $\kappa' = 0$. Moreover, our scheme parameter κ relates to the one used in [78] via $\kappa = -4b_{\text{ev}}$.

B.2 Reduction identities in light-cone components

We now list all the structures appearing in the matching to SCET from amplitudes involving two quarks and two leptons within our reduction scheme. They are

$$\begin{aligned}
& \frac{\not{n}\not{\bar{n}}}{4}\gamma_{\perp}^{\mu}P_L \otimes \frac{\not{\bar{n}}\not{n}}{4}\gamma_{\perp}^{\mu}P_L = \gamma_{\perp}^{\mu}P_L \otimes \frac{\not{n}\not{\bar{n}}}{4}\gamma_{\perp}^{\mu}P_L, \\
& \gamma_{\perp\mu}\gamma_{\perp\nu}\gamma_{\perp\rho}P_L \otimes \frac{\not{\bar{n}}\not{n}}{4}\gamma_{\perp}^{\mu}\gamma_{\perp}^{\nu}\gamma_{\perp}^{\rho}P_L = 4\gamma_{\perp}^{\mu}P_L \otimes \frac{\not{\bar{n}}\not{n}}{4}\gamma_{\perp}^{\mu}P_L \\
& \frac{\not{n}}{2}\gamma_{\perp}^{\mu}\gamma_{\perp}^{\nu}P_L \otimes \frac{\not{\bar{n}}\not{n}}{4}\gamma_{\perp}^{\mu}\gamma_{\perp}^{\nu}P_L = 4\frac{\not{n}}{2}P_L \otimes \frac{\not{\bar{n}}\not{n}}{4}P_L, \\
& \gamma_{\perp}^{\mu}P_L \otimes \frac{\not{\bar{n}}\not{n}}{4}k_{\perp}\gamma_{\perp}^{\mu}P_L = 2\frac{\not{n}\not{\bar{n}}}{4}k_{\perp}P_L \otimes \frac{\not{\bar{n}}\not{n}}{4}P_L, \\
& \frac{\not{n}\not{\bar{n}}}{4}\gamma_{\perp}^{\mu}P_L \otimes \frac{\not{\bar{n}}\not{n}}{4}k_{\perp}\gamma_{\perp}^{\mu}P_L = 2\frac{\not{n}\not{\bar{n}}}{4}k_{\perp}P_L \otimes \frac{\not{\bar{n}}\not{n}}{4}P_L, \\
& \frac{\not{n}}{2}\gamma_{\perp}^{\mu}\gamma_{\perp}^{\nu}P_L \otimes \frac{\not{\bar{n}}\not{n}}{4}k_{\perp}\gamma_{\perp}^{\mu}\gamma_{\perp}^{\nu}P_L = 4\frac{\not{n}}{2}P_L \otimes \frac{\not{\bar{n}}\not{n}}{4}k_{\perp}P_L, \\
& \frac{\not{n}}{2}\gamma_{\perp}^{\mu}\gamma_{\perp}^{\nu}P_L \otimes \frac{\not{\bar{n}}\not{n}}{4}k_{\perp}\gamma_{\perp}^{\mu}\gamma_{\perp}^{\nu}P_L = 0, \\
& \frac{\not{n}}{2}\gamma_{\perp}^{\mu}\gamma_{\perp}^{\nu}P_L \otimes \frac{\not{\bar{n}}\not{n}}{4}\gamma_{\perp}^{\mu}\gamma_{\perp}^{\nu}P_L = 0,
\end{aligned} \tag{B.4}$$

where k denotes the incoming momentum of the soft spectator quark. For amplitudes with an additional soft gluon in the initial state, we also need the following reductions

$$\begin{aligned}
& \gamma_{\perp}^{\mu}P_L \otimes \frac{\not{n}\not{\bar{n}}}{4}\not{\epsilon}_{\perp}^g\gamma_{\perp}^{\mu}P_L = 2\frac{\not{n}\not{\bar{n}}}{4}\not{\epsilon}_{\perp}^gP_L \otimes \frac{\not{\bar{n}}\not{n}}{4}P_L, \\
& \frac{\not{n}\not{\bar{n}}}{4}\gamma_{\perp}^{\mu}P_L \otimes \frac{\not{\bar{n}}\not{n}}{4}\not{\epsilon}_{\perp}^g\gamma_{\perp}^{\mu}P_L = 2\frac{\not{n}\not{\bar{n}}}{4}\not{\epsilon}_{\perp}^gP_L \otimes \frac{\not{\bar{n}}\not{n}}{4}P_L, \\
& \not{\epsilon}_{\perp}^g\gamma_{\perp}^{\mu}\gamma_{\perp}^{\nu}P_L \otimes \frac{\not{\bar{n}}\not{n}}{4}\gamma_{\perp}^{\mu}\gamma_{\perp}^{\nu}P_L = 4\frac{\not{n}\not{\bar{n}}}{4}\not{\epsilon}_{\perp}^gP_L \otimes \frac{\not{\bar{n}}\not{n}}{4}P_L, \\
& \frac{\not{n}\not{\bar{n}}}{4}\not{\epsilon}_{\perp}^g\gamma_{\perp}^{\mu}\gamma_{\perp}^{\nu}P_L \otimes \frac{\not{\bar{n}}\not{n}}{4}\gamma_{\perp}^{\mu}\gamma_{\perp}^{\nu}P_L = 4\frac{\not{n}\not{\bar{n}}}{4}\not{\epsilon}_{\perp}^gP_L \otimes \frac{\not{\bar{n}}\not{n}}{4}P_L, \\
& \frac{\not{n}}{2}k_{\perp}^g\not{\epsilon}_{\perp}^g\gamma_{\perp}^{\mu}\gamma_{\perp}^{\nu}P_L \otimes \frac{\not{\bar{n}}\not{n}}{4}\gamma_{\perp}^{\mu}\gamma_{\perp}^{\nu}P_L = 0, \\
& \frac{\not{n}}{2}k_{\perp}^g\gamma_{\perp}^{\mu}P_L \otimes \frac{\not{\bar{n}}\not{n}}{4}\not{\epsilon}_{\perp}^g\gamma_{\perp}^{\mu}P_L = 0, \\
& \frac{\not{n}}{2}\not{\epsilon}_{\perp}^g\gamma_{\perp}^{\mu}P_L \otimes \frac{\not{\bar{n}}\not{n}}{4}k_{\perp}^g\gamma_{\perp}^{\mu}P_L = 0,
\end{aligned} \tag{B.5}$$

where k^g and ϵ^g denote the incoming momentum and polarization vector of the additional soft gluon, respectively.

B.3 Cancellation of power-enhanced contributions

As explained in the main text, power-enhanced contributions to the amplitude, as they appear in the $B_s \rightarrow \mu^+ \mu^-$ decay, are absent in the charged-current decay [22]. In our calculation, they would however appear in intermediate steps if a different reduction scheme was chosen for the Dirac structures of SCET. To see the explicit cancellation, it is instructive to investigate the one-loop QED correction to the $b \rightarrow u \ell^- \bar{\nu}_\ell$ matrix element of the operator $\mathcal{O}_\ell^{V,LL}$ in (3.1), arising from photon exchange between the up quark and the lepton, and study its hard-collinear and collinear regions. In the hard-collinear region described in SCET-1, a subset of the terms one finds is

$$\mathcal{A}_{\ell u}^{\text{[hc]}} \supset -m_\ell \frac{Q_\ell Q_u \alpha}{8\pi\epsilon} \left(\frac{1}{n \cdot k} + \frac{2n \cdot p_\ell}{(n \cdot k)^2} - \frac{k_\perp^2}{4(n \cdot k)(\bar{n} \cdot p_\ell)} \right) \frac{\not{n}}{2} \gamma_\perp^\mu \gamma_\perp^\nu P_L \otimes \gamma_{\mu\perp} \gamma_{\nu\perp} P_L, \quad (\text{B.6})$$

where k and p_ℓ are the momenta of the spectator and the lepton, respectively. The first term in the brackets is power-enhanced by $\mathcal{O}(m_b/\Lambda_{\text{QCD}})$ with respect to the tree-level amplitude. In our reduction scheme, the Dirac structure in this expression reduces to zero directly, but in a more general scheme, where one would write

$$\frac{\not{n}}{2} \gamma_\perp^\mu \gamma_\perp^\nu P_L \otimes \gamma_{\mu\perp} \gamma_{\nu\perp} P_L \rightarrow \tilde{\kappa} \epsilon \frac{\not{n}}{2} P_L \otimes P_L, \quad (\text{B.7})$$

this contribution would appear in the hard-collinear jet functions as a finite term proportional to $\tilde{\kappa}$. It would cancel, however, against the collinear matrix element in SCET-2, which is found to be given by exactly the same expression, but with the opposite sign, i.e. $\mathcal{A}_{\ell u}^{[\text{c}]} = -\mathcal{A}_{\ell u}^{\text{[hc]}}$. In the region sum, the cancellation is apparent before any reductions, whereas in the EFT calculation the cancellation occurs once the jet functions and collinear matrix elements are combined, in an analogous fashion to the cancellation of κ in the LEFT, discussed in the previous section. Our scheme choice avoids the appearance of spurious super-leading terms with inverse powers of the spectator momentum from the start.

C Soft anomalous dimension of $F_\mp(\Lambda, \mu)$

Here we outline the calculation of the anomalous dimensions for the hadronic parameters $F_\mp(\Lambda, \mu)$ in (4.87). To derive them, one needs to compute the UV divergences of the soft matrix elements $S_{1,2}$ defined in (4.82). To this end, it is convenient to rewrite the θ_T functions entering these definitions in terms of a partial derivative, as shown in (4.39). Next, we express the soft matrix elements in the form

$$S_{1,2} = \frac{\mathcal{A}_1 + \mathcal{A}_2(\Lambda)}{\mathcal{A}_3}, \quad (\text{C.1})$$

where $\mathcal{A}_{1,2,3}$ denote the matrix elements

$$\begin{aligned} \mathcal{A}_1 &= \langle 0 | \bar{u}_s \Gamma b_v Y_n^{(\ell)\dagger} | B^- \rangle, \\ \mathcal{A}_2(\Lambda) &= -\langle 0 | (\bar{u}_s \bar{Y}_{\bar{n}}^{(u)}) \theta_T \left(\frac{-i\bar{n} \cdot \overleftarrow{\partial}_s}{\bar{n} \cdot v} - \Lambda \right) \Gamma (Y_n^{(\ell)\dagger} \bar{Y}_{\bar{n}}^{(u)\dagger} b_v) | B^- \rangle, \\ \mathcal{A}_3 &= \langle 0 | Y_n^{(\ell)\dagger} \bar{Y}_v^{(B)} | 0 \rangle, \end{aligned} \quad (\text{C.2})$$

with $\Gamma = (\not{n}/\bar{n} \cdot v) P_L$ for S_1 and $\Gamma = (\not{n}/n \cdot v) P_L$ for S_2 . It is convenient to present the results in terms of relative corrections to the tree-level matrix elements, i.e.

$$\mathcal{A}_i = \mathcal{A}_i^{\text{LO}} (1 + a_i). \quad (\text{C.3})$$

For this calculation, it is crucial to respect the appropriate $i0$ prescriptions for the Wilson lines in the n and v directions, as explained around (4.4). For photons with outgoing momentum k , the single-emission matrix elements of the Wilson lines read

$$\begin{aligned} \langle \gamma(k) | Y_n^{(\ell)\dagger} | 0 \rangle &= -Q_\ell e \frac{n \cdot \epsilon^*}{n \cdot k + v \cdot n \delta + i0}, \\ \langle \gamma(k) | \bar{Y}_v^{(B)} | 0 \rangle &= Q_B e \frac{v \cdot \epsilon^*}{v \cdot k + \frac{\delta}{2} - i0}, \end{aligned} \quad (\text{C.4})$$

where $\delta > 0$ regulates IR divergences [162]. With this prescription, we obtain

$$\begin{aligned} a_1 &= \frac{\alpha}{4\pi} \left[\frac{Q_b^2}{\epsilon} + \frac{Q_b Q_u}{\epsilon} - \frac{Q_u^2}{2\epsilon} - Q_\ell Q_b \left(\frac{1}{\epsilon^2} + \frac{1}{\epsilon} \ln \frac{\mu^2}{\delta^2} \right) \right. \\ &\quad \left. + \frac{Q_\ell Q_u}{\epsilon} \left(\int_0^\infty d\omega \phi_-(\omega, \mu) \ln \frac{\omega^2}{\delta^2} - 2 \right) \right] + \frac{3C_F \alpha_s}{8\pi\epsilon}, \\ a_2 &= \begin{cases} Q_\ell Q_u \frac{\alpha}{2\pi} \left[\frac{1}{\epsilon^2} + \frac{1}{\epsilon} \int_0^\infty d\omega \phi_-(\omega, \mu) \ln \frac{\mu^2}{\omega\Lambda} + \frac{1}{\epsilon} \right]; & \text{for } \Gamma = \frac{\not{n}}{\bar{n} \cdot v} P_L, \\ Q_\ell Q_u \frac{\alpha}{2\pi} \left[\frac{1}{\epsilon^2} + \frac{1}{\epsilon} \int_0^\infty d\omega \phi_-(\omega, \mu) \ln \frac{\mu^2}{\omega\Lambda} \right]; & \text{for } \Gamma = \frac{\not{n}}{n \cdot v} P_L, \end{cases} \quad (\text{C.5}) \\ a_3 &= -\frac{Q_B^2 \alpha}{4\pi} \left(\frac{1}{\epsilon^2} + \frac{1}{\epsilon} \ln \frac{\mu^2}{\delta^2} \right), \end{aligned}$$

where only a_2 differs for the two Dirac structures. Using these expressions, and introducing renormalization factors $Z_{F_\mp}(\Lambda, \mu)$ such that the renormalized matrix elements $S_1(\Lambda, \mu) = Z_{F_-}(\Lambda, \mu) S_1(\Lambda)$ and $S_2(\Lambda, \mu) = Z_{F_+}(\Lambda, \mu) S_2(\Lambda)$ are free of $1/\epsilon$ poles, we find

$$Z_{F_\mp}(\Lambda) = 1 + 3C_F \frac{\alpha_s}{8\pi\epsilon} + \frac{\alpha}{4\pi} \left\{ \frac{3Q_u^2}{2\epsilon} + Q_\ell Q_u \left[\frac{1}{\epsilon^2} + \frac{1}{\epsilon} \left((2 \pm 1) + \ln \frac{\mu^2}{\Lambda^2} \right) \right] \right\}, \quad (\text{C.6})$$

which leads directly to the expression (4.87) for the anomalous dimensions of $F_\mp(\Lambda, \mu)$. Finally, the anomalous dimensions of the "unsubtracted" parameters $F_\mp(\mu)$ are obtained by setting $a_2 = 0$. This yields the results quoted in (4.89).

D RG resummation with a running QED coupling

The derivation of the result (5.111) relied on the fact that the running of the coupling is neglected, as we have always done in this work. The formalism developed in [143] allows one to include the effects of the running of α in a systematic way. The main difference is that in this case one cannot choose s -dependent matching scales, because the matching conditions $\widetilde{W}_{us}(0) = \widetilde{W}_{us}(s, 2e^{-\gamma_E} s^{-1})$ and $\widetilde{W}_{usc}(0) = \widetilde{W}_{us}(s, 2e^{-\gamma_E} s^{-1} \frac{m_\ell}{m_B})$ then involve the QED coupling evaluated at s -dependent values $\alpha(2e^{-\gamma_E} s^{-1})$ and $\alpha(2e^{-\gamma_E} s^{-1} \frac{m_\ell}{m_B})$, respectively. This obviously complicates the inversion of the Laplace transformation.

The way out is to use matching scales that are independent of s , but still eliminate large logarithms in the matching conditions for typical values $s \sim 1/(2E_{\text{cut}})$. To begin, we recast the anomalous dimensions (5.106) in the form

$$\begin{aligned}\gamma_{us}(s, \mu) &= \gamma_{\text{cusp}}(\alpha) L_{us} + \gamma_{W_{us}}(\alpha), \\ \gamma_{usc}(s, \mu) &= -\gamma_{\text{cusp}}(\alpha) L_{usc} + \gamma_{W_{usc}}(\alpha),\end{aligned}\tag{D.1}$$

where $\gamma_{\text{cusp}}(\alpha)$ is the light-like cusp anomalous dimension of QED, whose explicit form can be derived from the corresponding quantity in QCD [102, 103] making the replacements $C_F \rightarrow Q_\ell^2$, $C_A \rightarrow 0$ and $T_F \rightarrow 1$. At one-loop order, we have

$$\gamma_{\text{cusp}}(\alpha) = \gamma_{W_{us}}(\alpha) = \gamma_{W_{usc}}(\alpha) = \frac{Q_\ell^2 \alpha}{\pi},\tag{D.2}$$

but in higher orders the three quantities can be different. Next, we introduce the QED β -function $\beta(\alpha) = d\alpha(\mu)/d \ln \mu$. The perturbative expansion coefficients of the anomalous dimensions and the β -function are defined as in (2.9). The one-loop coefficients are

$$\gamma_{\text{cusp},0} = \gamma_{W_{us},0} = \gamma_{W_{usc},0} = 4Q_\ell^2, \quad \beta_0 = -\frac{4}{3} \sum_f N_c^f Q_f^2,\tag{D.3}$$

where the sum extends over all fermion species with mass below the scale μ at which the coupling is evaluated. Next, we introduce RG functions via the integrals

$$\begin{aligned}S(\nu, \mu) &= -\int_\nu^\mu \frac{d\mu'}{\mu'} \gamma_{\text{cusp}}(\alpha(\mu')) \ln \frac{\mu'}{\nu} = -\int_{\alpha(\nu)}^{\alpha(\mu)} d\alpha \frac{\gamma_{\text{cusp}}(\alpha)}{\beta(\alpha)} \int_{\alpha(\nu)}^\alpha \frac{d\alpha'}{\beta(\alpha')}, \\ &= \frac{\gamma_{\text{cusp},0}}{2\beta_0^2} \left[\frac{4\pi}{\alpha(\nu)} \left(1 - \frac{1}{r} - \ln r \right) + \left(\frac{\gamma_{\text{cusp},1}}{\gamma_{\text{cusp},0}} - \frac{\beta_1}{\beta_0} \right) (1 - r + \ln r) + \dots \right], \\ a_{\text{cusp}}(\nu, \mu) &= -\int_\nu^\mu \frac{d\mu'}{\mu'} \gamma_{\text{cusp}}(\alpha(\mu')) = -\int_{\alpha(\nu)}^{\alpha(\mu)} d\alpha \frac{\gamma_{\text{cusp}}(\alpha)}{\beta(\alpha)} = \frac{\gamma_{\text{cusp},0}}{2\beta_0} \ln r + \dots,\end{aligned}\tag{D.4}$$

where $r = \alpha(\mu)/\alpha(\nu)$, and we have given the leading terms in the perturbative evaluation of the two quantities (see the Appendix of [163]). We also define analogous functions $a_{W_{us}}(\nu, \mu)$ and $a_{W_{usc}}(\nu, \mu)$.

The general solutions to the RG equations (5.105) can now be written in the form [143]

$$\begin{aligned}\widetilde{W}_{us}(s, \mu) &= \exp \left[-2S(\mu_0, \mu) - a_{\gamma_{us}}(\mu_0, \mu) \right] \left(\frac{\mu_0^2 s^2 e^{2\gamma_E}}{4} \right)^{-a_{\text{cusp}}(\mu_0, \mu)} \widetilde{W}_{us}(s, \mu_0), \\ \widetilde{W}_{usc}(s, \mu) &= \exp \left[2S(\mu'_0, \mu) - a_{\gamma_{usc}}(\mu'_0, \mu) \right] \left(\frac{\mu'^2_0 s^2 e^{2\gamma_E} m_B^2}{4m_\ell^2} \right)^{a_{\text{cusp}}(\mu'_0, \mu)} \widetilde{W}_{usc}(s, \mu'_0).\end{aligned}\tag{D.5}$$

The fact that s and E_{cut} are Laplace-conjugate variables suggests the choices $\mu_0 = 2E_{\text{cut}}$ and $\mu'_0 = 2E_{\text{cut}} \frac{m_\ell}{m_B}$ for the two matching scales, such that the initial conditions are free of large logarithms. The functions $\widetilde{W}_{us}(s, \mu_0)$ and $\widetilde{W}_{usc}(s, \mu'_0)$ depend on the various scales via the logarithms

$$L_{us}(\mu_0) = \ln \frac{\mu_0^2 s^2 e^{2\gamma_E}}{4}, \quad L_{usc}(\mu'_0) = \ln \frac{\mu'^2_0 s^2 e^{2\gamma_E} m_B^2}{4m_\ell^2}\tag{D.6}$$

and the running couplings $\alpha(\mu_0)$ and $\alpha(\mu'_0)$. In generalization of (5.108) we redefine

$$\widetilde{W}_{us}(s, \mu) \equiv \widetilde{W}_{us}(L_{us}(\mu_0), \mu_0), \quad \widetilde{W}_{usc}(s, \mu) \equiv \widetilde{W}_{usc}(L_{usc}(\mu'_0), \mu'_0).\tag{D.7}$$

We can then recast the general solutions in the form

$$\begin{aligned}\widetilde{W}_{us}(s, \mu) &= \exp \left[-2S(\mu_0, \mu) - a_{\gamma_{us}}(\mu_0, \mu) \right] \widetilde{W}_{us}(\partial_\eta, \mu_0) \left(\frac{\mu_0^2 s^2 e^{2\gamma_E}}{4} \right)^{\eta - a_{\text{cusp}}(\mu_0, \mu)} \Big|_{\eta=0}, \\ \widetilde{W}_{usc}(s, \mu) &= \exp \left[2S(\mu'_0, \mu) - a_{\gamma_{usc}}(\mu'_0, \mu) \right] \widetilde{W}_{usc}(\partial_\sigma, \mu'_0) \left(\frac{\mu'^2_0 s^2 e^{2\gamma_E} m_B^2}{4m_\ell^2} \right)^{\sigma + a_{\text{cusp}}(\mu'_0, \mu)} \Big|_{\sigma=0},\end{aligned}\tag{D.8}$$

which offers the advantage that the dependence on the Laplace variable s now takes a simple power-law form. It is thus a simple matter to invert the Laplace transform using (5.101). For the scale choices $\mu = 2E_{\text{cut}}$ and $\mu'_0 = 2E_{\text{cut}} \frac{m_\ell}{m_B}$, this leads to the final expression

$$\begin{aligned}R(E_{\text{cut}}, \mu) &= \exp \left[-2S(\mu_0, \mu) + 2S(\mu'_0, \mu) - a_{\gamma_{us}}(\mu_0, \mu) - a_{\gamma_{usc}}(\mu'_0, \mu) \right] \\ &\times \widetilde{W}_{us}(\partial_\eta, \mu_0) \widetilde{W}_{usc}(\partial_\sigma, \mu'_0) \frac{e^{-2\gamma_E (a_{\text{cusp}}(\mu_0, \mu'_0) - \eta - \sigma)}}{\Gamma[1 + 2(a_{\text{cusp}}(\mu_0, \mu'_0) - \eta - \sigma)]} \Big|_{\eta=\sigma=0},\end{aligned}\tag{D.9}$$

where we have used the relation

$$a_{\text{cusp}}(\mu_0, \mu) - a_{\text{cusp}}(\mu'_0, \mu) = a_{\text{cusp}}(\mu_0, \mu'_0).\tag{D.10}$$

To make contact with our result (5.111), we neglect the scale dependence of α and evaluate the integrals in (D.4) to obtain

$$S(\nu, \mu) = -\frac{Q_\ell^2 \alpha}{8\pi} \ln^2 \frac{\mu^2}{\nu^2}, \quad a_{\text{cusp}}(\nu, \mu) = -\frac{Q_\ell^2 \alpha}{2\pi} \ln \frac{\mu^2}{\nu^2},\tag{D.11}$$

where $a_{W_{us}}(\nu, \mu)$ and $a_{W_{usc}}(\nu, \mu)$ are equal to $a_{\text{cusp}}(\nu, \mu)$ at one-loop order. Inserting the explicit values of the scales μ_0 and μ'_0 , we then obtain

$$R(E_{\text{cut}}, \mu) = \left(\frac{\mu^2 m_B}{(2E_{\text{cut}})^2 m_\ell} \right)^{-\gamma_{\text{soft}}} \widetilde{W}_{us}(\partial_\eta) \widetilde{W}_{usc}(\partial_\sigma) \frac{e^{-2\gamma_E \left(\frac{Q_\ell^2 \alpha}{2\pi} \ln \frac{m_B^2}{m_\ell^2} - \eta - \sigma \right)}}{\Gamma \left[1 + 2 \left(\frac{Q_\ell^2 \alpha}{2\pi} \ln \frac{m_B^2}{m_\ell^2} - \eta - \sigma \right) \right]} \Big|_{\eta=\sigma=0}, \quad (\text{D.12})$$

where the matching conditions no longer depend on the scales. At one-loop order, we have

$$\widetilde{W}_{us}(\partial_\eta) \widetilde{W}_{usc}(\partial_\sigma) = 1 + \frac{Q_\ell^2 \alpha}{2\pi} \left[\frac{\partial_\eta^2 - \partial_\sigma^2}{2} + \partial_\eta + \partial_\sigma + 2 - \frac{\pi^2}{3} \right] + \mathcal{O}(\alpha^2). \quad (\text{D.13})$$

But we can actually do better. Integrating the RG equations for fixed coupling yields the solutions

$$\widetilde{W}_{us}(L_{us}) = \exp \left[\frac{Q_\ell^2 \alpha}{2\pi} \left(\frac{L_{us}^2}{2} + L_{us} \right) \right] \exp \left[-\frac{Q_\ell^2 \alpha}{2\pi} \left(\frac{L_{us}^2(\mu_0)}{2} + L_{us}(\mu_0) \right) \right] \widetilde{W}_{us}(L_{us}(\mu_0)), \quad (\text{D.14})$$

and similarly for $\widetilde{W}_{usc}(L_{usc})$. The fact that these expressions must be independent of the matching scales μ_0 and μ'_0 implies that the logarithms in the matching conditions must cancel those in the second exponential. We can thus upgrade relation (D.13) to

$$\widetilde{W}_{us}(\partial_\eta) \widetilde{W}_{usc}(\partial_\sigma) = \exp \left[\frac{Q_\ell^2 \alpha}{2\pi} \left(\frac{\partial_\eta^2 - \partial_\sigma^2}{2} + \partial_\eta + \partial_\sigma \right) \right] \left[1 + \frac{Q_\ell^2 \alpha}{2\pi} \left(2 - \frac{\pi^2}{3} \right) + \mathcal{O}(\alpha^2) \right]. \quad (\text{D.15})$$

We now define new variables $\eta_\pm = \eta \pm \sigma$ and derivatives $\partial_\pm = \partial/\partial\eta_\pm$, in which case the derivative operator in round parenthesis takes the form $(2\partial_+ \partial_- + 2\partial_+)$. Using the fact that the expression on which the differential operators act only involves η_+ , we can set $\partial_- \rightarrow 0$ and obtain

$$R(E_{\text{cut}}, \mu) = \left(\frac{\mu^2 m_B}{(2E_{\text{cut}})^2 m_\ell} \right)^{-\gamma_{\text{soft}}} \left[1 + \frac{Q_\ell^2 \alpha}{2\pi} \left(2 - \frac{\pi^2}{3} \right) + \mathcal{O}(\alpha^2) \right] \times \exp \left(\frac{Q_\ell^2 \alpha}{\pi} \partial_+ \right) \frac{e^{-2\gamma_E \left(\frac{Q_\ell^2 \alpha}{2\pi} \ln \frac{m_B^2}{m_\ell^2} - \eta_+ \right)}}{\Gamma \left[1 + 2 \left(\frac{Q_\ell^2 \alpha}{2\pi} \ln \frac{m_B^2}{m_\ell^2} - \eta_+ \right) \right]} \Big|_{\eta_+=0}. \quad (\text{D.16})$$

The remaining exponential derivative operator has the effect of shifting the value of η_+ away from zero by an amount $\frac{Q_\ell^2 \alpha}{\pi}$, so that one exactly recovers the relation (5.111).

References

- [1] N. Davidson, T. Przedzinski and Z. Was, *PHOTOS interface in C++: Technical and Physics Documentation*, *Comput. Phys. Commun.* **199** (2016) 86–101, [1011.0937].
- [2] L. Dai, C. Kim and A. K. Leibovich, *Universal lepton universality violation in exclusive processes*, *Phys. Rev. D* **105** (2022) L031301, [2103.03963].
- [3] M. Bordone, G. Isidori and A. Pattori, *On the Standard Model predictions for R_K and R_{K^*}* , *Eur. Phys. J. C* **76** (2016) 440, [1605.07633].
- [4] G. Isidori, S. Nabeebaccus and R. Zwicky, *QED corrections in $\bar{B} \rightarrow \bar{K} \ell^+ \ell^-$ at the double-differential level*, *JHEP* **12** (2020) 104, [2009.00929].
- [5] G. Isidori, D. Lancierini, S. Nabeebaccus and R. Zwicky, *QED in $\bar{B} \rightarrow \bar{K} \ell^+ \ell^-$ LFU ratios: theory versus experiment, a Monte Carlo study*, *JHEP* **10** (2022) 146, [2205.08635].
- [6] E. Baracchini and G. Isidori, *Electromagnetic corrections to non-leptonic two-body B and D decays*, *Phys. Lett. B* **633** (2006) 309–313, [hep-ph/0508071].
- [7] D. Bigi, M. Bordone, P. Gambino, U. Haisch and A. Piccione, *QED effects in inclusive semi-leptonic B decays*, *JHEP* **11** (2023) 163, [2309.02849].
- [8] N. Carrasco, V. Lubicz, G. Martinelli, C. T. Sachrajda, N. Tantalo, C. Tarantino et al., *QED Corrections to Hadronic Processes in Lattice QCD*, *Phys. Rev. D* **91** (2015) 074506, [1502.00257].
- [9] D. Giusti, V. Lubicz, G. Martinelli, C. T. Sachrajda, F. Sanfilippo, S. Simula et al., *First lattice calculation of the QED corrections to leptonic decay rates*, *Phys. Rev. Lett.* **120** (2018) 072001, [1711.06537].
- [10] C. T. Sachrajda, M. Di Carlo, G. Martinelli, D. Giusti, V. Lubicz, F. Sanfilippo et al., *Radiative corrections to semileptonic decay rates*, *PoS LATTICE2019* (2019) 162, [1910.07342].
- [11] A. Desiderio et al., *First lattice calculation of radiative leptonic decay rates of pseudoscalar mesons*, *Phys. Rev. D* **103** (2021) 014502, [2006.05358].
- [12] R. Frezzotti, M. Garofalo, V. Lubicz, G. Martinelli, C. T. Sachrajda, F. Sanfilippo et al., *Comparison of lattice QCD+QED predictions for radiative leptonic decays of light mesons with experimental data*, *Phys. Rev. D* **103** (2021) 053005, [2012.02120].
- [13] M. Di Carlo, M. T. Hansen, A. Portelli and N. Hermansson-Truedsson, *Relativistic, model-independent determination of electromagnetic finite-size effects beyond the pointlike approximation*, *Phys. Rev. D* **105** (2022) 074509, [2109.05002].
- [14] P. Boyle et al., *Isospin-breaking corrections to light-meson leptonic decays from lattice simulations at physical quark masses*, *JHEP* **02** (2023) 242, [2211.12865].

- [15] G. Gagliardi, F. Sanfilippo, S. Simula, V. Lubicz, F. Mazzetti, G. Martinelli et al., *Virtual photon emission in leptonic decays of charged pseudoscalar mesons*, *Phys. Rev. D* **105** (2022) 114507, [2202.03833].
- [16] R. Frezzotti, N. Tantalo, G. Gagliardi, F. Sanfilippo, S. Simula, V. Lubicz et al., *Lattice calculation of the D_s meson radiative form factors over the full kinematical range*, *Phys. Rev. D* **108** (2023) 074505, [2306.05904].
- [17] R. Di Palma, R. Frezzotti, G. Gagliardi, V. Lubicz, G. Martinelli, C. T. Sachrajda et al., *Kaon radiative leptonic decay rates from lattice QCD simulations at the physical point*, *Phys. Rev. D* **111** (2025) 114523, [2504.08680].
- [18] M. Beneke, P. Böer, J.-N. Toelstede and K. K. Vos, *QED factorization of non-leptonic B decays*, *JHEP* **11** (2020) 081, [2008.10615].
- [19] M. Beneke, P. Böer, G. Finauri and K. K. Vos, *QED factorization of two-body non-leptonic and semi-leptonic B to charm decays*, *JHEP* **10** (2021) 223, [2107.03819].
- [20] M. Beneke, P. Böer, J.-N. Toelstede and K. K. Vos, *Light-cone distribution amplitudes of light mesons with QED effects*, *JHEP* **11** (2021) 059, [2108.05589].
- [21] M. Beneke, P. Böer, J.-N. Toelstede and K. K. Vos, *Light-cone distribution amplitudes of heavy mesons with QED effects*, *JHEP* **08** (2022) 020, [2204.09091].
- [22] M. Beneke, C. Bobeth and R. Szafron, *Enhanced electromagnetic correction to the rare B -meson decay $B_{s,d} \rightarrow \mu^+ \mu^-$* , *Phys. Rev. Lett.* **120** (2018) 011801, [1708.09152].
- [23] M. Beneke, C. Bobeth and R. Szafron, *Power-enhanced leading-logarithmic QED corrections to $B_q \rightarrow \mu^+ \mu^-$* , *JHEP* **10** (2019) 232, [1908.07011].
- [24] C. Cornella, M. König and M. Neubert, *Structure-dependent QED effects in exclusive B decays at subleading power*, *Phys. Rev. D* **108** (2023) L031502, [2212.14430].
- [25] S. Nabeebaccus and R. Zwicky, *Resolving charged hadrons in QED – gauge invariant interpolating operators*, *JHEP* **11** (2022) 101, [2209.06925].
- [26] M. Rowe and R. Zwicky, *Structure-dependent QED in $B^- \rightarrow \ell^- \bar{\nu}(\gamma)$* , *JHEP* **07** (2024) 249, [2404.07648].
- [27] D. Becirevic, B. Haas and E. Kou, *Soft Photon Problem in Leptonic B -decays*, *Phys. Lett. B* **681** (2009) 257–263, [0907.1845].
- [28] Y. G. Aditya, K. J. Healey and A. A. Petrov, *Faking $B_s \rightarrow \mu^+ \mu^-$* , *Phys. Rev. D* **87** (2013) 074028, [1212.4166].
- [29] BABAR collaboration, B. Aubert et al., *A search for $B^+ \rightarrow \ell^+ \nu_\ell$ Recoiling Against $B^- \rightarrow D^0 \ell^- \bar{\nu} X$* , *Phys. Rev. D* **81** (2010) 051101, [0912.2453].

- [30] BABAR collaboration, J. P. Lees et al., *Evidence of $B^+ \rightarrow \tau^+ \nu$ decays with hadronic B tags*, *Phys. Rev. D* **88** (2013) 031102, [1207.0698].
- [31] BELLE collaboration, I. Adachi et al., *Evidence for $B^- \rightarrow \tau^- \bar{\nu}_\tau$ with a Hadronic Tagging Method Using the Full Data Sample of Belle*, *Phys. Rev. Lett.* **110** (2013) 131801, [1208.4678].
- [32] BELLE collaboration, B. Kronenbitter et al., *Measurement of the branching fraction of $B^+ \rightarrow \tau^+ \nu_\tau$ decays with the semileptonic tagging method*, *Phys. Rev. D* **92** (2015) 051102, [1503.05613].
- [33] BELLE-II collaboration, I. Adachi et al., *Measurement of $B^+ \rightarrow \tau^+ \nu_\tau$ branching fraction with a hadronic tagging method at Belle II*, 2502.04885.
- [34] PARTICLE DATA GROUP collaboration, S. Navas et al., *Review of particle physics*, *Phys. Rev. D* **110** (2024) 030001.
- [35] BELLE-II collaboration, W. Altmannshofer et al., *The Belle II Physics Book*, *PTEP* **2019** (2019) 123C01, [1808.10567].
- [36] BELLE-II collaboration, L. Aggarwal et al., *Snowmass White Paper: Belle II physics reach and plans for the next decade and beyond*, 2207.06307.
- [37] Y. Amhis, M. Hartmann, C. Hensens, D. Hill and O. Sumensari, *Prospects for $B_c^+ \rightarrow \tau^+ \nu_\tau$ at FCC-ee*, *JHEP* **12** (2021) 133, [2105.13330].
- [38] X. Zuo, M. Fedele, C. Hensens, D. Hill, S. Iguro and M. Klute, *Prospects for B_c^+ and $B^+ \rightarrow \tau^+ \nu_\tau$ at FCC-ee*, *Eur. Phys. J. C* **84** (2024) 87, [2305.02998].
- [39] M. Beneke, G. Buchalla, M. Neubert and C. T. Sachrajda, *QCD factorization for exclusive, nonleptonic B meson decays: General arguments and the case of heavy light final states*, *Nucl. Phys. B* **591** (2000) 313–418, [hep-ph/0006124].
- [40] M. Beneke, G. Buchalla, M. Neubert and C. T. Sachrajda, *QCD factorization in $B \rightarrow \pi K, \pi\pi$ decays and extraction of Wolfenstein parameters*, *Nucl. Phys. B* **606** (2001) 245–321, [hep-ph/0104110].
- [41] M. Beneke, T. Feldmann and D. Seidel, *Systematic approach to exclusive $B \rightarrow V l^+ l^-$, $V\gamma$ decays*, *Nucl. Phys. B* **612** (2001) 25–58, [hep-ph/0106067].
- [42] M. Beneke and L. Vernazza, *$B \rightarrow \chi_{cJ} K$ decays revisited*, *Nucl. Phys. B* **811** (2009) 155–181, [0810.3575].
- [43] M. Benzke, S. J. Lee, M. Neubert and G. Paz, *Factorization at Subleading Power and Irreducible Uncertainties in $\bar{B} \rightarrow X_s \gamma$ Decay*, *JHEP* **08** (2010) 099, [1003.5012].
- [44] M. Benzke, S. J. Lee, M. Neubert and G. Paz, *Long-Distance Dominance of the CP Asymmetry in $B \rightarrow X_{s,d} + \gamma$ Decays*, *Phys. Rev. Lett.* **106** (2011) 141801, [1012.3167].

- [45] M. A. Ebert, I. Moulton, I. W. Stewart, F. J. Tackmann, G. Vita and H. X. Zhu, *Subleading power rapidity divergences and power corrections for q_T* , *JHEP* **04** (2019) 123, [1812.08189].
- [46] I. Moulton, I. W. Stewart and G. Vita, *Subleading Power Factorization with Radiative Functions*, *JHEP* **11** (2019) 153, [1905.07411].
- [47] M. Beneke, M. Garny, R. Szafron and J. Wang, *Violation of the Kluberg-Stern-Zuber theorem in SCET*, *JHEP* **09** (2019) 101, [1907.05463].
- [48] I. Moulton, I. W. Stewart, G. Vita and H. X. Zhu, *The Soft Quark Sudakov*, *JHEP* **05** (2020) 089, [1910.14038].
- [49] M. Beneke, A. Broggio, S. Jaskiewicz and L. Vernazza, *Threshold factorization of the Drell-Yan process at next-to-leading power*, *JHEP* **07** (2020) 078, [1912.01585].
- [50] I. Moulton, G. Vita and K. Yan, *Subleading power resummation of rapidity logarithms: the energy-energy correlator in $\mathcal{N} = 4$ SYM*, *JHEP* **07** (2020) 005, [1912.02188].
- [51] Z. L. Liu and M. Neubert, *Factorization at subleading power and endpoint-divergent convolutions in $h \rightarrow \gamma\gamma$ decay*, *JHEP* **04** (2020) 033, [1912.08818].
- [52] M. Beneke, M. Garny, S. Jaskiewicz, R. Szafron, L. Vernazza and J. Wang, *Large- x resummation of off-diagonal deep-inelastic parton scattering from d -dimensional refactorization*, *JHEP* **10** (2020) 196, [2008.04943].
- [53] Z. L. Liu, B. Mecaj, M. Neubert and X. Wang, *Factorization at subleading power, Sudakov resummation, and endpoint divergences in soft-collinear effective theory*, *Phys. Rev. D* **104** (2021) 014004, [2009.04456].
- [54] Z. L. Liu, B. Mecaj, M. Neubert and X. Wang, *Factorization at subleading power and endpoint divergences in $h \rightarrow \gamma\gamma$ decay. Part II. Renormalization and scale evolution*, *JHEP* **01** (2021) 077, [2009.06779].
- [55] M. Beneke, M. Garny, S. Jaskiewicz, J. Strohm, R. Szafron, L. Vernazza et al., *Next-to-leading power endpoint factorization and resummation for off-diagonal “gluon” thrust*, *JHEP* **07** (2022) 144, [2205.04479].
- [56] G. Bell, P. Böer and T. Feldmann, *Muon-electron backward scattering: a prime example for endpoint singularities in SCET*, *JHEP* **09** (2022) 183, [2205.06021].
- [57] T. Feldmann, N. Gubernari, T. Huber and N. Seitz, *Contribution of the electromagnetic dipole operator O_7 to the $\bar{B}_s \rightarrow \mu^+\mu^-$ decay amplitude*, *Phys. Rev. D* **107** (2023) 013007, [2211.04209].
- [58] Z. L. Liu, M. Neubert, M. Schnubel and X. Wang, *Factorization at next-to-leading power and endpoint divergences in $gg \rightarrow h$ production*, *JHEP* **06** (2023) 183, [2212.10447].

- [59] T. Hurth and R. Szafron, *Refactorisation in subleading $B \rightarrow X_s \gamma$* , *Nucl. Phys. B* **991** (2023) 116200, [2301.01739].
- [60] G. Buchalla, A. J. Buras and M. E. Lautenbacher, *Weak decays beyond leading logarithms*, *Rev. Mod. Phys.* **68** (1996) 1125–1144, [hep-ph/9512380].
- [61] E. E. Jenkins, A. V. Manohar and P. Stoffer, *Low-Energy Effective Field Theory below the Electroweak Scale: Operators and Matching*, *JHEP* **03** (2018) 016, [1709.04486].
- [62] E. E. Jenkins, A. V. Manohar and P. Stoffer, *Low-Energy Effective Field Theory below the Electroweak Scale: Anomalous Dimensions*, *JHEP* **01** (2018) 084, [1711.05270].
- [63] E. Eichten and B. R. Hill, *An Effective Field Theory for the Calculation of Matrix Elements Involving Heavy Quarks*, *Phys. Lett. B* **234** (1990) 511–516.
- [64] H. Georgi, *An Effective Field Theory for Heavy Quarks at Low Energies*, *Phys. Lett. B* **240** (1990) 447–450.
- [65] B. Grinstein, *The Static Quark Effective Theory*, *Nucl. Phys. B* **339** (1990) 253–268.
- [66] M. Neubert, *Heavy quark symmetry*, *Phys. Rept.* **245** (1994) 259–396, [hep-ph/9306320].
- [67] C. W. Bauer, S. Fleming, D. Pirjol and I. W. Stewart, *An Effective field theory for collinear and soft gluons: Heavy to light decays*, *Phys. Rev. D* **63** (2001) 114020, [hep-ph/0011336].
- [68] C. W. Bauer, D. Pirjol and I. W. Stewart, *Soft collinear factorization in effective field theory*, *Phys. Rev. D* **65** (2002) 054022, [hep-ph/0109045].
- [69] C. W. Bauer, S. Fleming, D. Pirjol, I. Z. Rothstein and I. W. Stewart, *Hard scattering factorization from effective field theory*, *Phys. Rev. D* **66** (2002) 014017, [hep-ph/0202088].
- [70] M. Beneke, A. P. Chapovsky, M. Diehl and T. Feldmann, *Soft collinear effective theory and heavy to light currents beyond leading power*, *Nucl. Phys. B* **643** (2002) 431–476, [hep-ph/0206152].
- [71] N. Isgur and M. B. Wise, *Weak transition form factors between heavy mesons*, *Phys. Lett. B* **237** (1990) 527–530.
- [72] A. F. Falk, H. Georgi, B. Grinstein and M. B. Wise, *Heavy Meson Form-factors From QCD*, *Nucl. Phys. B* **343** (1990) 1–13.
- [73] M. Neubert, *Model independent extraction of V_{cb} from semileptonic decays*, *Phys. Lett. B* **264** (1991) 455–461.
- [74] M. B. Wise, *Chiral perturbation theory for hadrons containing a heavy quark*, *Phys. Rev. D* **45** (1992) R2188.

- [75] T.-M. Yan, H.-Y. Cheng, C.-Y. Cheung, G.-L. Lin, Y. C. Lin and H.-L. Yu, *Heavy quark symmetry and chiral dynamics*, *Phys. Rev. D* **46** (1992) 1148–1164.
- [76] G. Burdman and J. F. Donoghue, *Union of chiral and heavy quark symmetries*, *Phys. Lett. B* **280** (1992) 287–291.
- [77] E. V. Shuryak, *Hadrons Containing a Heavy Quark and QCD Sum Rules*, *Nucl. Phys. B* **198** (1982) 83–101.
- [78] W. Dekens and P. Stoffer, *Low-energy effective field theory below the electroweak scale: matching at one loop*, *JHEP* **10** (2019) 197, [1908.05295].
- [79] W. J. Marciano and A. Sirlin, *Radiative corrections to $\pi_{\ell 2}$ decays*, *Phys. Rev. Lett.* **71** (1993) 3629–3632.
- [80] C. W. Bauer, D. Pirjol and I. W. Stewart, *Factorization and endpoint singularities in heavy to light decays*, *Phys. Rev. D* **67** (2003) 071502, [hep-ph/0211069].
- [81] M. Beneke and T. Feldmann, *Factorization of heavy to light form-factors in soft collinear effective theory*, *Nucl. Phys. B* **685** (2004) 249–296, [hep-ph/0311335].
- [82] T. Becher, R. J. Hill and M. Neubert, *Factorization in $B \rightarrow V\gamma$ decays*, *Phys. Rev. D* **72** (2005) 094017, [hep-ph/0503263].
- [83] J. Chay and C. Kim, *Collinear effective theory at subleading order and its application to heavy-light currents*, *Phys. Rev. D* **65** (2002) 114016, [hep-ph/0201197].
- [84] A. V. Manohar, T. Mehen, D. Pirjol and I. W. Stewart, *Reparameterization invariance for collinear operators*, *Phys. Lett. B* **539** (2002) 59–66, [hep-ph/0204229].
- [85] T. Becher, A. Broggio and A. Ferroglia, *Introduction to Soft-Collinear Effective Theory*, vol. 896. Springer, 2015, 10.1007/978-3-319-14848-9.
- [86] R. J. Hill and M. Neubert, *Spectator interactions in soft collinear effective theory*, *Nucl. Phys. B* **657** (2003) 229–256, [hep-ph/0211018].
- [87] S. Alte, M. König and M. Neubert, *Effective Field Theory after a New-Physics Discovery*, *JHEP* **08** (2018) 095, [1806.01278].
- [88] B. O. Lange and M. Neubert, *Factorization and the soft overlap contribution to heavy to light form-factors*, *Nucl. Phys. B* **690** (2004) 249–278, [hep-ph/0311345].
- [89] M. Beneke and T. Feldmann, *Multipole expanded soft collinear effective theory with non-Abelian gauge symmetry*, *Phys. Lett. B* **553** (2003) 267–276, [hep-ph/0211358].
- [90] A. J. Buras and P. H. Weisz, *QCD Nonleading Corrections to Weak Decays in Dimensional Regularization and 't Hooft-Veltman Schemes*, *Nucl. Phys. B* **333** (1990) 66–99.

- [91] M. J. Dugan and B. Grinstein, *On the vanishing of evanescent operators*, *Phys. Lett. B* **256** (1991) 239–244.
- [92] S. Herrlich and U. Nierste, *Evanescent operators, scheme dependences and double insertions*, *Nucl. Phys. B* **455** (1995) 39–58, [[hep-ph/9412375](#)].
- [93] J. Fuentes-Martín, M. König, J. Pagès, A. E. Thomsen and F. Wilsch, *Evanescent operators in one-loop matching computations*, *JHEP* **02** (2023) 031, [[2211.09144](#)].
- [94] N. Tracas and N. Vlachos, *Two-loop calculations in QCD and the $\Delta I = 1/2$ rule in non-leptonic weak decays*, *Phys. Lett. B* **115** (1982) 419.
- [95] X.-D. Ji and M. J. Musolf, *Subleading logarithmic mass dependence in heavy meson form-factors*, *Phys. Lett. B* **257** (1991) 409–413.
- [96] C. W. Bauer and A. V. Manohar, *Shape function effects in $B \rightarrow X_s \gamma$ and $B \rightarrow X_u l \bar{\nu}$ decays*, *Phys. Rev. D* **70** (2004) 034024, [[hep-ph/0312109](#)].
- [97] S. W. Bosch, B. O. Lange, M. Neubert and G. Paz, *Factorization and shape function effects in inclusive B meson decays*, *Nucl. Phys. B* **699** (2004) 335–386, [[hep-ph/0402094](#)].
- [98] T. Becher and M. Neubert, *On the Structure of Infrared Singularities of Gauge-Theory Amplitudes*, *JHEP* **06** (2009) 081, [[0903.1126](#)].
- [99] T. Becher and M. Neubert, *Infrared singularities of QCD amplitudes with massive partons*, *Phys. Rev. D* **79** (2009) 125004, [[0904.1021](#)].
- [100] M. Beneke, Y. Kiyo and D. s. Yang, *Loop corrections to subleading heavy quark currents in SCET*, *Nucl. Phys. B* **692** (2004) 232–248, [[hep-ph/0402241](#)].
- [101] R. J. Hill, T. Becher, S. J. Lee and M. Neubert, *Sudakov resummation for subleading SCET currents and heavy-to-light form-factors*, *JHEP* **07** (2004) 081, [[hep-ph/0404217](#)].
- [102] G. P. Korchemsky and A. V. Radyushkin, *Renormalization of the Wilson Loops Beyond the Leading Order*, *Nucl. Phys. B* **283** (1987) 342–364.
- [103] I. A. Korchemskaya and G. P. Korchemsky, *On lightlike Wilson loops*, *Phys. Lett. B* **287** (1992) 169–175.
- [104] M. Neubert, *Renormalization-group improved calculation of the $B \rightarrow X_s \gamma$ branching ratio*, *Eur. Phys. J. C* **40** (2005) 165–186, [[hep-ph/0408179](#)].
- [105] J. Chay, C. Kim, Y. G. Kim and J.-P. Lee, *Soft Wilson lines in soft-collinear effective theory*, *Phys. Rev. D* **71** (2005) 056001, [[hep-ph/0412110](#)].
- [106] I. Feige and M. D. Schwartz, *An on-shell approach to factorization*, *Phys. Rev. D* **88** (2013) 065021, [[1306.6341](#)].

- [107] R. Goerke and M. Luke, *Power Counting and Modes in SCET*, *JHEP* **02** (2018) 147, [1711.09136].
- [108] A. G. Grozin and M. Neubert, *Asymptotics of heavy meson form-factors*, *Phys. Rev. D* **55** (1997) 272–290, [hep-ph/9607366].
- [109] B. O. Lange and M. Neubert, *Renormalization group evolution of the B meson light cone distribution amplitude*, *Phys. Rev. Lett.* **91** (2003) 102001, [hep-ph/0303082].
- [110] S. J. Lee and M. Neubert, *Model-independent properties of the B-meson distribution amplitude*, *Phys. Rev. D* **72** (2005) 094028, [hep-ph/0509350].
- [111] M. Beneke, G. Finauri, K. K. Vos and Y. Wei, *QCD light-cone distribution amplitudes of heavy mesons from boosted HQET*, *JHEP* **09** (2023) 066, [2305.06401].
- [112] H. Kawamura, J. Kodaira, C.-F. Qiao and K. Tanaka, *B-meson light cone distribution amplitudes in the heavy quark limit*, *Phys. Lett. B* **523** (2001) 111, [hep-ph/0109181].
- [113] V. M. Braun, Y. Ji and A. N. Manashov, *Higher-twist B-meson Distribution Amplitudes in HQET*, *JHEP* **05** (2017) 022, [1703.02446].
- [114] A. Vogt, *Leading logarithmic large-x resummation of off-diagonal splitting functions and coefficient functions*, *Phys. Lett. B* **691** (2010) 77–81, [1005.1606].
- [115] A. A. Almasy, G. Soar and A. Vogt, *Generalized double-logarithmic large-x resummation in inclusive deep-inelastic scattering*, *JHEP* **03** (2011) 030, [1012.3352].
- [116] M. Neubert, *Symmetry breaking corrections to meson decay constants in the heavy quark effective theory*, *Phys. Rev. D* **46** (1992) 1076–1087.
- [117] S. Fleming, A. H. Hoang, S. Mantry and I. W. Stewart, *Top Jets in the Peak Region: Factorization Analysis with NLL Resummation*, *Phys. Rev. D* **77** (2008) 114003, [0711.2079].
- [118] S. Fleming, A. H. Hoang, S. Mantry and I. W. Stewart, *Jets from massive unstable particles: Top-mass determination*, *Phys. Rev. D* **77** (2008) 074010, [hep-ph/0703207].
- [119] D. A. Bryman, P. Depommier and C. Leroy, *$\pi \rightarrow e\nu$, $\pi \rightarrow e\nu\gamma$ decays and related processes*, *Phys. Rept.* **88** (1982) 151–205.
- [120] J. Bijnens, G. Ecker and J. Gasser, *Radiative semileptonic kaon decays*, *Nucl. Phys. B* **396** (1993) 81–118, [hep-ph/9209261].
- [121] C. G. Boyd and B. Grinstein, *Chiral and heavy quark symmetry violation in B decays*, *Nucl. Phys. B* **442** (1995) 205–227, [hep-ph/9402340].
- [122] G. Chiladze, A. F. Falk and A. A. Petrov, *Radiative leptonic B_c decays in effective field theory*, *Phys. Rev. D* **60** (1999) 034011, [hep-ph/9811405].

- [123] S. Kürten, M. Zanke, B. Kubis and D. van Dyk, *Dispersion relations for $B^- \rightarrow \ell^- \bar{\nu}_\ell \ell'^- \ell'^+$ form factors*, *Phys. Rev. D* **107** (2023) 053006, [2210.09832].
- [124] P. L. Cho and H. Georgi, *Electromagnetic interactions in heavy hadron chiral theory*, *Phys. Lett. B* **296** (1992) 408–414, [hep-ph/9209239].
- [125] P. Colangelo, F. De Fazio and G. Nardulli, *Radiative heavy meson transitions*, *Phys. Lett. B* **316** (1993) 555–560, [hep-ph/9307330].
- [126] M. E. Luke and A. V. Manohar, *Reparametrization invariance constraints on heavy particle effective field theories*, *Phys. Lett. B* **286** (1992) 348–354, [hep-ph/9205228].
- [127] G. Amoros, M. Beneke and M. Neubert, *Two loop anomalous dimension of the chromomagnetic moment of a heavy quark*, *Phys. Lett. B* **401** (1997) 81–90, [hep-ph/9701375].
- [128] A. F. Falk and M. Neubert, *Second order power corrections in the heavy quark effective theory. 1. Formalism and meson form-factors*, *Phys. Rev. D* **47** (1993) 2965–2981, [hep-ph/9209268].
- [129] F. E. Low, *Bremsstrahlung of very low-energy quanta in elementary particle collisions*, *Phys. Rev.* **110** (1958) 974–977.
- [130] H. Georgi, *Weak Interactions and Modern Particle Theory*. Benjamin/Cummings, 1984.
- [131] J. L. Goity, *Chiral perturbation theory for $SU(3)$ breaking in heavy meson systems*, *Phys. Rev. D* **46** (1992) 3929–3936, [hep-ph/9206230].
- [132] B. Grinstein, E. E. Jenkins, A. V. Manohar, M. J. Savage and M. B. Wise, *Chiral perturbation theory for f_{D_s}/f_D and B_{B_s}/B_B* , *Nucl. Phys. B* **380** (1992) 369–376, [hep-ph/9204207].
- [133] H.-Y. Cheng, C.-Y. Cheung, G.-L. Lin, Y. C. Lin, T.-M. Yan and H.-L. Yu, *Corrections to chiral dynamics of heavy hadrons: $SU(3)$ symmetry breaking*, *Phys. Rev. D* **49** (1994) 5857–5881, [hep-ph/9312304].
- [134] I. W. Stewart, *Extraction of the $D^* D \pi$ coupling from D^* decays*, *Nucl. Phys. B* **529** (1998) 62–80, [hep-ph/9803227].
- [135] J. Gasser and H. Leutwyler, *Chiral Perturbation Theory to One Loop*, *Annals Phys.* **158** (1984) 142.
- [136] J. Gasser and H. Leutwyler, *Chiral Perturbation Theory: Expansions in the Mass of the Strange Quark*, *Nucl. Phys. B* **250** (1985) 465–516.
- [137] J. Wess and B. Zumino, *Consequences of anomalous Ward identities*, *Phys. Lett. B* **37** (1971) 95–97.

- [138] E. Witten, *Global Aspects of Current Algebra*, *Nucl. Phys. B* **223** (1983) 422–432.
- [139] F. De Fazio and M. Neubert, *$B \rightarrow X_u l \bar{\nu}_l$ decay distributions to order α_s* , *JHEP* **06** (1999) 017, [[hep-ph/9905351](#)].
- [140] M. Neubert, *Analysis of the photon spectrum in inclusive $B \rightarrow X_s \gamma$ decays*, *Phys. Rev. D* **49** (1994) 4623–4633, [[hep-ph/9312311](#)].
- [141] A. G. Grozin and G. P. Korchemsky, *Renormalized sum rules for structure functions of heavy mesons decays*, *Phys. Rev. D* **53** (1996) 1378–1390, [[hep-ph/9411323](#)].
- [142] M. Neubert, *Advanced predictions for moments of the $\bar{B} \rightarrow X_s \gamma$ photon spectrum*, *Phys. Rev. D* **72** (2005) 074025, [[hep-ph/0506245](#)].
- [143] T. Becher and M. Neubert, *Threshold resummation in momentum space from effective field theory*, *Phys. Rev. Lett.* **97** (2006) 082001, [[hep-ph/0605050](#)].
- [144] M. Wirbel, B. Stech and M. Bauer, *Exclusive Semileptonic Decays of Heavy Mesons*, *Z. Phys. C* **29** (1985) 637.
- [145] G. Burdman, Z. Ligeti, M. Neubert and Y. Nir, *The Decay $B \rightarrow \pi l \nu$ in Heavy Quark Effective Theory*, *Phys. Rev. D* **49** (1994) 2331–2345, [[hep-ph/9309272](#)].
- [146] BELLE collaboration, M. Gelb et al., *Search for the rare decay of $B^+ \rightarrow \ell^+ \nu_\ell \gamma$ with improved hadronic tagging*, *Phys. Rev. D* **98** (2018) 112016, [[1810.12976](#)].
- [147] K. G. Chetyrkin, J. H. Kuhn and M. Steinhauser, *RunDec: A Mathematica package for running and decoupling of the strong coupling and quark masses*, *Comput. Phys. Commun.* **133** (2000) 43–65, [[hep-ph/0004189](#)].
- [148] B. Pullin and R. Zwicky, *Radiative decays of heavy-light mesons and the $f_{H,H^*,H_1}^{(T)}$ decay constants*, *JHEP* **09** (2021) 023, [[2106.13617](#)].
- [149] H.-D. Li, C.-D. Lü, C. Wang, Y.-M. Wang and Y.-B. Wei, *QCD calculations of radiative heavy meson decays with subleading power corrections*, *JHEP* **04** (2020) 023, [[2002.03825](#)].
- [150] RBC, UKQCD collaboration, J. M. Flynn, P. Fritzsche, T. Kawanai, C. Lehner, B. Samways, C. T. Sachrajda et al., *The $B^* B \pi$ Coupling Using Relativistic Heavy Quarks*, *Phys. Rev. D* **93** (2016) 014510, [[1506.06413](#)].
- [151] V. M. Belyaev, V. M. Braun, A. Khodjamirian and R. Ruckl, *$D^* D \pi$ and $B^* B \pi$ couplings in QCD*, *Phys. Rev. D* **51** (1995) 6177–6195, [[hep-ph/9410280](#)].
- [152] A. Khodjamirian, B. Melić, Y.-M. Wang and Y.-B. Wei, *The $D^* D \pi$ and $B^* B \pi$ couplings from light-cone sum rules*, *JHEP* **03** (2021) 016, [[2011.11275](#)].
- [153] FLAVOUR LATTICE AVERAGING GROUP (FLAG) collaboration, Y. Aoki et al., *FLAG Review 2024*, [2411.04268](#).

- [154] HPQCD collaboration, B. Colquhoun, C. T. H. Davies, R. J. Dowdall, J. Kettle, J. Koponen, G. P. Lepage et al., *B-meson decay constants: a more complete picture from full lattice QCD*, *Phys. Rev. D* **91** (2015) 114509, [1503.05762].
- [155] ETM collaboration, V. Lubicz, A. Melis and S. Simula, *Masses and decay constants of $D_{(s)}^*$ and $B_{(s)}^*$ mesons with $N_f = 2 + 1 + 1$ twisted mass fermions*, *Phys. Rev. D* **96** (2017) 034524, [1707.04529].
- [156] T. Nishikawa and K. Tanaka, *QCD Sum Rules for Quark-Gluon Three-Body Components in the B Meson*, *Nucl. Phys. B* **879** (2014) 110–142, [1109.6786].
- [157] A. Khodjamirian, R. Mandal and T. Mannel, *Inverse moment of the B_s -meson distribution amplitude from QCD sum rule*, *JHEP* **10** (2020) 043, [2008.03935].
- [158] V. M. Braun, A. N. Manashov and N. Offen, *Evolution equation for the higher-twist B-meson distribution amplitude*, *Phys. Rev. D* **92** (2015) 074044, [1507.03445].
- [159] BELLE collaboration, M. T. Prim et al., *Search for $B^+ \rightarrow \mu^+ \nu_\mu$ and $B^+ \rightarrow \mu^+ N$ with inclusive tagging*, *Phys. Rev. D* **101** (2020) 032007, [1911.03186].
- [160] J. Chay, C. Kim and A. K. Leibovich, *Quark mass effects in the soft-collinear effective theory and $\bar{B} \rightarrow X_s \gamma$ in the endpoint region*, *Phys. Rev. D* **72** (2005) 014010, [hep-ph/0505030].
- [161] M. Beneke, M. Garny, R. Szafron and J. Wang, *Anomalous dimension of subleading-power N-jet operators. Part II*, *JHEP* **11** (2018) 112, [1808.04742].
- [162] J.-y. Chiu, A. Fuhrer, A. H. Hoang, R. Kelley and A. V. Manohar, *Soft-Collinear Factorization and Zero-Bin Subtractions*, *Phys. Rev. D* **79** (2009) 053007, [0901.1332].
- [163] T. Becher, M. Neubert and B. D. Pecjak, *Factorization and Momentum-Space Resummation in Deep-Inelastic Scattering*, *JHEP* **01** (2007) 076, [hep-ph/0607228].